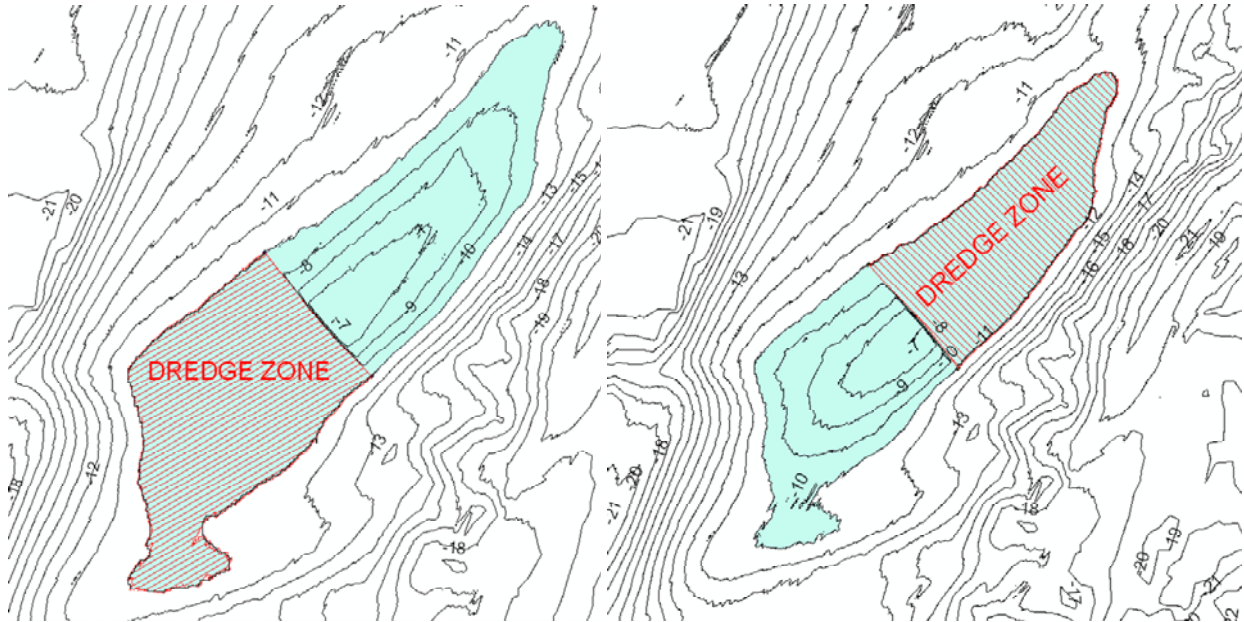# INVESTIGATION OF DREDGING GUIDELINES TO MAINTAIN AND PROTECT THE GEOMORPHIC INTEGRITY OF OFFSHORE RIDGE AND SHOAL REGIMES

Detailed Morphologic Evaluation of Offshore Shoals

PREPARED FOR:
U.S. DEPARTMENT OF THE INTERIOR
MINERALS MANAGEMENT SERVICE

MMS U.S. Department of the Interior
Minerals Management Service

INVESTIGATION OF DREDGING GUIDELINES TO MAINTAIN AND PROTECT THE GEOMORPHIC INTEGRITY OF OFFSHORE RIDGE AND SHOAL REGIMES

Detailed Morphologic Evaluation of Offshore Shoals

Authors
Dr. Mohammad Dibajnia
Dr. Robert B. Nairn

January 2010

MMS **U.S. Department of the Interior**
Minerals Management Service

DISCLAIMER

This report was prepared under contract between the Minerals Management Service (MMS) and W.F. Baird & Associates Ltd. This report has been reviewed technically by the MMS, and it has been approved for publication. Approval does not signify that the contents necessarily reflect the views and policies of the MMS, nor does mention of trade names or commercial products constitute endorsement or recommendation for use. It is, however, exempt from review and compliance with the MMS editorial standards.

TABLE OF CONTENTS

LIST OF FIGURES

LIST OF TABLES

1.0   INTRODUCTION

W.F. Baird & Associates Ltd. (Baird) was retained by the Minerals Management Service (MMS) for execution of the project "Investigation of Dredging Guidelines to Maintain and Protect the Geomorphic Integrity of Offshore Ridge and Shoal Regimes/Detailed Morphologic Evaluation of Offshore Shoals".

Motivation for this study developed over a period of ten years beginning with the design of several shoreline protection projects for the Assateague Island National Seashore, south of Ocean City, Maryland in the late 1990s (USACE, 1998). MMS partnered with the U.S. Army Corps of Engineers Baltimore District to design and test the viability of strategic dredging on Great Gull Bank the borrow area selected for the project. During dredging, the crest of the shoal was avoided, and a maximum dredge depth on the shoal flanks was maintained (Amato, 2002). Concerns over the importance of the mid-Atlantic shoal fields to fish migration and feeding by Federal and state agencies led to heightened awareness of their preservation (Vasslides and Able, 2008; Slacum et al., in press) and more careful planning of their use in beach construction projects including the Atlantic Coast of Maryland Shoreline Protection Project (USACE, 2008).

Similar dredging strategies to that employed at Great Gull Bank have been proposed for other projects, including limiting the dredge volume to a relative percentage of the original shoal volume. In support of this approach, some have suggested there may be a critical depth of dredging below which shoals should not be dredged provided wave-induced sediment transport is paramount to shoal crest elevation and geometry (Hayes and Nairn, 2004). Others have added that there may be a relative water depth and/or shoal height and size for which recovery may be constrained. Recognizing that a better understanding of the processes that maintain these features is necessary, the MMS designed and funded this study.

The purpose of the present study was thus to formulate and recommend offshore dredging guidelines to protect and maintain the morphologic integrity of the ridge and shoal features found on the Outer Continental Shelf (OCS) which are being targeted as sand borrow sites for beach nourishment and coastal restoration efforts. The guidelines are supported by an improved understanding of the morphologic evolution of ridge and shoal features through morphometric analysis, field measurements, and numerical modeling. The objective of the guidelines will be to allow dredging of ridge and shoal features, at the same time as protecting their integrity and the habitat for benthos and fish provided by these features.

The focus of the study was on Delmarva Atlantic Coast area, i.e. the area offshore Delaware, Maryland and Virginia between Delaware Bay and Chesapeake Bay. Shoals in this area are technically regarded as sand ridges (see Section 2.1). However, we will also use the more general term of "shoal" to refer to sand ridges throughout this report.

To assess the impacts of dredging on Offshore Ridge and Shoal features, it is essential that a better understanding of the processes that maintain these features be developed. There have been numerous previous studies considering effect of waves and currents on shaping shoals or

shoreface-attached ridges (e.g. Duane et al. 1972, Swift et al. 1972, Field 1980, Figueiredo et al. 1981, Swift and Field 1981, Pattiaratchi and Collins 1987, Trowbridge 1995, Dyer and Huntley 1999, Snedden and Dalrymple 1999, Restrepo, Calvete et al. 2001, Maa et al. 2004, Sanay et al. 2007). A new conceptual model presented in Hayes and Nairn (2004) demonstrates how waves shoaling and refracting up either side of a ridge off the coast of Maryland and Delaware result in convergence of sand transport over the crest of the ridge, thus maintaining the ridge even after it is detached from shore face processes. The possibility that these ridges might deflate or disappear as a consequence of dredging, resulting in dramatic changes in wave conditions along the shore, is a major concern.

It is the purpose of this project to investigate shoal self-sustainability mechanisms through a combination of field surveys and numerical modeling, and to determine its universality for other ridge and shoal features. With this understanding established and verified, the next step is to determine to what extent dredging and removal of some of the shoal volume may influence the maintenance processes. The findings will provide the basis for developing guidelines to protect the integrity of these features. Ideally the guidelines should to be universal and related to non-dimensional characteristics of the shoals, such as ratio of crest height to depth height, or volume removed to initial volume.

A series of scientific questions may be formulated to provide a framework for addressing the objectives of this project as follows:

1. At what rate are ridge and shoal features created, potentially replacing features that are diminished through dredging? The rate and direction of migration of these features may provide a clue to answering this question.

2. What are the relative roles of waves and currents in maintaining the geomorphic integrity of existing ridge and shoal features? Hayes and Nairn (2004) suggested a hypothesis that waves are the primary controlling mechanism in OCS waters; this hypothesis must be rigorously tested.

3. Is there a critical threshold for dredging that once crossed, ridge and shoal features may deflate, losing their morphologic integrity?

4. Ridges and shoals come in many shapes and sizes in different wave/tidal settings. Is it possible to develop universal criteria for protecting the morphologic integrity of these features, possibly related to dimensionless characteristics such as ratios of crest depth to shoal height, length to width, volume removed to initial volume and storm wave height to crest height? If universal criteria can be established, they would provide the basis for developing guidelines to protect the morphologic integrity of these features. If universal criteria cannot be established, it may be necessary to specify site-specific analysis following a recommended set of procedures to evaluate each case individually.

2.0   LITERATURE REVIEW

In this section a brief review of previous studies and a list of available information are presented.

2.1   Previous Studies

This section provides a brief selected summary of a rich and complex literature on sand ridges. In addition to several key references mentioned in Section 1.0, Van Rijn (1998) provided a comprehensive review of sand waves, ridges and banks in the context of Coastal Geomorphology. He classified these features according to their orientation to the dominant current direction, to the orientation of the coastline and to the presence of particular coastal features (spit, headland, inlet, etc.), as follows:

- Current-transverse sand waves and ridges,

- Current-oblique sand ridges and banks,

- Current-parallel sand ridges and banks,

- Shoreface-connected sand ridges,

- Headland-attached banks and shoals,

- Spit-attached banks and shoals,

- Estuary mouth banks and shoals.

According to van Rijn (1998), the ridge and shoal features found on the Outer Continental Shelf east of the United States are classified as Current-oblique sand banks and ridges. Linear sand bodies oblique to the main current direction are found in a variety of geomorphological settings such as on open shelf seas, adjacent to convergent or divergent coastlines (straits), and off coastal headlands. Linear sand bodies in open shelf seas are often divided into tidal sand banks found in tide-dominated settings and smaller-scale sand ridges found in storm-generated ridges (Mid Atlantic Shelf), but they are also found in a setting where tidal currents and storms both may be important.   Generally, the landward end of the ridge is situated ahead (in the direction of the dominant current) of the seaward end of the ridge. The downcurrent (seaward) slopes tend to be steeper and finer grained. The ridges tend to migrate slowly (1 to 3 m per year) in the dominant current direction. Swift and Field (1981) determined that large shoals of the region may migrate at rates ranging from 2 to 12 m (6 to 40 ft) per year, generally to the southeast. Maryland Geological Survey monitoring of Borrow Areas 2 and 3 presented in USACE (2008) determined that those two features are migrating to the south at a rate of 4.5 to 9 m (15 to 30 ft) per year.

Van Rijn (1998) found significant morphological differences between active tide-dominated sand banks and storm-dominated sand ridges. The orientation of the tidal sand banks is related primarily to the dominant peak tidal current direction, while the orientation of the storm sand ridges seems to be imposed by the direction of the storm-driven near-bed currents with respect to the coastline. Tidal sand banks are generally higher than storm sand ridges: the former have heights up to 40 meters, while the latter are up to 10 meters. Tidal sand banks may be steeper (6° or less) than storm sand ridges (2° or less) and they generally have sharper crests. Tidal sand banks have larger spacings than storm ridges and they are generally longer. Typical spacings range between 2 to 30 km for tidal sand banks and 0.5 to 5 km for storm sand ridges. Tidal sand banks are up to 70 km long, storm sand ridges up to 20 km.

Van Rijn (1998) explains that an important feature of many sand bank systems is the lateral coherence of the individual sand bodies. Shoreface sand bodies almost always occur in fields, often with a very constant spacing between the ridges. Generally, sand banks consist of medium to coarse sand (0.4 to 0.8 mm) and are considered as sources of sediment. Sand banks are quite stable features. Mega-ripples and sand waves may migrate over the banks in regions, where the velocities are large enough to initiate particle motion. Closely related to the strength and direction of the currents, sediments are circulating round and over the bank. The crest axis of the bank deviates typically 20° (anticlockwise rotation on the Northern hemisphere) from the direction of the dominant peak tidal current, which may be caused by Coriolis effects.

According to Van Rijn (1998), sand ridges with heights up to 10 m extend for tens of kilometers in the Atlantic Bight off the east coast of the USA. They have spacings of 2 to 5 km and they are attached to the shoreface (depths of about 5 m) at their southwest end at angles of 20° to 40°. The ridges are abundant on the Delmarva (Delaware-Maryland-Virginia) peninsula between Delaware and Chesapeake Bays. Tidal currents (micro-tidal range) are relatively weak in the Middle Atlantic shelf. The axes of the ridges are aligned with the direction of approach of storm winds/waves generated by 'northeasters' producing strong southwesterly currents. Common features are

- Ridges are formed and maintained by tide- and wind-driven currents along relatively flat sandy coasts formed during the Holocene Epoch on a marine transgressive surface;

- Ridges make an angle between 20° and 50° with the shoreline;

- The landward ends of the ridges are situated ahead of the seaward ends (in the direction of the dominant current);

- The ridges migrate in the dominant current direction;

- The downflank slopes are steeper and finer grained than the upflank slopes.

Lankneus et al. (1994) studied the morphological behaviour on one (Middlekerke bank) of the Flemish sand banks in front of the southern North Sea coast of Belgium. The bank has a slight

oblique orientation with respect to the local coastline. Each of the Flemish banks is about 20 to 30 km long, 10 to 20 m high and 1 to 2 km wide. The water depths at the crest vary between 20 and 4 m below the low water level at spring tide (tidal range of about 4 m). Coarser (0.4 mm) sediments occur in the higher parts, whereas finer sediments (0.2 mm) are located in the deeper parts between the banks. The crest zone of the bank is covered with asymmetric sand dunes (lengths up to 150 m and heights up to 5m) and mega-ripples (lengths up to 20 m) on the flanks. Analysis of regular bathymetric survey results shows the presence of considerable volumetric changes (±25 %) along several transects. The volume seems to decrease in periods of stormy weather (dispersion by wave action) after which the sand is carried back to the bank (volume increase). On the long term there is a dynamic equilibrium. Analysis of pre-storm and post-storm survey results at two selected areas shows that the mega—ripples may disappear under storm conditions and that the sand dune heights may become smaller (by about 1 m). There was hardly any change in volume at both locations over the time interval of the surveys.

Huthnance (1982) studied ridge formation and orientation for situations far away from the shoreline. He analyzed the linearized depth-averaged hydrodynamic equations in combination with a sand transport function and the bed evolution equation, and showed that the oblique orientation of the ridge (infinitely long ridge in water far away from shorelines) is essential for ridge growth. Maximum growth occurs at a spacing of about 250h (h= depth) and at an angle of about ±30° (with a variation of about 10° depending on various parameters) between the current vector and the longest ridge axis. The basic mechanism is that the current velocities on the upstream flank are slightly larger than those on the downstream flank in case of oblique orientation resulting in net tide-averaged sand flux towards the crest on both flanks (convergence). The net current and sand transport on the flanks is directed towards the crest of the ridge, both for the flood and ebb phase of the tide. The actual orientation (clockwise or anti-clockwise) of the ridge axis with respect to the dominant current direction will depend on the orientation of the initially present bed perturbation, the latter being dependent on factors like topographical configuration and orientation of the coastline. If the flood- and ebb—tidal currents are unequal in magnitude and/or direction, then the sand ridge will be asymmetric with the steep flank facing the direction of the net transport vector. The Coriolis term was found to enhance the growth of the ridges and to turn the ridge axis in a more anti—clockwise direction (on the northern hemisphere) with respect to the direction of the tidal wave propagation.

Based on Huthnance's work, De Vriend (1990) has developed a mathematical model, with which the effect of a number of phenomena on the growth rate of the ridges can be evaluated. The growth of a sand bank orientated obliquely to the flow is predicted to occur for any combination of tidal velocity amplitude, mean water depth, bottom roughness and sediment transport. Assuming the model to be correct, this means that the presence of such banks in a tidal setting like the North Sea, rather than the absence would be the normal situation.

The ridge formation theory of Huthnance (1982) requires a sufficient sand source, currents to move the sand, and an irregularity on the sea floor around which the ridges are initiated. McBride and Moslow (1991) postulated that one of the initial irregularities is a segment of an ebb-tidal delta abandoned by inlet migration. These theories of origin provide little information on how these features maintain their form once they are detached from the shore, yet remain in a zone of active wave attack (i.e. in depths less than 20 m). Snedden and Dalrymple (1999)

indicate that shoals in water depths less than approximately 20 m are migrating shoreward through the influence of Stokes Drift under fair-weather waves based on the work of McHone (1973). However, this model does not explain the maintenance of the form of linear shoal and ridge features.

Recent work for MMS by Condrey (personal communications) on Ship Shoal offshore Louisiana, and Slacum et al. (2010) on shoals offshore Maryland/Delaware, and Vasslides and Able (2008) have found that ridge and shoal features may have important ecological functions in terms of fish and benthos habitat at certain times of the year and day (evening). In addition, in some cases these ridge and shoal features provide protection from wave attack to adjacent shorelines.

Hayes and Nairn (2004) in an investigation for MMS, completed a literature review of understanding of the distribution, genesis, maintenance and characteristics of linear ridge and shoal features. Ridge and swale topography is exceptionally well developed on the continental shelves of the Mid-Atlantic Bight (see Figure 2.1) and the northeastern Gulf of Mexico (see Figure 2.2). In both cases, these linear ridges are oriented parallel to the predominant wave approach direction, suggesting a common process for their evolution and maintenance. Most researchers have concluded that ridges were derived from shore faces of barrier islands as they retreated across the shelf in response to rising sea level and tides or storm-driven currents maintain them. Hayes and Nairn (2004) demonstrated how waves shoaling and refracting up either side of the Fenwick ridge (Figure 2.3) off the coast of Maryland and Delaware result in convergence of sand transport over the crest of the ridge (Figure 2.4), thus maintaining the ridge even after it is detached from shore face processes. They concluded that predominant storm waves originating from the northeast (nor'easters) cause shoals on the Mid-Atlantic Bight to align and migrate along a northeast/southwest axis while preserving their overall shape/integrity.
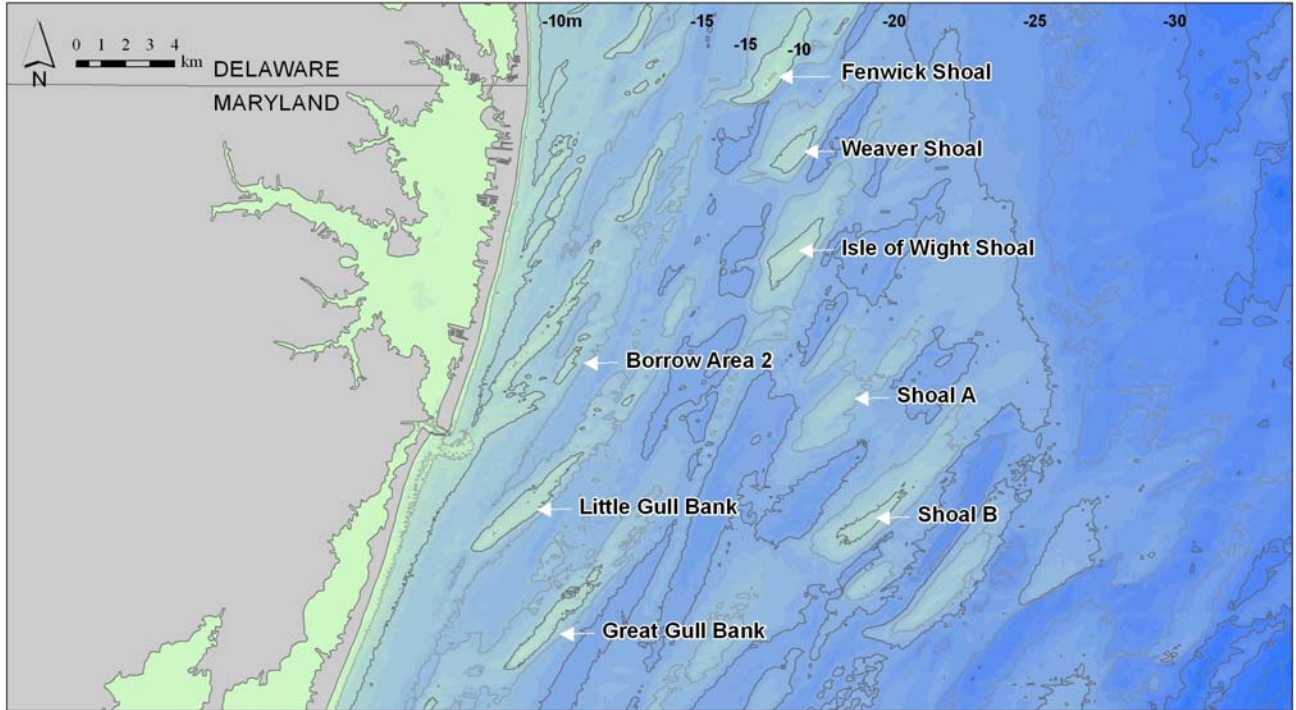
Figure 2.1 Example of ridge and swale topography typical of the Mid-Atlantic Bight region.
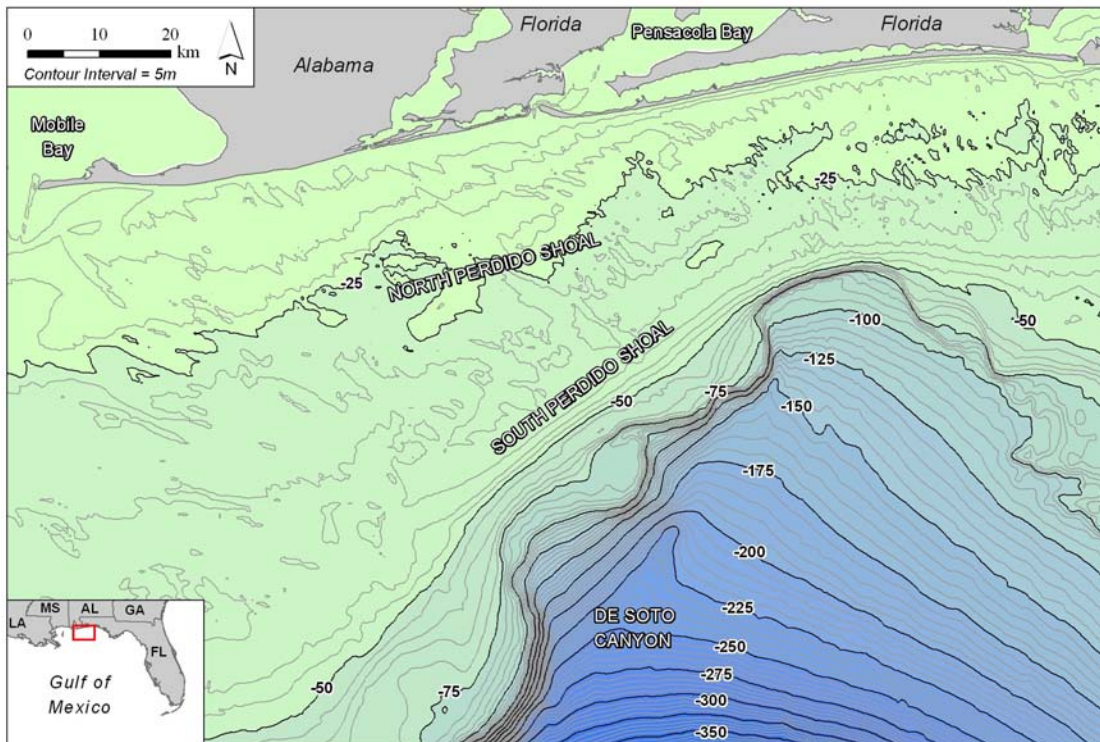
Figure 2.2 Continental shelf in the north-eastern Gulf of Mexico showing detailed bathymetry at 5 m contour intervals. Thicker contours are at 25 m intervals.
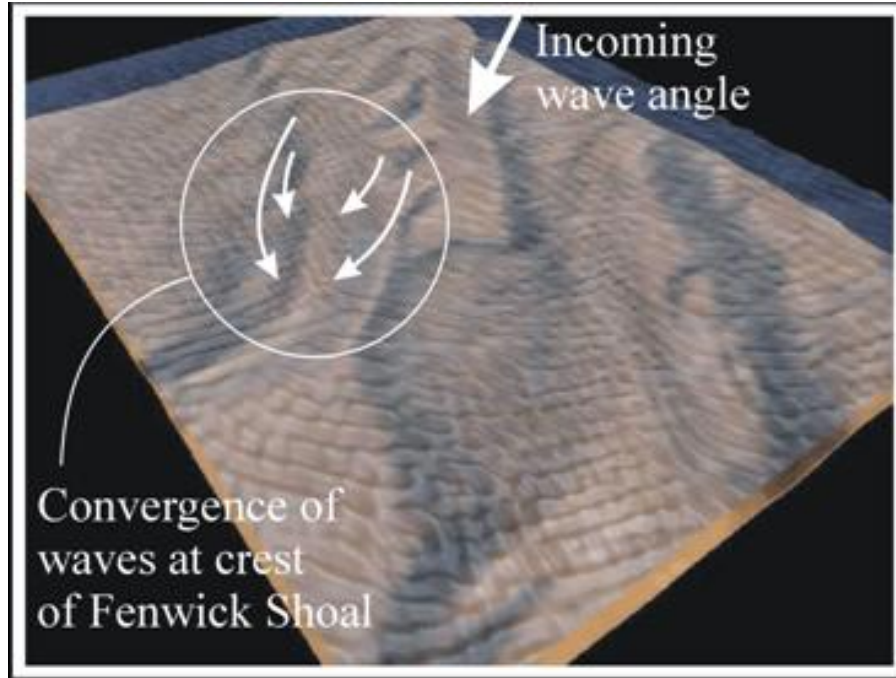
Figure 2.3 A snapshot of wave action predicted with a Boussinesq numerical model over the Fenwick and Weaver Shoals shown in Figure 2.1.
The results are for a 3 m significant wave height, 16-second period and ENE direction. Waves wrap around and up the slopes on either side of the shoal, converging at the crest (from Hayes and Nairn, 2004).
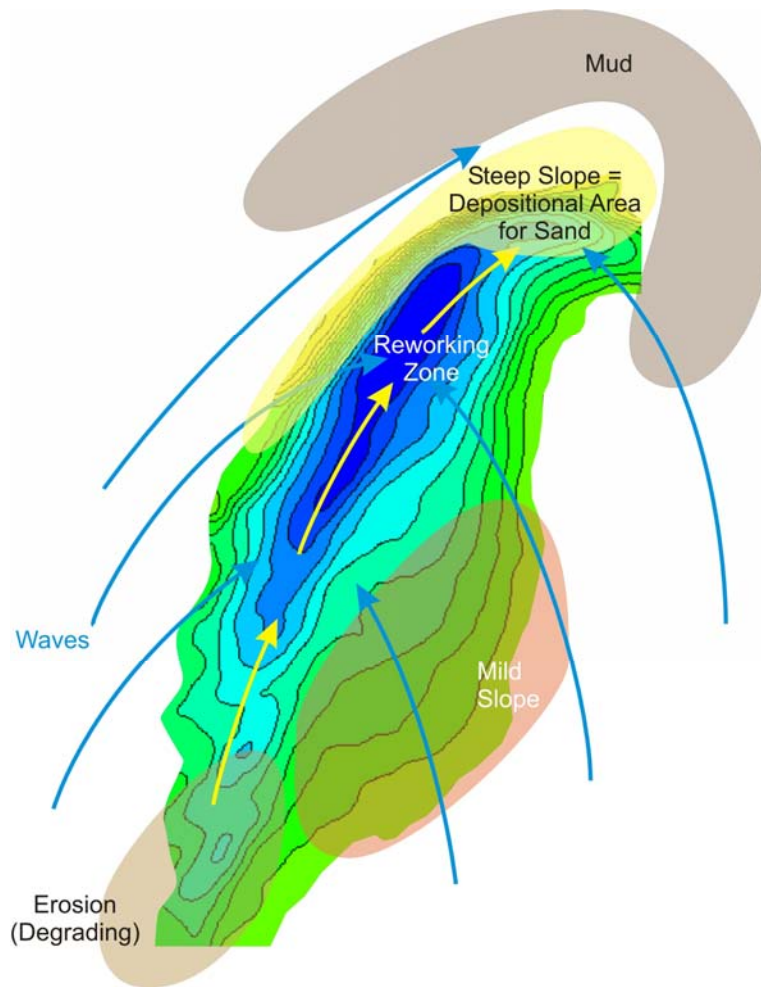
Figure 2.4 Schematics of the wave and sand transport processes that may serve to maintain the shape of Fenwick shoal. The shoal is migrating in the direction of the "steep slope" on its southeast side.

2.2 Available Data

As discussed in Section 1.0, the focus of the present study was on Delmarva Atlantic Coast area, i.e. the area offshore Delaware, Maryland and Virginia between Delaware Bay and Chesapeake Bay. The study area is part of the ridge and swale topography of the Mid-Atlantic Bight formed by wave/storm dominated sand ridges. This section provides a summary of various available data for the study area.

2.2.1 Bathymetric Data

The following bathymetry data were considered for use in the present study. Refer to Figure 2.1 for the mentioned locations.

1880 Charts at GGB, IOW, Weaver, Fenwick, Shoal A, Borrow Area 2 including 2 charts obtained from NOAA Office of Coast Survey's Historical Map & Chart Project Image Catalog (http://historicalcharts.noaa.gov/). Chart 1 is entitled 'From Cape Henlopen to Fenwick's Island' and Chart 2 entitled 'From Isle of Wight to Green Run Inlet'. Both charts are at 1:80,000 scale, with soundings in fathoms at Mean Low Water (MLW). The charts contain both soundings and contours. Soundings are coarse; distance between soundings varies from 500 m to 1000 m. Due to concerns over accuracy, it was decided not rely on these charts in the present analysis.

*1929 Field Sheet covering IOW, Weaver and Fenwic*k (US Coast and Geodetic Survey Register No. 4951) obtained from NOAA Office of Coast Survey's Historical Map & Chart Project Image Catalog (http://historicalcharts.noaa.gov/). Soundings were surveyed between Sept 4 and Oct 31, 1929, at 1:20,000 scale. Soundings are in feet referenced to Mean Low Water (MLW). The reference level is assumed to be at Ocean City.

1975 Hydrographic Survey (Survey ID = H09579) obtained from the NOAA National Ocean Service (NOS) – Geodas. The data provides full coverage of IOW, but partial coverage of Weaver & Shoal A. Soundings are in feet at 1:20,000 scale and referenced to Mean Low Water (MLW). The reference level is assumed to be at Ocean City.

1978 Hydrographic Surveys (Survey ID = H09764 and H09759) obtained from the NOAA National Ocean Service (NOS) – Geodas. The survey provides full coverage of GGB, Fenwick, Borrow Area 2, and partial coverage of Weaver and Shoal A. Soundings are in feet referenced to Mean Low Water (MLW) at scale 1:20,000 scale. The reference level is assumed to be at Ocean City.

1999 Survey at Great Gull Bank (GGB) was surveyed for USACE, Baltimore District, by Ocean Surveys Inc. in 1999.   Survey lines are at about 500 ft (150 m) intervals; distance between soundings varies from 5-10 ft (1.5 to 3 m, on average). Depths are reported in feet and referenced to Mean Lower Low Water (MLLW) at Ocean City, Maryland. The data is available in digital XYZ format.

2002 Surveys at Weaver, Isle of Wight (IOW) and Shoal A completed by USACE, Baltimore District. Survey lines are at about 500 ft (150 m) intervals; distance between soundings varies from 20-30 ft (6 to 9 m, on average). Vertical datum is Mean Lower Low Water (1960-1978 tidal epoch) US Survey Feet at Ocean City. The data is available in digital XYZ format.

2002 Survey at Great Gull Bank (GGB) was surveyed for USACE, Baltimore District, by Weeks Marine Inc. on December 31, 2002. The survey provides a partial coverage of shoal with survey lines at 500 ft (150 m) intervals. Depths are in feet and referenced to Mean Lower Low Water (MLLW) at Ocean City, Maryland, fishing pier. Digital XYZ data was not available.

2003 Survey at Great Gull Bank (GGB) surveyed for USACE, Baltimore District, by Weeks Marine Inc. in 2003. Survey lines at 500 ft (150 m) intervals. Depths are in feet and referenced

to Mean Lower Low Water (MLLW) at Ocean City, Maryland, fishing pier. Digital XYZ data was not available.

National Ocean Service (NOS) hydrographic survey data of the entire Mid Atlantic Bight (http://map.ngdc.noaa.gov/website/mgg/nos_hydro/viewer.htm)

2.2.2   Waves

The National Data Buoy Center (NDBC) owns and maintains a number of wave buoys in the Atlantic. The closest wave buoy to the present study site is NDBC Buoy 44009 (Lat 38.464 N, Long 74.702 W, see Figure 2.5). Currently, this is a 3 m discus buoy deployed at 28 m water depth off Ocean City, recording wind and wave conditions (http://www.ndbc.noaa.gov/station_page.php?station=44009). The data from the 44009 buoy is available since 1984; however, directional wave data is only available for the 1996 to 1998 period. The buoy does not currently record wave direction. Figure 2.6 shows the wave rose and Figure 2.7 shows the wave point rose measured by 44009 in 1996-1998 period.

Analysis of the data indicates that between 1996 and 1998, about 27% of the time waves were from the NE quadrant and about 50% of the time from the SE quadrant. Significant wave height was larger than 3 m for 2.7% of the time, 2/3 of which arrived from the NE quadrant. There were 41 events (i.e. 0.16% of the time) with wave heights larger than 6 m, of which 35 were from NE and only 6 from SE quadrants.
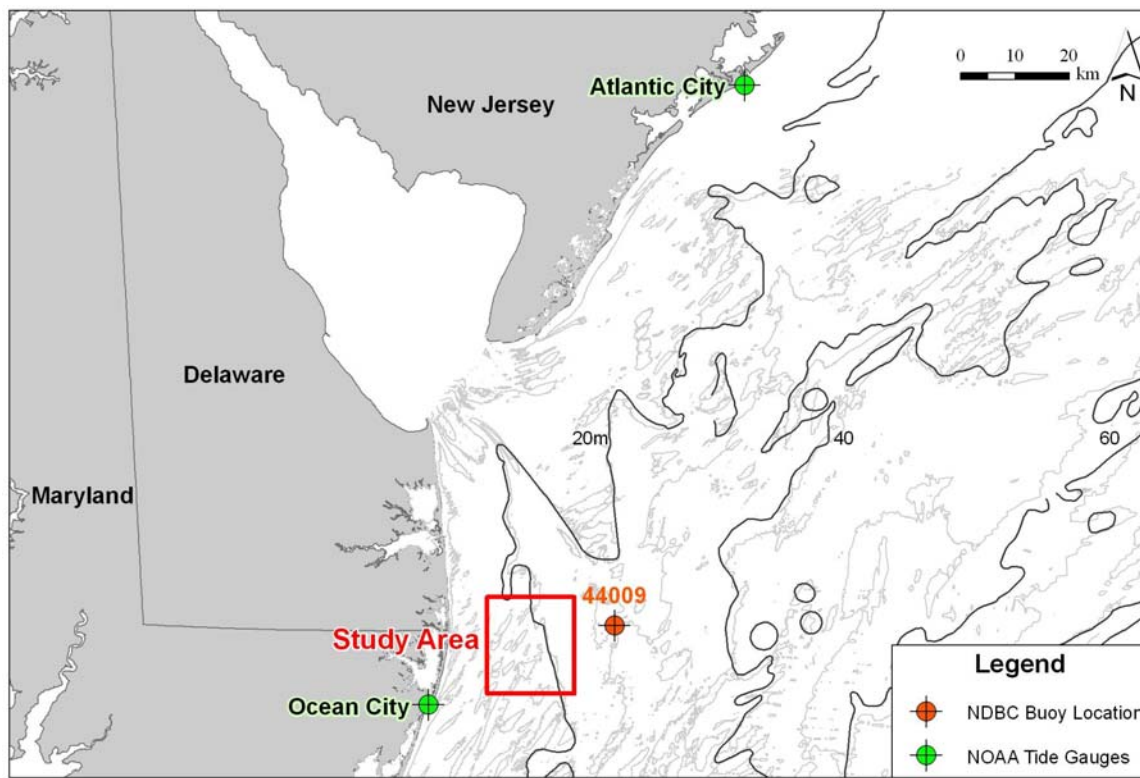
Figure 2.5 Wave and water level data locations.
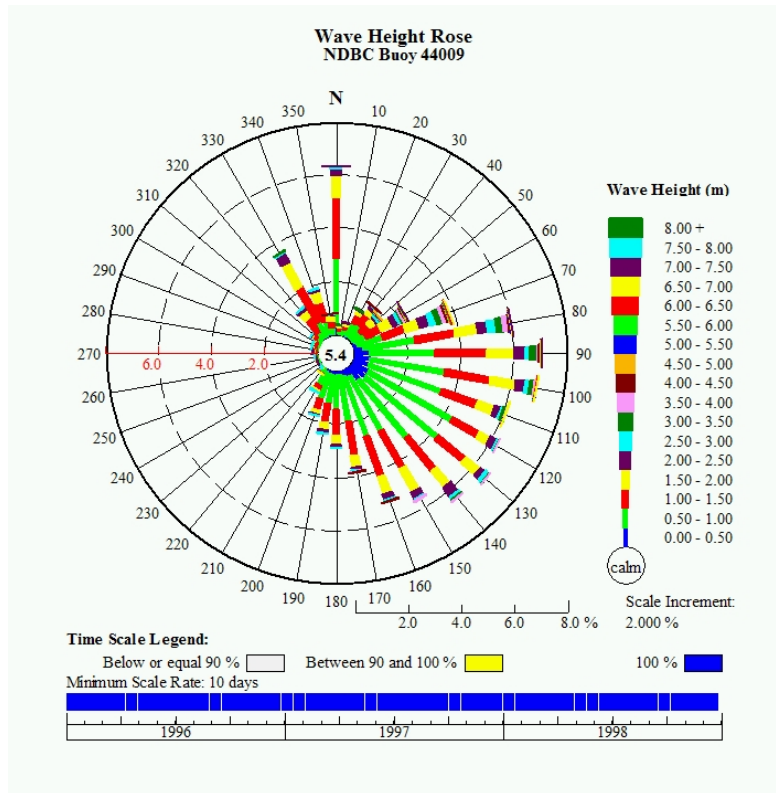
Figure 2.6 44009 wave rose (1996-1998).
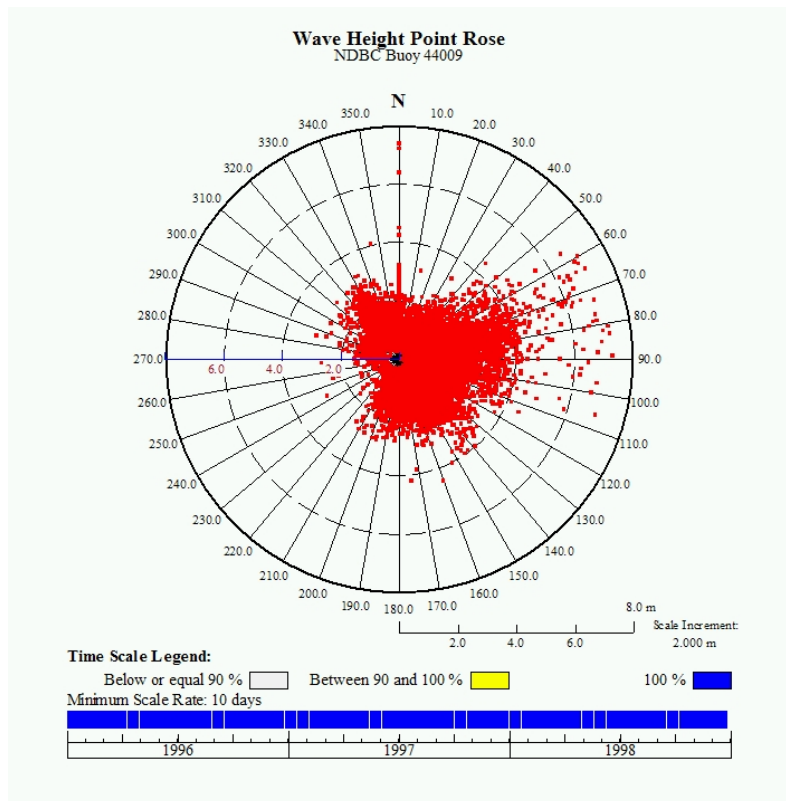
Figure 2.7 44009 wave point rose (1996-1998).

Other available wave data is by the Coastal and Hydraulics Laboratory of USACE who maintains a bottom mounted directional wave gage (MD002) at 9 m water depth off Ocean City, MD (Lat 38.34 N, Long 75.07 W) since 1988. Wave data is collected for 17 minutes at 1 Hz starting at the top of the hour. Data are transmitted to the Engineer Research and Development Center (ERDC) and are posted to the Internet (http://sandbar.wes.army.mil/public_html/pmab2web/htdocs/md002.html).

2.2.3   Water Levels

Water level data in exposed ocean environment are available from NOAA's National Ocean Service (NOS) gages at Atlantic City (Station ID: 8534720 since 1911) and Ocean City (Station ID: 8570283 since 1978). See Figure 2.5 for the locations. Tidal range at Atlantic City is around 1.4 m (4.6 ft). It is about 0.75 m (2.5 ft) at Ocean City. A comparison of data from the two stations with water level measurements of the present study is provided later in this report. The mean sea level trend in the area is 3.99 mm/year rise with a 95% confidence interval of +/- 0.18 mm/yr based on monthly mean sea level data from 1911 to 2006 at Atlantic City. This is equivalent to a change of about 40 cm (1.31 feet) in 100 years.

2.2.4   Currents

The study area experiences severe tropical and extratropical storms during the summer and early autumn. These seasonal storms often track along a corridor running parallel to the coast between the shelf break and several tens of kilometers inland. In late autumn and winter months severe northeasters are formed through rapid cyclogenesis associated with the Gulf Stream off Cape Hatteras. These storms are believed to play a disproportionately large role in the transport of particulate material on the continental shelf (Glenn et al. 2008, Lentz 2008). Sediment transport processes on continental shelves are often characterized in terms of the turbulent interactions between combined waves and large-scale current systems. High bottom shear stress associated with the thin oscillatory wave boundary layer acts to mobilize and transport the sediment in wave direction, and at the same time, makes the sediment available for transport by the mean currents. The combination is an enhanced sediment transport mechanism, since the turbulence associated with the thicker pure current boundary layer may not be sufficient to initiate sediment motion.

Available data options for defining a "long-term climate" for the large-scale oceanic currents are scarce. The MMS Environmental Studies Program sponsored Princeton University and Old Dominion University to implement the Princeton Ocean Model (~5 km cell, 3 hr step) and hindcast meteorological and oceanographic conditions between 1993 and 2010 for the Mid Atlantic Bight. The data was not available for use in defining a long-term climate for the present study. Our search indicated that the Mid-Atlantic Regional Coastal Ocean Observing System (MARCOOS) is presently the only dataset available to us providing such data. MARCOOS uses an extensive array of HF radar stations to measure surface currents over the Mid Atlantic Bight (MAB) continental shelf. The HF Radar network is capable of providing surface current maps across the shelf from Cape Cod, MA to Cape Hatteras, NC during high sea state conditions associated with coastal storms. Nested within this shelf coverage are high resolution systems in the five sub-regions (Chesapeake Bay, Delaware Bay, NY Harbor, Long Island Sound and

Southern New England Bays and Sounds). The network is currently made up of 29 sites. The system initially started in 2001 and continued to expand since then. The large data footprint over MAB is available since early 2007. The reader is encouraged to visit http://www.marcoos.us/ for further information.

Maritime Safety was the main purpose for development of MARCOOS system. Measured surface current maps by the Mid-Atlantic HF Radar network are used (1) by the Coast Guard to improve their Search And Rescue (SAR) activities and (2) by NOAA HazMat to improve emergency response to hazardous spills. HF Radar information fill the gap between the inshore NOAA PORTS and offshore NDBC buoy stations and allow SAR operations to be optimized. Hourly time series of MARCOOS surface currents for the period between January 2007 and July 31, 2008, was provided to Baird by Dr. Scott Glenn and Dr. Josh Kohut of Coastal Ocean Observation Laboratory of Rutgers University, NJ. Figure 2.8 shows the overall MARCOOS grid locations in MAB. Figure 2.9 presents an example snapshot of MARCOOS surface current data. Figure 2.10 shows MARCOOS grid points close to the present study site.
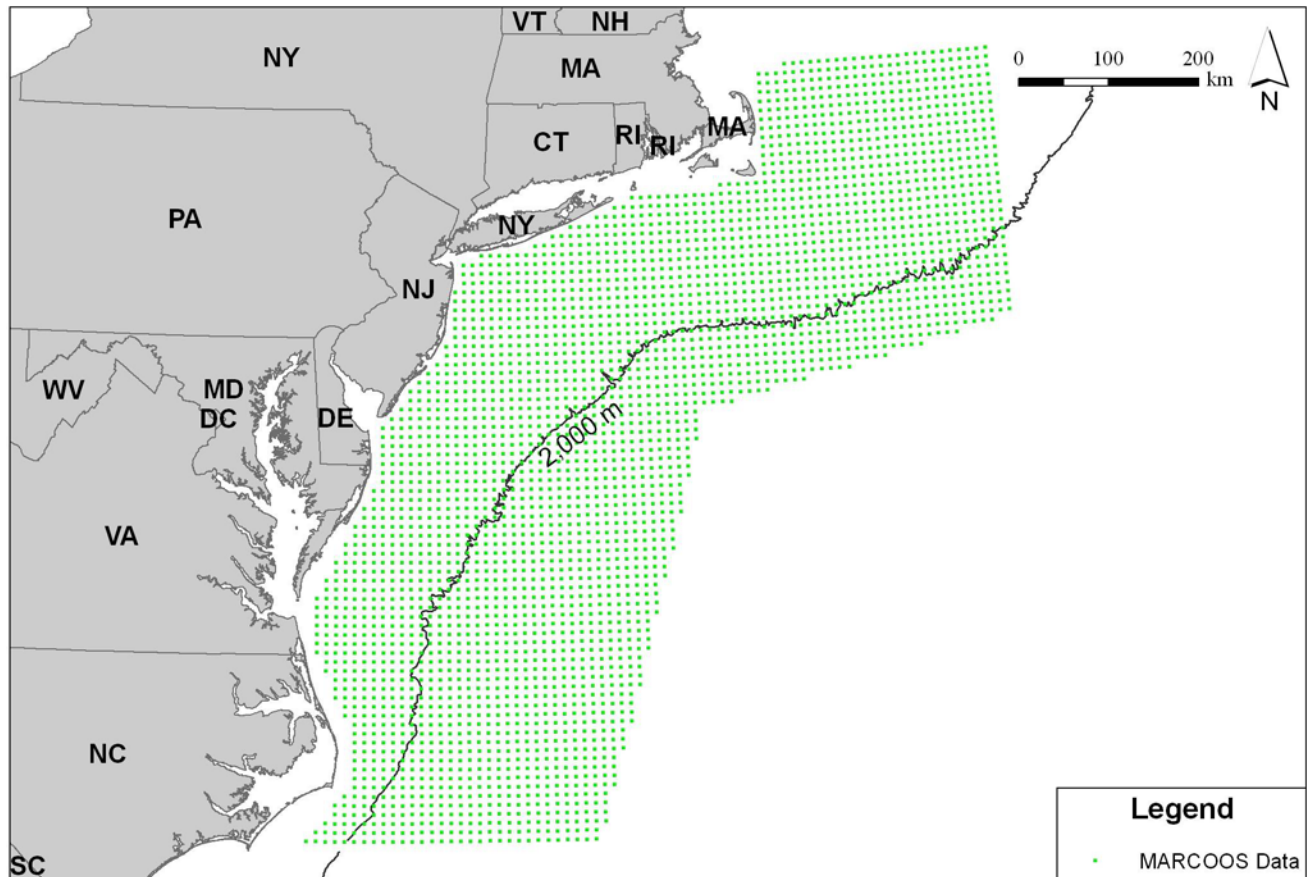
Figure 2.8 MARCOOS surface current measurement grid over MAB.
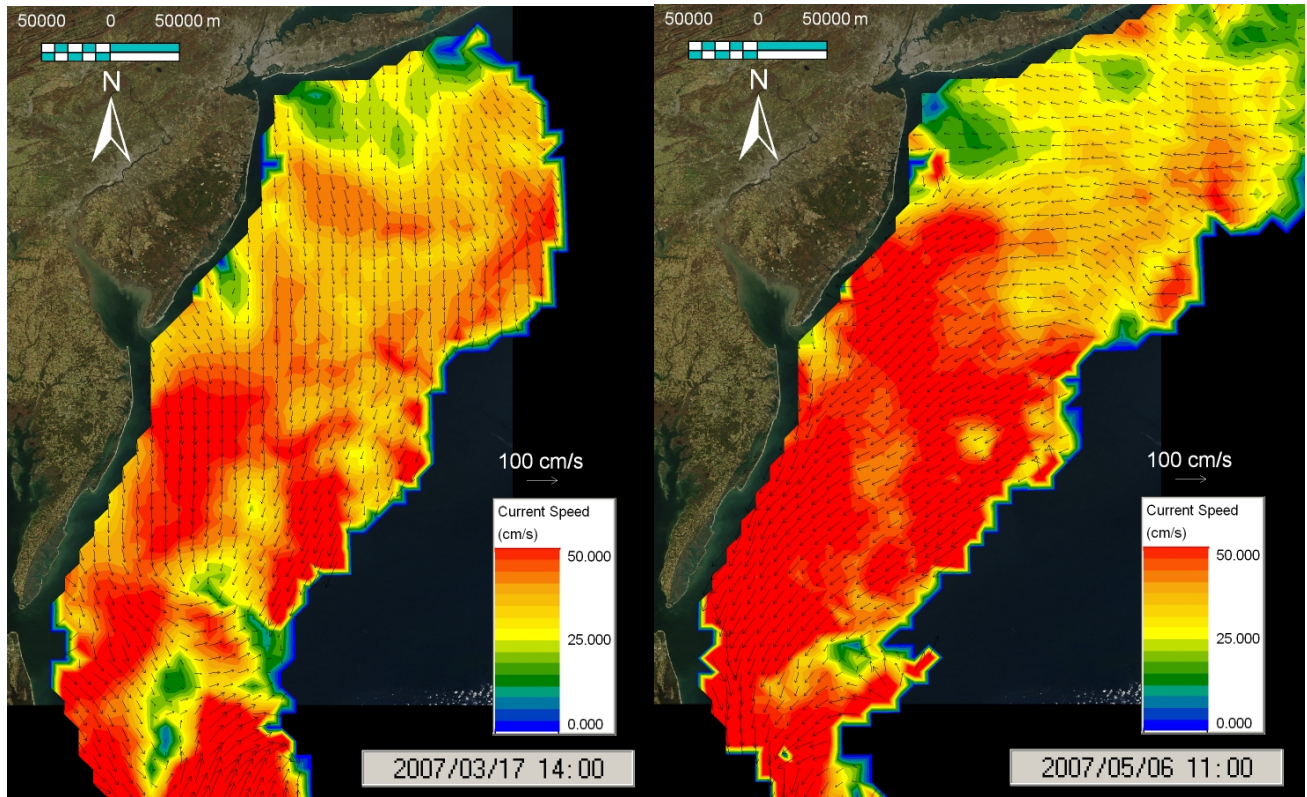
Figure 2.9 Example snapshots of MARCOOS surface current data.
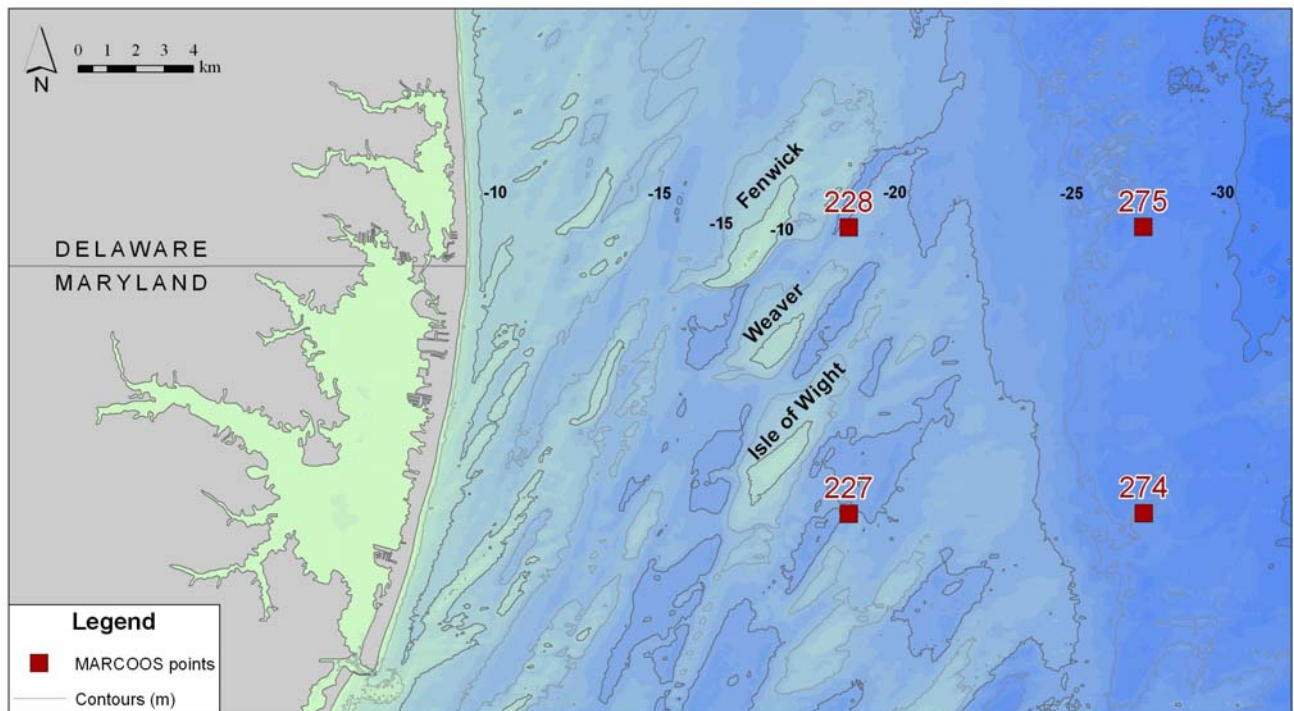
Figure 2.10 MARCOOS grid points in the vicinity of the present study site.

2.2.5   *Seabed Classification*

A Seabed Classification System to classify seabed conditions in the Isle of Wight shoal area from acoustic reflection properties has been used by Maryland Geological Survey (MGS) to classify seabed in Isle of Wight area. The material presented in this section has been provided by Mr. Bob Conkwright of MGS. Seabed classification at Isle of Wight has been completed based on QTC VIEW 4 acoustic data, VIMS seafloor imagery and sampling, as well as MGS vibracores and grab samples. The full VIMS data set is available on DVD through OCS Study MMS 2000-055.

Seabed classes represent distinct bottom types based on acoustic reflectivity characteristics. In the Isle of Wight study, seabed classes were divided into four groups:

Shoal crest: The crests of shoals Fenwick, Weaver, and Isle of Wight typically contain large-scale bedforms such as sand waves and large ripples. The surface is medium sand and displays a low concentration of biogenic surface structures. Scattered shell fragments are the dominant biogenic feature. Because shoal crests are relatively shallow (< 10 m deep) the surface is constantly reworked and bedforms are mostly transient. Figure 2.11 shows a pair of in-situ core and surface photos taken in this environment.

Shoal flank: The shoal flank bottom type is similar to the shoal crest, but typically contains coarser sediment and somewhat greater biogenic productivity. Echinoderms and bivalves are observed on the flanks more often than the crests. Smaller scale bedforms are commonly observed. Figure 2.12 shows the coarser surface sediments encountered on the shoal flanks.

Intershoal: The areas between shoals are predominantly covered by medium to fine sand. Small-scale bedforms are common in the intershoal areas. Biogenic productivity is generally higher than on the shoals (Figure 2.13).

Patch-mat: This bottom type is characterized by fine sediments and relatively high biogenic productivity. Mats and patches of tube worm colonies are common. This bottom type generally occurs in the deeper troughs between shoals where thin deposits of fine to muddy sand overlay muds (Figure 2.14).

A more complete description of these bottom types can be found in Diaz et al (2003). Furthermore, QTC acoustic bottom mapping data were processed by MGS in ESRI ArcGIS to produce a map of bottom types. Figure 2.15 displays the resulting bottom class map for the Isle of Wight Shoal area.

Cross-section

Overhead
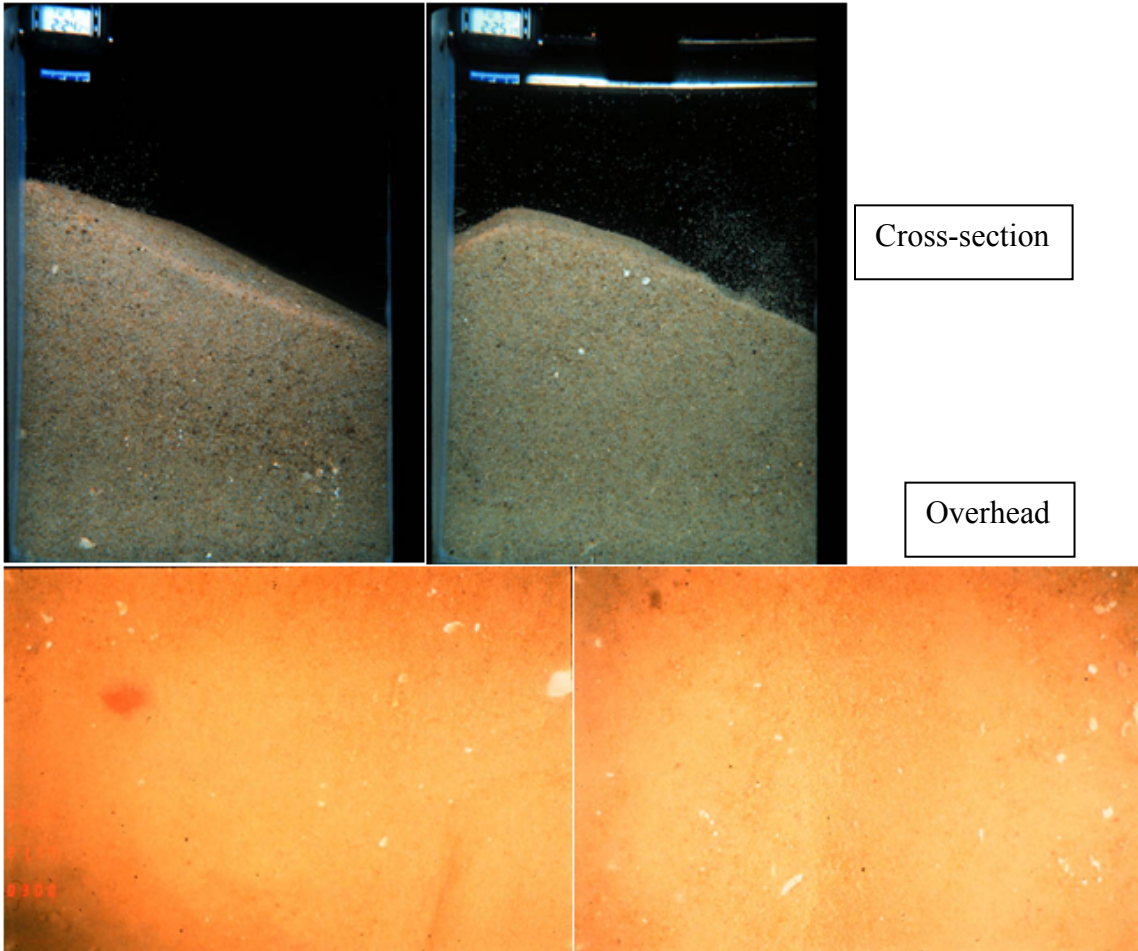
Figure 2.11 VIMS imagery of shoal crest bottom type (Maryland Geological Survey).
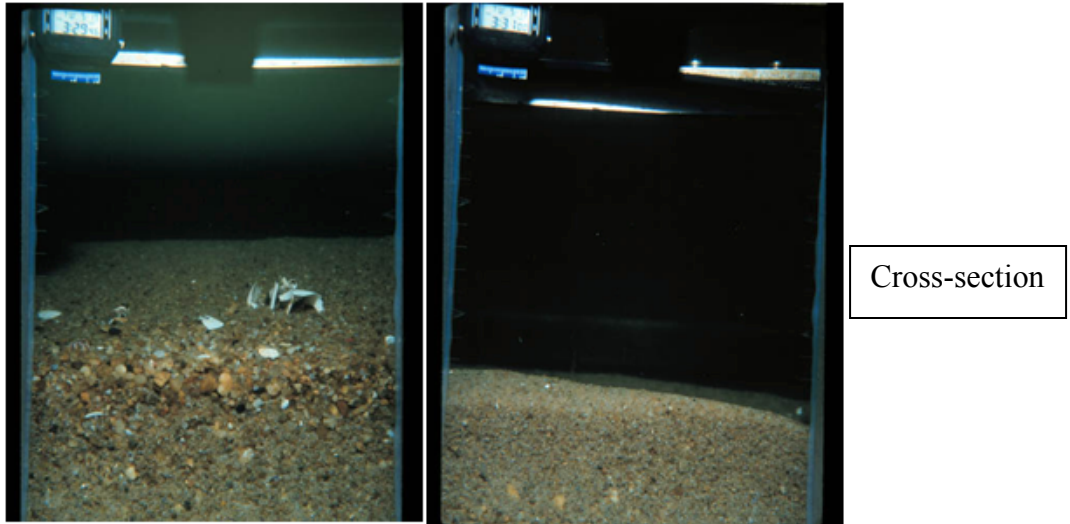
No surface images available

Figure 2.12 VIMS bottom imagery from shoal flank (Maryland Geological Survey).
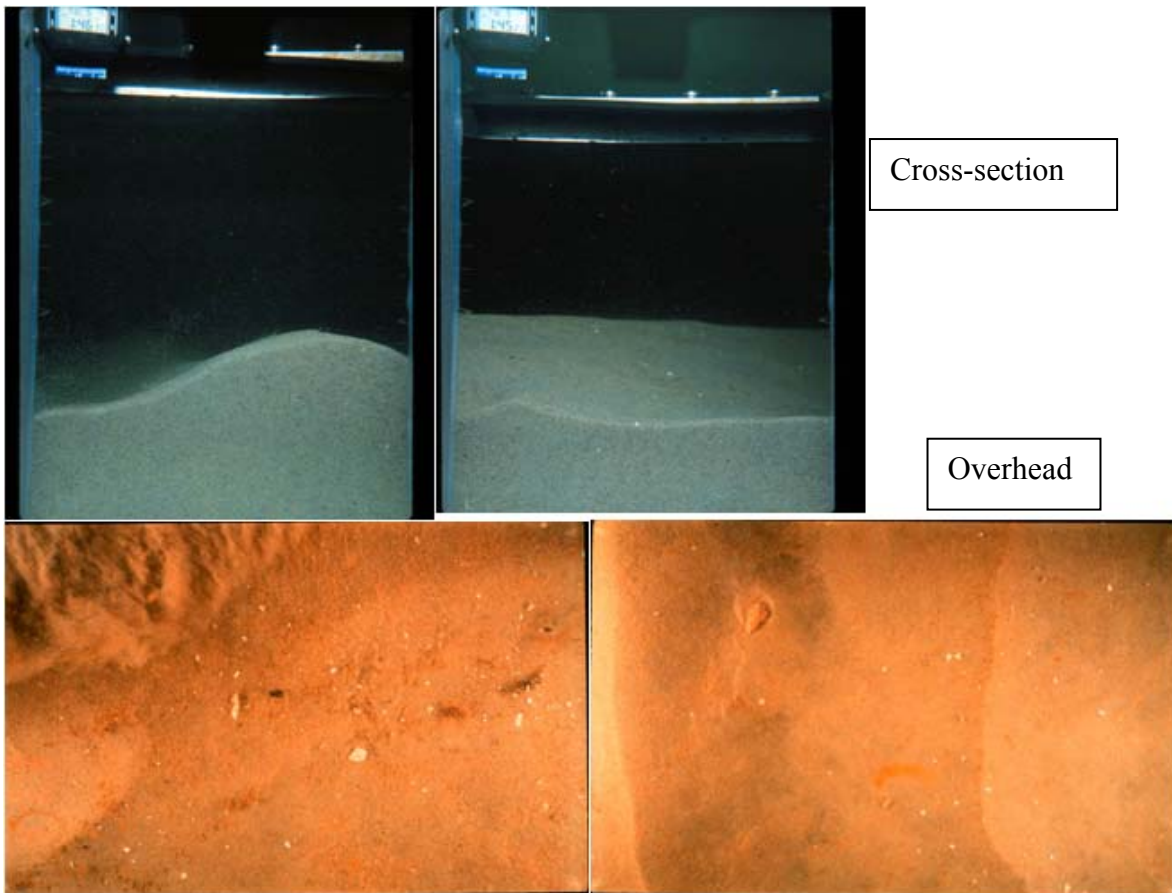
Figure 2.13 Typical intershoal bottom, from VIMS imagery (Maryland Geological Survey).

Cross-section

Overhead
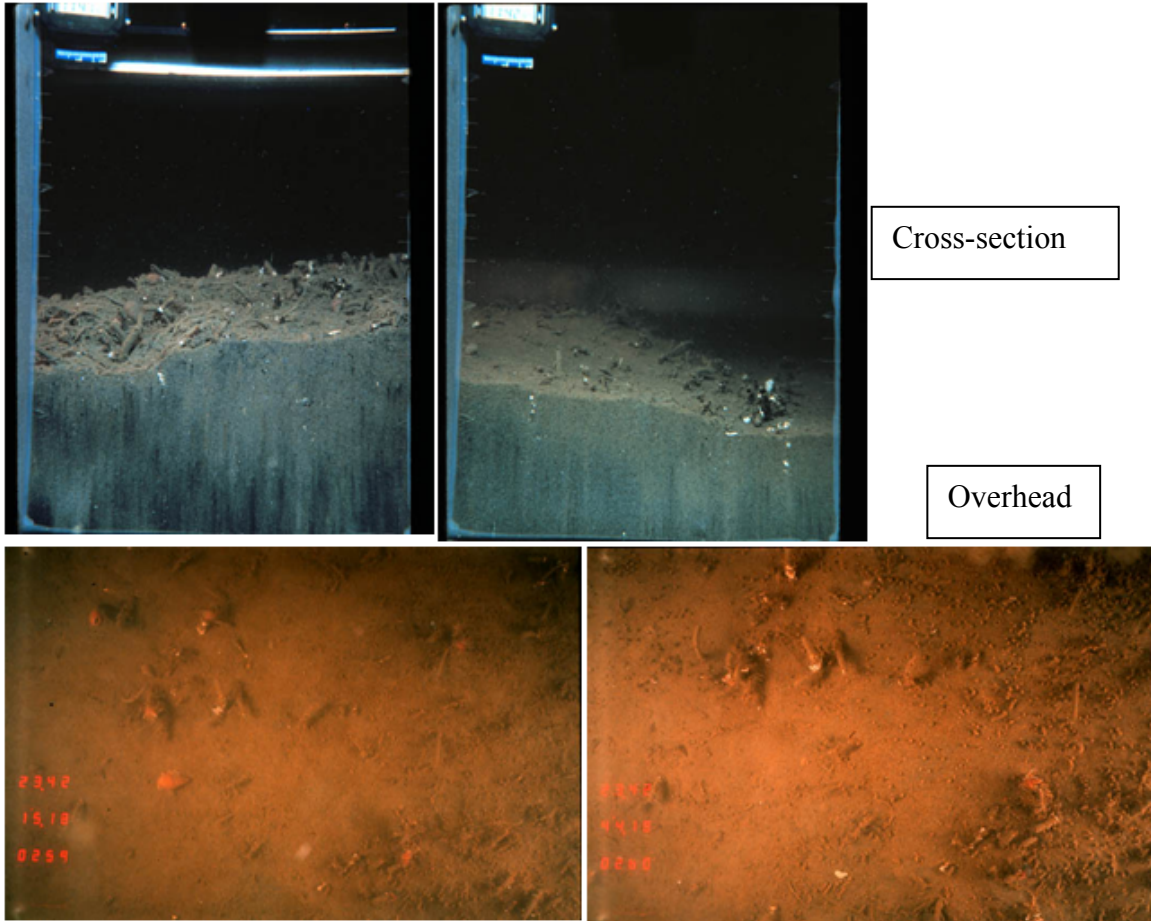
Figure 2.14 Patch-mat bottom type from VIMS imagery (Maryland Geological Survey).

Isle of Wight Surface Types

type

shoal crest
shoal flank
patch-mat
intershoal
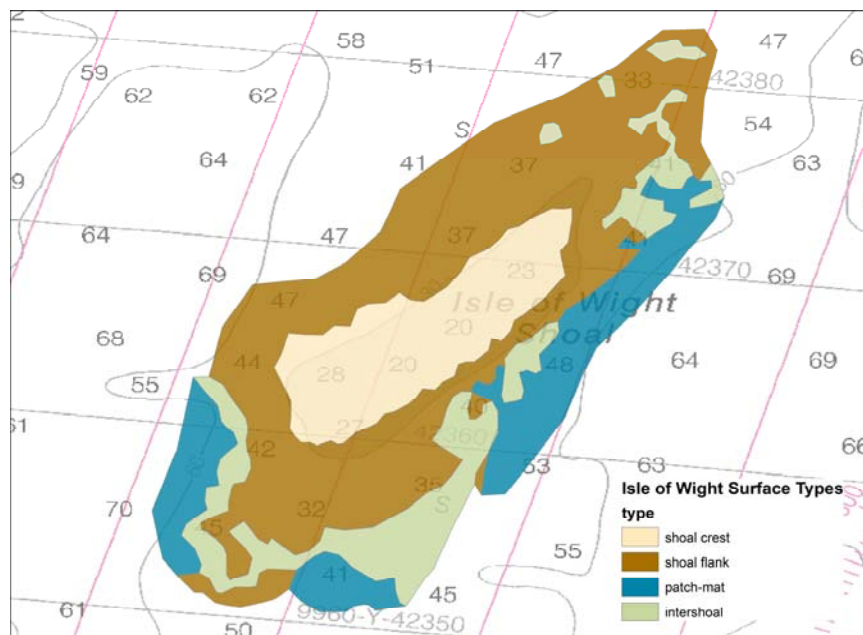
Figure 2.15 Isle of Wight Shoal bottom types (by Maryland Geological Survey).

3.0   METHODOLOGY

The following methodology was employed:

- Literature survey and review of available data

- Selection of a representative shoal for detail study

- Field Measurements

- Evaluation of the effect of the contributing factors (waves, tides, currents)

- Morphometric analysis of shoal parameters

- Conceptual shoal evolution model

- Numerical modeling of shoal morphology change

- Numerical modeling and evaluation of various dredging scenarios

- Development of dredging guidelines

Literature review and available data were discussed in the previous section. Regarding the selection of a representative shoal for detail studies, the U.S. Army Corps of Engineers, Baltimore District has released a Final Supplemental Environmental Impact Statement (USACE, August 2008) for the "Atlantic Coast of Maryland Shoreline Protection Project" to evaluate the impacts of dredging several new offshore shoals to provide sand for the project for the years 2010-2044. It is estimated that between 6,800,000 and 15,000,000 cubic yards of sand would be needed through 2044, depending on future storminess. Offshore borrow sources to obtain up to 15,000,000 cubic yards of sand were thus identified. Three offshore shoals located in Federal waters were recommended: Weaver Shoal, Isle of Wight Shoal, and Shoal "A" (see Figure 2.1). Sub-areas on each shoal were delineated based on suitability of sand for beach nourishment purposes. Sand at Shoal "B," also known as Bass Grounds or First Lump, was also found suitable, however that shoal is currently an important fishing ground. The U.S. Fish and Wildlife Service and National Marine Fisheries Service recommended that Shoal "B" not be utilized at this time.

For selection of detail study site/shoal, several shoals recommended in USACE 2008 were considered.   The idea was to select a shoal which has morphodynamics that are representative of the wave-dominated settings of the area. For this purpose, the shoal needed to be shallow enough to be morphologically dynamic and have an overall NE-SW orientation to promote wave focusing under predominant storm events of the site. Other criteria were dredging priority and

historic bathymetry data availability. Table 3.1 provides the final summary of criteria used to arrive at the shoal best suited for instrumentation and numerical modeling for the present study (note: GGB is Great Gull Bank). Migration rates provided in this table were determined through comparison of the location of the shoal footprint (-30 ft m contour) in NOAA Raster Navigational Charts with the same contour from most recent surveys. The Isle of Wight shoal was selected for this study as it had the most favorable rating and was preferred to Weaver Shoal owing to its shallower crest depth.

Table 3.1 – Criteria for Shoal Selection for Detailed Investigation.

	Migration Rate m/year	Crossing Waves	Dredging Priority	Bathy Data Availability	Crest Height (m)	Dredged Before
Fenwick	3 ~ 4 m/yr	○	✖	1978	5.5	✖
Isle of Wight	4 ~ 5 m/yr	○	○	1929, 1978, 2002	6.5	✖
Weaver	4 ~ 5 m/yr	○	○	1929, 1978, 2002	8.5	✖
GGB	5 ~ 6 m/yr	○	✖	1880, 1978, 1999, 2003, 2002	6.0	○
Shoal A	4 ~ 5 m/yr	Δ	○	1978, 2002	11	✖
Borrow Area 2	7.5 ~ 9 m/yr	✖	?	1978, 1986, 1988, 1991, 2004	9.5	○

○ Positive   Δ Possible   ✖ Negative

Following selection of Isle of Wight shoal as detail study site, a field measurement program was prepared and executed to investigate contributions from various hydrodynamic forces to evolution of this shoal. A morphometric analysis of shoal parameters was also completed to determine most important shoal parameters contributing to shoal geomorphic integrity. A morphology change model was then setup and calibrated using data collected for Isle of Wight. The model was applied to investigate various dredging scenarios and develop dredging guidelines. These tasks are explained in detail in the following sections.

4.0   FIELD MEASUREMENTS

The purpose of field measurements was to arrive at a better understanding of hydrodynamic forces (waves and currents) in the study area and evaluate their relative contribution to morphodynamics of the shoals. The objective is to define the required input driving forces to the numerical model of shoal morphology evolution. A field measurement program was thus prepared by Baird and executed by Alpine Ocean including two hydrographic surveys, surface sediment sampling and analysis, and deployment and retrieval of three ADCPs (Acoustic Doppler Current Profilers) to measure waves and currents.

4.1   ADCP Measurements

Storm season in the NW Atlantic is generally between January and May. Three ADCPs were deployed from the last week of February to around the end of May 2007, providing almost 3 months of recorded data. Figure 4.1 shows deployment locations. One ADCP was deployed in 25 m depth about 12 km northeast of the Isle of Wight shoal to capture offshore incident waves. This is referred to as Deepwater ADCP hereafter. Two other ADCPs were deployed at 10 m depth on southeast (SE) and northwest (NW) side slopes of the shoal to measure refracting waves focusing towards the shoal crest. They will be referred to as SE and NW ADCP, respectively, hereafter. Figures 4.2 to 4.4 show combined time series of parts of the recorded data by the Deepwater ADCP for the months of March, April and May. The data presented in these figures in order from top to the bottom include water temperature and wave period, wave height and wave direction, water levels and air pressure, wind speed vectors, and measured current velocity vectors by the ADCPs at three levels (near the surface, mid-depth and near the bottom). Air pressure and wind speed data are from NDBC Buoy 44009.

Severe storms were recorded on March 2, March 17, April 16, May 7 and May 18 during the three-month deployment. The storms on March 17, May 7 and May 18 were nor'easters. Measured current velocities indicate the presence of both tidal and storm-driven currents. Different storm events illustrate a temporal variability in system response. For example, the event on April 16 (Figure 4.3) involves a changing wind direction, compared to the events on March 17 (Figure 4.2) and May 18 (Figure 4.4) where winds blew mostly from northeast. Examination of wave directions indicates that the latter two events are nor'easters while the former event (April 16) is a southeasterly storm.   Combined time series plots for NW and SE ADCPs are presented in Appendix A. Detailed analysis of the measured data is presented in sections 5.1 and 5.2.
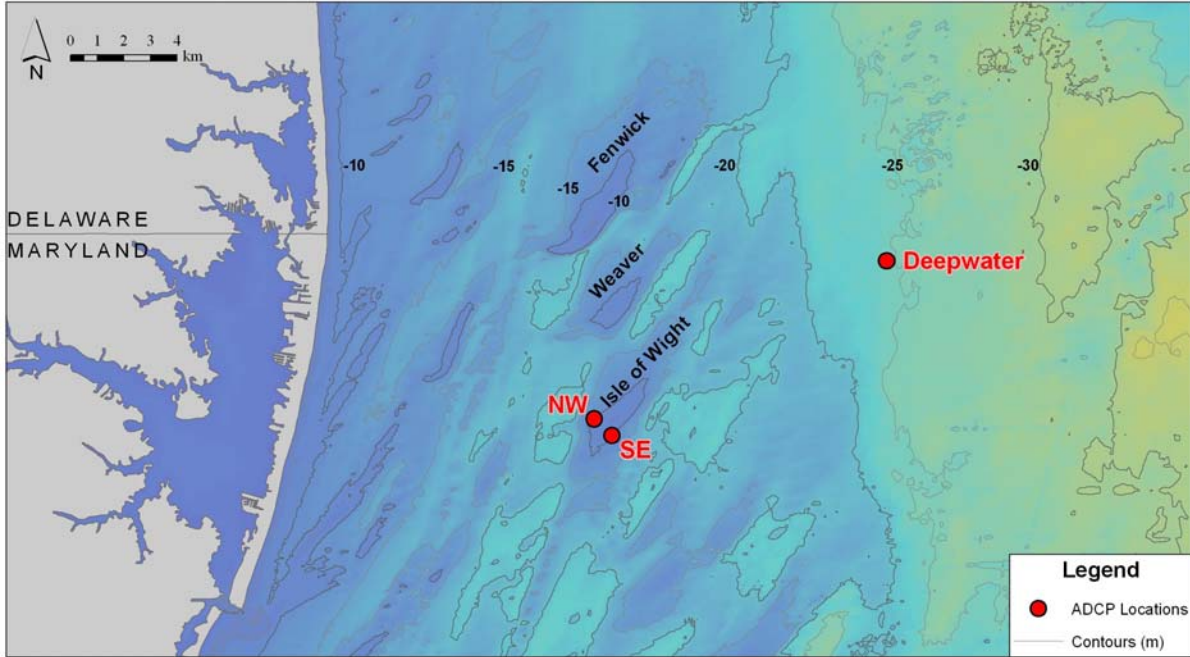
Figure 4.1 Instrument deployment locations.
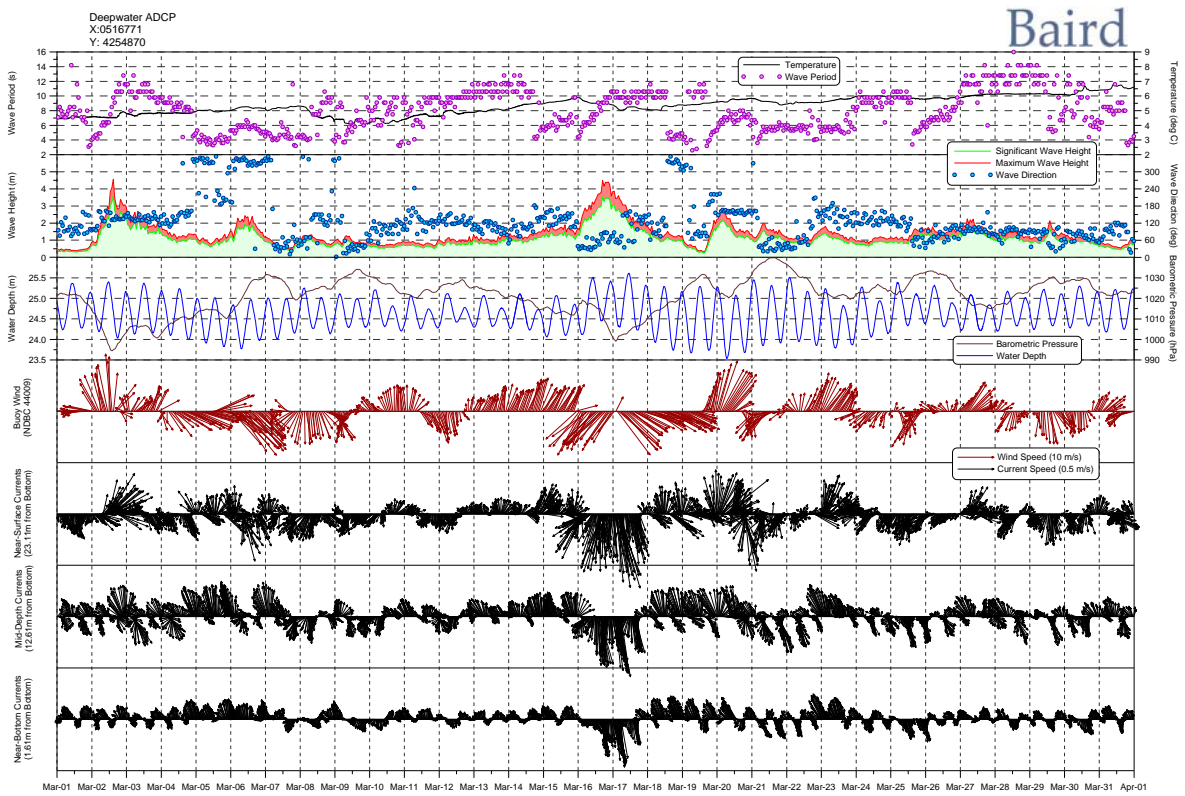
Figure 4.2 Waves and currents measured by the Deepwater ADCP during March 2007.
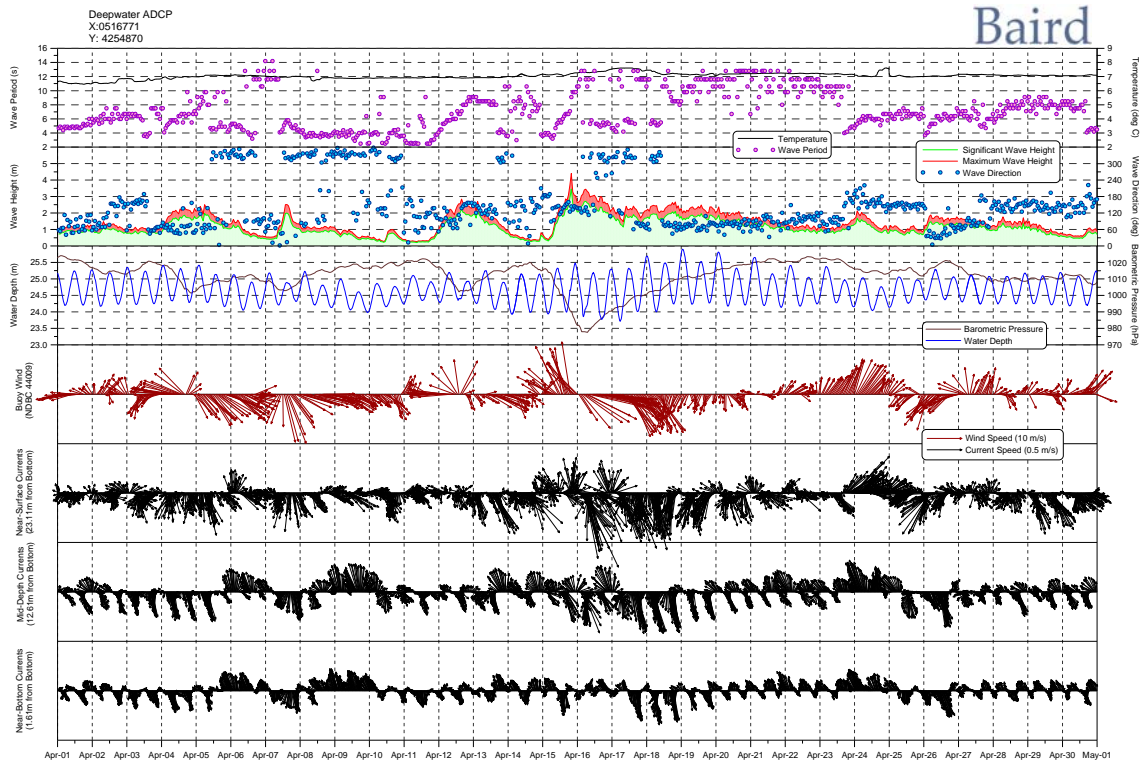
Figure 4.3 Waves and currents measured by the Deepwater ADCP during April 2007.
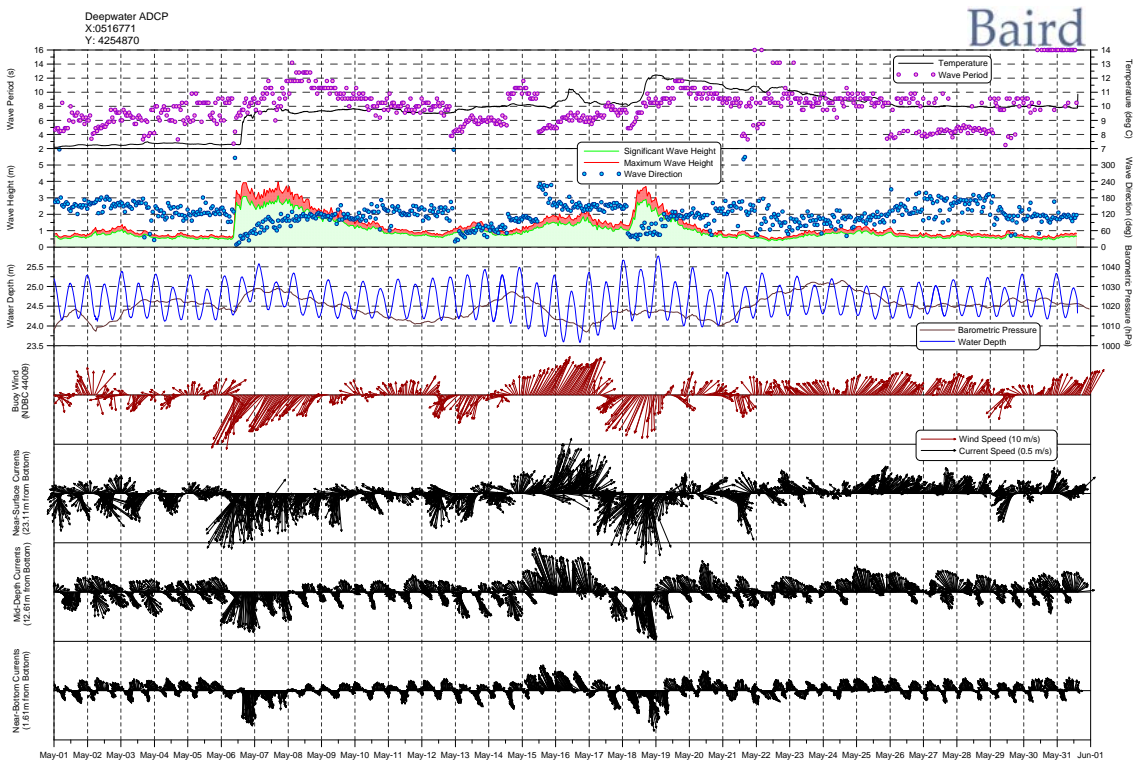
Figure 4.4 Waves and currents measured by the Deepwater ADCP during May 2007.

4.2 Hydrographic Surveys

Two hydrographic surveys of the migrating edge of Isle of Wight were considered and scheduled around the beginning and after completion of the present field work. The idea was to provide a detailed description of morphologic evolution of the shoal feature in response to waves and currents that would be measured between the two surveys. Survey schedule was subjective to wave conditions at the site which proved to be persistently higher than the threshold for boat operation during the winter of 2007.

The first hydrographic survey was completed in three missions in April 2007 based on available weather windows. For this survey, water levels were measured by the ADCPs. Upon reviewing the results, Baird recommended Alpine Ocean to complete the second hydrographic survey in one mission under continuous tidal and water level conditions. This required a 3 successive day window of calm wave conditions for survey operations and resulted in a considerable delay in completion of this task. Alpine Ocean was finally able to conduct the second hydrographic survey during the second week of January 2008, again in three missions (January 8, 10 and 12, 2008, based on available weather windows). A tide gage was simultaneously deployed to record water levels during the survey, however the gage was found to have malfunctioned on retrieval. Water level information from Atlantic City and Ocean City gages was used to process the second survey data (see Section 5). A single beam echosounder was used and survey line spacing was 50 m for both surveys. Figures 4.5 and 4.6 show survey lines of the first and second surveys, respectively.
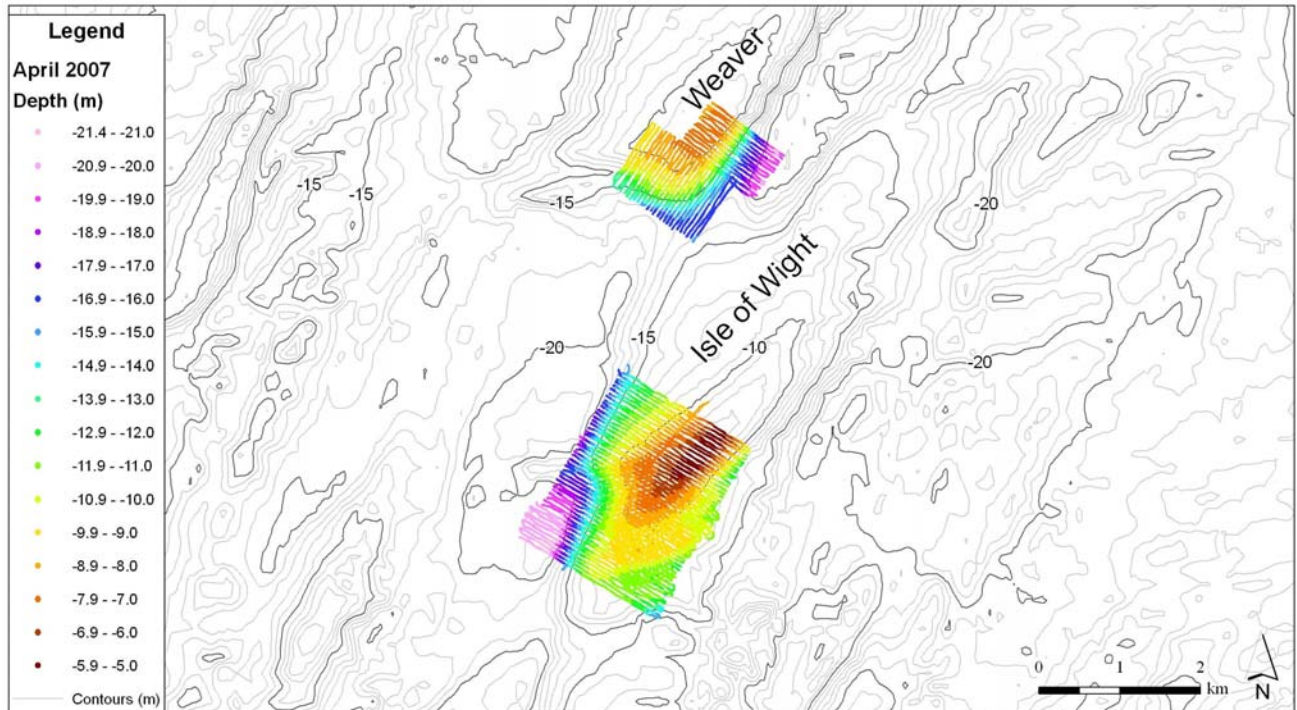
Figure 4.5 First hydrographic survey data (April 2007).
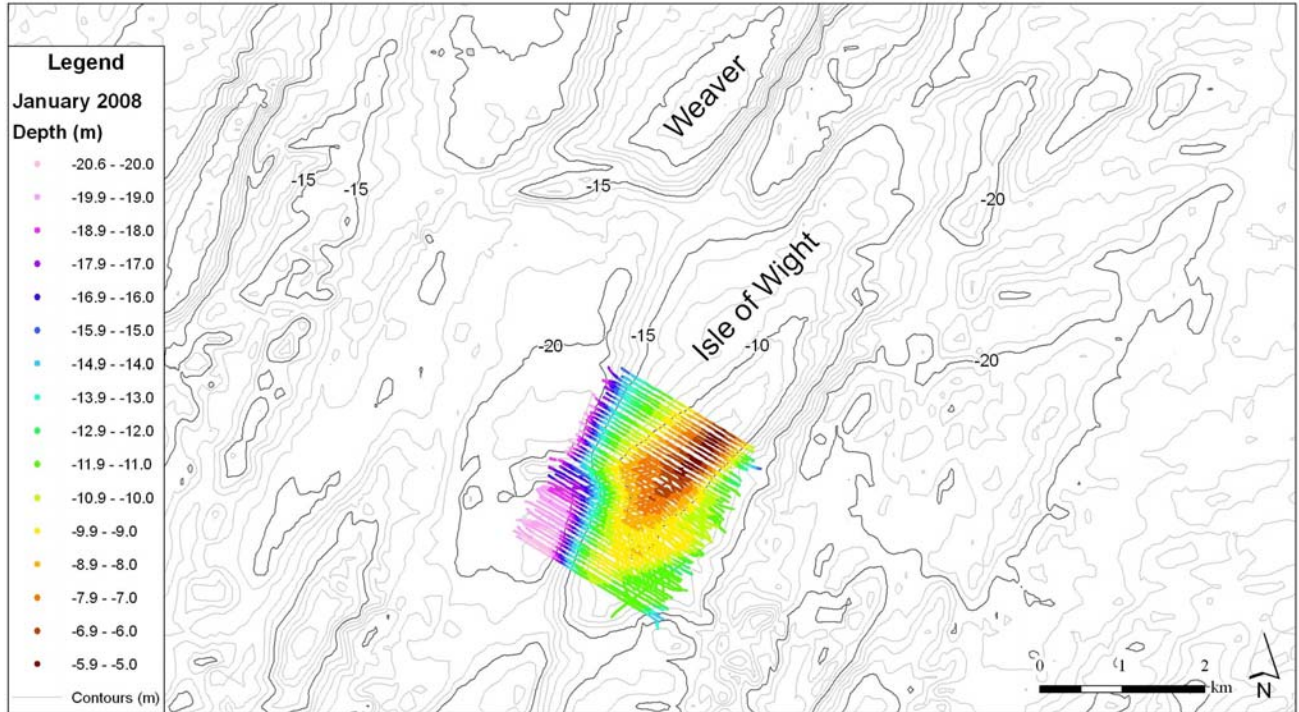
Figure 4.6 Second hydrographic survey data (January 2008).

The vertical resolution of the echosounder was 1 cm. In other words the reading from the echosounder was in 1 cm increments. The Horizontal resolution is a factor of the angle of transmission of the transducer. The deeper the water depth, the more the beam spreads and the less detail can be resolved. In the present case a transducer which transmits a 9° beam was used. Thus the range of resolution in the survey area was from about 45 cm in 3 of water to 3 m in 21 m of water.

4.3   Sediment Sampling and Grain Size Analysis

A total of 25 surface sediment samples were taken from the Isle of Wight shoal during the period of instrument deployments.   Sieve analysis of the surficial sediment samples was subsequently completed.   Figure 4.7 shows median grain size (D_{50}) and percentage sand content of each sample.   The area is covered with sand.   The grain size is coarser on the NW side of the shoal and finer on the SE side of it.

Figure 4.8 provides the MGS seabed classification (Section 2.2.5) overlaid on the present results. Median grain size in the shoal crest area (as defined by MGS) ranges from 0.4 mm to 1. 2 mm (medium to very coarse sand). This is to some extent different from QTC data which indicates medium sand for the shoal crest area. Over the shoal flank, the present data mostly shows a median grain size of 0.3 mm except on the west flank where D_{50} ranges from 0.7 mm to 1.5 mm (coarse to very coarse sand). Again this is somewhat different from QTC data that finds coarser sand over shoal flanks than over the shoal crest. It is our opinion that grain size distribution on a

morphodynamically active shoal is subject to temporal variability and depends on the type and intensity of hydrodynamic forcing that prevailed prior to sediment sampling. Generally, the movement of graded sands involves various processes (or modes of transport) such as static armoring (where fine sand is winnowed away by waves and/or currents leaving behind a lag of coarse material), dynamic armoring (where coarser grains become mobile as a layer on top of the smooth surface formed by the underlying fine sediment), and sediment sorting (resulting from different behavior of fine and coarse sand under same hydrodynamic conditions). The prevailing mode of transport is a function of intensity and type of driving forces as well as percentage and grain size of fine and coarse sediments in the mixture. Under extreme storm events, however, it is expected that both fine and coarse sediments are mobilized and move together (Dibajnia and Watanabe, 2000).
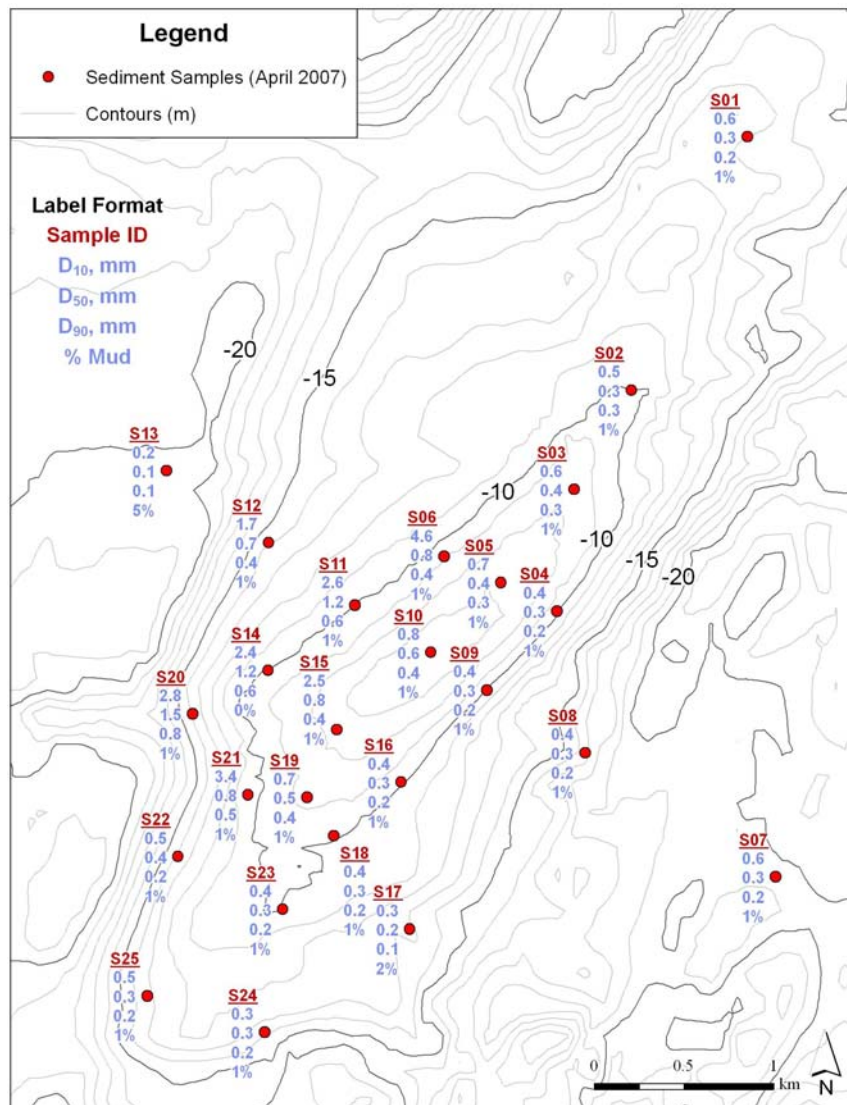
Figure 4.7 Sediment sample locations and sieve analysis results.

28
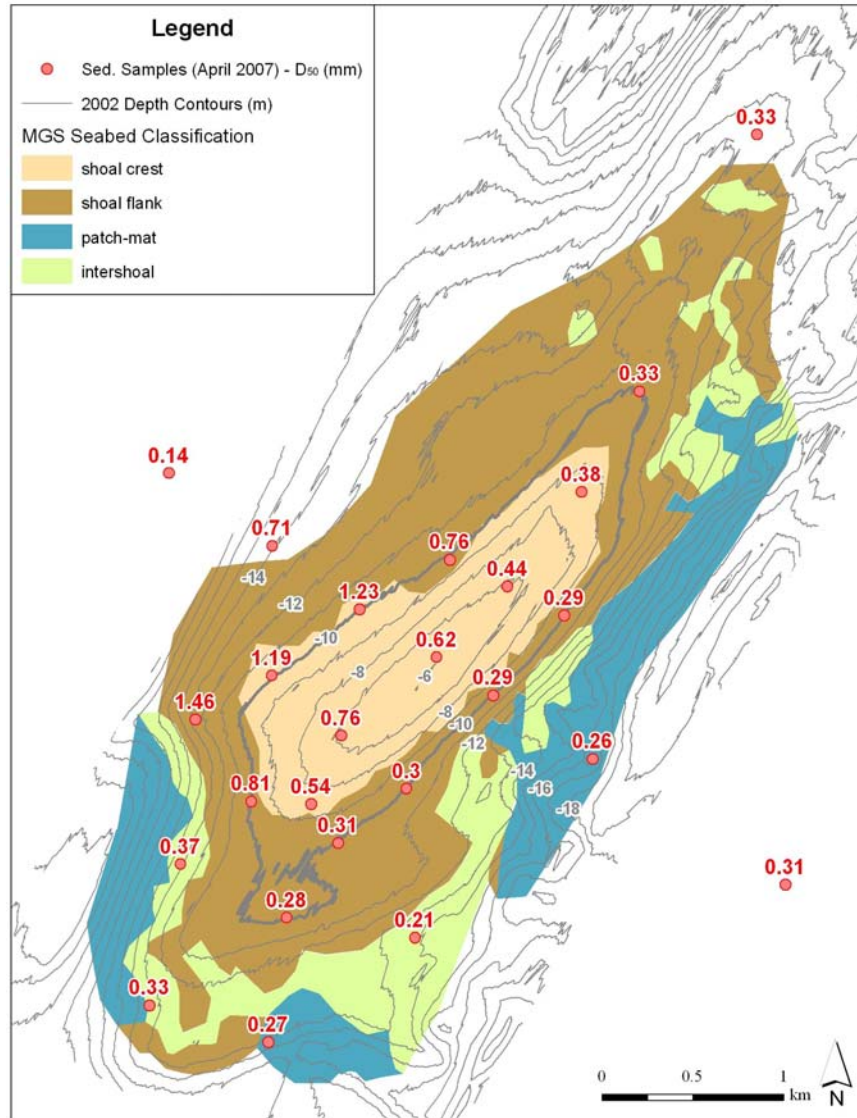
Figure 4.8 Sieve analysis results (D$_{50}$) of the present study on MGS seabed classification.

5.0 DATA ANALYSIS

This section provides an analysis of various measured data described in Section 4.0.

5.1 Waves

Measured wave rose by the Deepwater ADCP is presented in Figure 5.1 and Figure 5.2 provides the corresponding wave height point rose. Analysis of the data indicates that between Feb 28 and May 31, 2007, about 29% of the time waves were from the NE quadrant and about 59% of the time from the SE quadrant. Significant wave height was larger than 2 m for 7% of the time, arriving equally from SE and NE quadrants. There were 16 events with wave heights larger than 3 m (i.e. 0.73% of the time), of which 11 were from NE and 5 from SE quadrants. Maximum recorded significant wave height was 3.6 m.
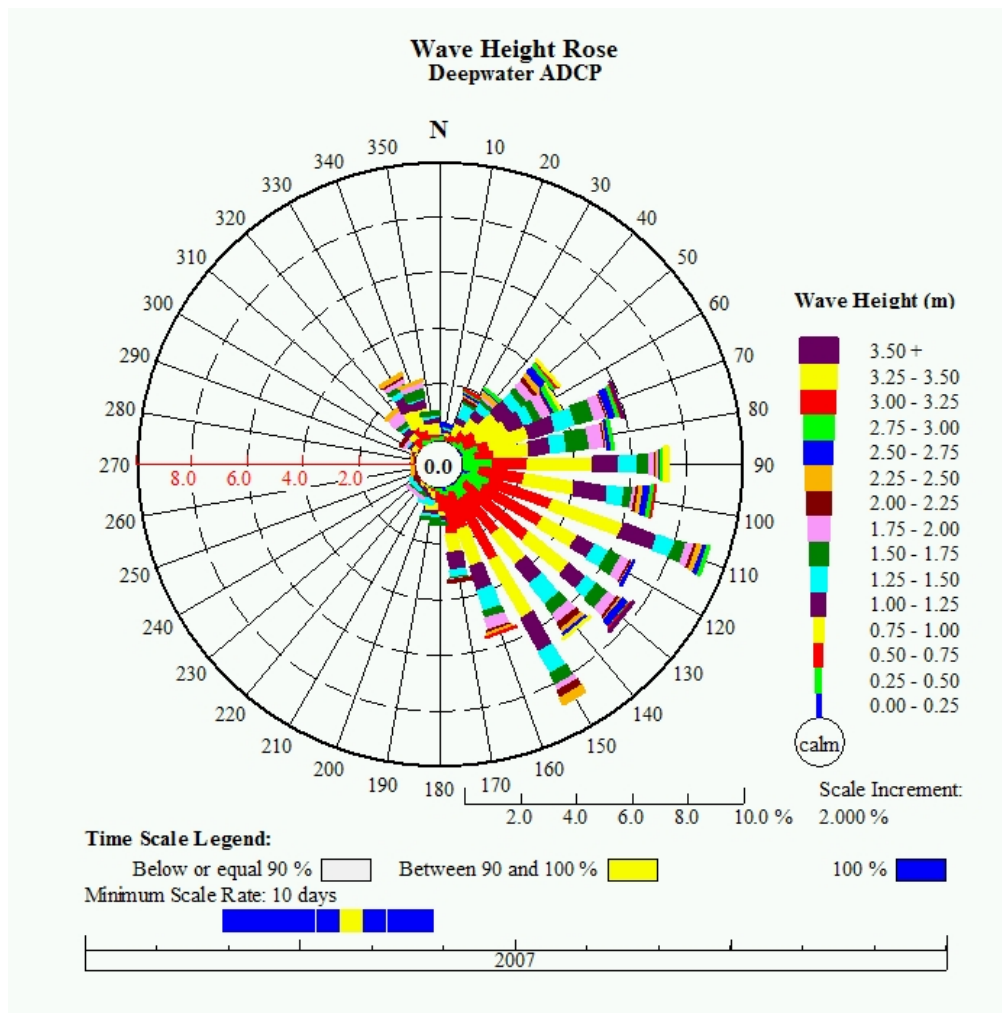
Figure 5.1 Deepwater ADCP wave rose (Feb 28 to May 31, 2007).
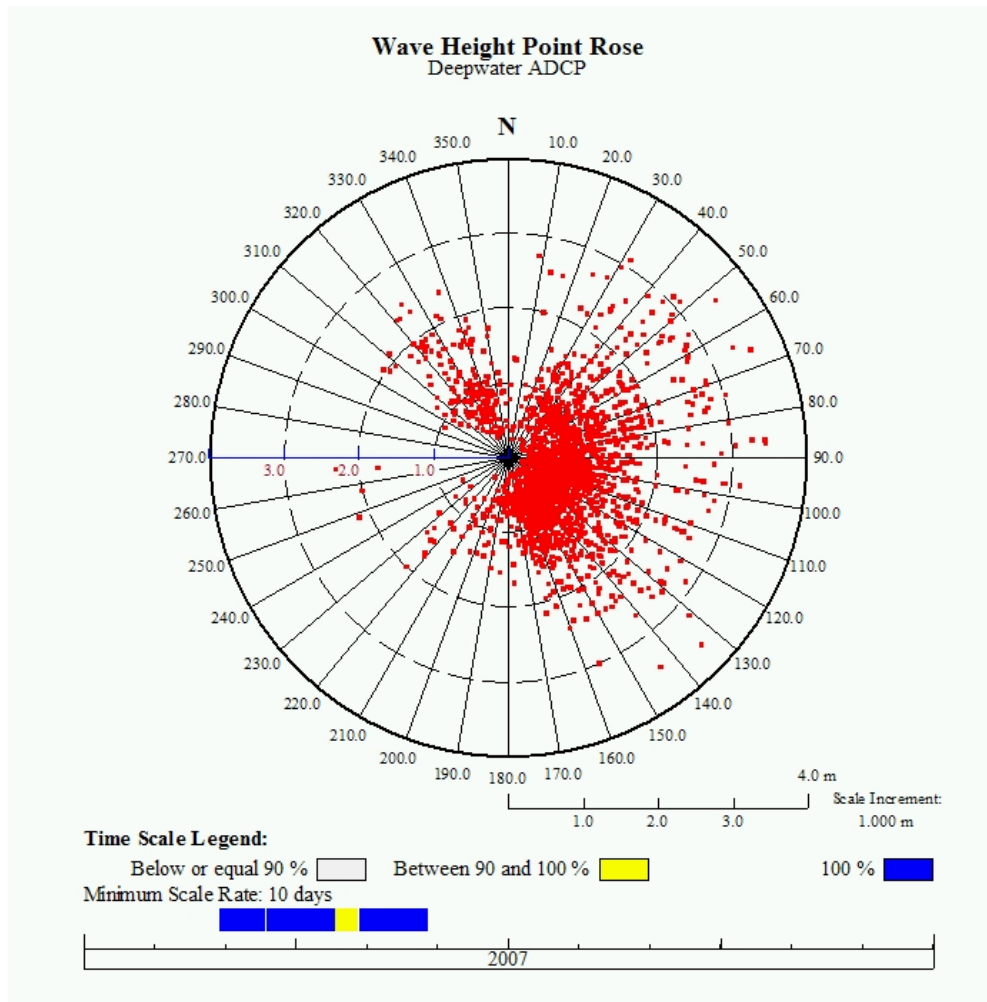
Figure 5.2 Deepwater ADCP wave point rose (Feb 28 to May 31, 2007).

It is noted that compared to NDBC Buoy 44009 data discussed in Section 2.2.2, the present measured wave climate does not include extreme storm events (including nor'easters) with wave heights larger than 4 m. Figure 5.3 shows annual distribution of nor'easter events with significant wave height larger than 3 m since 1991 recorded by NDBC Buoy 44014. This is a directional wave buoy deployed at 48 m depth approximately 200 km south of the present study site. The figure shows number of hours in each year in the 18-year hourly record where the wave height was larger than 3 m and wave direction was from the 0 to 75 degree window. Annual average number of nor'easter hours, as defined in the above, was found to be about 196 hours or 8.2 days per year with a standard deviation of 93 hours (3.9 days). The year 1993 with 360 hours and 1998 with 74 hours had the most and least nor'easter activity, respectively. The year 2007 with 116 hours was one of the years with less than average nor'easter activity.
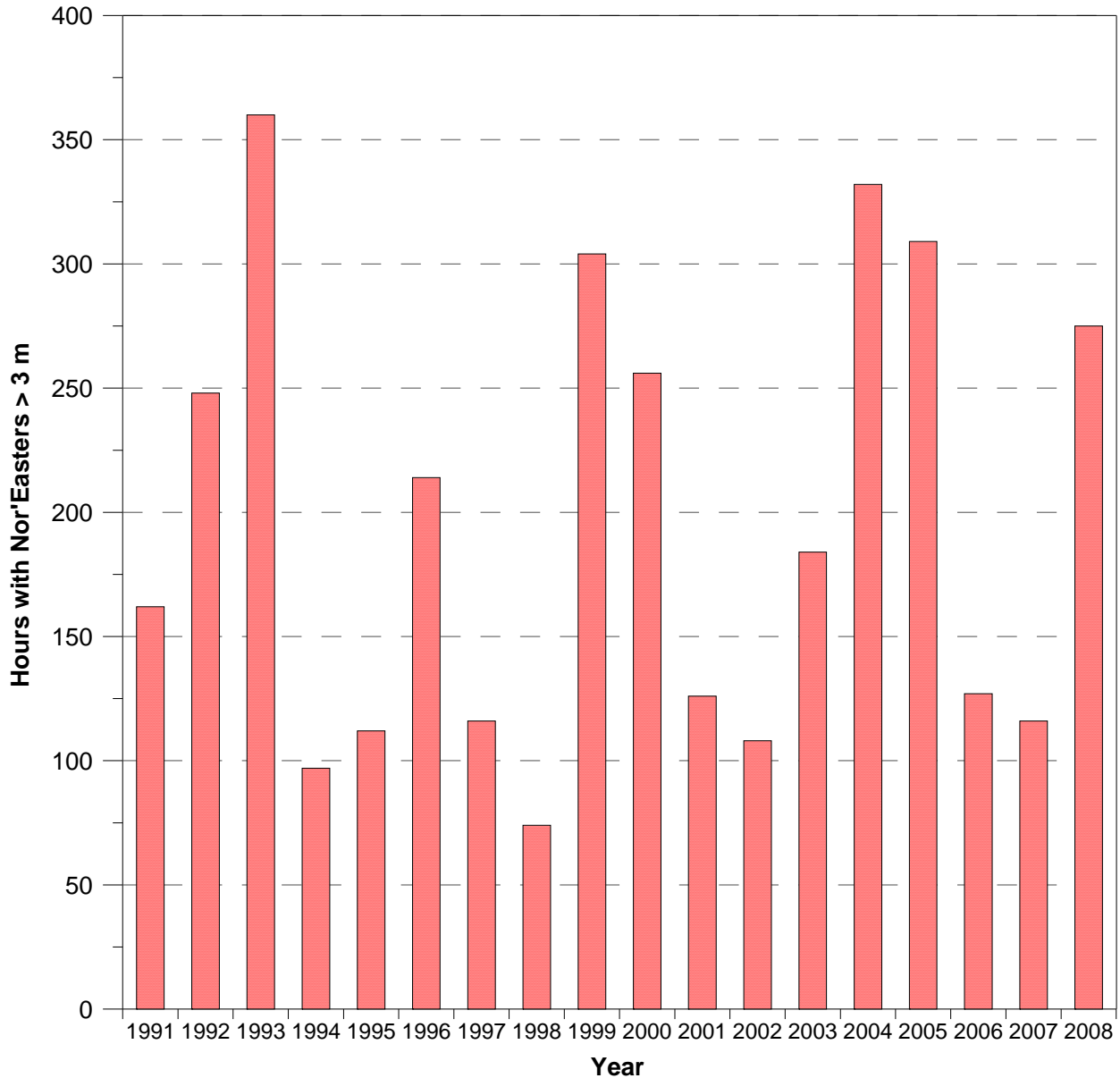
Figure 5.3 Annual distribution of percentage of nor'easters since 1991.

Measured wave rose by SE ADCP is presented in Figure 5.4. Compared to the Deepwater ADCP wave rose (Figure 5.1), waves arrive from a narrower directional window at this location. The SE flank of IOW is nearly in NE-SW direction. Waves from NE quadrant undergo considerable refraction before arriving at this location. Figure 5.5 shows comparison of wave heights measured at the SE and the Deepwater locations. Larger waves, typically characterized by longer periods, are subject to transformation (refraction/shoaling) evidenced by increasing scatter with larger wave height. Wave height at SE location is generally about 0.94 times the wave height at the Deepwater location.
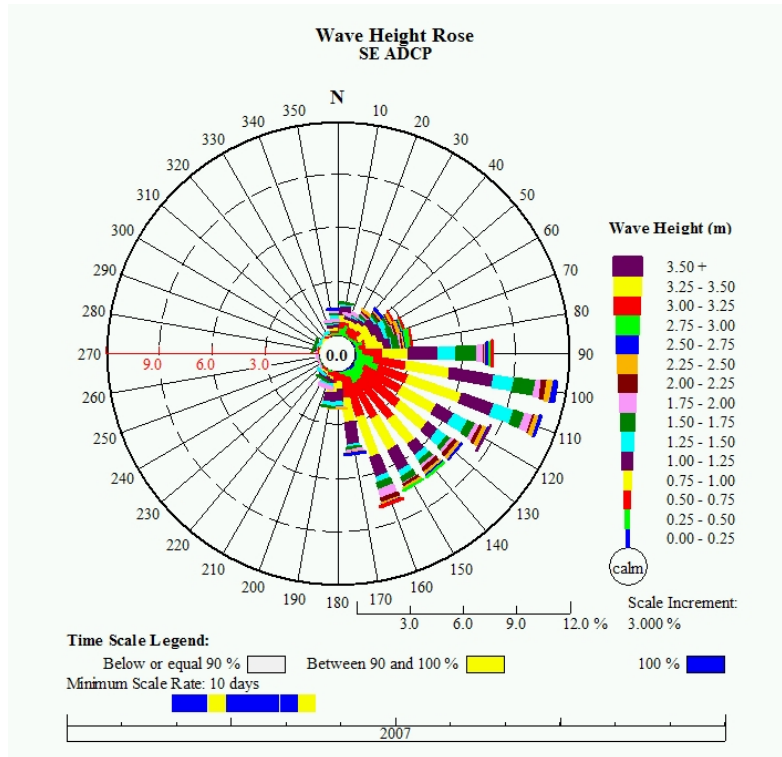
Figure 5.4 SE ADCP wave rose (Feb 28 to May 24, 2007).
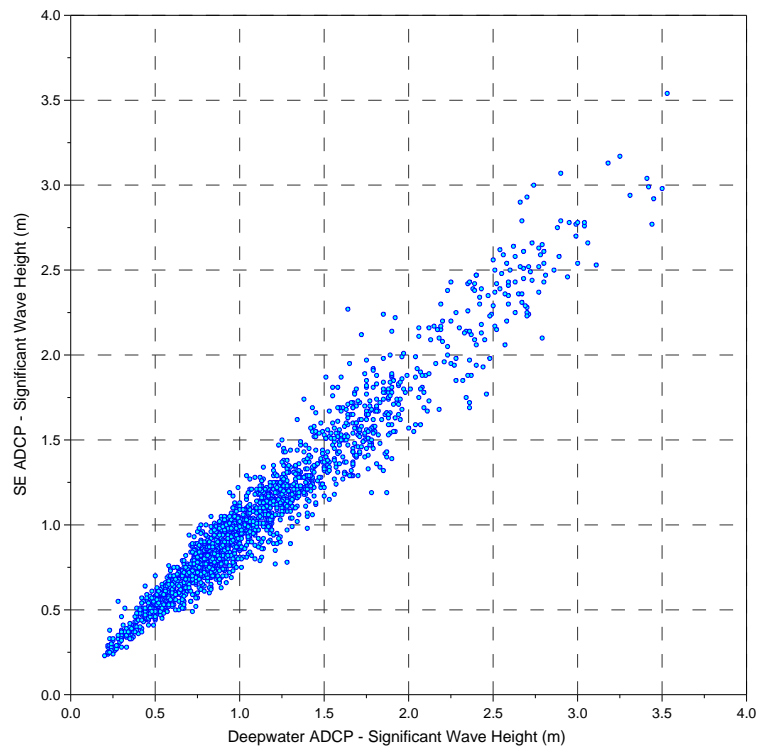
Figure 5.5 SE ADCP wave height vs. Deepwater ADCP wave height.

Similarly, measured wave rose by NW ADCP is presented in Figure 5.6. Compared to the Deepwater ADCP wave rose (Figure 5.1), waves arrive from a wider directional window at this location. The NW flank of IOW has a nearly 53°orientation measured clockwise from the North. Waves from N to NE direction refract towards NW direction, while waves from the SE quadrant undergo a complicated refraction pattern before arriving at this location. Figure 5.7 shows comparison of wave heights measured at the NW and the Deepwater locations. Wave height at NW location is generally as large as the wave height at the Deepwater location.
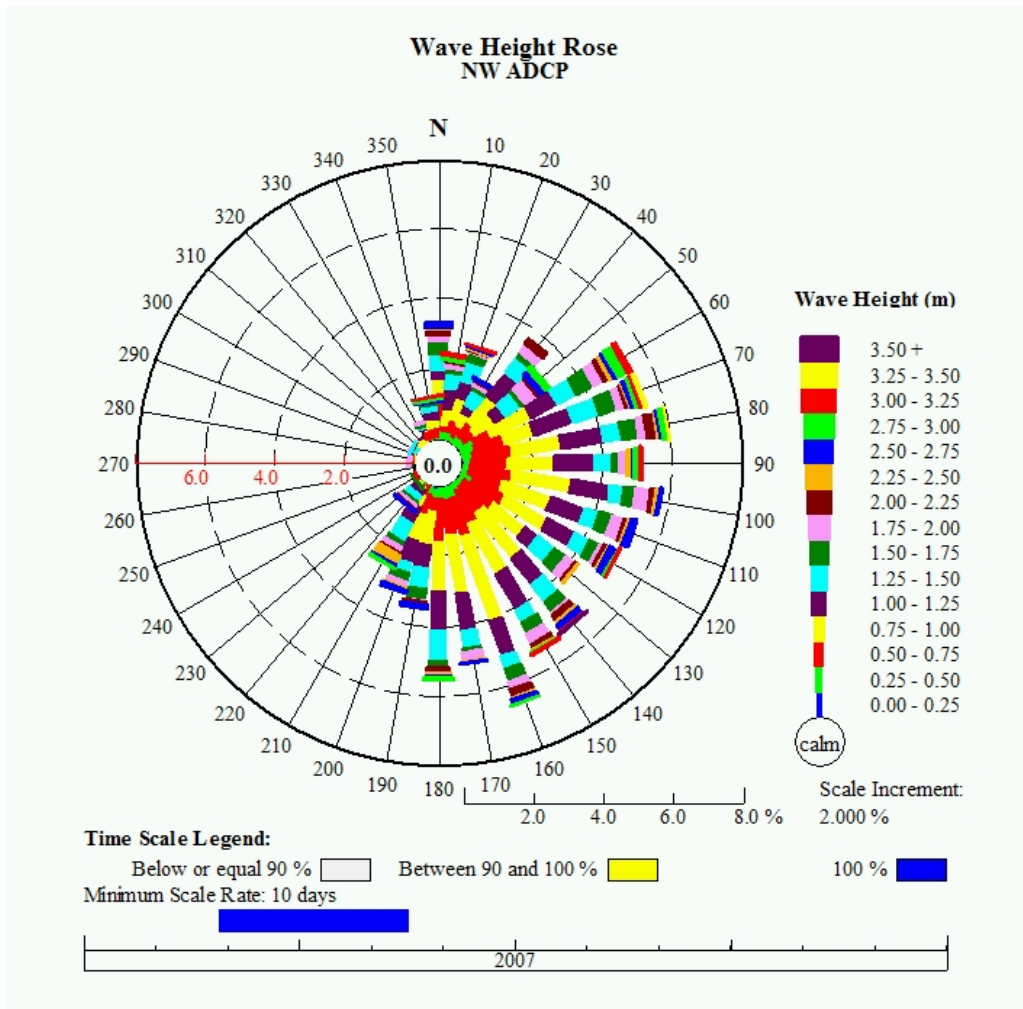
Figure 5.6 NW ADCP wave rose (Feb 28 to May 24, 2007).
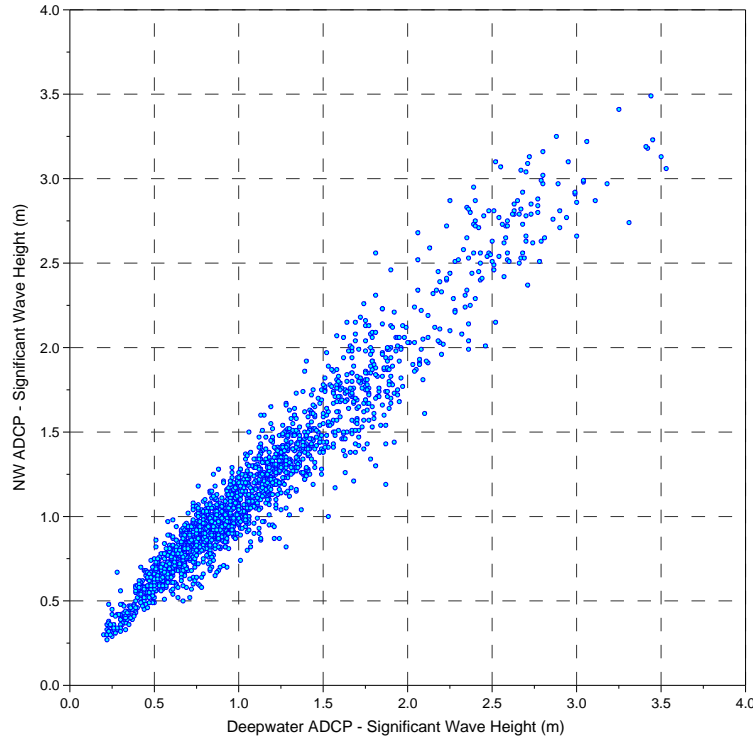
Figure 5.7 NW ADCP wave height vs. Deepwater ADCP wave height.

5.2   Currents

As discussed in Section 4.1, measured current velocities indicate the presence of both tidal and storm-driven currents. The March 17, 2007 event is further investigated as an example here. Figure 4.2 indicates that this was a nor'easter (wave directions from NE) with wave heights exceeding 3 m. Winds were from NE and then NW during the passage of this storm. Atmospheric pressure dropped to 1000 hPa and the storm was accompanied by strong southward currents superseding the background tidal currents.

Time series analysis of the measured north-south component of near-bottom current velocity by the ADCPs was completed in frequency domain for the entire measurement period. First, the tidal analysis module of MIKE ZERO was used to separate the tidal signal from the measured record. Figure 5.8 shows the resulting tidal and residual components together with the original input time series for the period between Mar 13 and Mar 21, 2007 at the SE ADCP as an example. The residual component contains frequencies both higher and lower than the tidal frequencies. Subsequently, FFT analysis with a low-pass filter (cutoff frequency of $1/30$ hr^{-1}) was used to separate storm-driven subtidal components from the residual. Figure 5.9 shows the residual and resulting subtidal components corresponding to the above period. It shows the existence of a southward current reaching a maximum velocity of about 22 cm/s on March 17, 2007. The subtidal velocity magnitude is comparable to that of the tidal component. Similar results were obtained at other ADCP locations.
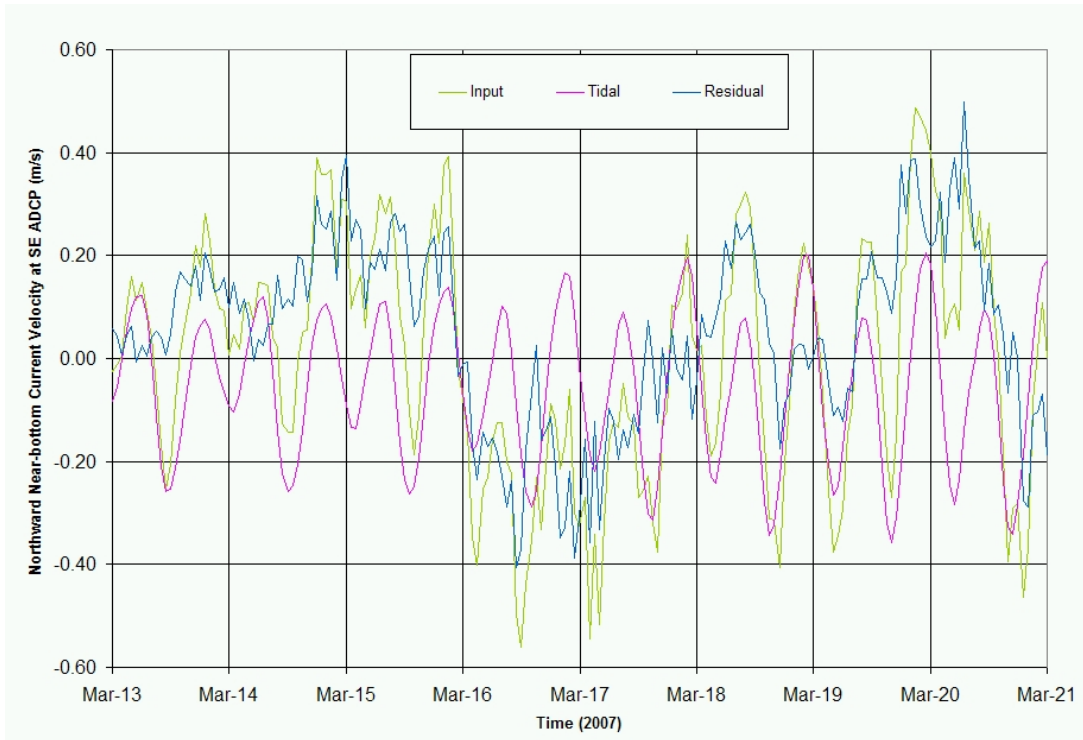
Figure 5.8 Example of tidal and residual components of the measured near-bottom velocity.
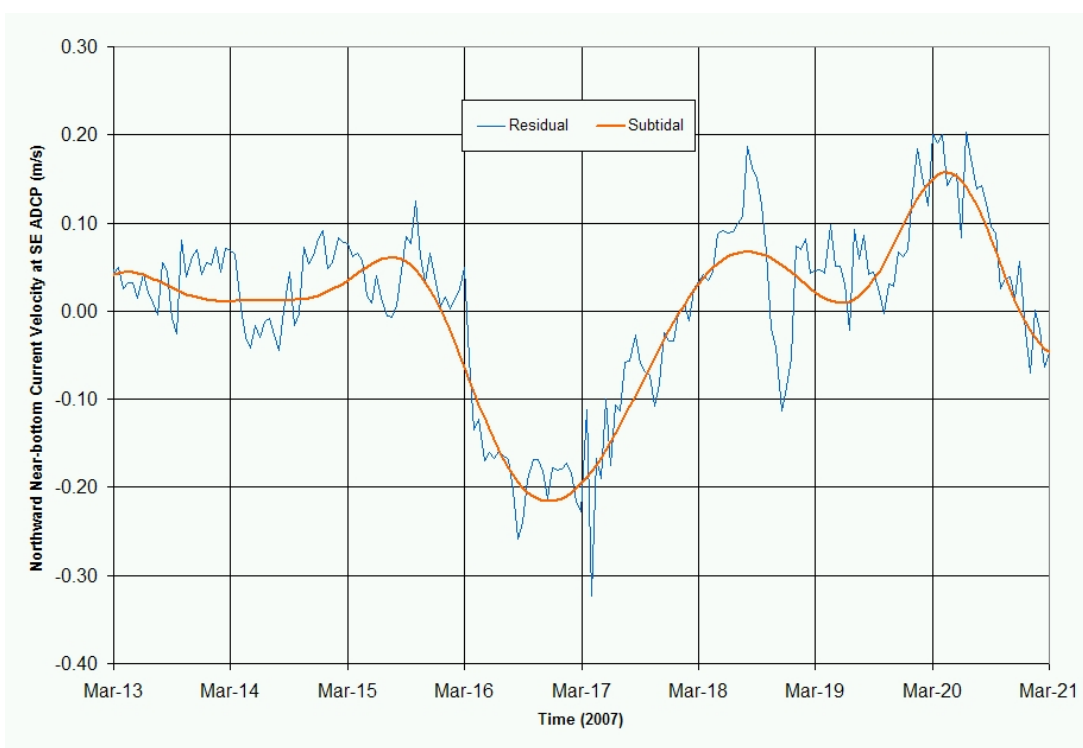
Figure 5.9 Example of subtidal component extracted from the residual near-bottom velocity.

A similar time series analysis was conducted on water surface elevation data. Figure 5.10 shows the extracted subtidal component of water surface elevation at the Deepwater ADCP through the month of March 2007. The corresponding near-bottom tidal and subtidal northward velocity components are also plotted in this figure. It shows that the near-bottom southward current reached a maximum velocity of about 40 cm/s on March 17, 2007 at the location of this sensor. Figure 5.6 indicates that each subtidal current event is associated with a corresponding subtidal rise or drop in water levels. The observed southward current on March 17 corresponds to a subtidal rise of about 40 cm in water surface elevation. This is also confirmed by comparison of predicted and measured tides at NOAA's Ocean City Inlet tide gage as shown in Figure 5.11.
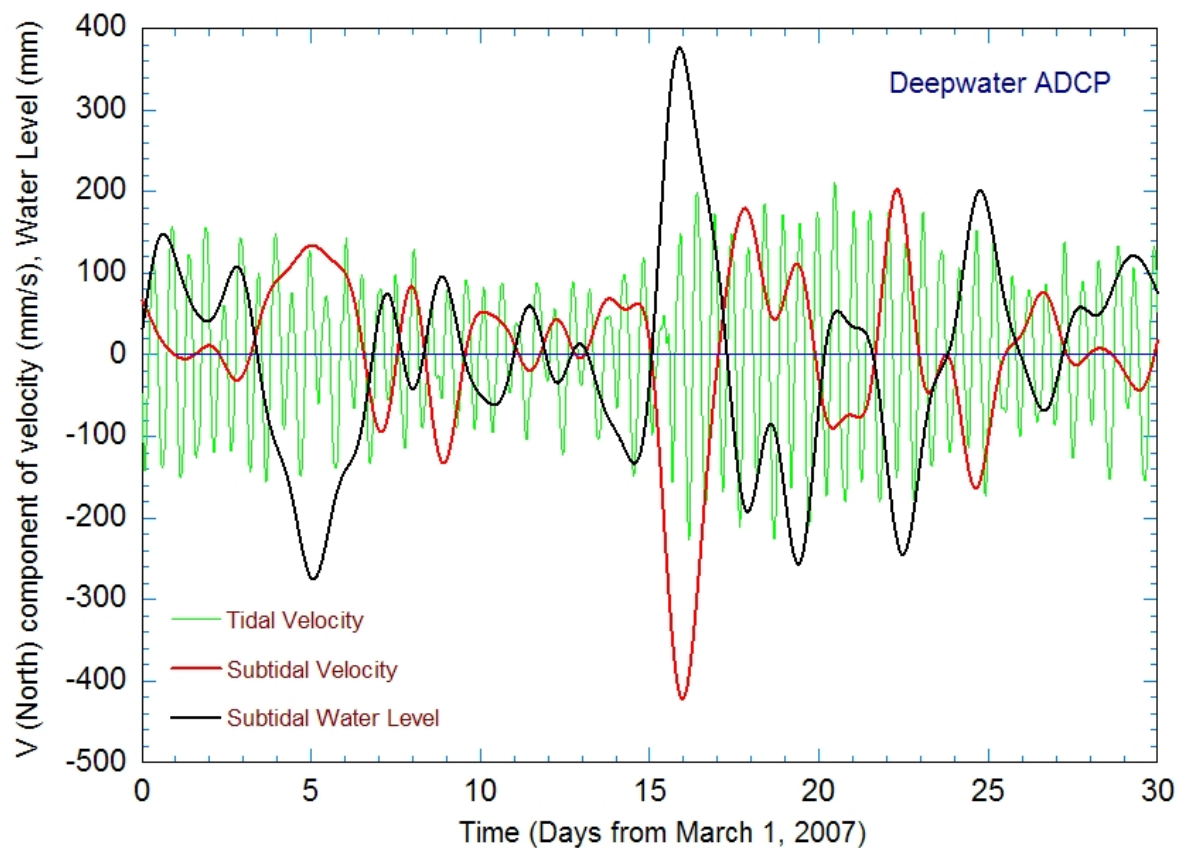
Figure 5.10 Relation between subtidal components of velocity and water level.
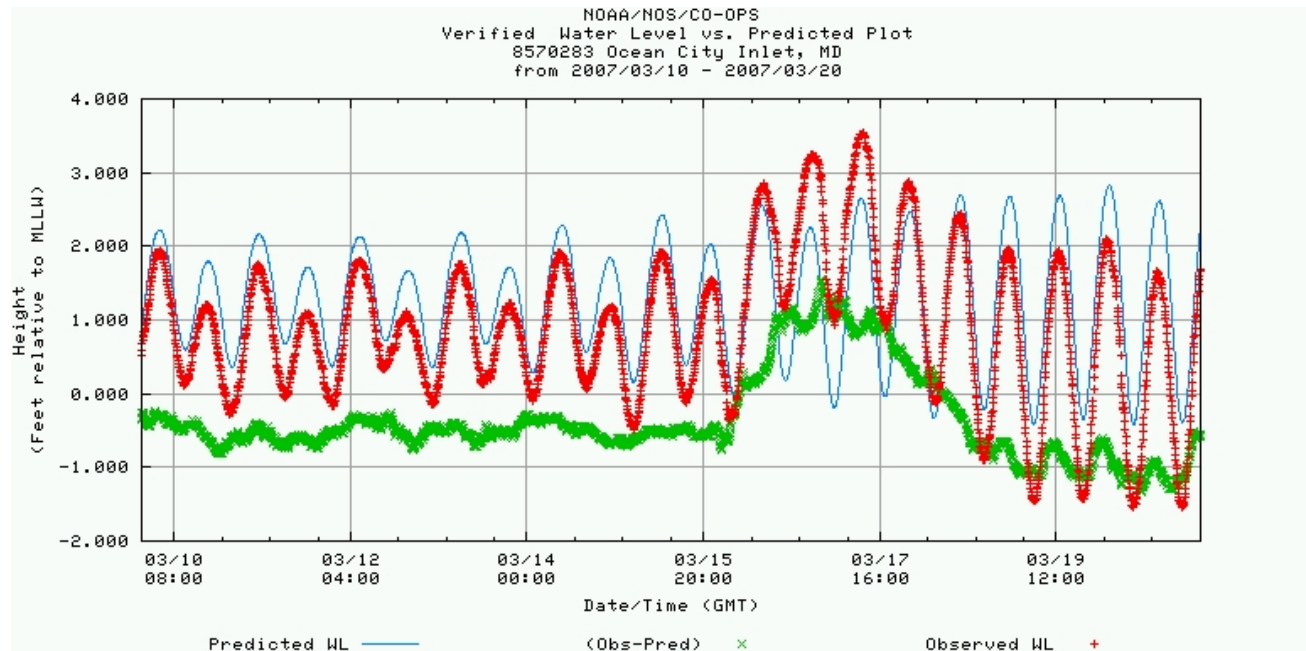
Figure 5.11 Comparison between measured and predicted tides by NOAA at Ocean City in March 2007.

Synoptic scale gradients in atmospheric pressure are known to cause circulations over the continental-shelf in the Middle Atlantic Bight. Synoptic scale motions are generally characterized by periods in excess of 2 days and horizontal-length scales in excess of 500 km. The synoptic scale weather disturbances are generally caused by baroclinic instability. Figure 5.12 shows locations of several NDBC buoys in Northwest Atlantic including the Buoy 44009 which is located close to the present study site. Values of pressure difference between this buoy and the other buoys were compared with the observed sub-tidal fluctuations in the water level. Strong correlation was observed with pressure differences between 44009 and 44005 as well as 44027 as shown in Figure 5.13. Note that as a general rule there is a 10 mm increase in sea level for every mbar (hPa) drop in atmospheric pressure. It is therefore concluded that synoptic scale pressure gradients and their associated wind storms in general, and nor'easters in particular, result in large scale circulations (Figure 2.9) and generation of important subtidal current components in the study area.

The focus in the above discussion was on southerly flow associated with the barotropic pressure gradient of sea surface and winds. It should be noted that there may be a comparable northerly response under the presence of persistent winds and/or different barotropic conditions (note March 20 event in Figure 5.9 for example). However, the significance of southerly flows during nor'easters is because these flows are accompanied with large waves and it is the combined effect of large waves and strong currents that has a significant impact on sediment transport (see Section 6.1 for more discussion).
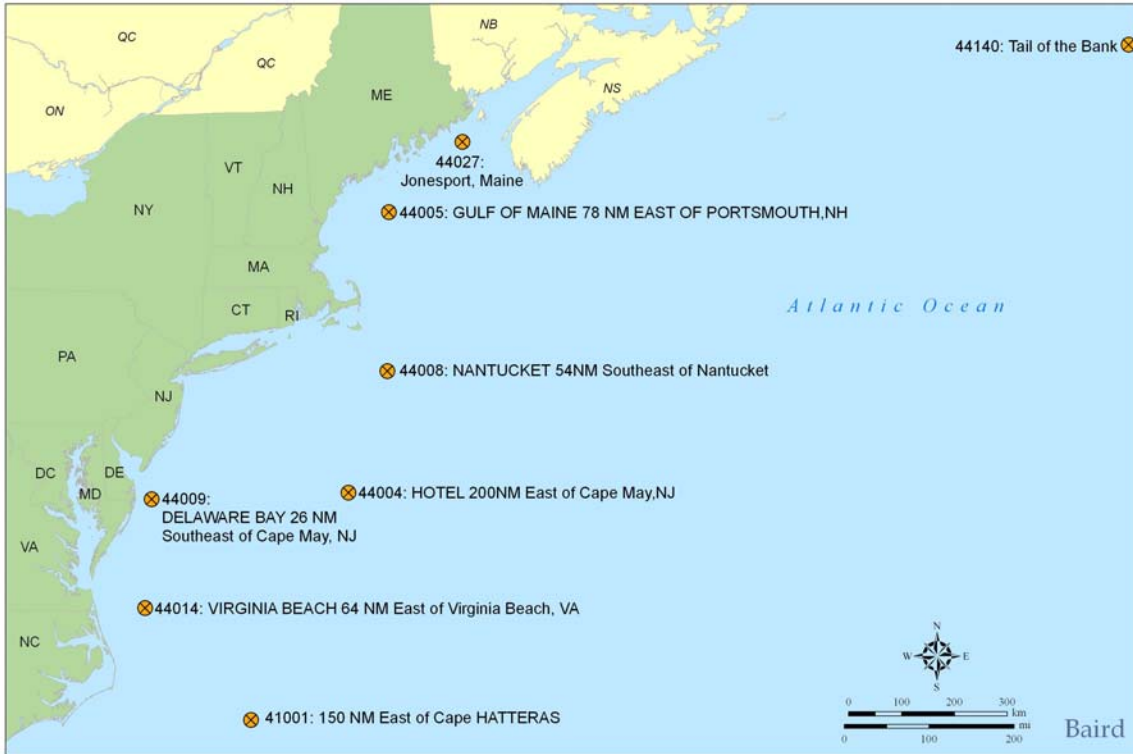
Figure 5.12 Locations of various NDBC buoys across Northwest Atlantic.
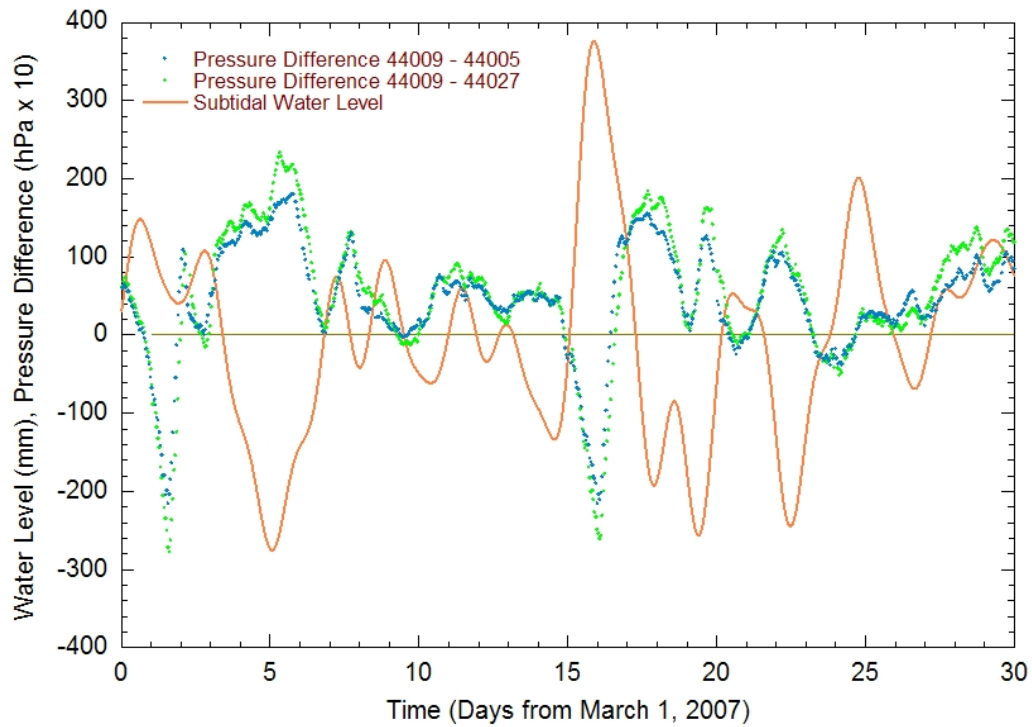
Figure 5.13 Relation between subtidal water level fluctuations and pressure gradients in NW Atlantic.

5.3   Hydrographic Surveys

Water level info Water level information is required for processing depth sounding data collected from a boat. The first hydrographic survey was completed during ADCP deployment period, i.e. between March and May 2007. Water level information recorded by ADCPs was therefore used to process survey data. The second hydrographic survey, however, was completed in January 2008. A tide gage was simultaneously deployed but was found to have malfunctioned on retrieval. The nearest tide stations to the site are Ocean City Inlet, MD (Station ID: 8570283) and Atlantic City, NJ (Station ID: 8534720). Baird examined tide records at these stations against measured tidal levels at the site by the ADCPs.

Figures 5.14 and 5.15 show correlation between Ocean City Inlet (OC Inlet) and Atlantic City (AC) tide levels and the ADCP measured data, respectively. In Figure 1, OC Inlet tides show a regression coefficient of 0.8291 with the ADCP data; they should be divided by 0.6618 to represent the tides at the project site (i.e. OC Inlet tides are about 2/3 of the project site tides). In Figure 2, AC tides show a regression coefficient of 0.9181 with the ADCP data, i.e. a much better correlation than OC tides. AC tides should be divided by 1.1501 to represent the tides at the project site (i.e. AC tides are slightly larger than the project site tides). It was found that a weighted average of 85% AC plus 15% OC Inlet tide would give the highest correlation (0.919) with ADCP data as shown in Figure 5.16. The weighted average values were divided by 1.0768 to represent the tides at the project site and the resulting time series was used to process the second hydrographic survey data.

$$y = 0.6618x$$
$$R^2 = 0.8291$$
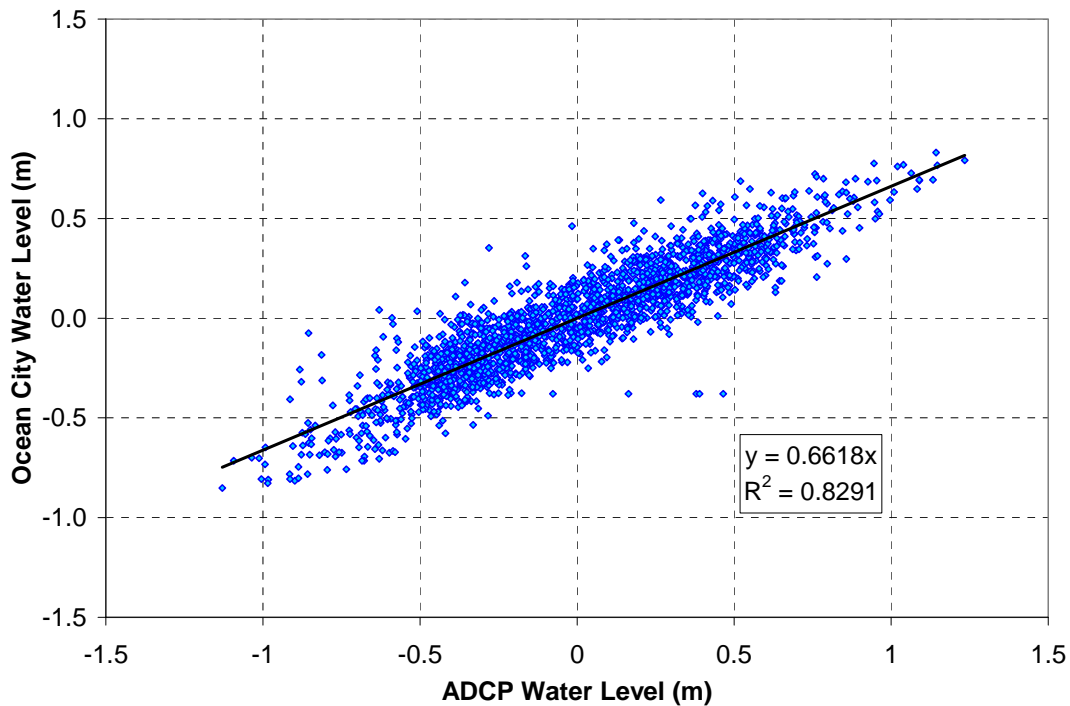
Figure 5.14 Relation between water levels measured at Ocean City Inlet and by the ADCP.
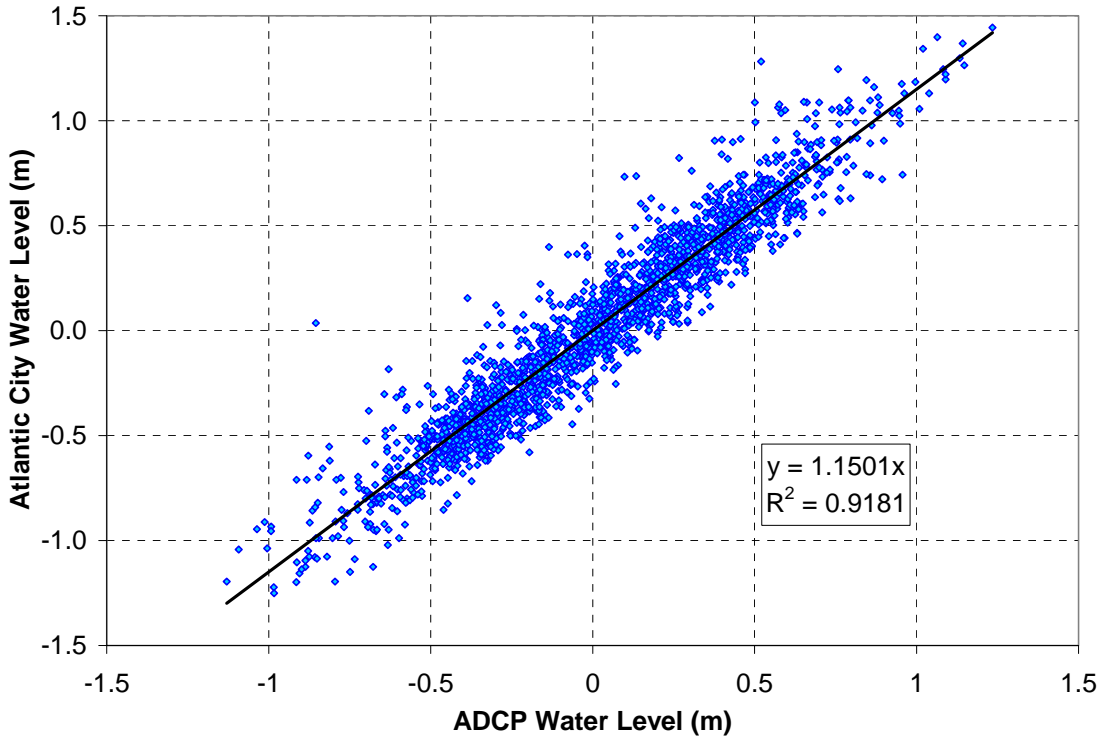
Figure 5.15 Relation between water levels measured at Atlantic City and by the ADCP.
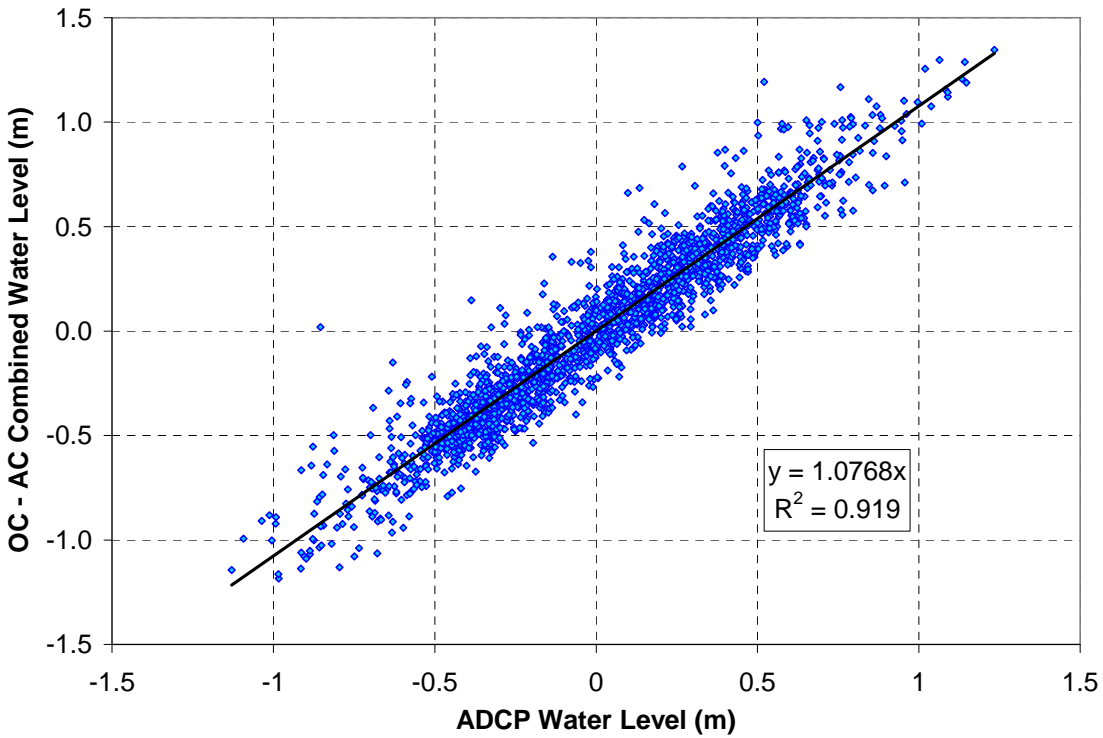
Figure 5.16 Relation between water levels measured at Atlantic City and by the ADCP.

5.4   Comparison with Historic Charts and Surveys in GIS

The bathymetric data explained in Section 2.2.1 and the present hydrographic surveys were used to study the change in bottom elevations around the Isle of Wight since 1929. Figure 5.17 shows the comparison (depth change) between the 2007 and 2008 surveys collected in the present study. Depth change values range from -0.75 m to +1.25 m. The comparison does not provide a meaningful trend of bottom evolution. It was found that errors commonly involved in a hydrographic survey are comparable in magnitude to the annual rate of change of bottom morphology in the study area, affecting short-term bathymetry comparisons. Byrnes et al. (2002) provide estimates of acoustic depth measurement accuracy for various project conditions. The estimated RMS (95 percent) error for the present project conditions is ± 1.0 ft (± 0.3 m). The combined error from both surveys would thus be ± 0.6 m, comparable to the values of depth change shown in Figure 5.17. It was, therefore, decided to focus on long-term morphological evolution of the shoals such that survey errors become negligible against actual changes in bottom elevations.
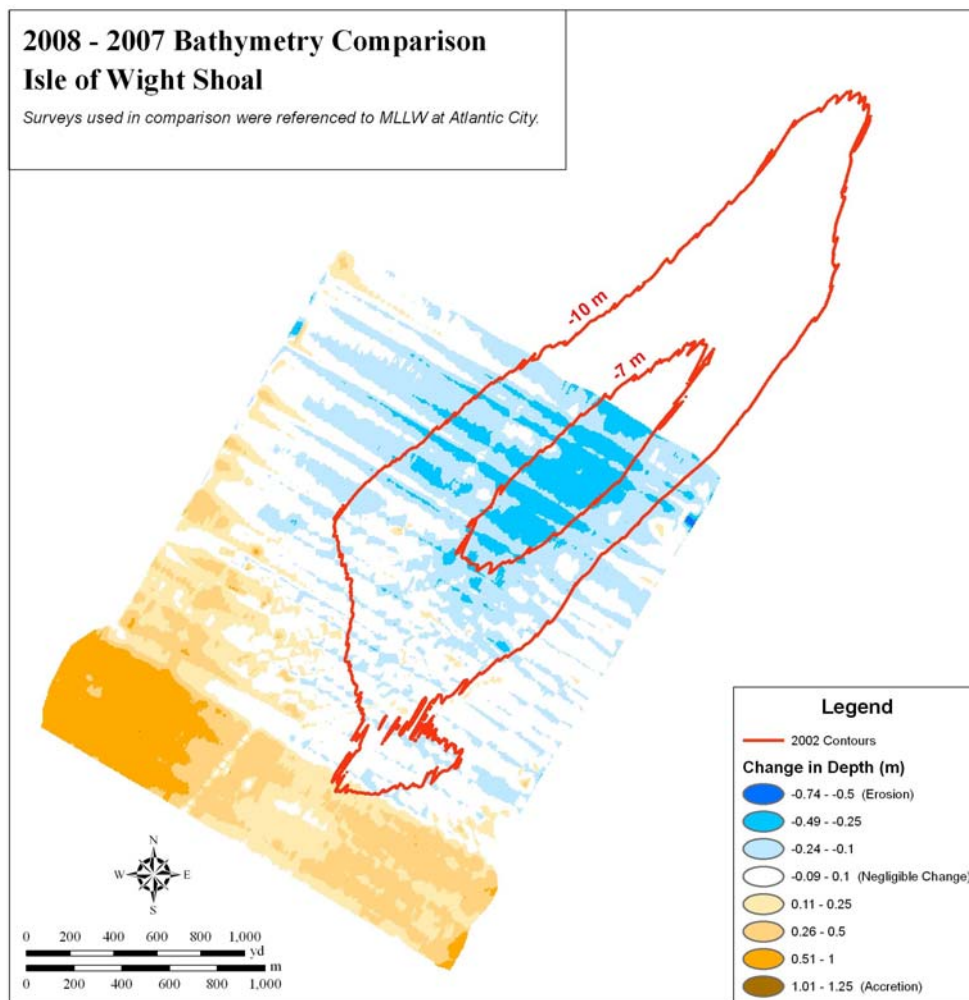
Figure 5.17 Comparison between 2007 and 2008 surveys of the present study around IOW.

The USACE 2002 Surveys of Weaver and Isle of Wight, the 1929 Field Sheet, and the 1975 survey as described in Section 2.2.1 were selected to look at long-term bathymetry comparisons around Isle of Wight. The selected surveys cover the entire IOW shoal. They were referenced to MLLW at Ocean City, and the effect of sea level rise was taken into account (~ 4 mm/year).

Figure 5.18 provides a plot of bottom elevation change at IOW between 1929 and 2002. Comparison area is limited by the extent of the 1929 survey. Erosion and accretion are shown with blue and brown colors, respectively. The -7 m and -10 m contours from both surveys are also shown. While the -10 m contour shows an overall southward movement, the -7 m contour seems to have moved in the SW direction. It is expected that shoal crest will be more dynamic than deeper parts of the shoal; therefore the crest shows a more random behavior than the main body of the shoal. Also note that the NW flank of IOW has a milder slope of its SE flank. Therefore, survey inaccuracies are more amplified on the NW flank.
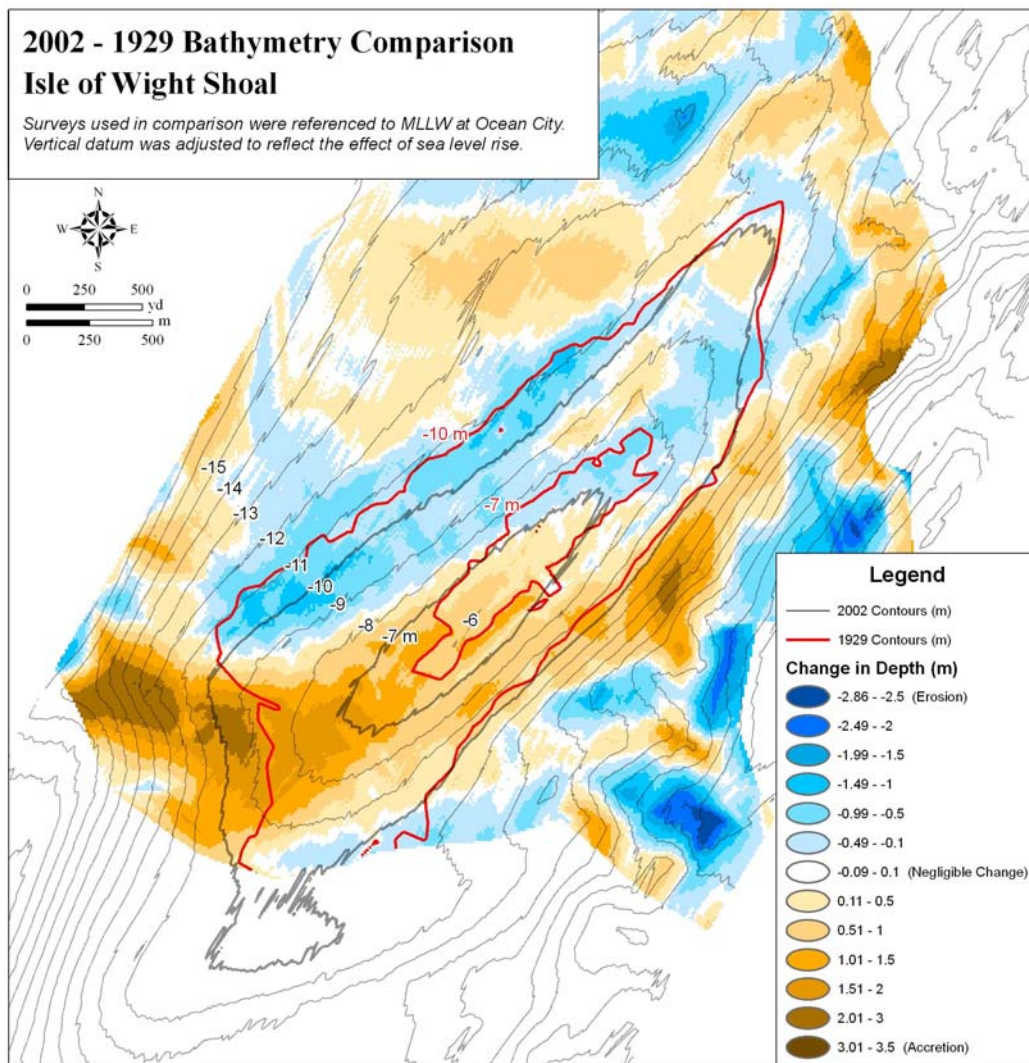
Figure 5.18 Comparison between 1929 and 2002 surveys around IOW.

Calculation of erosion and accretion volumes indicates a total accretion of about 2.8 million m³ and total erosion of 1.9 million m³ over the comparison area in the 73-year comparison period. The difference is attributed to the comparison area being limited, thus not covering all relevant accretion and erosion features, and to possible survey and datum inaccuracies.

Figure 5.19 provides a plot of bottom elevation change at IOW between 1975 and 2002. Comparison area is limited by the extent of the 2002 survey and covers a much larger area than the previous comparison (the north end quarter of the area is not shown in the figure). The -7 m and -10 m contours from both surveys are also shown. Both the -10 m and the -7 m contours show movement in SW direction. A corresponding accumulation area is observed on the west side of the shoal. The reasons behind the differences observed between 1929-2002 and 1975-2002 comparisons are not clear. One possibility could be long-term (decadal or longer) shifts/variations in the wave and current climate of the area due to the variability in the North Atlantic Oscillation (NAO). It is generally believed that the leading edge (i.e. the edge on the migration side) of a shoal has a much steeper slope than its trailing edge resulting in the asymmetric shape of the shoals. Looking at depth contours in Figure 5.19, it appears that IOW has two steep sides on its south and west edges. This may be an indication that IOW has two westerly and southerly migration components corresponding to the above observations.
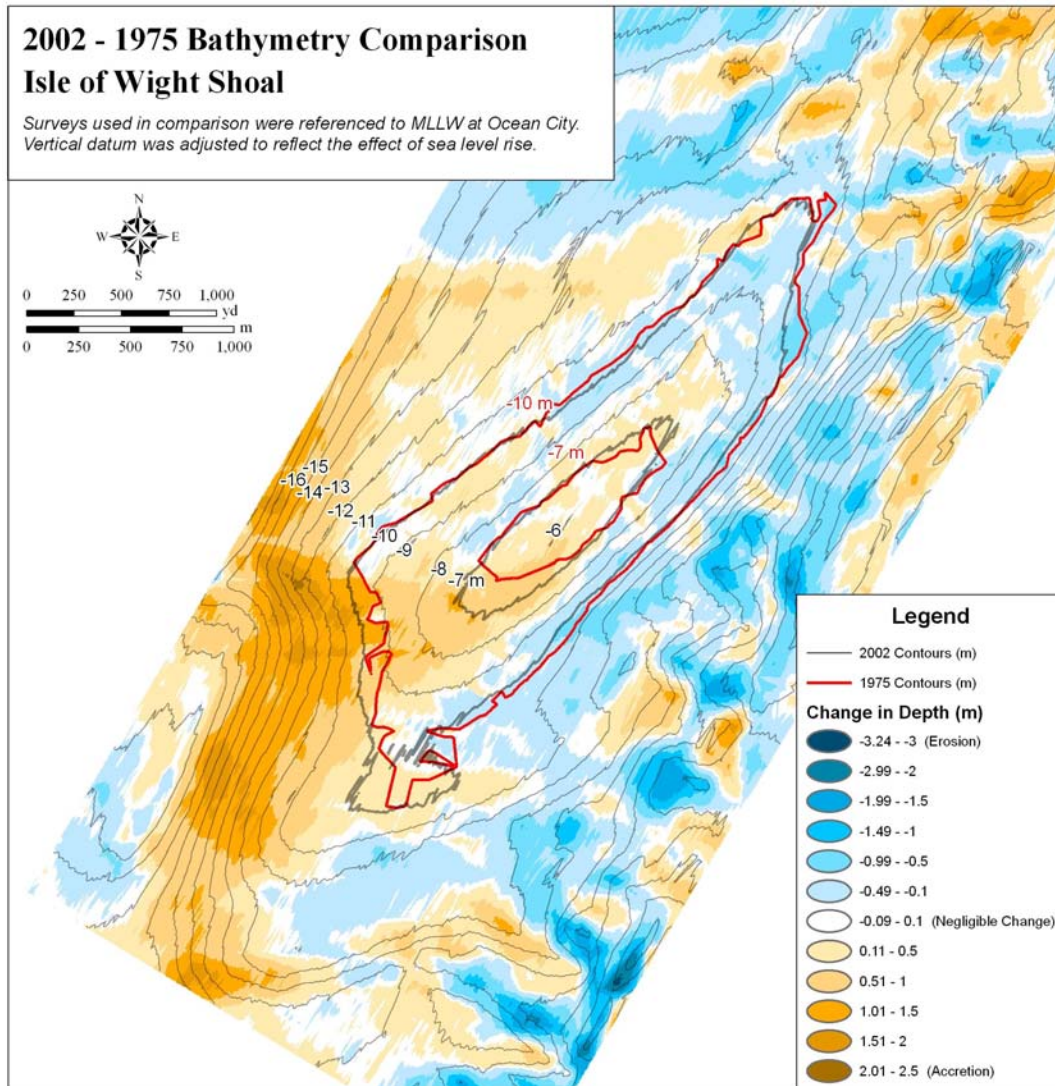
Figure 5.19 Comparison between 1975 and 2002 surveys around IOW.

Calculation of erosion and accretion volumes (Figure 5.19) indicates a total accretion of about 4.4 million m^3 and total erosion of 4.7 million m^3 over the comparison area in the 28-year comparison period. The numbers are reasonably close as a result of relatively large comparison area.

Figure 5.20 provides a plot of bottom elevation change at Weaver between 1975 and 2002. Comparison area is limited by the extent of the 2002 survey. Weaver has a deeper crest than Isle of Wight. The -10 m contours from both surveys are also shown and show a movement towards the south (note that the red contour in this figure belongs to 1975). A corresponding accumulation area is observed on the south side of the shoal. Calculation of erosion and accretion volumes indicates a total accretion of about 4.0 million m^3 and total erosion of 3.3 million m^3 over the comparison area in the 28-year comparison period. The difference is

attributed to the comparison area being limited, thus not covering all relevant accretion and erosion features, and to possible survey and datum inaccuracies.
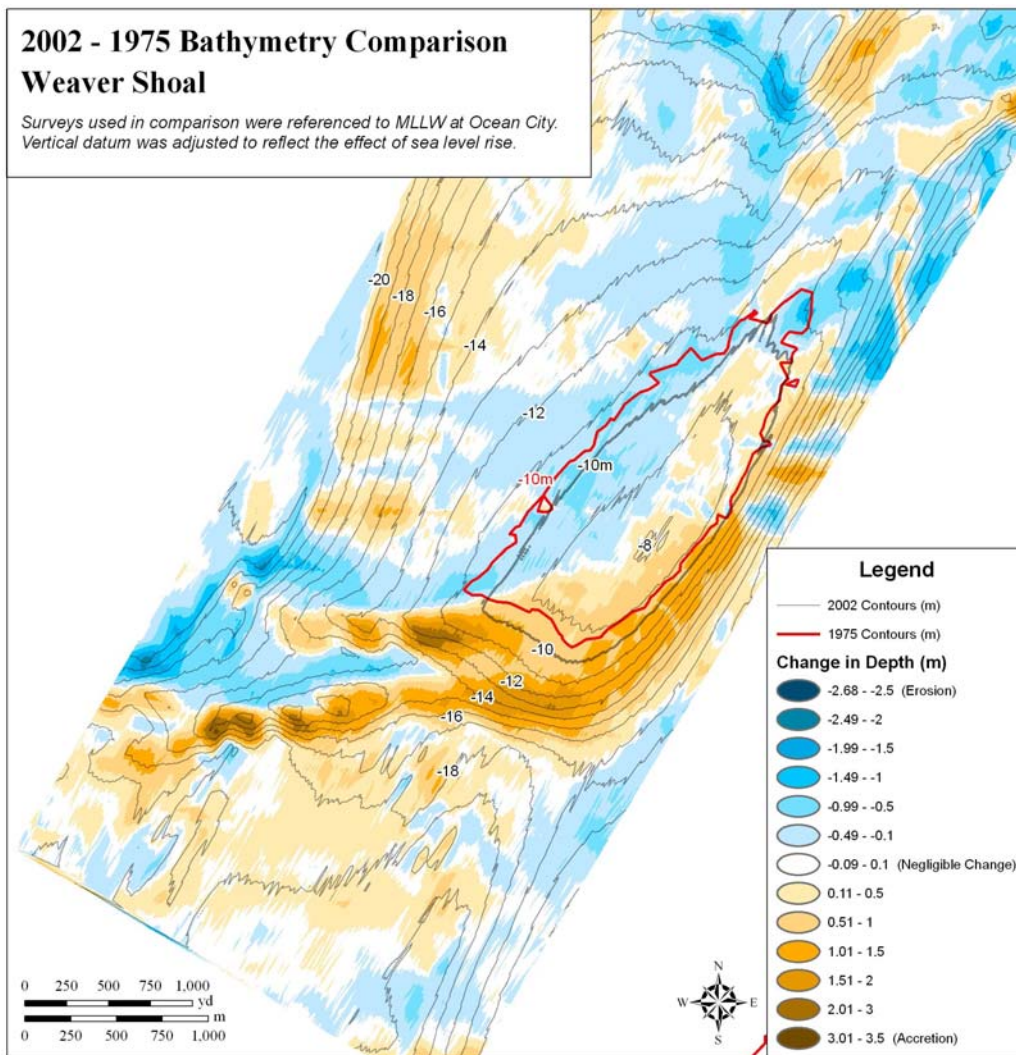
Figure 5.20 Comparison between 1975 and 2002 surveys around Weaver.

5.5   Analysis of Shoal Parameters

An analysis of shoal geometric parameters was completed and is presented in this section. This analysis complements previous comparable efforts completed off the Delmarva Peninsula/Atlantic by Duane et al. (1972), Figueiredo et al. (1981), and McBride and Moslow (1991) among others. The objectives of this task are 1) to better understand shoal features, their genesis, evolution and maintenance, and 2) to support development of dredging guidelines. Regarding the guidelines, the focus will be to identify possible minimums that should not be crossed (e.g. shoal height, width, length, volume, etc.) and to determine if the target shoals are special or unique in some way. Selected shoal parameters are shoal Height (H), shoal Length (L), shoal Width (W), shoal Base Depth (BD), shoal Crest Depth (CD), shoal Orientation (Azimuth), shoal Volume (V), and shoal Distance from Shore (DS). Figures 5.21 and 5.22 provide definitions for most of the above parameters. The parameters and their ratios were plotted against each other in several ways. A summary of the findings is provided here.
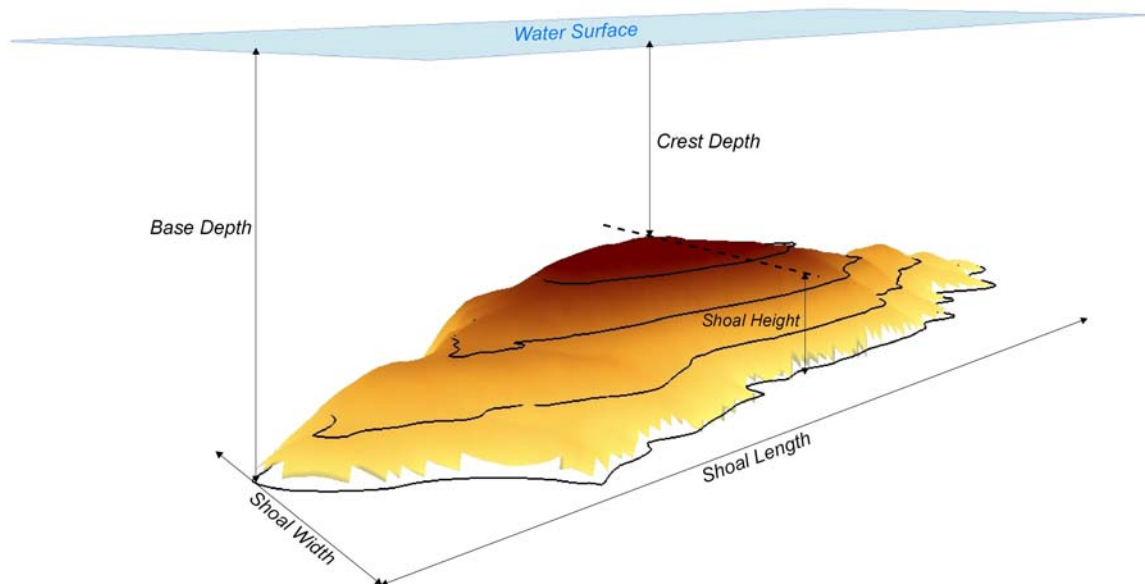
Figure 5.21 Definitions of Shoal Parameters

Shoals were identified in this study for the area offshore Delaware, Maryland and Virginia between Delaware Bay and Chesapeake Bay. Figure 5.23 shows the study area. Offshore shoals between 10 m and 40 m depth contour were considered. Bathymetry of the area was obtained from National Ocean Service (NOS) hydrographic survey data (see Section 2.2.1). The data was processed using ESRI® ArcMap™ 9.3.1 and the bathymetry was interpolated as a grid with 50 m resolution. Using classification techniques, the grid was displayed in the GIS such that shoals could be identified from visual interpretation. Shoal locations were also identified using cross-shelf bathymetry profiles taken through the interpolated grid and from hydrographic charts. Shoal location and parameter data were stored as shapefiles, while bathymetric profiles were stored as feature classes in a geodatabase. Shoal parameters were delineated in the GIS using heads-up digitizing. Heads-up digitizing is the manual delineation of features observed on a

computer screen, often from digital imagery or maps. This approach is commonly used for delineation of features from digital imagery or other base data for GIS analysis (Moore et al., 2003; Zuzek et al., 2003; Wozencraft et al., 2001). Parameters such as Crest Depth and Base Depth were interpreted from the bathymetric profiles taken through the interpolated grid and also from bathymetric contours generated from the grid.

Figure 5.24 shows a typical cross-shelf profile. The above approach allowed for shoals with height of greater than 6 m to be identified. Exclusion of shoals below 6 m shoal height was justified given the relatively low potential for such shoals to be considered economically viable targets for beach fill/dredging operations. Shoals with length shorter than 2 km were also not considered. In total 130 profiles were investigated and 181 offshore shoals identified.

The identified shoals are shown in Figure 5.23. Of these, 7 are in or offshore Delaware, 50 in or offshore Maryland and 124 in or offshore Virginia waters. Note that two shoals (one immediately south of Cape Henlopen on the northern boundary of the study area and another offshore the central Virginia barrier islands) have a distinct NW-SE orientation, suggesting these features may be tidally-influenced and/or geologically controlled. These shoals, however, were not excluded from the analysis as they represent a very small population in the overall dataset.
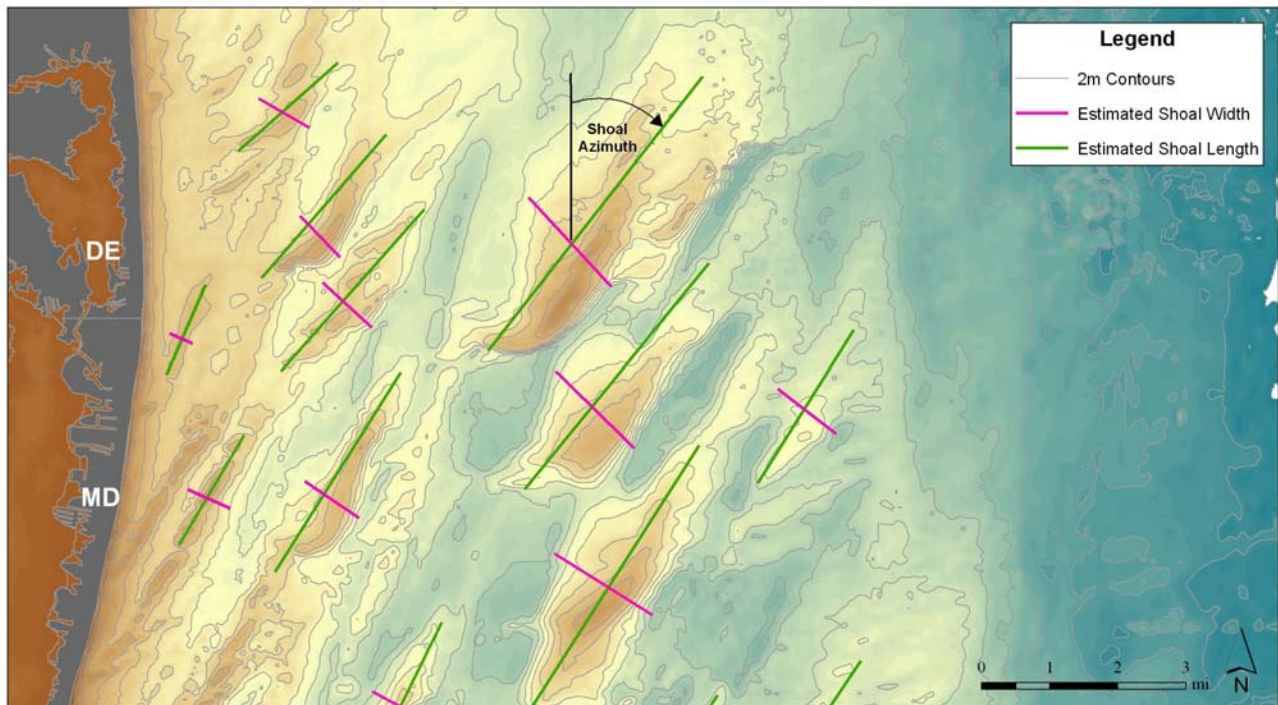
Figure 5.22 Definition of Shoal Length, Width and Azimuth
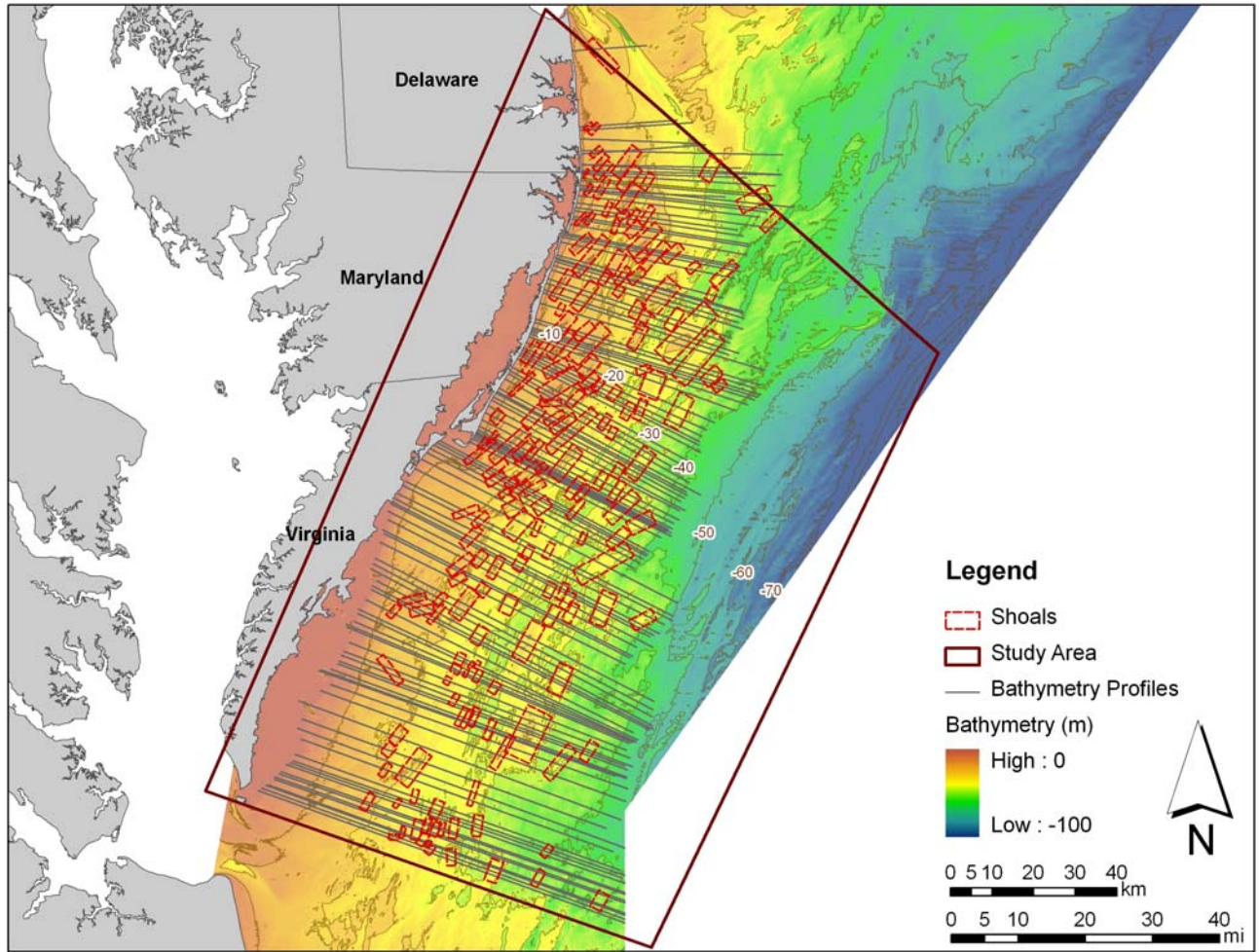
Figure 5.23 Study area, cross-shelf profiles and identified shoals
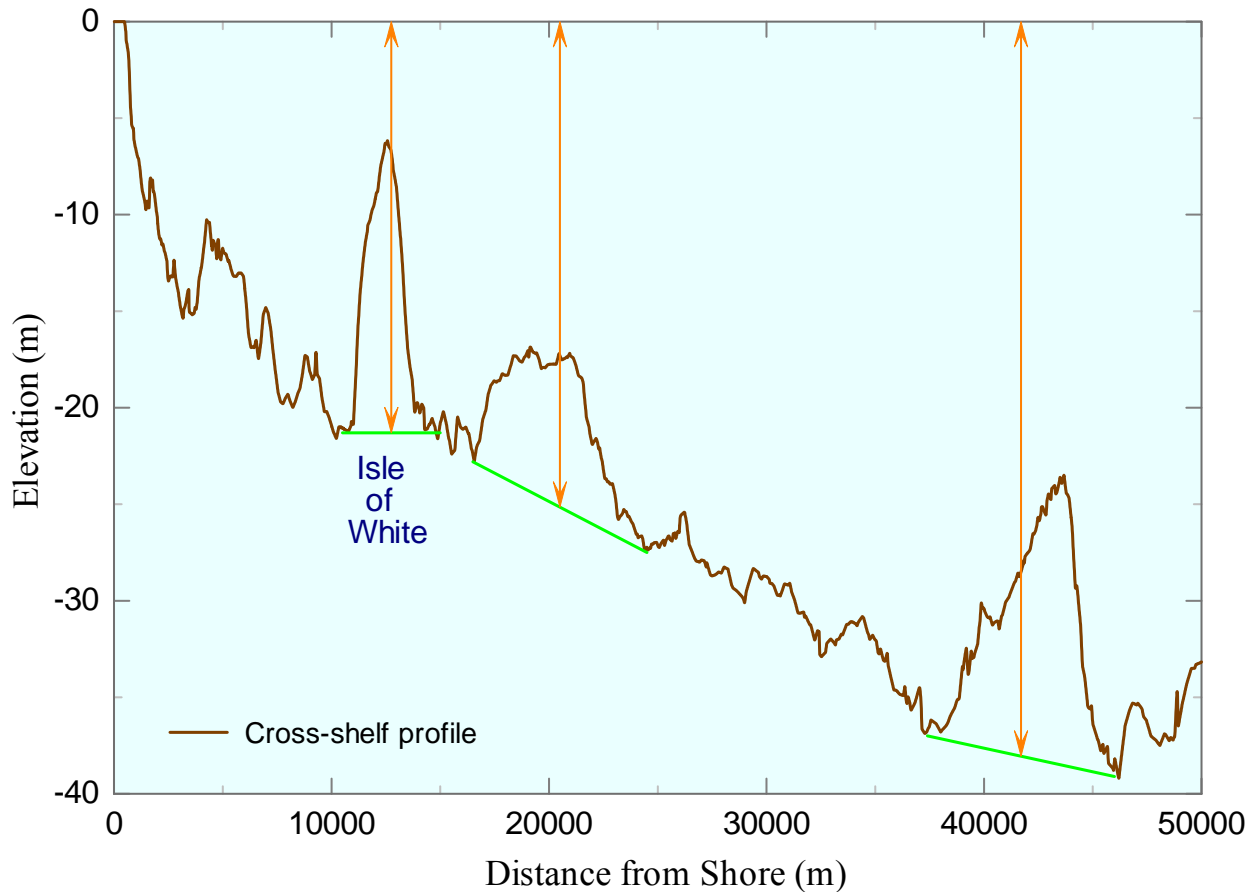
Figure 5.24 Shoal identification and definition of Base Depth (orange arrows) on a cross-shelf profile

A plot of the number of shoals in different depth ranges (Figure 5.25) shows that most of the shoals are located in water depths of 20 to 35 m.

The Width vs. Length (W-L) plot of Figure 5.26 shows that shoal length varies between 2 km (i.e. the minimum shoal Length considered) and 16 km, while shoal width ranges from 500 m to 5 km. The data in this figure is color coded by Base Depth class. Shoals in deeper depth class show a slightly higher Width to Length ratio (i.e. shoals in shallower depths seem to be more elongated than those in deeper depths; see Figure 5.49 and the corresponding discussion). Shoal width generally increases with the shoal length for all depth classes.
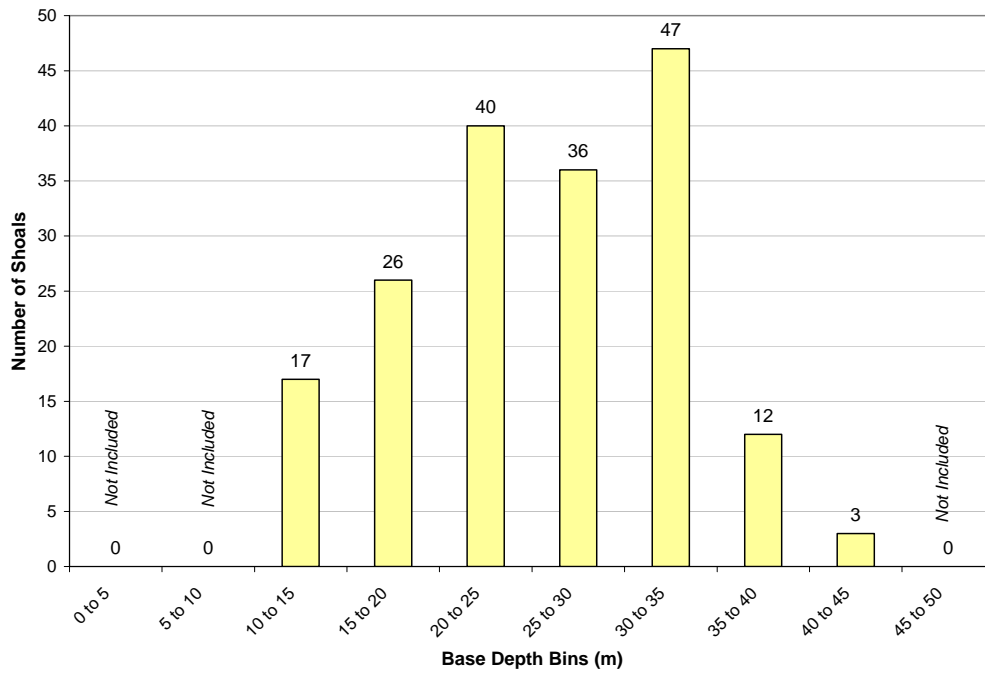
Figure 5.25 Shoal count for different Base Depth ranges
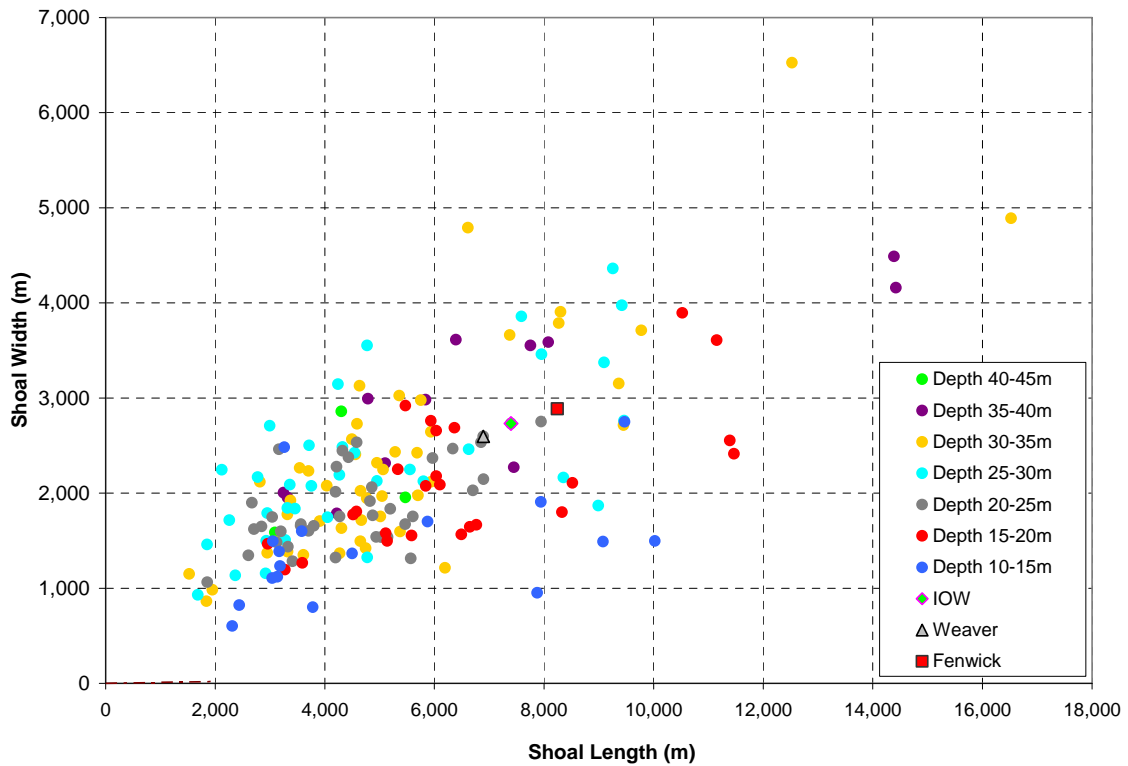
Figure 5.26 Shoal Width vs. Shoal Length

The Crest Depth vs. Base Depth (CD-BD) plot (Figure 5.27) suggests the existence of upper and lower Crest Depth limits for each Base Depth as shown by the two dash lines. The upper limit is simply because only shoals with height greater than 6 m are included in the present dataset. The lower limit may suggest a minimum Crest Depth for a given Base Depth. The CD-BD plot also indicates that minimum Crest Depth is about 5 m and occurs in 10 m to 20 m Base Depth range. It is expected that shoal height is limited by the local wave and current intensity. The minimum Crest Depth is in the same order as the 1-year return period storm wave height which is about 5 m. Note that the transport potential of waves and currents increases with decreasing water depth. It appears that at this site, waves and currents would wash away any accumulation of sand above 5 m depth.

It should be noted that a smaller minimum Crest Depth may be possible in shoals attached to spit complex and shoreface-attached sand ridges, but such shoals/shoreface-attached ridges were not generally considered in the present database.

A plot of Crest Depth vs. Distance from Shore (DS) (Figure 5.28) indicates that the minimum Crest Depth increases linearly with increasing distance from shore. From the above two figures it may be concluded that shoal growth has ceased once the shoal Base Depth became larger than 25 m under rising water level. In other words, shoals with Base Depth greater than 25 m do not grow in height anymore.
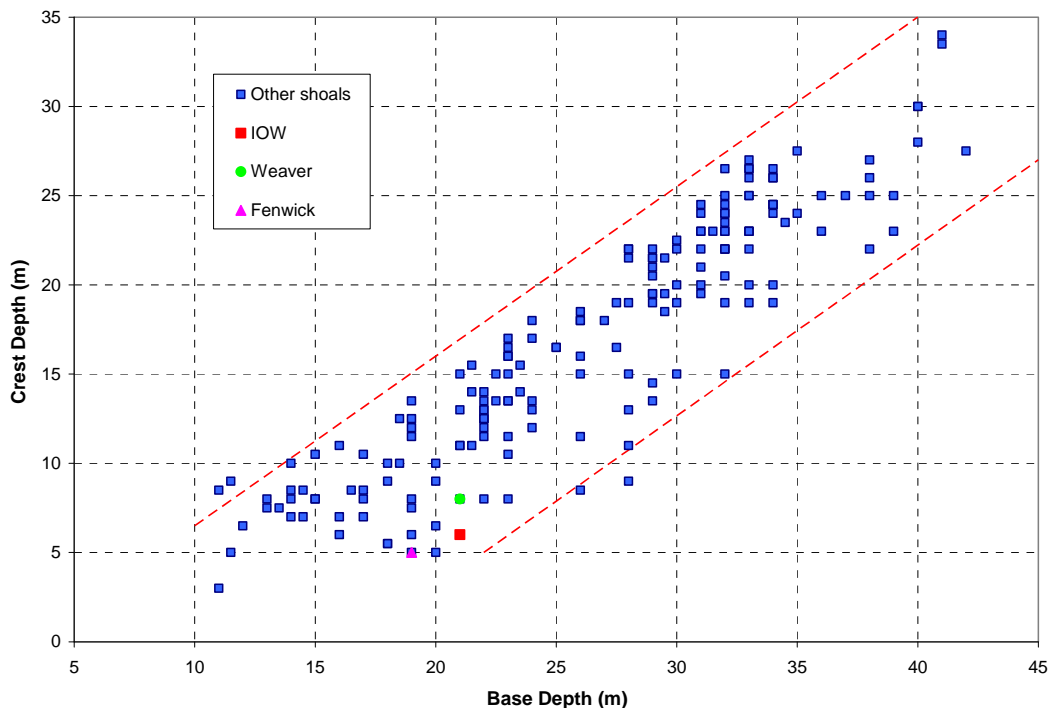
Figure 5.27 Shoal Crest Depth vs. Base Depth
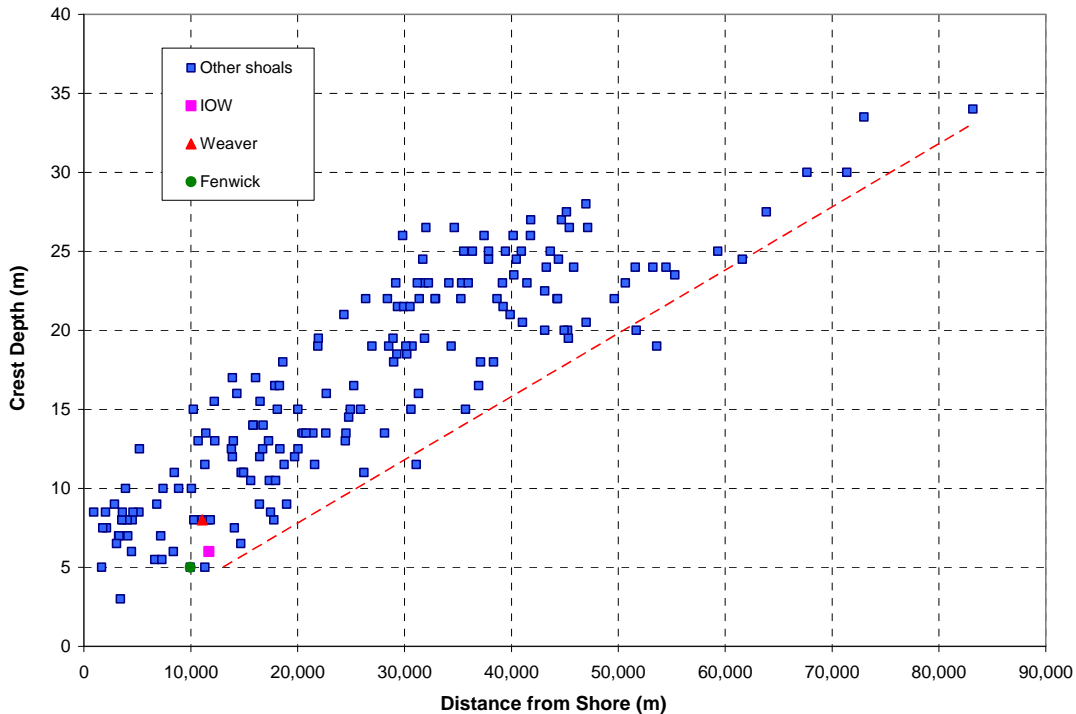
Figure 5.28 Shoal Crest Depth vs. Distance from Shore

The Height vs. Base Depth (H-BD) plot presented in Figure 5.29 indicates that shoal Height could grow to as much as 75% of the Base Depth (red dash line in the figure). Highest shoals occur in 25 m to 30 m Base Depth range. The highest shoal in the present database is 19 m high located in 28 m depth. However, not all the shoals in this depth range are high. Fenwick shoal is in 19 m Base Depth, Isle of Wight (IOW) and Weaver shoals are in 21 m Base Depth. While Fenwick and IOW have H/BD values close to 0.75, Weaver and many other shoals have much smaller H/BD values. This is likely not a result of lack of sand availability as there is enough sand around Weaver. It may be concluded that shoal growth is not entirely a function of today's waves and currents influence. Other factors such as initial geometry, distance from updrift or surrounding shoals, etc. may be involved.

It is noted that on a transgressive shore, a deeper Base Depth is expected to represent an older shoreline position. Assuming that all shoals were initiated at the shoreline at some point in time (e.g. Hayes and Nairn, 2004), then the greater the Base Depth, the older is a shoal. Therefore, the zone between 0 m and 25 m to 30 m Base Depth may be considered as the Shoal Height Growth Zone under a rising sea level. The 30 m Base Depth may be considered as the limit of wave influence beyond which the balance changes in favor of current dominated processes (in the wave-current coexisting system of the study area). Beyond 30 m depth, shoal height shows a decreasing trend indicative of existence of a possible Shoal Height Decrease Zone. The rate of height decrease with increasing depth, however, is much less than the rate of height increase in the growth zone (Figure 5.29).

The plot of H/BD vs. Base Depth (Figure 5.30) indicates that the maximum relative shoal height (H/BD) increases with Base Depth until 20 m depth and decreases for depths deeper than 20 m. If the relative shoal height (H/BD) is considered as the shoal growth index, then Figure 5.30 indicates that Shoal Height Growth Zone ends at about 20 m depth, i.e. in a shallower depth than indicated by Figure 5.29. This is because beyond the 20 m depth, the process of shoal crest building by waves is not strong enough to build the shoal sufficiently high to reach the minimum Crest Depth of 5 m. In other words the 20 m to 30 m Base Depth range may be considered as a transition zone over which the predominant forcing changes from wave-dominated at 20 m depth to current-dominated at 30 m depth. Accordingly, IOW, Weaver and Fenwick are located just before the start of the transition zone.

The plot of Height vs. Distance from Shore (DS) presented in Figure 5.31 shows similar trends. The DS parameter represents the age or maturity of a shoal on the transgressive Mid-Atlantic shore. Shoal Height increases with distance from the shore. Note that the horizontal axis is in logarithmic scale and therefore the relation is not linear. Maximum shoal Height is observed at about 20 km from the shore, beyond which the shoal height starts to decrease. In either of the above figures, Fenwick, IOW and Weaver are located in the Growth Zone. They thus have the potential to rebuild themselves to their existing height once being dredged. On the other hand, shoals located in waters deeper than 30 m are not expected to re-grow in height if dredged.
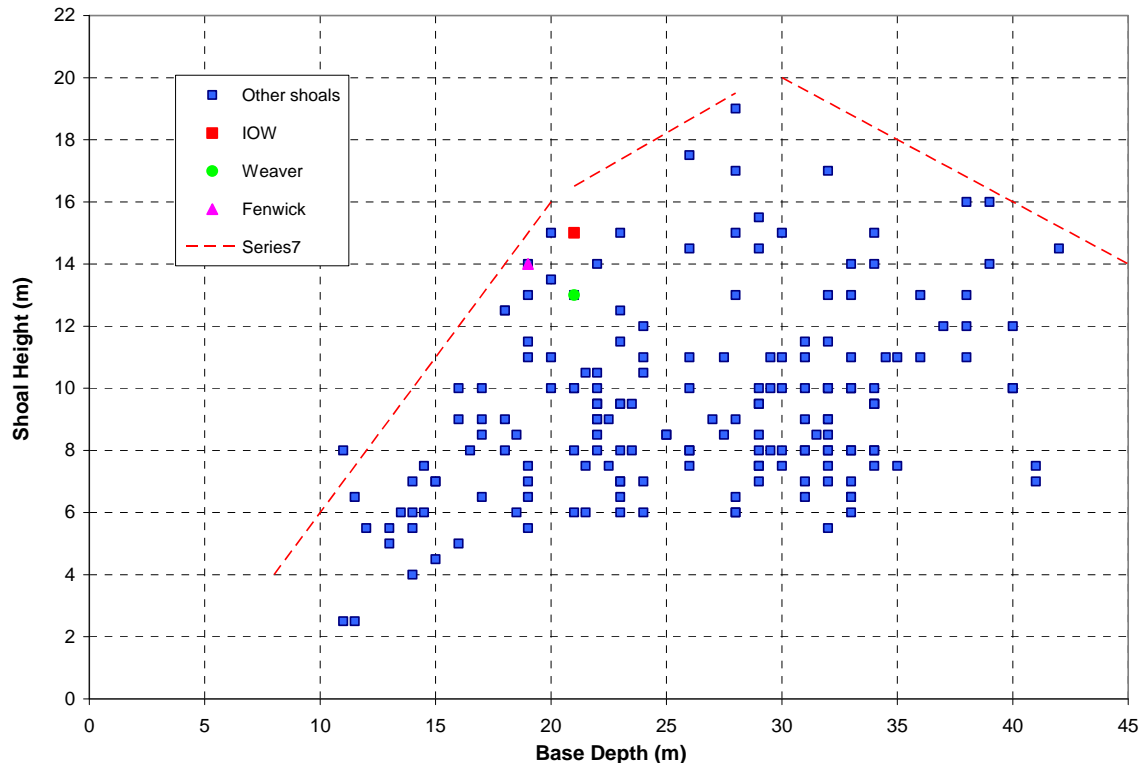
Figure 5.29 Shoal Height vs. Base Depth (the dataset mainly includes shoals with height greater than 6 m)
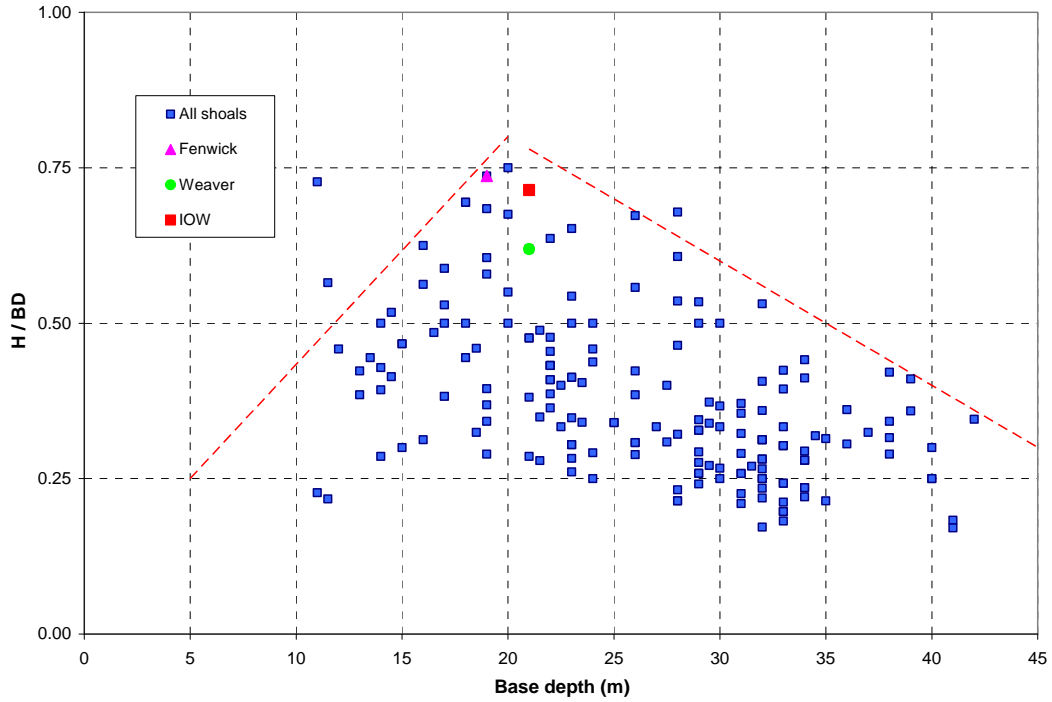
Figure 5.30 H/BD vs. Base Depth (mainly for shoals with height greater than 6 m)
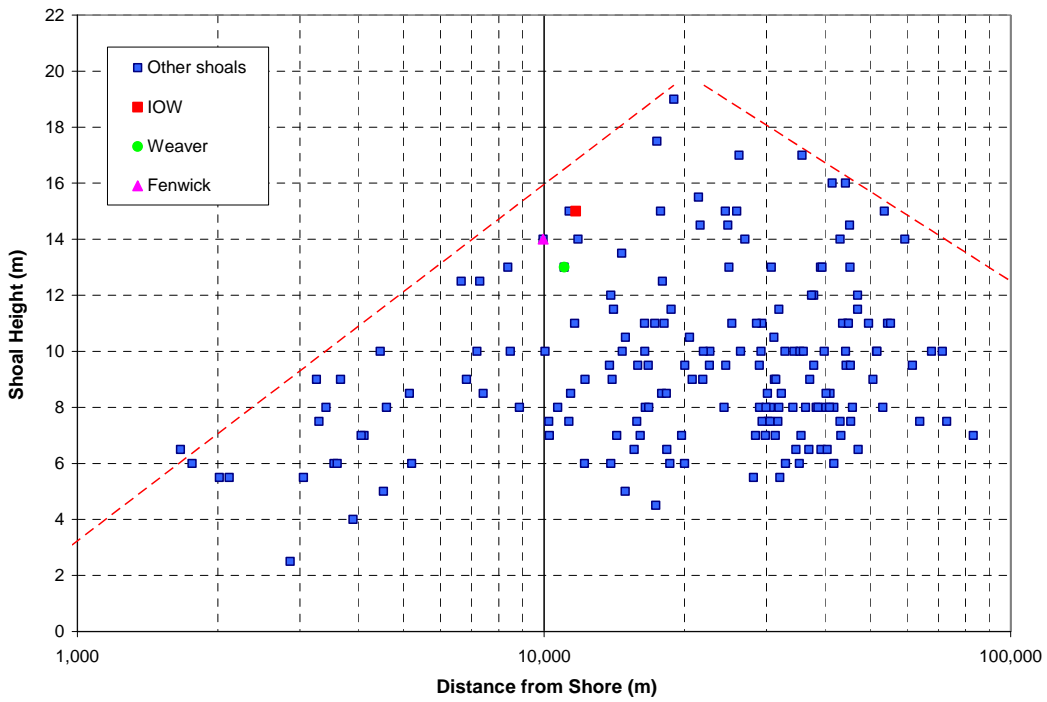
Figure 5.31 Shoal Height vs. Distance from Shore (the dataset mainly includes shoals with height greater than 6 m)
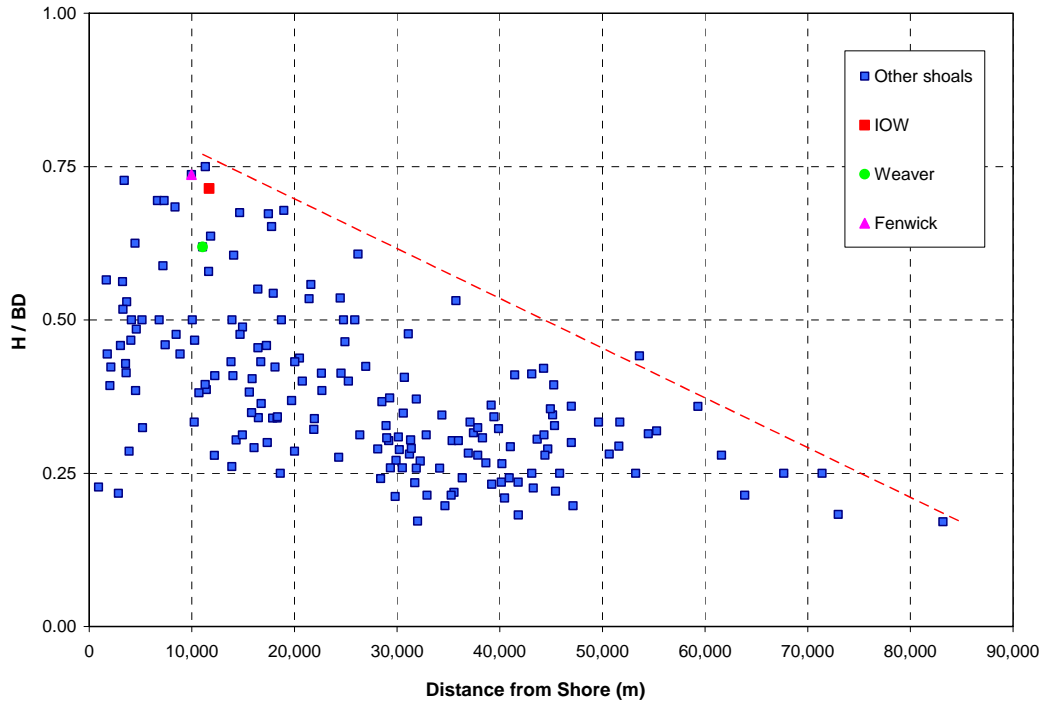
Figure 5.32 Relative shoal height (H/BD) vs. Distance from Shore

A plot of the relative shoal height (H/BD) vs. Distance from Shore (Figure 5.32) shows that maximum H/BD occurs at distance of about 11 km from the shore and decreases linearly with DS afterwards.

Shoal Volume was calculated in two ways as 1) the volume above the Base Depth plane in ArcMap, and 2) $L \times H \times W / 3$. Comparison between the results indicated that shoal Volume above the Base Depth may be calculated using the following formulation:

$$\text{Shoal Volume} = 0.53 \times L \times H \times W$$

Weaver has a volume of about 100 million m^3 above its Base Depth while IOW and Fenwick have volumes close to 140 million m^3.

A plot of shoal Base Area vs. Base depth (Figure 5.33) indicates that maximum shoal footprint Area increases with increasing BD until about 35 m depth. Base Area was defined as the area of the "bounding rectangle" in ArcMap for calculation of volume. It is roughly equivalent to the product of Length times Width. Fenwick, IOW and Weaver, all have large Areas close to the maximum observed in their depth range.
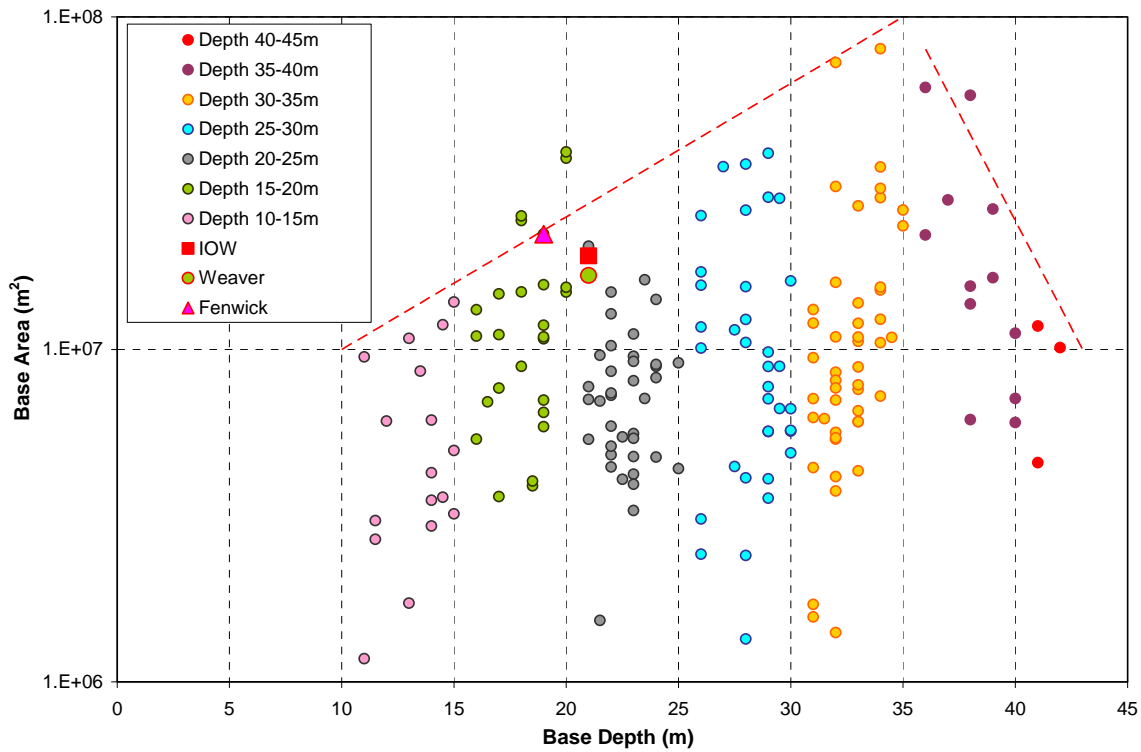
Figure 5.33 Shoal Base Area vs. Base Depth

A plot of shoal Volume vs. Base Depth (Figure 5.34) indicates that maximum shoal Volume increases with increasing BD until about 35 m depth. Fenwick, IOW and Weaver, all have large volumes close to the maximum observed in their depth range.

The Height vs. Length (H-L) plot of Figure 5.35 shows that longer shoals tend to be higher in an asymptotic manner. However, not all the shoals with the same length grow as high.   The H/L ratio (shoal steepness along its longer axis) does not exceed 1/200 (dash-dot line in the figure).
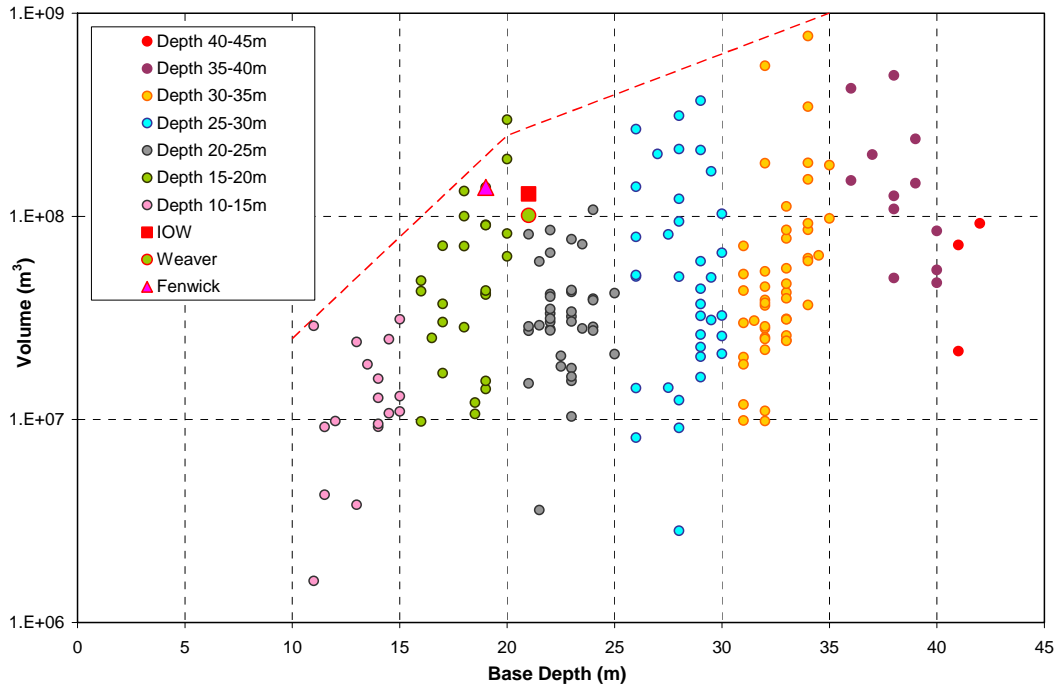
Figure 5.34 Shoal Volume vs. Base Depth
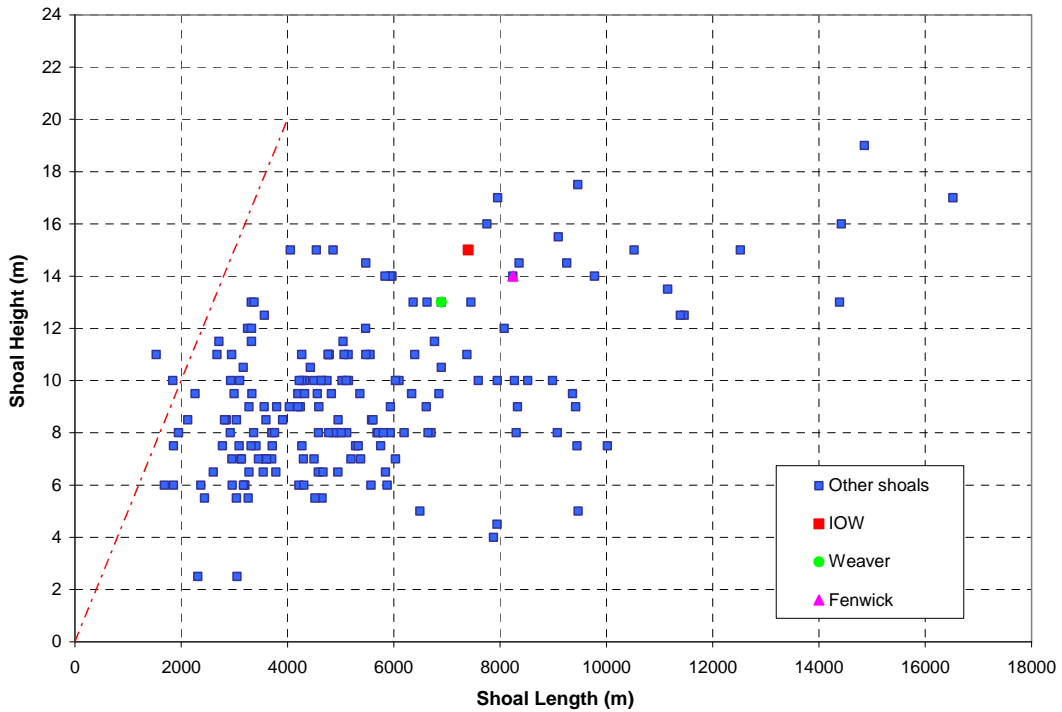
Figure 5.35 Shoal Height vs. Length (the dataset mainly includes shoals with length longer than 2 km and height greater than 6 m)

Similarly, the Height vs. Width (H-W) plot (Figure 5.36) shows that wider shoals tend to be higher in an asymptotic manner. However, not all the shoals with the same width grow as high. Higher shoals have widths in 3 to 6 km range, but the highest shoal is not the widest. This may be a result of wave focusing effects. Shoals are expected to become narrower and grow in height under focusing waves. Shoals in deeper water have a wide range of height and width. In shallower depths, shoals are narrower and their height is limited by the depth. The H/W ratio (shoal steepness along its shorter axis) does not exceed 1/100 (dash-dot line in the figure). Maximum shoal Width increases with shoal Base Depth in general (BD-W plot, Figure 5.37). Similarly, maximum shoal Length increases with increasing Base Depth (BD-L plot, Figure 5.38).

The above observations may be summarized as follows. Maximum shoal Width, Length and Base Area all increase to approximately 35 m depth and decrease thereafter. Maximum shoal Height increases to approximately 30 m depth, but the rate of increase in the 20 m to 30 m depth range is less than the same rate in the 10 m to 20 m depth range. As a result, maximum shoal volume increases to approximately 35 m depth and decreases thereafter. However, the rate of increase in shoal Volume in the 20 m to 35 m depth range is less than the same rate in the 10 m to 20 m depth range (Figure 5.34).
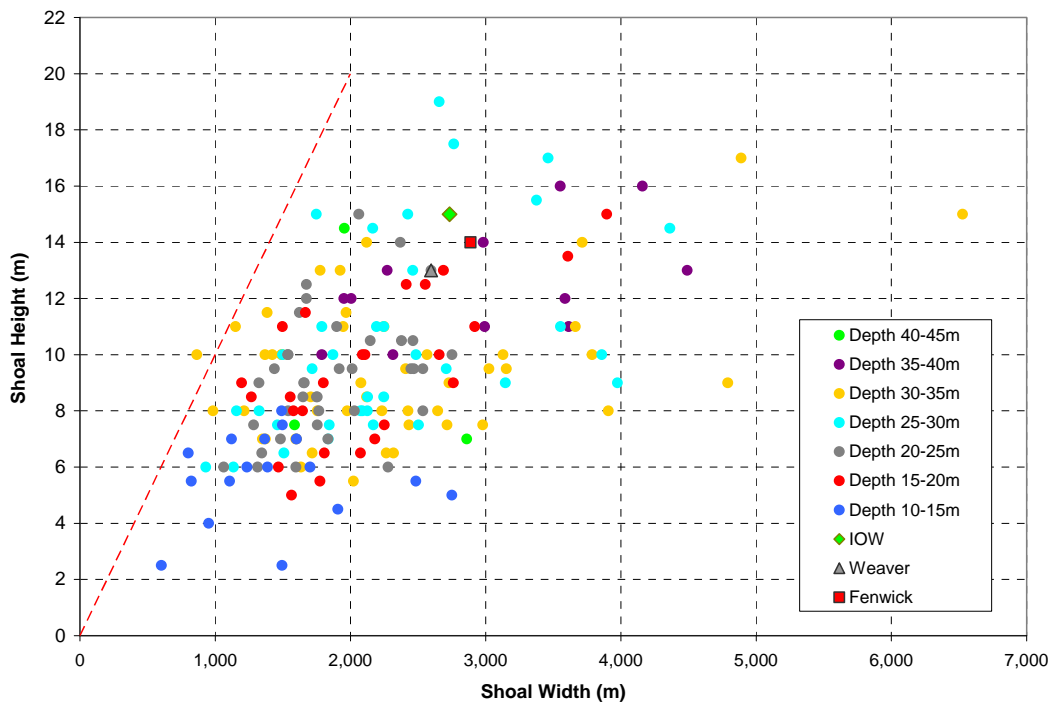
Figure 5.36 Shoal Height vs. Width (mainly for shoals with height greater than 6 m)
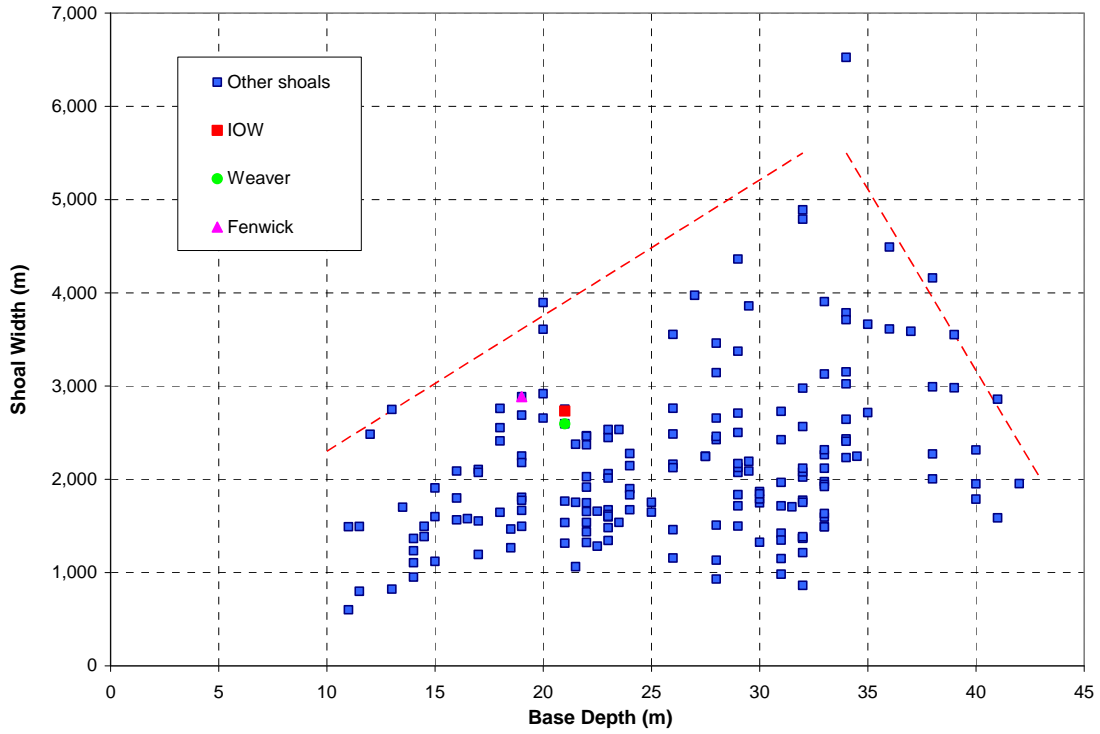
Figure 5.37 Shoal Width vs. Base Depth
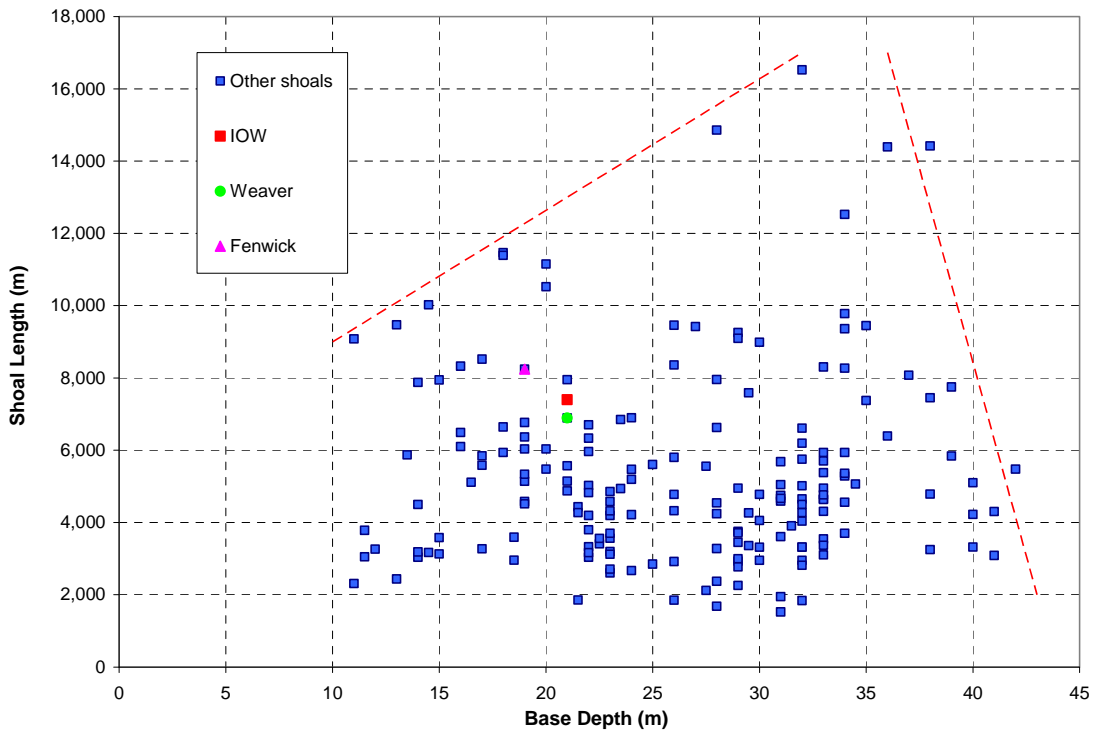
Figure 5.38 Shoal Length vs. Base Depth (mainly for shoals with Length longer than 6 m)

The plot of Azimuth (orientation of shoal longer axis measured clockwise from north) vs. H presented in Figure 5.39 indicates that shoal Azimuth ranges between 20° to 60° in the study area. Higher shoals tend to be more focused around the NE (45°) direction. This suggests that shoals with orientation close to NE grow larger. Figure 5.40 provides a plot of shoal Azimuth vs. relative shoal height (H/BD) and indicates that almost all shoals with H/BD larger than 0.5 have more or less an NE orientation and are located in less than 30 m of water. Scatter in azimuth is high when H/BD < 0.5. Therefore, shoals with H/BD > 0.5 have the potential to rebuild themselves (likely to their existing height) once being dredged.

As discussed earlier, the minimum Crest Depth in the present study area is 5 m (Figure 5.27). Therefore, a relative shoal height of 0.75 can only be achieved in a Base Depth of 20 m or deeper. Similarly, a relative shoal height of 0.5 corresponds to a fully grown shoal in 10 m Base Depth. Shoals in waters shallower than 20 m may still grow under rising sea levels. Considering that the relative shoal height of the shoals with Base Depth deeper than 20 m decreases with increasing the Base Depth (Figure 5.30), maximum shoal Height growth in the present study area is expected to happen landward of the 20 m depth contour.
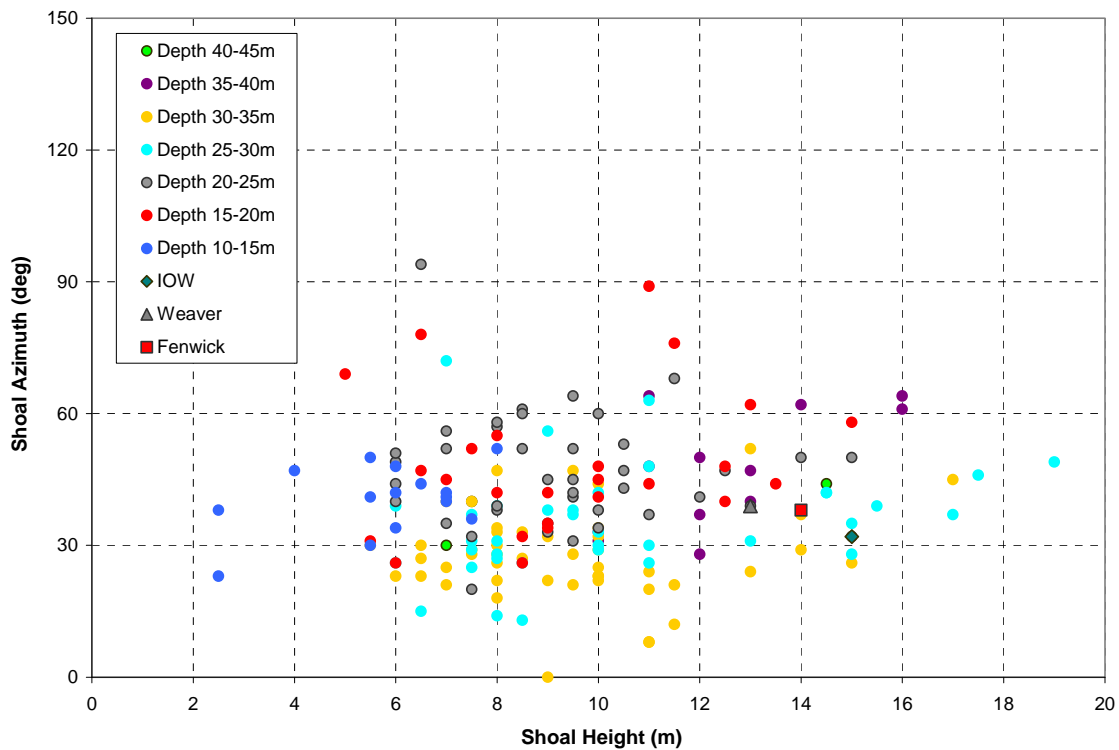
Figure 5.39 Shoal Azimuth vs. Height

It is noted that although most shoals in the 10 m to 25 m BD range have an Azimuth more or less close to NE direction, they did not all grow towards the limiting H/BD value at the corresponding depth. Although some of these shoals may still grow/be growing (particularly under rising sea levels), it is likely that shoal growth is not entirely a function of wave influence

and other factors such as initial shoal geometry/geology, sand availability, proximity to other shoals, etc. are also important. At a certain depth, shoals that have reached their corresponding maximum relative shoal height are more likely to re-grow once they are dredged.
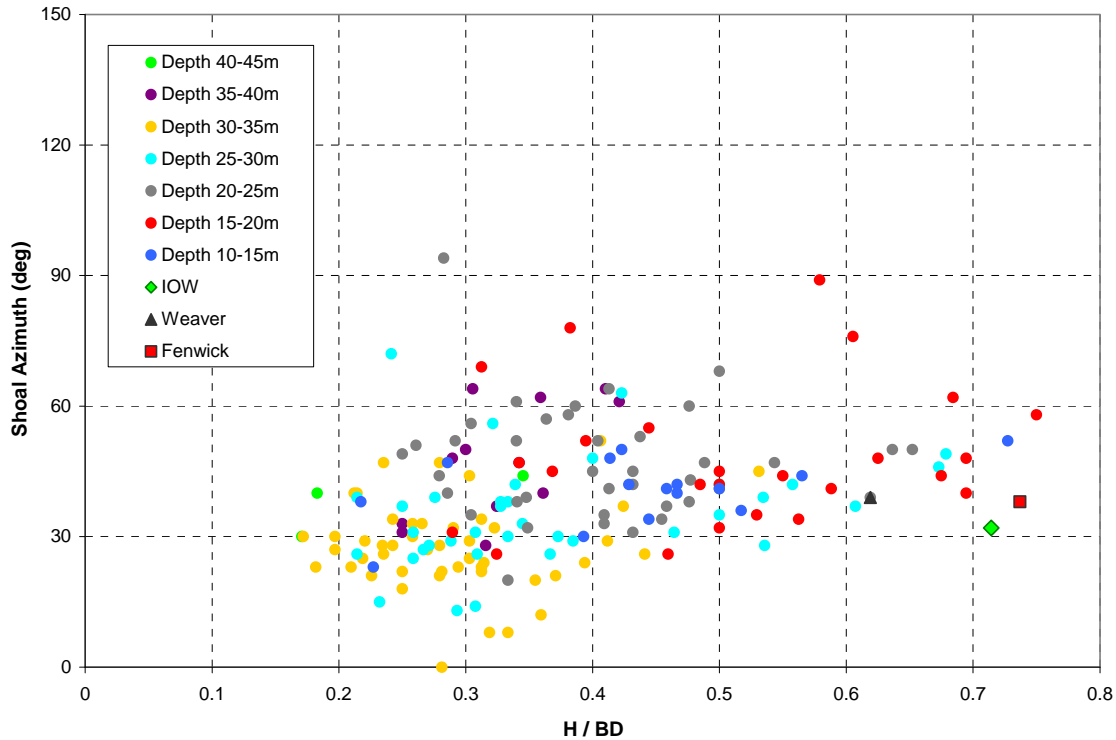
Figure 5.40 Shoal Azimuth vs. Relative Shoal Height (H/BD)

A plot of shoal Azimuth vs. shoal Base Depth (Figure 5.41) shows that almost all shoals with Base Depth less than 25 m have an Azimuth of 30° to 60° indicating the importance of wave action (which is dominated by nor'easters) in shaping the geometry of the shoals over the Shoal Height Growth Zone. There is a group of shoals in 25 m to 35 m Based depth range that feature a more northerly orientation (10° to 40°) relative to the shoals in other depth ranges. These shoals mostly have H/BD values of less than 0.5 (Figure 5.40), i.e. they did not grow fully in height. Figure 5.42 shows the spatial distribution of shoals color coded based on the Azimuth. Shoals with Azimuth less than 30° (pink circles) are more or less located along the 30 m depth contour. Considering that on a transgressive shore, a deeper Base Depth is expected to represent an older shoreline position, it is possible that this group of shoals belong to a previous historic time with a more northerly wave climate. Accordingly, it is possible that the reduction in wave influence observed over the transition zone (i.e. over the 20 m to 30 m depth range) is partly a result of northerly orientation of the shoals in the 25 m to 35 m depth range. Beyond 35 m depth, shoal Azimuth is again in the 30° to 60° range.
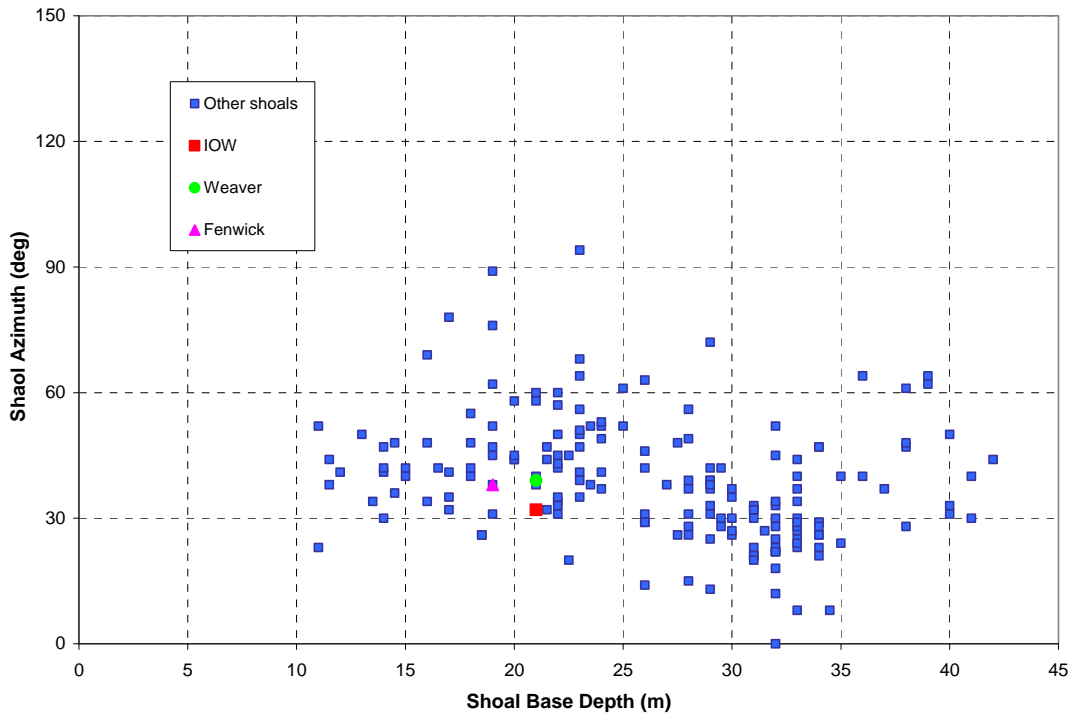
Figure 5.41 Shoal Azimuth vs. Base Depth
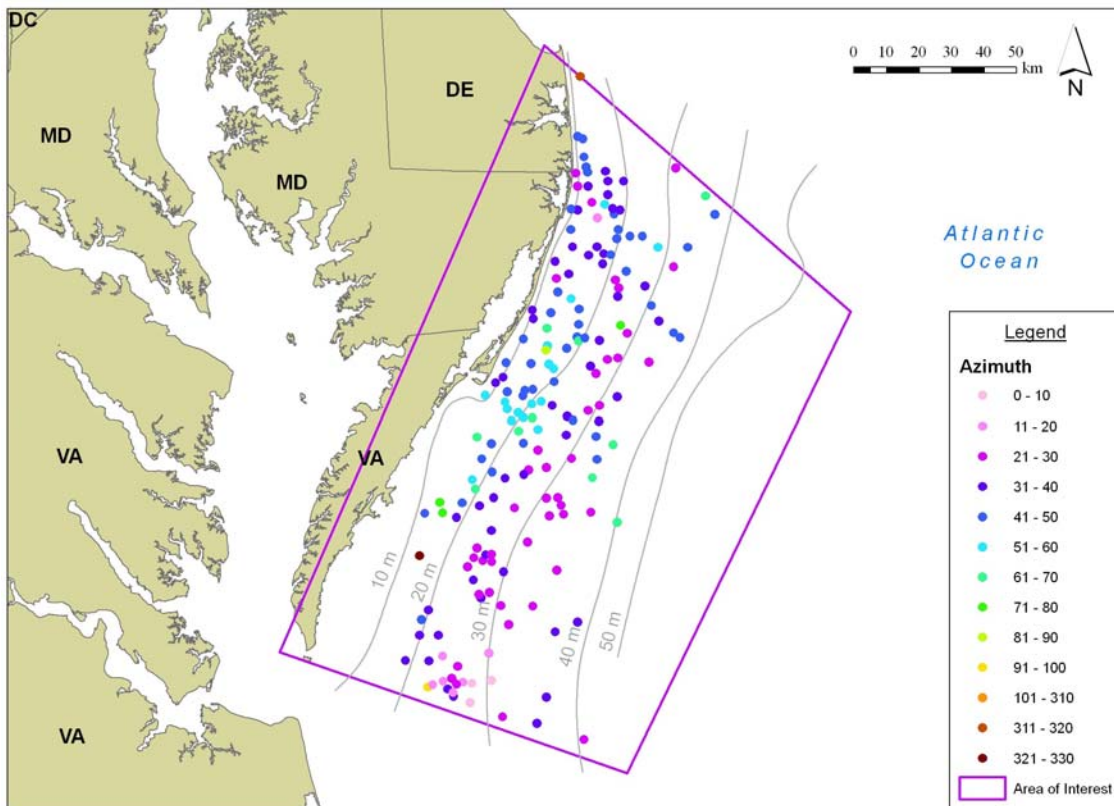
Figure 5.42 Spatial distribution of shoal Azimuth in the study area

A plot of shoal Azimuth vs. Crest Depth (Figure 5.43) shows an overall decreasing trend in shoal Azimuth with increasing Crest Depth. Shoals with smaller Crest Depth have an Azimuth closer to NE direction, while shoals with larger Crest Depth fall more in the 10° to 40° azimuth range. This is because of the fact that shoals with smaller Crest Depth are more influenced by waves and their corresponding focusing process. Such shoals occur mostly in 10 m to 25 m Base Depth range. As mentioned earlier, it is possible that shoals in 25 m to 35 m depth range belong to an earlier historic wave climate with more northerly wave components.
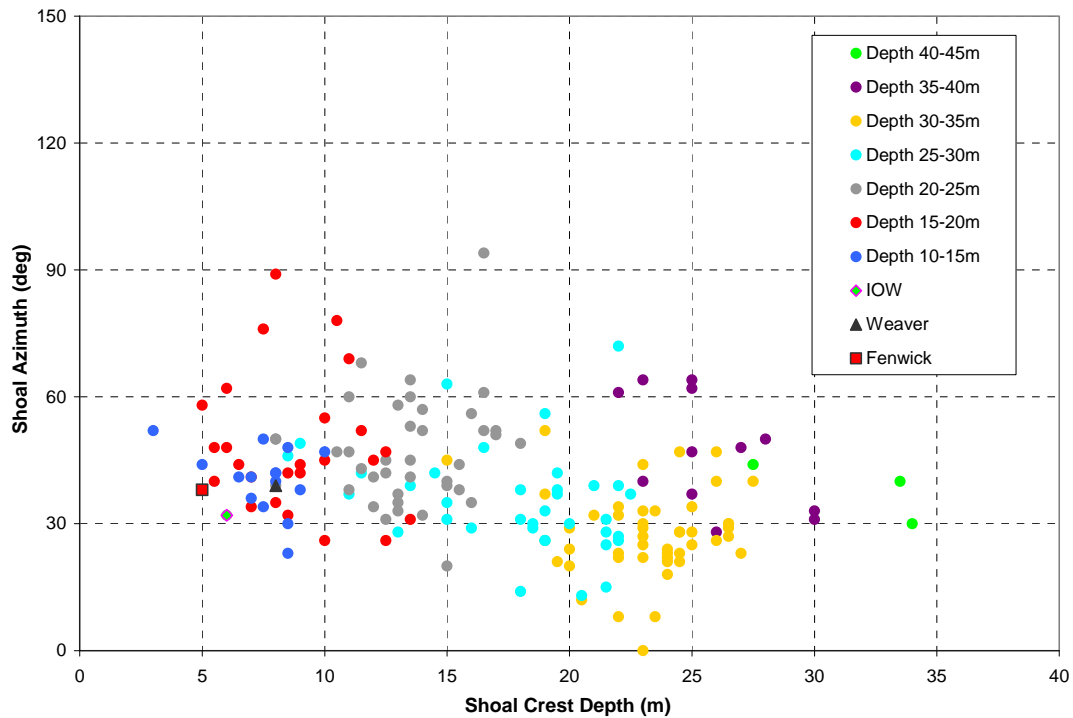
Figure 5.43 Shoal Azimuth vs. Crest Depth

A plot of shoal Azimuth vs. Length is presented in Figure 5.44 and indicates that longer shoals have more or less an NE orientation, emphasizing the importance of wave action on shoal elongation (Length growth).
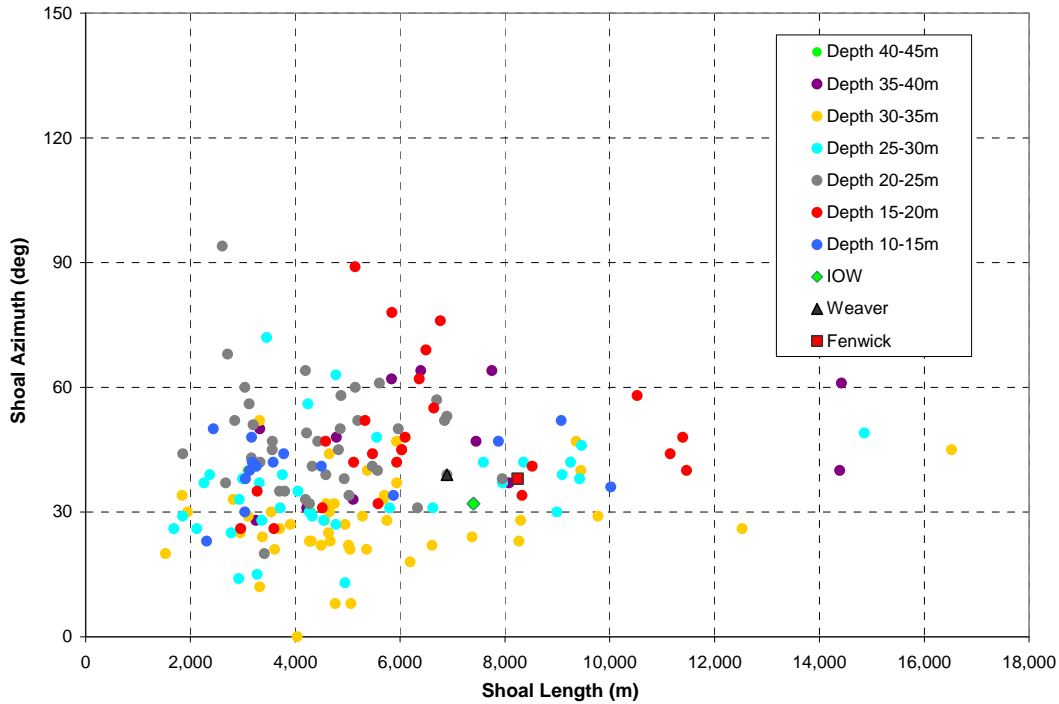
Figure 5.44 Shoal Azimuth vs. Length

One of the objectives of the present analysis was to look for possible universal criteria for protecting the morphologic integrity of shoal features. Such criteria, if they exist, have to be in the form of dimensionless characteristics such as ratios of Crest Depth to shoal Height, Length to Width etc. An analysis using dimensionless variables H/L, H/W, H/BD and W/L is provided in the following.

A plot of H/L vs. BD is provided in Figure 5.45. H/L ranges from 1/1000 to 5/1000 (1/200). The range is narrower in shallower water (< 20 m) and is between 1/1000 to 2/1000, obviously because shoal Height is limited by water depth. For IOW, H/L=2/1000.

Figure 5.46 provides a plot of H/W vs. BD. H/W ranges from 1/500 to 1/100. Isle of Wight has an H/W value of about 1/200.

A plot of W/L vs. H/BD is provided in Figure 5.47. W/L ranges between 0.2 and 0.8, but is mostly in the 0.2 to 0.6 range (i.e. shoal Length is generally 1.5 to 5 times of the shoal Width). The relative shoal height (H/BD) ranges from 0.2 to 0.75. Shoals with higher H/BD values (H/BD > 0.5) have W/L values smaller than 0.4 and are therefore more elongated. IOW and Fenwick have H/BD values of 0.71 and 0.74, respectively, (i.e. they have grown nearly to the maximum relative shoal height). For Weaver, H/BD value is 0.62. They have W/L ratios just under 0.4 (i.e. shoal Length is roughly 2.5 times the Width).
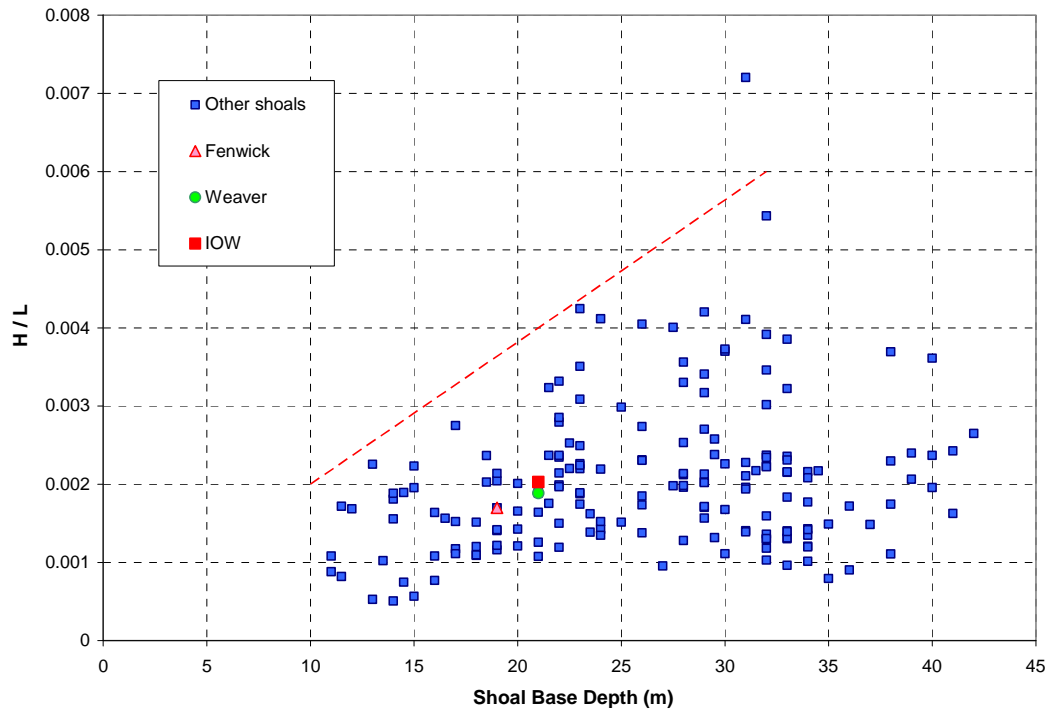
Figure 5.45 H/L vs. Base Depth
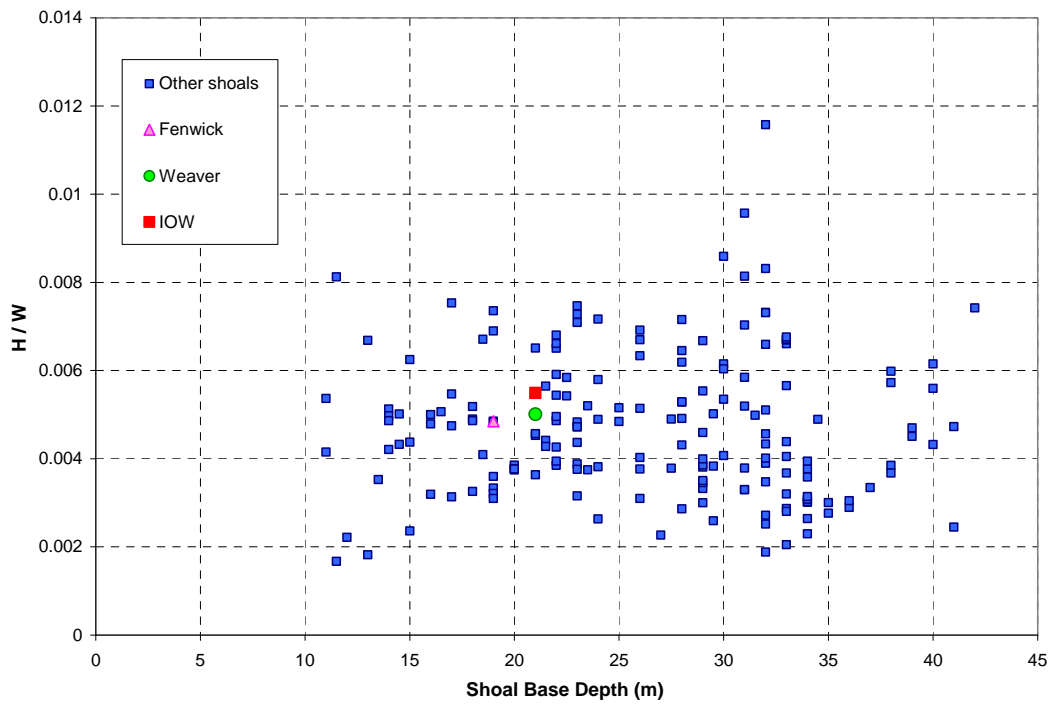
Figure 5.46 H/W vs. Base Depth
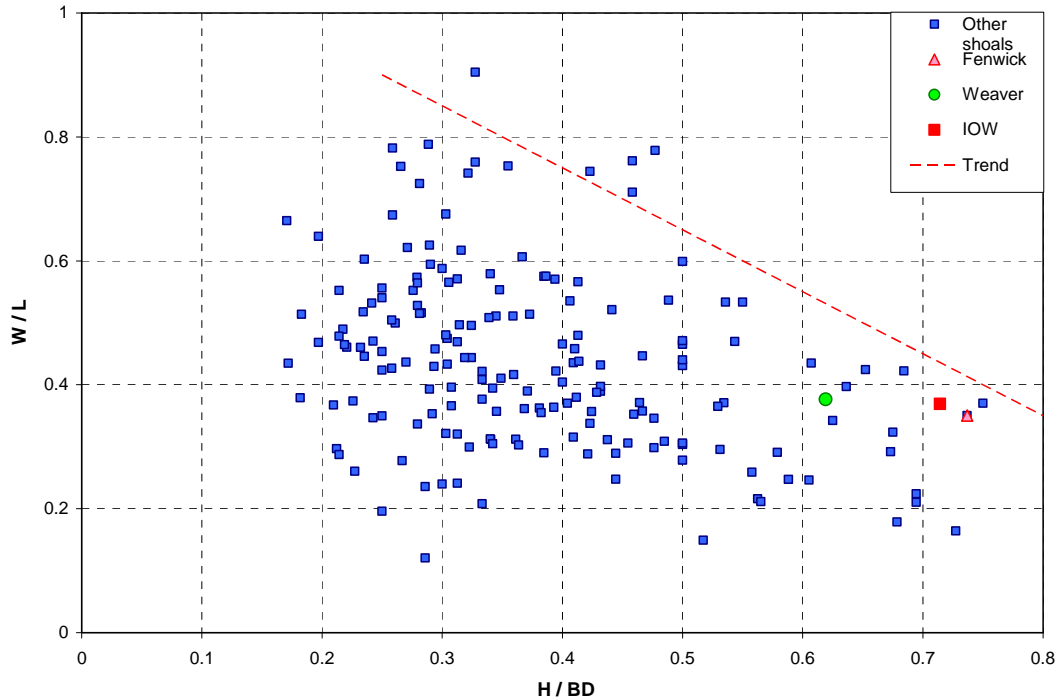
Figure 5.47 W/L vs. H/BD

Figure 5.48 presents a plot of H/BD vs. shoal Length. This plot suggests that there is an upper limit for H/BD value at each shoal Length. The maximum H/BD value of 0.75 occurs at a shoal Length of about 10 km. Maximum value of H/BD at each shoal Length becomes smaller for both shorter and longer length values, although sample population for longer shoals is small. This suggests that longer shoals have the potential to grow higher, indicating a wave-dominated shoal maintenance mechanism.
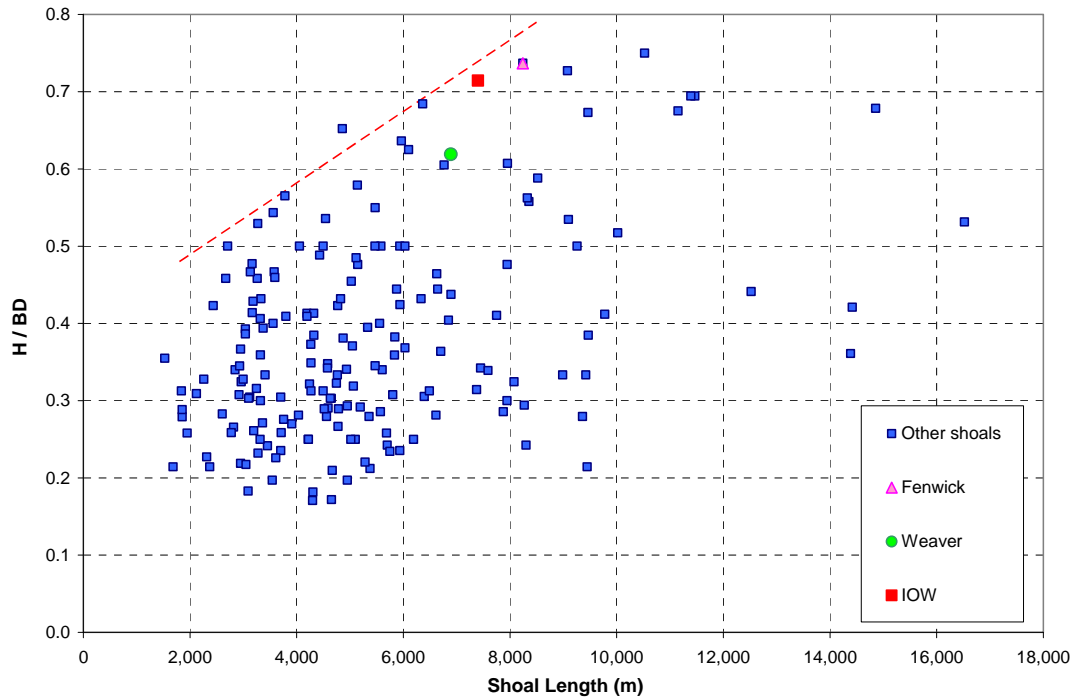
Figure 5.48 H/BD vs. Length

The plot of W/L vs. BD presented in Figure 5.49 indicates that W/L is generally smaller in shallower depths, i.e. shoals with shallower Base Depth tend to be more elongated than those in deeper water. However, note that the data is largely scattered.

Figure 5.50 provides a plot of W/L vs. shoal Height. No clear trend is observed.   Higher shoals (> 14 m) have W/L between 2 to 4. W/L for Fenwick, Weaver and IOW is between 2.5 and 3.
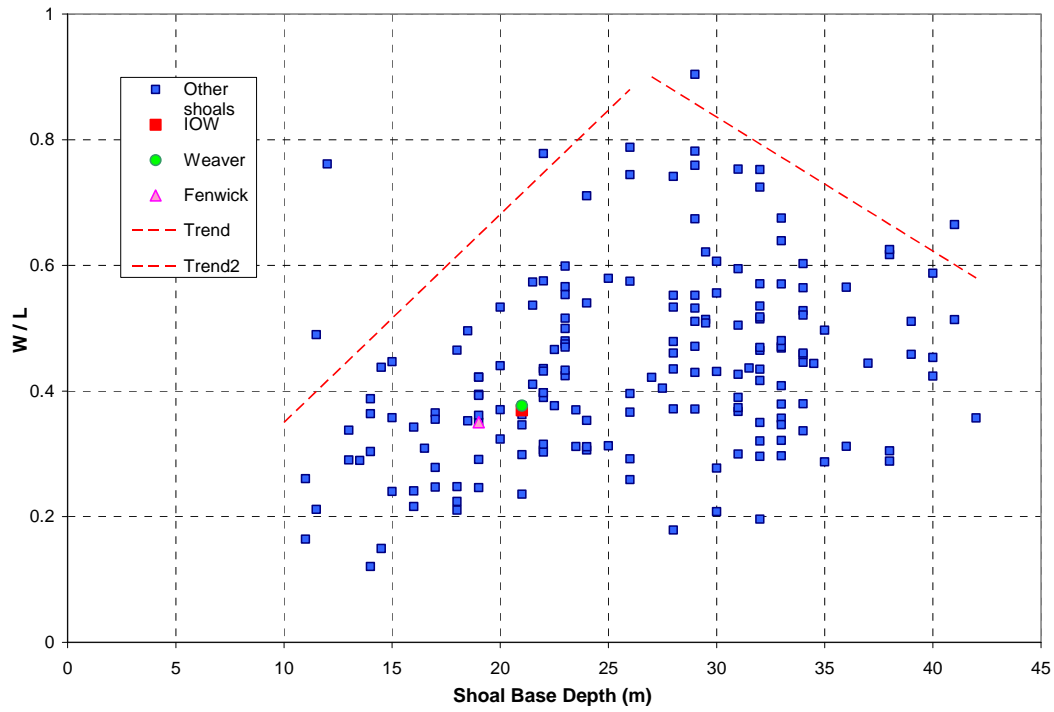
Figure 5.49 W/L vs. Base Depth
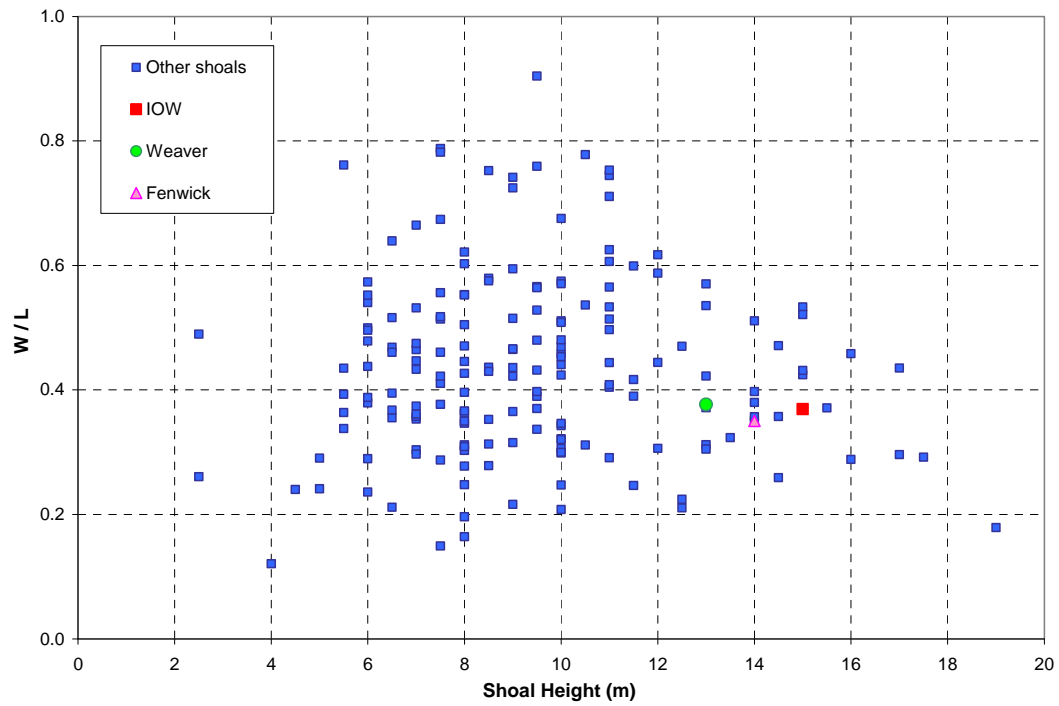
Figure 5.50 W/L vs. shoal Height

Summary:

More than 180 offshore shoals were identified and analyzed in the study area. The dataset contains a wide range of shoals resulting in large scatter when shoal parameters are plotted against each other. A universal relationship was not observed between those parameters. Nevertheless, several important trends provided insight into shoal behavior and morphologic evolution. The data suggests that wave influence on the shoals is limited to shoals with Base Depth of less than 30 m. Waves were found to be the primary factor in shoal height growth and maintenance (as opposed to currents that have a greater influence on shoal migration as discussed later in Section 6.7 of this report).

The Shoal Height Growth Zone was identified to be between 10 m and 30 m depth. This zone was further divided into two areas. In the 10 m to 20 m depth range, shoals can potentially grow in height up to the minimum Crest Depth of 5 m. In the 20 m to 30 m depth range, shoals may still grow but to a lesser extent. The 20 m to 30 m Base Depth range is a transition zone over which the predominant forcing changes from wave-dominated at 20 m depth to current-dominated at 30 m depth.

The Relative Shoal Height defined as the ratio of shoal Height to Base Depth (H/BD) was found to be an appropriate indicator of the shoal growth. $(H/BD)_{max}$ varies from 0.5 at 10 m depth to 0.75 at 20 m depth. A shoal that has reached the maximum relative shoal height of its Base Depth may be considered to be a fully grown shoal at that depth, but may still grow under rising sea levels. Such a shoal is more likely to re-grow and rebuild itself to the same height upon being dredged.

Maximum shoal Width, Length and Base Area all increase to approximately 35 m depth and decrease thereafter. Maximum shoal Height increases to approximately 30 m depth, but the rate of increase in the 20 m to 30 m depth range (i.e. in the transition zone) is less than the same rate in the 10 m to 20 m depth range. As a result, maximum shoal volume increases to approximately 35 m depth and decreases thereafter. However, the rate of increase in shoal Volume in the 20 m to 35 m depth range is less than the same rate in the 10 m to 20 m depth range.

Larger shoals are located in 15 to 25 m depth range and are oriented more or less in NE direction. They have length to width ratios of greater than 2. However, not all the shoals in the above depth range have grown to the same extent. Although some of these shoals may still grow/be growing (particularly under rising sea levels), it is likely that shoal growth is not entirely a function of wave influence and other factors such as initial shoal geometry/geology, sand availability, proximity to other shoals, etc. are also important. At a certain depth, shoals that have reached their corresponding maximum relative shoal height are more likely to re-grow once they are dredged.

Shoals located in waters deeper than 30 m show a decrease in height with increasing depth representing a possible Shoal Height Decrease Zone beyond 30 m depth. These shoals are not expected to grow, once being dredged. On a transgressive shoreline and considering that shoals are created at the shore, the age of a shoal is directly related to distance from shore. There is a

group of shoals in 25 m to 35 m Base Depth range featuring a more northerly orientation (10° to 40°) relative to the shoals in other depth ranges. It is possible that this group of shoals belong to a previous historic time with a more northerly wave climate.

6.0   NUMERICAL MODELING

Development of the morphology model is discussed in this section. Our modeling approach was finalized mainly based on the findings from field measurements regarding driving forces as discussed in Section 6.1. The morphology model requires several modules for calculation of waves, currents, sediment transport rates and corresponding changes in bottom elevations. A model selection discussion is provided in section 6.2. Section 6.3 presents the selected calculation domain, while sample calculation results are provided in Section 6.4. The model was run for the conditions of field measurements and the results are evaluated against the measured data in section 6.5. A discussion of selection of input driving forces for long-term morphology simulations is provided in section 6.6. In Section 6.7, model runs are completed for existing conditions and long-term evolution of the Isle of Wight shoal is predicted. Model predictions are compared with historical evolution of this shoal since 1929.

6.1   Modeling Approach

The modeling approach was finalized based on the findings from field measurements regarding driving forces. Note that in sections 6.1 through 6.5 the 3-month field measurement data is used for model selection, testing, and model validation. Development of model input driving forces for simulation of long-term morphologic evolution of shoals is discussed in Section 6.6.

An analysis of the field data was completed in Section 5 to identify the processes and driving forces involved in morphological evolution of the shoals. The results indicated that there are three driving forces that could affect movement of the sediment in the study area, i.e. waves, tides and subtidal currents. In order to examine the relative contribution of each component, the complete recorded near-bottom velocity data was given as input to a sediment transport model and the corresponding transport rates were calculated.

Figure 6.1 shows the resulting cumulative sand transport volumes from March 1, 2007 for about 3 months (calculated using Van Rijn sediment transport model). In this figure, transport rates are presented as two east-west and north-south components that are positive eastward and northward, respectively. They have been calculated for three different combinations of driving forces, namely; 1) waves only, 2) waves and tides, and 3) waves, tides and subtidal currents (called as waves and currents in the figure). Two important observations are made from this figure. The first observation is that sediment transport mainly occurs under certain storm events such as the event around Day 17 (March 17) or the one around Day 66 (May 6). These are both nor'easter events. The second observation is related to contribution from each forcing mechanism. It is observed that while inclusion of tides (more precisely tidal currents) has only a minor effect on the transport rates, inclusion of subtidal currents almost doubles the calculated transport volumes.

The above analysis indicates that synoptic scale pressure gradients associated with nor'easters result in large scale circulations that play an important role in movement of sediment in the study area. These sediment transport calculations for representative conditions indicate that the

contribution of subtidal currents is as important as that from nor'easter waves themselves. Calculation of large scale circulations across Northwestern Atlantic Ocean requires complicated coupled meteorological and hydrodynamic modeling and is beyond the scope of the present study. The other alternative is to use the measured wave and flow conditions as the input driving force to the model. Using the measured data has the advantage that it includes both locally generated and large scale wave and current events.

Our approach is, therefore, to use the measured wave and flow conditions as the input driving forces to the shoal morphology evolution model. Input conditions would include waves and tidal and subtidal currents at the offshore boundary of the calculations domain. Waves will be transformed through the calculation domain using a spectral wave transformation model. A hydrodynamic model will be used to calculate currents inside the calculation domain. Subsequently, sediment transport rates and corresponding shoal morphology change will be calculated.
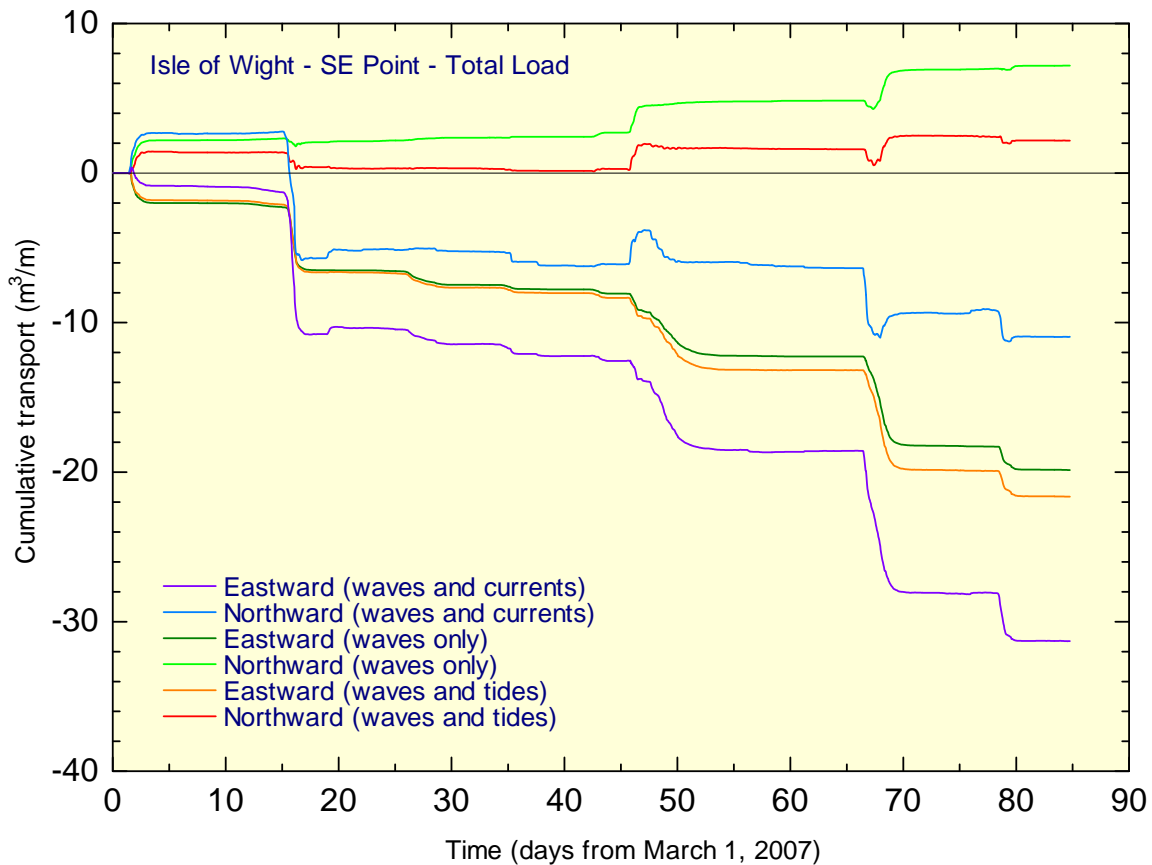
Figure 6.1 Cumulative sediment transport volumes calculated for the period of field measurements using Van Rijn sediment transport model.

6.2   Model Selection

As discussed in section 5.5, waves are believed to have a primary role in the growth and maintenance of shoal features. Therefore, accurate simulation of waves over the calculation domain is of critical importance. An analysis of calculated wave field over the shoals by standard spectral wave models and its sensitivity to wave direction and grid orientation was completed and the results are presented in this section. It is noted that the accepted rule is that standard (half-plane) spectral wave models (such as the Baird in-house *HYDROSED*, STWAVE or MIKE21 NSW) can handle wave directions of up to 45 deg relative to the grid orientation (in the direction of wave propagation). It is, therefore, expected that a north-south (N-S) grid can handle NE waves (nor'easters) as well as other more frequent waves from E and SE directions for the present study area.

For this sensitivity analysis, transformation of 45 deg (NE) incident waves (H= 4 m and T=10 s) over the shoals was examined using two different grids. One is a large N-S grid and the other a 45° rotated grid. The N-S grid was extended beyond the shoals area to both north and south to completely avoid the effect of lateral boundaries. The rotated grid is aligned with the incident wave direction and expected to provide the base results for comparison. Figure 6.2 shows the two calculation domains (note that north is to the left of this figure and east is to the top). The Isle of Wight (IOW) Shoal is the most right of the three shoals in the middle of the rotated grid.
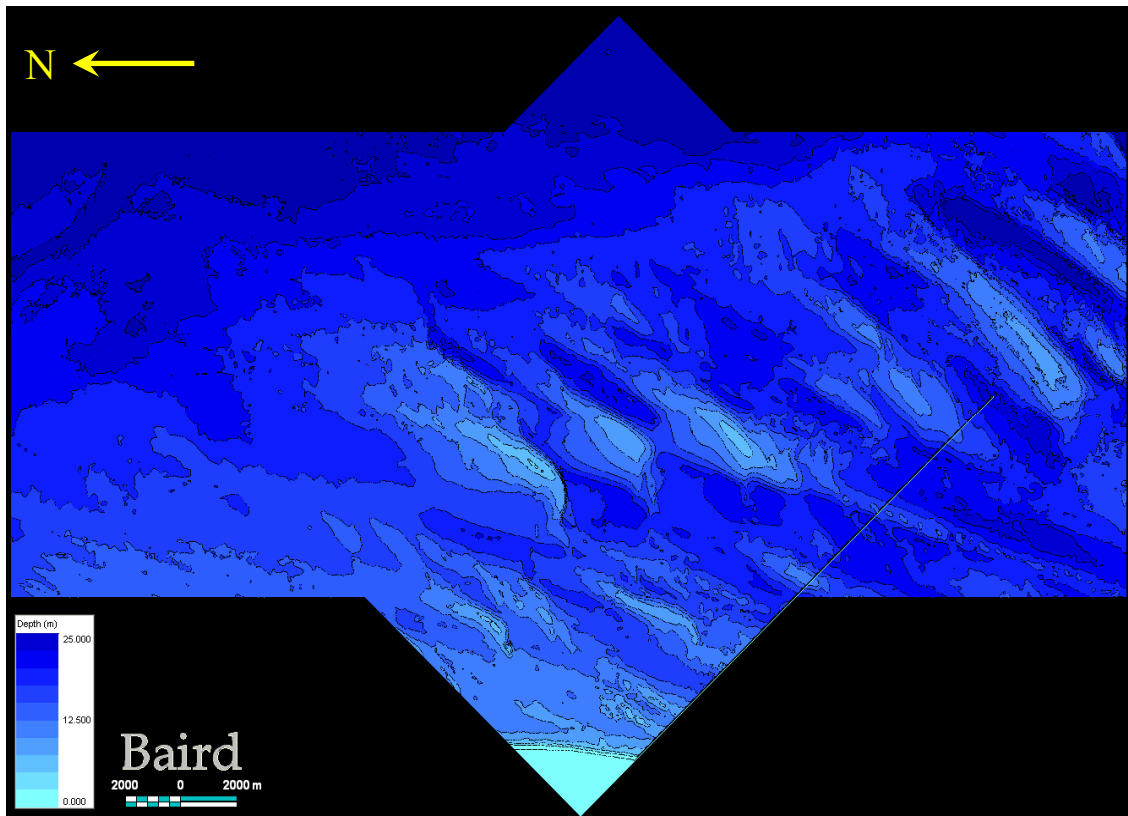
Figure 6.2 N-S and rotated calculation grids

Calculation results by *HYDROSED* are shown in Figure 6.3. Red vectors correspond to the large N-S grid. It is observed that with the N-S grid, wave refraction occurs mostly on the SE flank of the IOW shoal, while with the rotated grid, refraction occurs equally on both SE and NW flanks. The difference in wave direction around IOW Shoal is up to 15 degrees. Discrepancy in calculated wave directions is more dramatic on the curved slope south side of the Fenwick Shoal (first shoal from the left). Similar results were obtained with STWAVE and MIKE21 NSW half-plane models.

Generally, these shoals feature a number of slopes in various directions and provide severe conditions for refraction and wave focusing calculations by conventional half-plane spectral wave transformation models. This results in inaccuracies in calculated wave directions even if the models are applied within the recommended ±45° limitation.
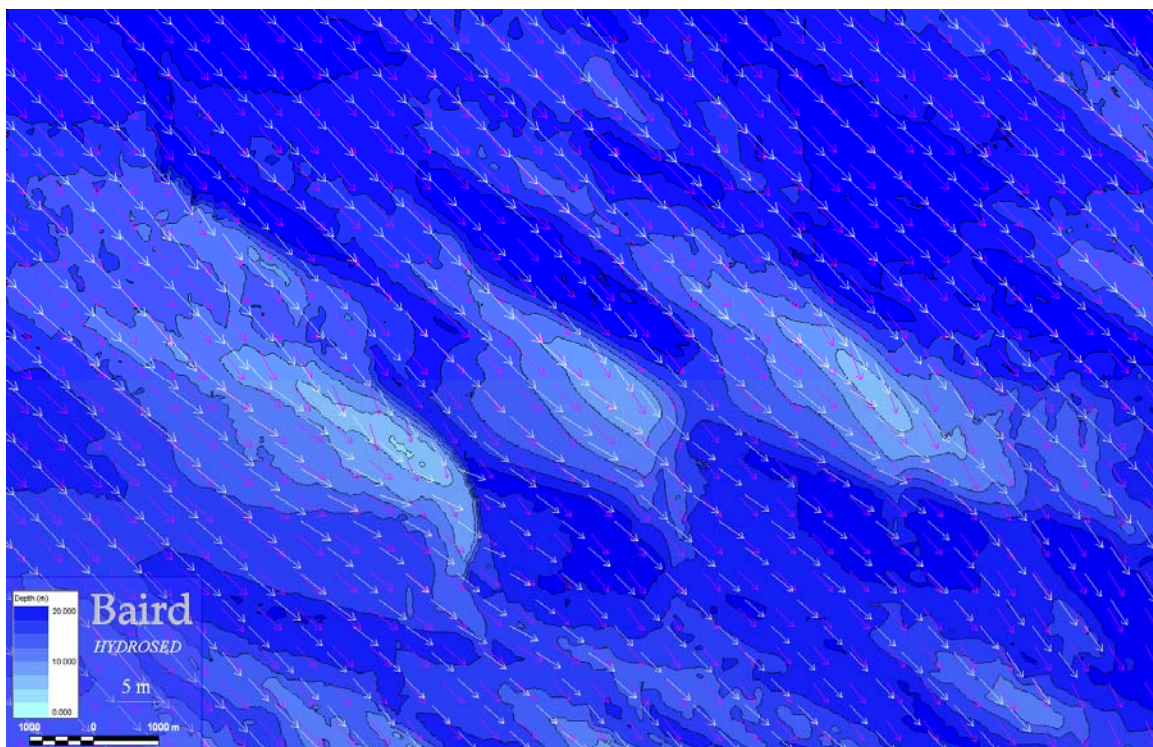
Figure 6.3 *Calculated wave directions using half-plane spectral models for the two different grids. Red vectors correspond to the large N-S grid.*

It is not practical to rotate the grid for every wave direction. Therefore, the option to improve the accuracy of wave direction calculations over the shoal is to use a full-plane wave model. Calculated wave directions using SWAN and MIKE21 SW full-plane wave models are shown in Figures 6.4 and 6.5, respectively. Figure 6.4 shows that SWAN results with the N-S grid are in close agreement with *HYDROSED* results using rotated grid. Similarly, Figure 10 shows that calculated wave directions by MIKE21 SW full-plane model are insensitive to the choice of grid (N-S vs. rotated) and in either case are in close agreement with *HYDROSED* results using rotated grid.
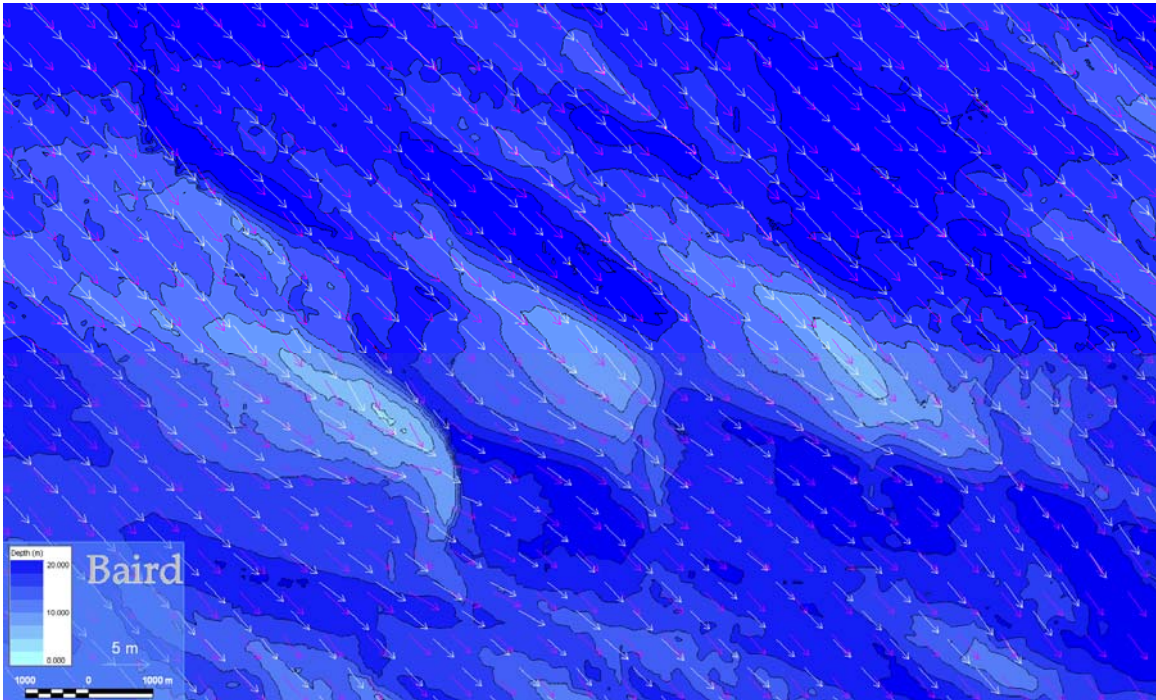
Figure 6.4 *HYDROSED* **wave directions (white) using the rotated grid vs. SWAN wave directions (pink) using the N-S grid**
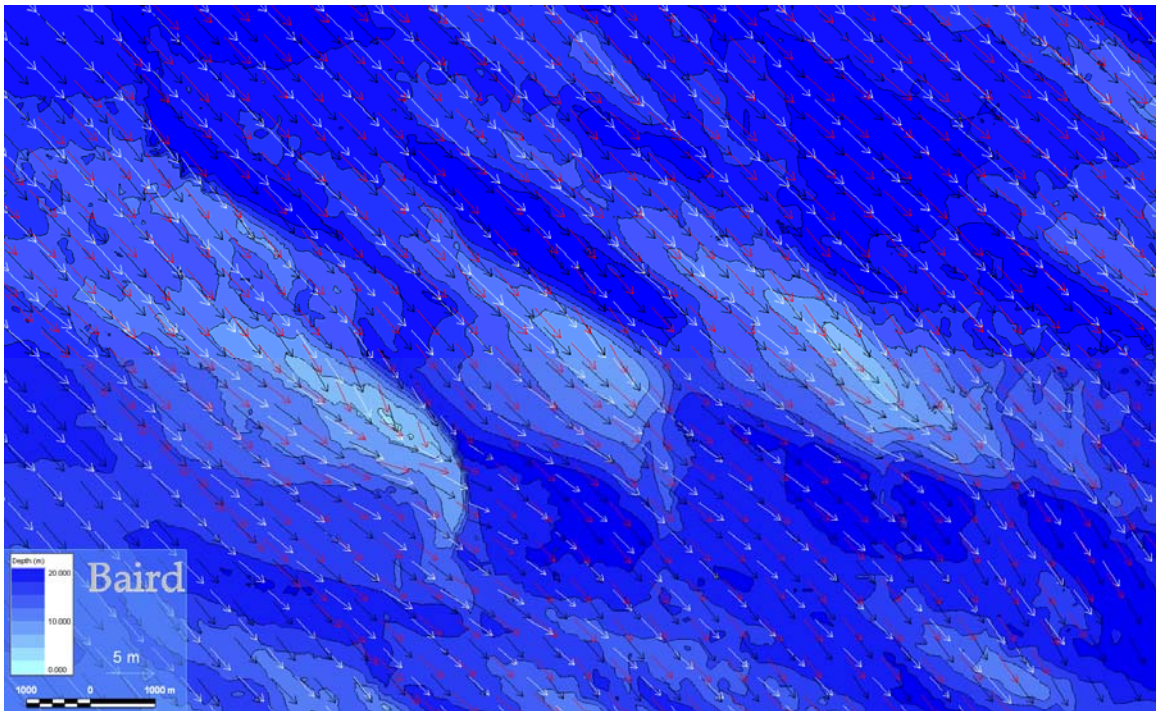
Figure 6.5 *HYDROSED* **wave directions (white) using the rotated grid vs. MIKE21 SW wave directions (black) using the N-S grid and MIKE21 SW wave directions (red) using the rotated grid**

It was, therefore, decided to use the SWAN model for the current morphology simulation effort. The advantage of SWAN was that the source code is publicly available and could be integrated into the morphology model.

A simple hydrodynamic module was developed and integrated into the morphology model to calculate currents within the calculation domain. The main concern was regarding the significant calculation time generally required by hydrodynamic models to converge. For long-term morphology change simulations, this could lead to impractical simulation times. Therefore, a site-specific finite difference depth-averaged hydrodynamic model was developed to minimize the required calculation time. The hydrodynamic model is derived by input depth-averaged current conditions at the model boundary as well as radiation stresses predicted with the spectral wave transformation model to calculate tidal, subtidal, and wave generated currents within the calculation domain. The model is based on depth-averaged momentum and continuity equations proposed by Nishimura (1988). Wind forcing is not applied within the calculation domain of the hydrodynamic model, but the effect of winds is included on the input currents at the domain boundary.

Two sediment transport formulations were considered for this study: 1) the sediment transport formulation of Van Rijn for waves and depth averaged currents (Van Rijn 1993, 2000), and 2) the sheet flow transport formulation of Dibajnia and Watanabe (1992) as extended by Dibajnia et al (2001) and referred to as D&W formula hereafter. It is expected that sheet flow transport is predominant over the shoals during extreme nor'easter events. The two models provided very similar results. The D&W formula was used as it required less calculation time.

6.3   Model Domain

A large calculation domain was selected containing Fenwick, Weaver and Isle of Wight shoals to incorporate possible effects of neighboring shoals and bathymetry on the wave and current fields around Isle of Wight. The calculation domain was 16.5 km in east-west direction and 26.64 km in north-south direction as shown in Figure 6.6. The calculation domain is surrounded by water (open boundary) without any land boundary. For calculation of currents by the hydrodynamic model, however, at least one closed boundary is required to avoid model instabilities. Therefore, the calculation domain was doubled towards the west by repeating the bathymetry as shown in Figure 6.7.

Different grid sizes were used for different modules of the morphology change model. For the SWAN wave model, a 60 m × 60 m mesh was used resulting in a 275 × 441 grid. For the hydrodynamic model, the mesh size was increased to 120 m × 120 m to keep calculation time within practical limits. For the sediment transport and morphology change model a finer 30 m × 30 m mesh was used to better capture shoal movement which is expected to be in the order of only a few meters per year.
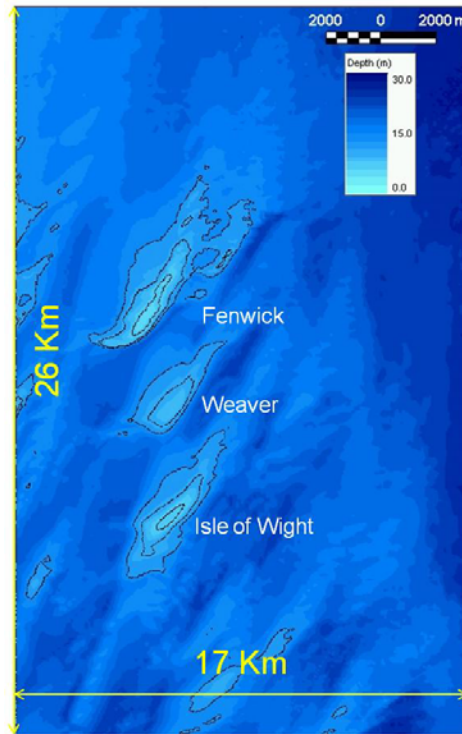
Figure 6.6 Calculation domain and bathymetry.
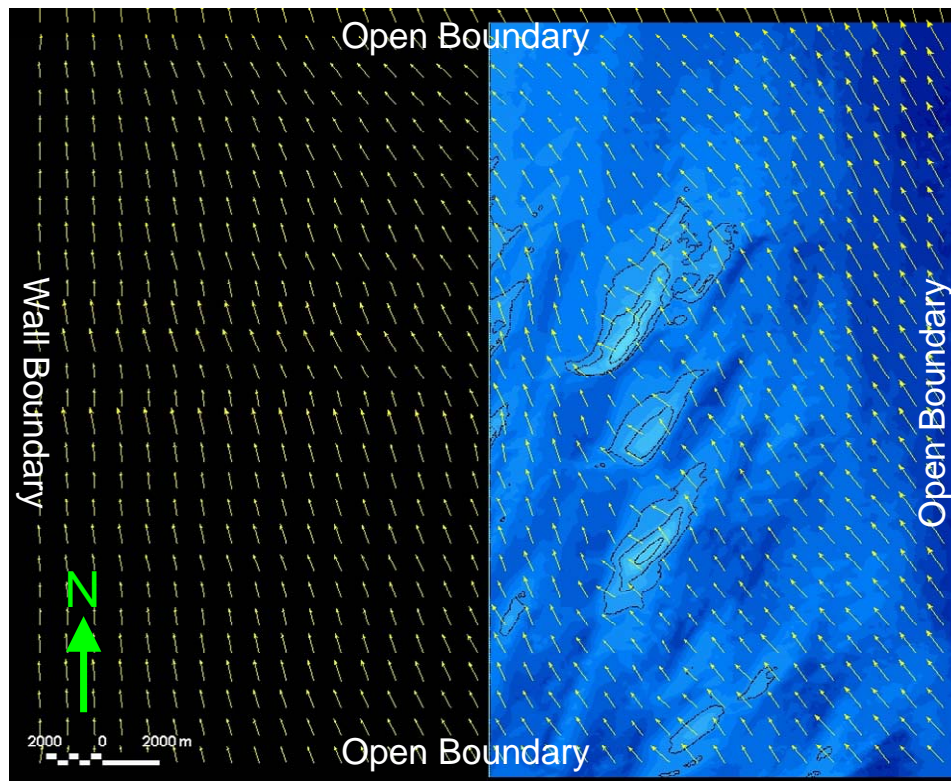
Figure 6.7 Calculation domain for the hydrodynamic model.

6.4 Sample Calculations

Two sample calculation results are presented in this section to demonstrate the model performance. Predicted waves, currents and sediment transport vectors are presented for each case.

Figure 6.8 shows waves and currents vectors for NE (45°) waves of H= 4 m, T=10 s with 0.5 m/s currents from the north. The conditions correspond to those during a rather strong nor'easter. Wave focusing over the shoals is notable in Figure 6.8, particularly over Fenwick and Isle of Wight shoals which have shallower crest depths compared to Weaver. Corresponding wave-induced radiation stresses force the currents on top of the shoals to run along the shoal axes (towards southwest). Figure 6.9 shows sediment transport vectors for the above conditions. Transport of sediment is mainly limited to shallower areas over the shoals. For Isle of Wight and Weaver, transport direction is towards the southwest under this wave condition. Over the Fenwick, transport is also towards southwest along the shoal crest, but becomes more southward over the west tail of the shoal.

Figure 6.8 Calculated wave height and direction (left) and current velocity vectors over bathymetry (right) for a nor'easter conditions (H=4 m, T=10 s waves from NE with 0.5 m/s currents from the north). Depth contours are also shown in both figures to identify shoal locations.

Figure 6.9 Calculated sediment transport rate vectors (m³/m/s) over bathymetry for the nor'easter conditions. Depth contours are also shown to identify shoal locations.

Figure 6.10 shows waves and currents vectors for SE (135°) waves of H= 4 m, T=10 s with 0.7 m/s currents from the southeast. The conditions correspond to those during a strong southeasterly event. It is mentioned again that southeasterly events are not as frequent as nor'easters. Waves follow classical refraction processes without significant wave focusing over the shoals under these conditions. The input current from southeast is slightly modified over and around the shoals but maintains it overall direction towards southeast. Figure 6.11 shows sediment transport vectors for the above conditions. As in the previous case, transport of sediment is mainly limited to shallower areas over the shoals. For Isle of Wight, Weaver and Fenwick, transport direction is towards the northwest under this wave condition.
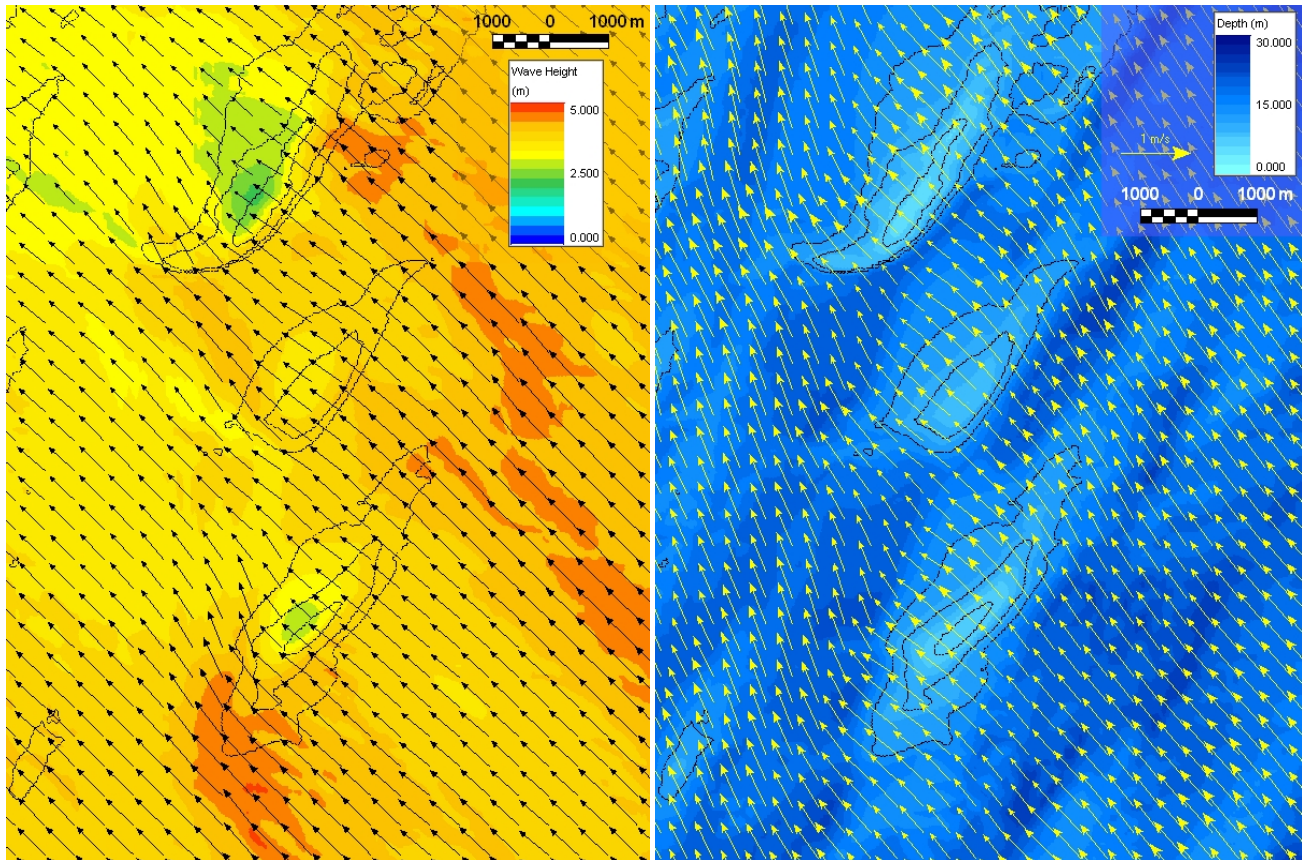
Figure 6.10 Calculated wave height and direction (left) and current velocity vectors over bathymetry (right) for a southeasterly event (H=4 m, T=10 s waves from SE with 0.7 m/s currents from the southeast). Depth contours are also shown in both figures to identify shoal locations.

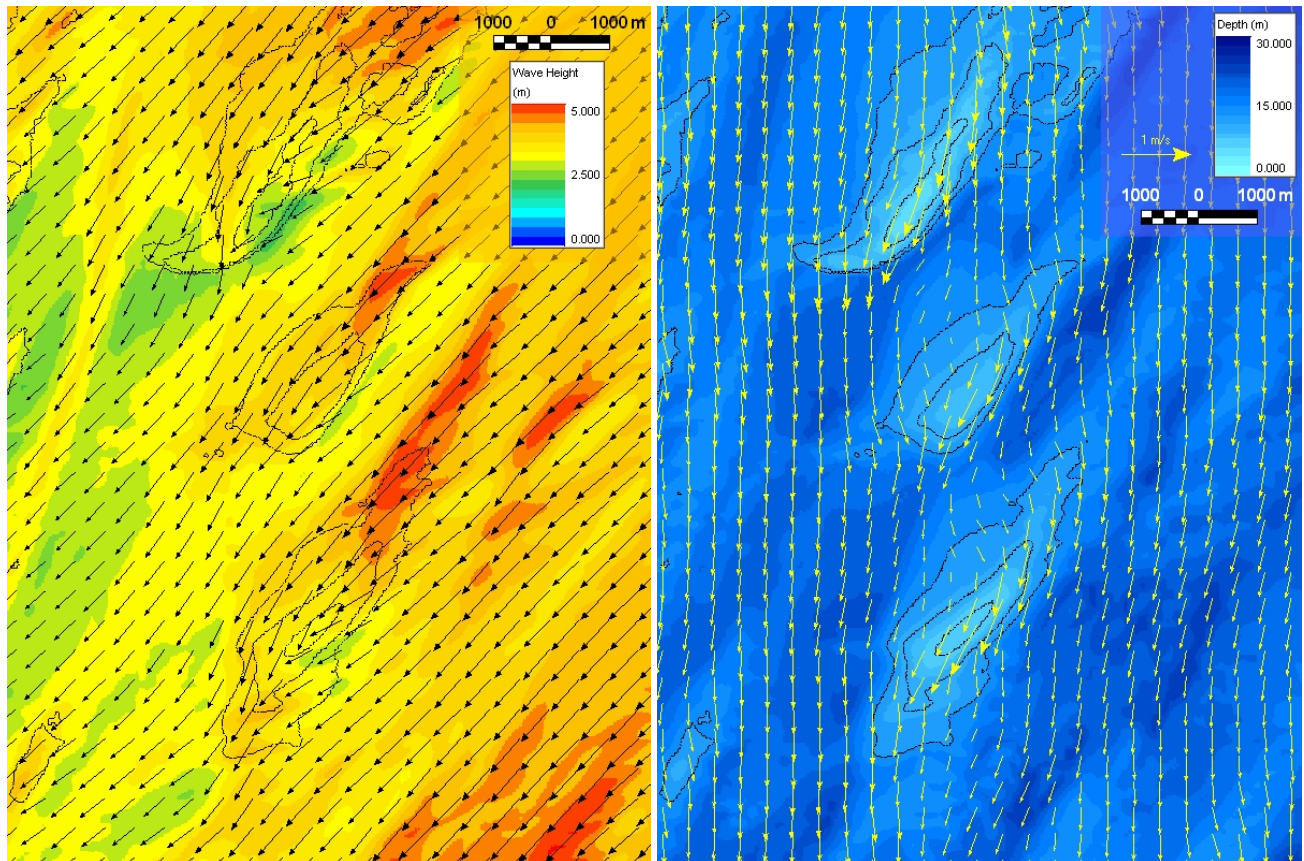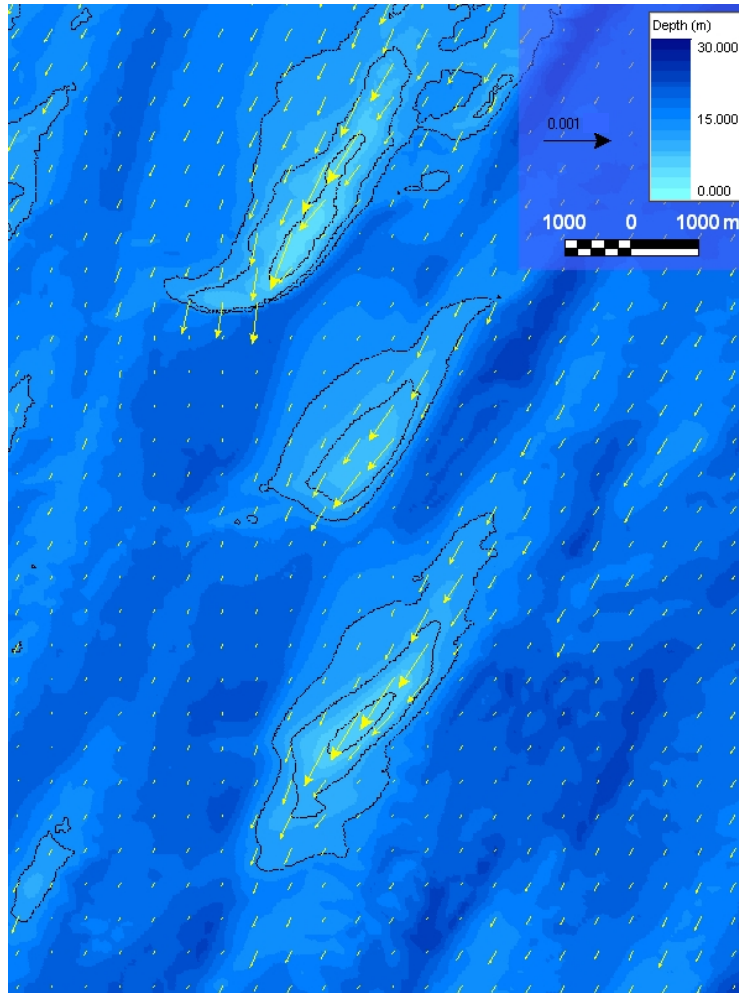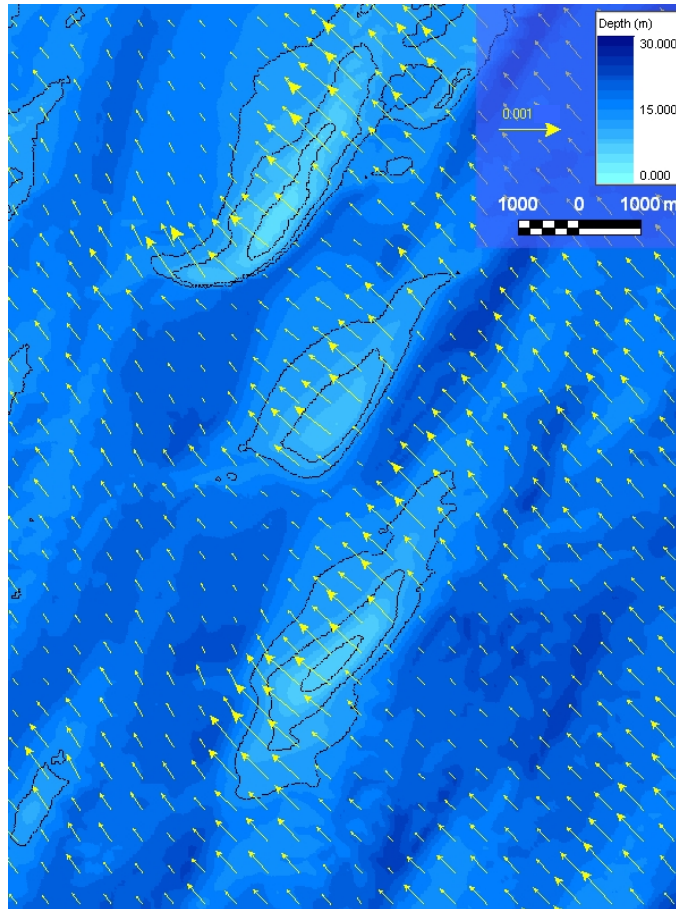**Figure 6.11 Calculated sediment transport rate vectors (m³/m/s) over bathymetry for the nor'easter conditions. Depth contours are also shown to identify shoal locations.**

6.5 Comparison with Measurements

Waves and depth-averaged currents measured by the deepwater ADCP (at 25 m depth) were used as input to the above model. Calculated waves and currents at the location of SE and NW ADCPs were compared with measurements. Figures 6.12 and 6.13 show comparisons between measured and calculated wave height at SE and NW ADCP locations, respectively. Modeled wave heights are in general slightly (10% to 20%) higher than corresponding measured values. Bottom friction and its corresponding energy dissipation were discarded in the wave calculations. It is noted that while bottom friction works to dissipate wave energy over a wide shallow shelf, winds may continue generating waves thus providing more energy to the wave field. It is therefore important to consider the effect of bottom friction and wind forcing simultaneously. Considering the large extent of the present calculation area, however, proper model calibrations to include the effect of winds and bottom friction require additional field data and analysis which are beyond the scope of this study. The observed differences are within the range of natural variability of the wave field at the study site. Therefore, the observed agreement with measurements is considered to be very good and sufficient for the purpose of long-term morphological modeling.
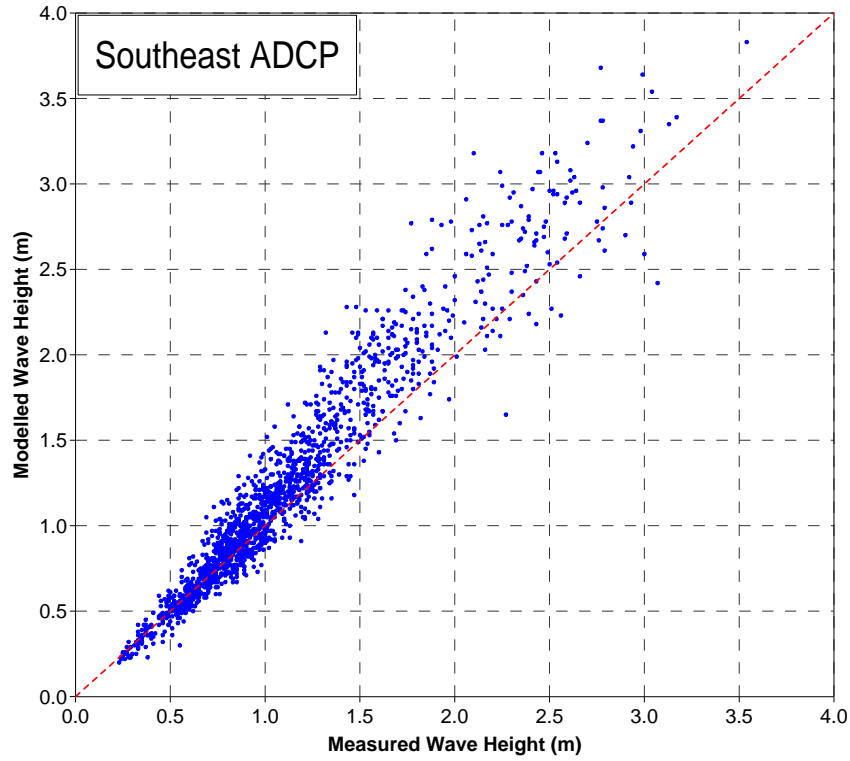
Figure 6.12 Measured vs. model wave height at SE ADCP.
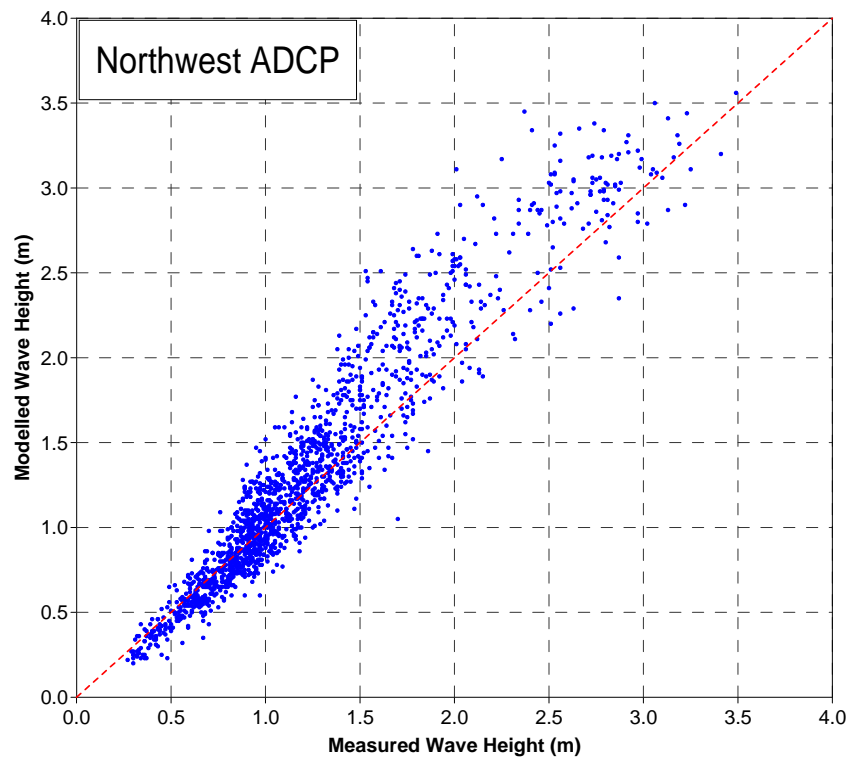
Figure 6.13 Measured vs. model wave height at NW ADCP.

Time series comparisons for 2 nor'easter events of March 17 and May 6, 2007, at SE and NW ADCP locations are shown in Figures 6.14 to 6.17. Shown in these figures in order from top to bottom panels are: measured and calculated wave direction, measured and calculated wave height, measured and calculated depth-averaged current velocity as well as input offshore current velocity, wind speed vectors as measured by NDBC Buoy 44009, measured and calculated depth-averaged current vectors, and measured and offshore input current vectors.

Figure 6.14 shows the comparison at SE ADCP location for the period of March 13 to 19, 2007, which includes the nor'easter event of March 17. Figure 6.14 indicates that the model does a great job in simulating wave height and direction during the storm event. Regarding simulation of the current velocity (third panel), the model performance between March 13 and March 16 is less than expected. Predicted currents are almost identical to the input deepwater currents and weaker than the measurements. Measured currents over the above period are believed to be wind-driven and the observed discrepancy is attributed to the neglect of winds over the calculation domain. Similarly from March 16 to March 18, i.e. during the storm, the model has underestimated the current velocity. In fact, Figure 6.14 indicates that the input offshore current velocity (green line in the third panel) better represents the measured current velocity (orange line) than the model predictions during the March 17 storm event. Looking at wind speed vectors (fourth panel) and measured velocity vectors (orange vectors in the fifth panel) it appears that subtidal currents during a nor'easter were further enhanced by the contemporary local winds. This resulted in an almost uniform depth-averaged current over the entire study area during the March 17 storm event. Figure 6.15 shows the comparison at NW ADCP location for the period of March 13 to 19, 2007. Results are similar to those of Figure 6.14.

Figures 6.16 and 6.17 show time series comparison results during the nor'easter event of May 6, 2007, at SE and NW ADCP locations, respectively. Again good agreement is observed between measured and predicted wave height and direction. Depth-averaged currents at SE and NW locations during the storm are better represented by the offshore input depth-averaged current velocity than by the model predictions. This is attributed to the effect of winds in enhancing the subtidal currents (note that synoptic scale pressure gradients result in both subtidal sea level rise and winds in the same direction). The subtidal component has a very long wavelength and its corresponding current velocity may be considered as uniform over the depth (long wave assumption). Wind driven currents are created by the wind exerting stress on the sea surface. This stress causes the surface water to move, and this movement is transmitted through vertical mixing to the underlying water to a depth that is dependent mainly on the strength and persistence of the wind. When the wind blows for a sufficiently long time, such as during a nor'easter, wind-driven currents extend to the sea bottom resulting in a well-mixed current profile. Under a uniform wind field, this results in a uniform depth-averaged current field.

It is possible that the model performance in simulating currents can be improved with the inclusion of winds. However, we note from Section 6.1 that sediment transport in the present study area mainly occurs during extreme events and, therefore, model performance in simulating extreme events is the most important. The above comparisons suggest that during extreme events it is sufficient to use the measured depth-averaged current velocity uniformly over the entire calculation domain.   The practice of inclusion of winds in the hydrodynamic model and

corresponding model calibrations, once completed, would provide similar results and was not pursued here.

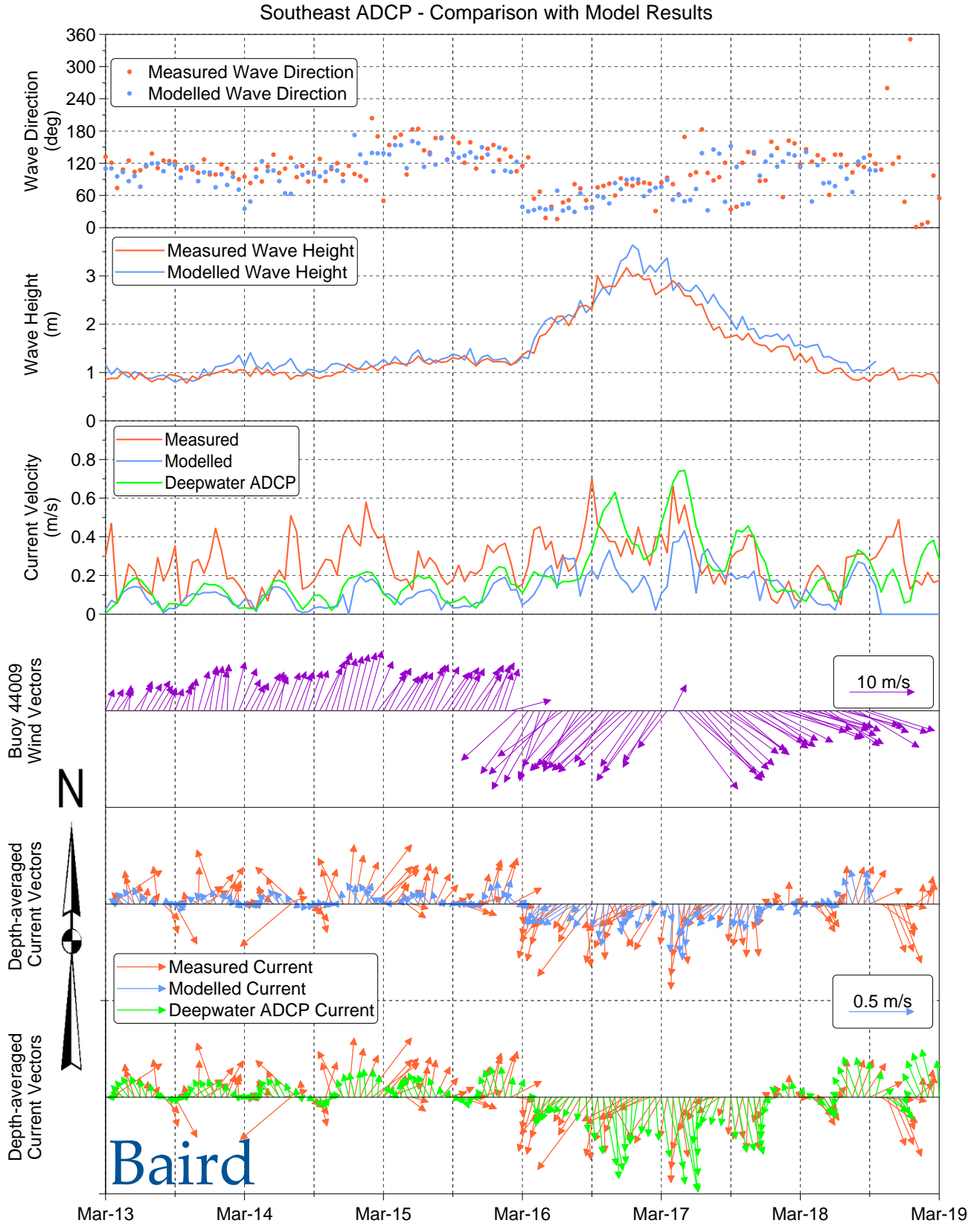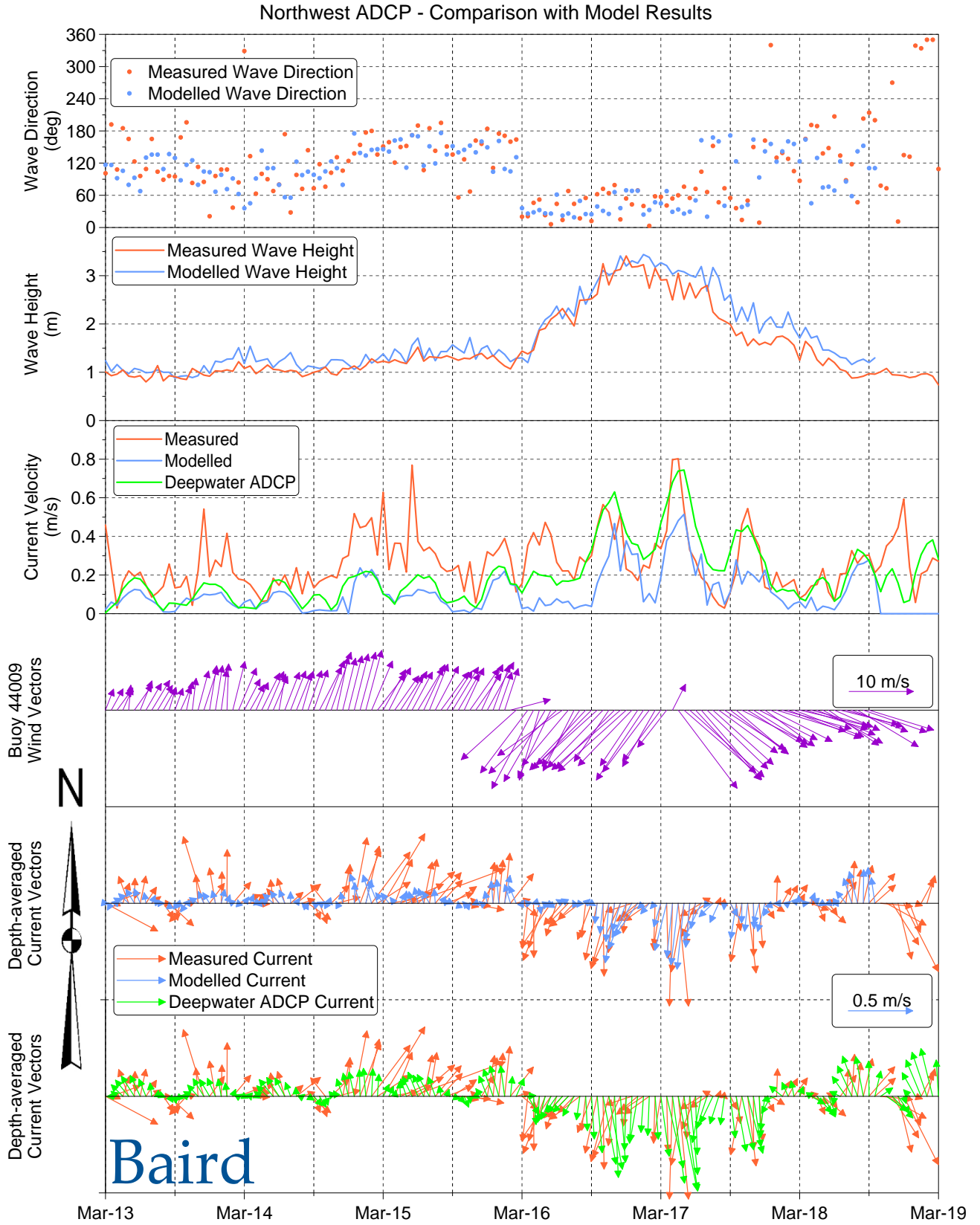**Figure 6.14 Measured vs. model waves and currents at SE ADCP for March 13 to 19, 2007.**

Figure 6.15 Measured vs. model waves and currents at NW ADCP for March 13 to 19, 2007.
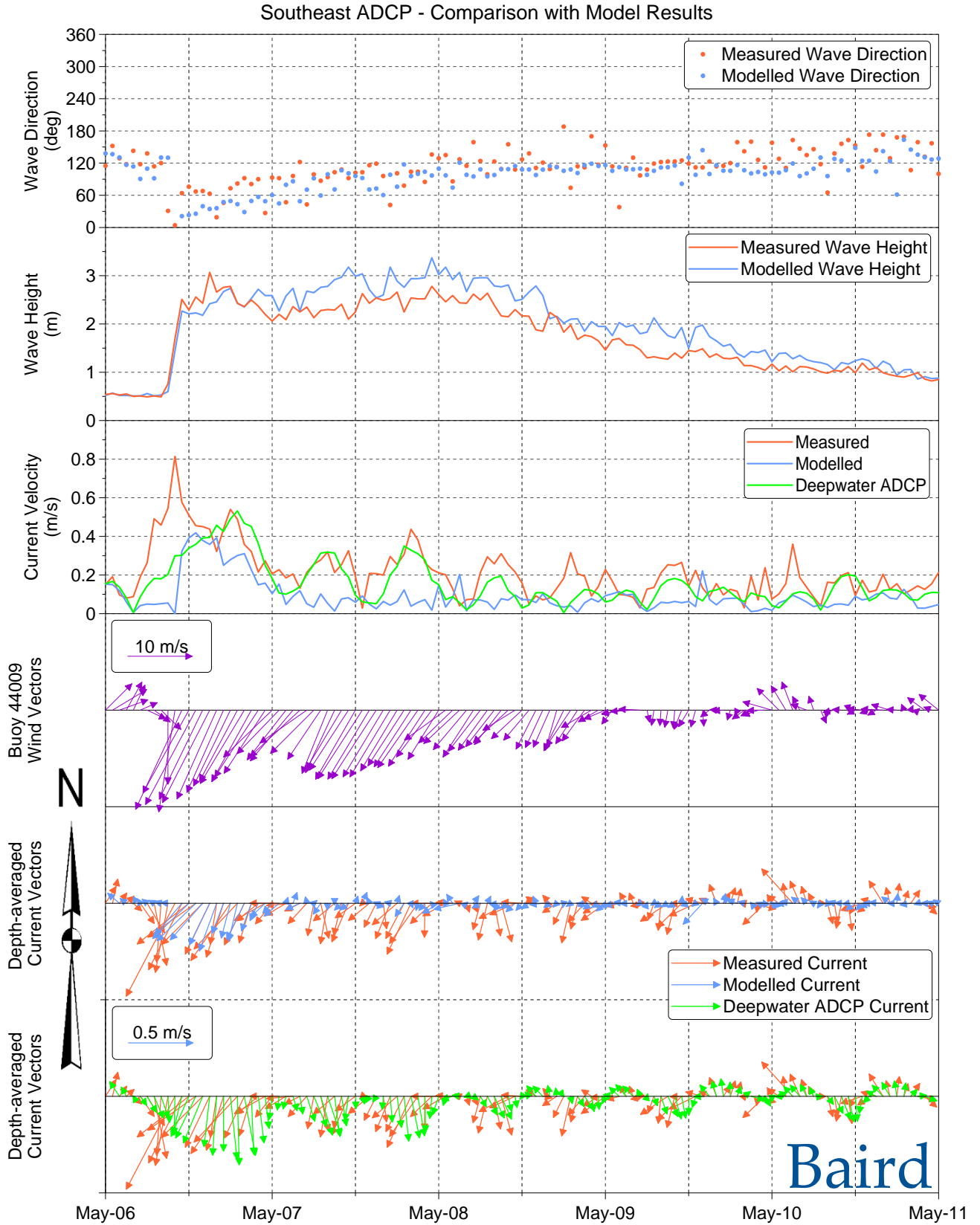
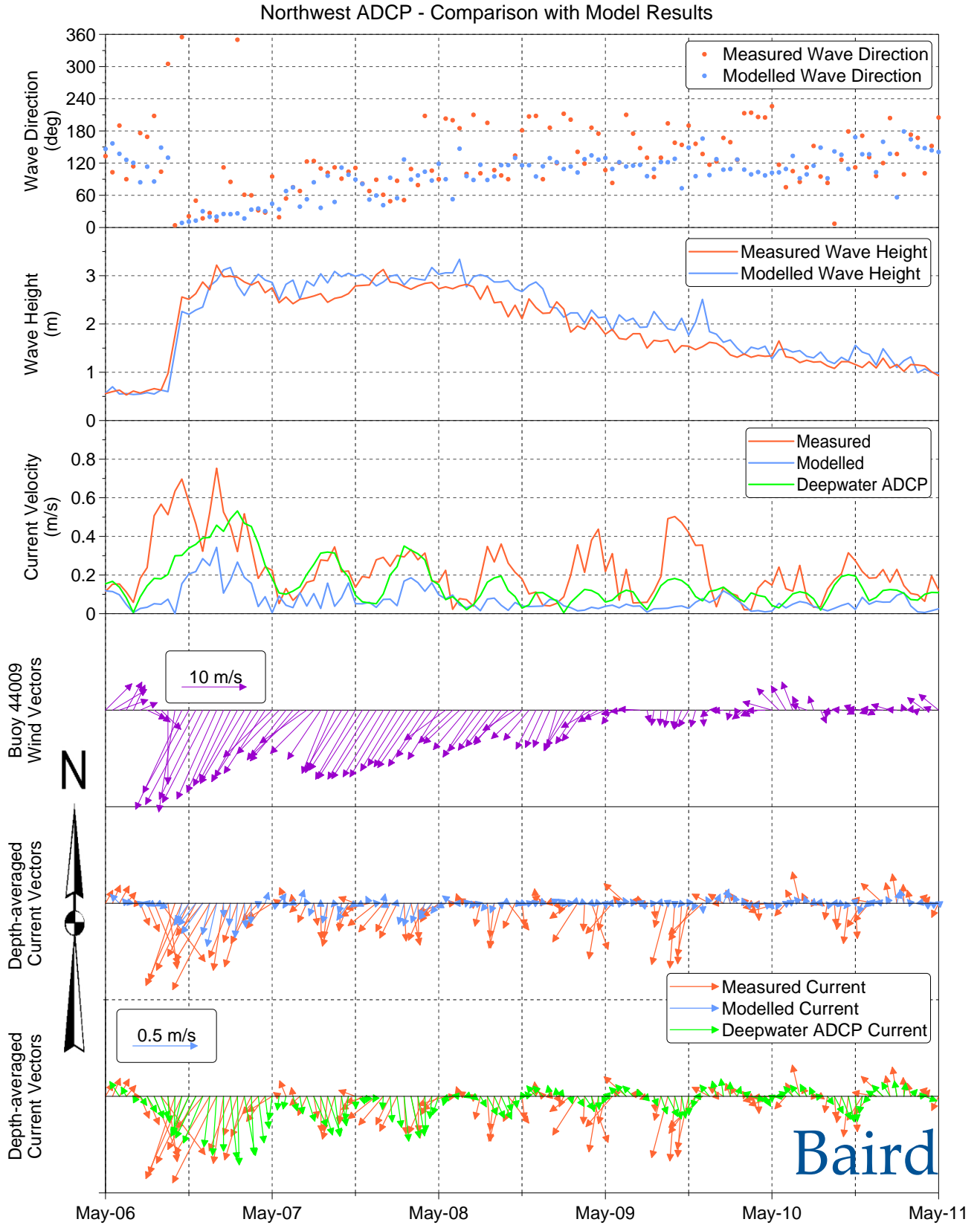Figure 6.16 Measured vs. model waves and currents at SE ADCP for May 6 to 11, 2007.

Northwest ADCP - Comparison with Model Results

Figure 6.17 Measured vs. model waves and currents at NW ADCP for May 6 to 11, 2007.

6.6 Selection of Input Driving Forces for Long-Term Morphologic Modeling

The numerical model offshore boundary is at the location of the deepwater ADCP. However, comparison between ADCP wave data and the data from NDBC Buoy 44009 (Section 5.1) showed that the 3-month measured wave climate of this study does not include extreme nor'easter events as 2007 was a year of low nor'easter activity. Moreover, the 3-month data does not include a complete annual cycle of events and was found to be biased towards southeasterly events. In other words, it includes an almost equal number of southeasterly and nor'easter events, while the long-term wave statistics from the buoys in the area show that nor'easters are the predominant extreme storms. Therefore, the ADCP data are not appropriate to be used as input to the long-term morphology model.

It was decided to use a combination of NDBC Buoy waves and MARCOOS currents data (Section 2.2.4) to create the model input boundary conditions. A complete full-year time series was desired to avoid, to the extent possible, statistical bias of the events. The one year period from August 1, 2007 to July 31, 2008 was selected. This period was selected because 1) there are fewer gaps in MARCOOS surface velocity data compared to earlier periods and 2) wave activity at the site is minimal during July and August and, therefore, the above period coincides with the local "wave year" rather than the calendar year.

The closest wave buoy to the present study site is NOAA Buoy 44009. This buoy, however, does not record wave direction. Figure 6.18 shows the relationship between measured wave height at the deepwater ADCP and that measured by 44009 during March to May 2007 ADCP deployment period. A relation of $H_{ADCP} = 0.835 \times H_{44009}$ is observed. Thus, wave height measured by Buoy 44009 was multiplied by 0.835 and used at the model boundary. A one to one relationship was assumed for the wave period. Record gaps in 44009 data were filled using a relationship with measured wave heights at MD002.

Regarding wave direction, a close review of wave and wind time series recorded by Buoy 44009 showed a strong correlation between winds and waves during storm events. Figure 6.19 shows an example during the nor'easter event of May 2008. In this figure, wave height, wind speed and wind direction measured by 44009 are shown. The wind speed has been scaled (divided by 4) to make the comparison more convenient. The strong relation between winds and waves indicates a locally generated wave field and suggests that wave directions should be very close to the recorded wind directions. The next closest wave buoy of interest is NDBC Buoy 44014 which is a directional wave buoy deployed at 48 m depth approximately 200 km south of the present study site. For comparison, recorded wave directions at this buoy are also shown in Figure 6.19 (green dots). In the absence of direct measurements of wave direction, it is reasonable to assume that wind directions measured by 44009 also represent the wave direction during storm events.
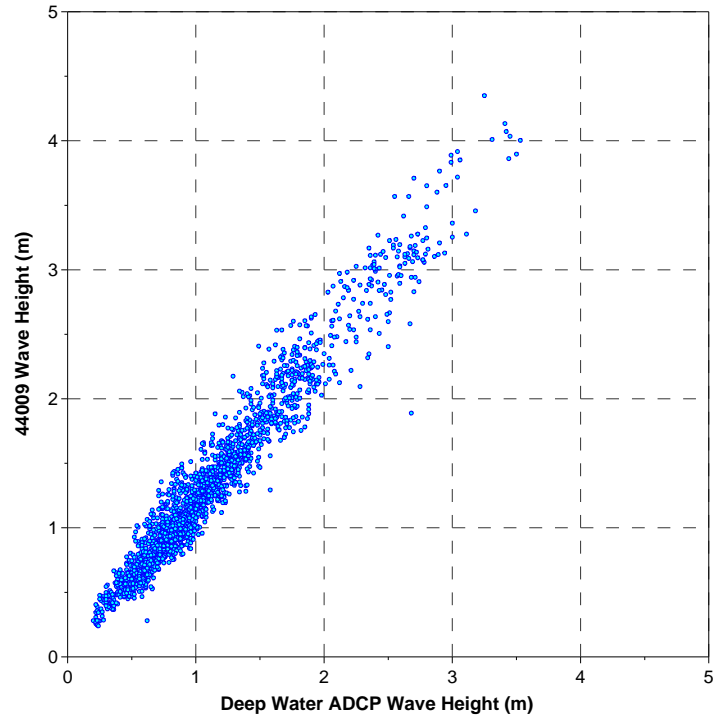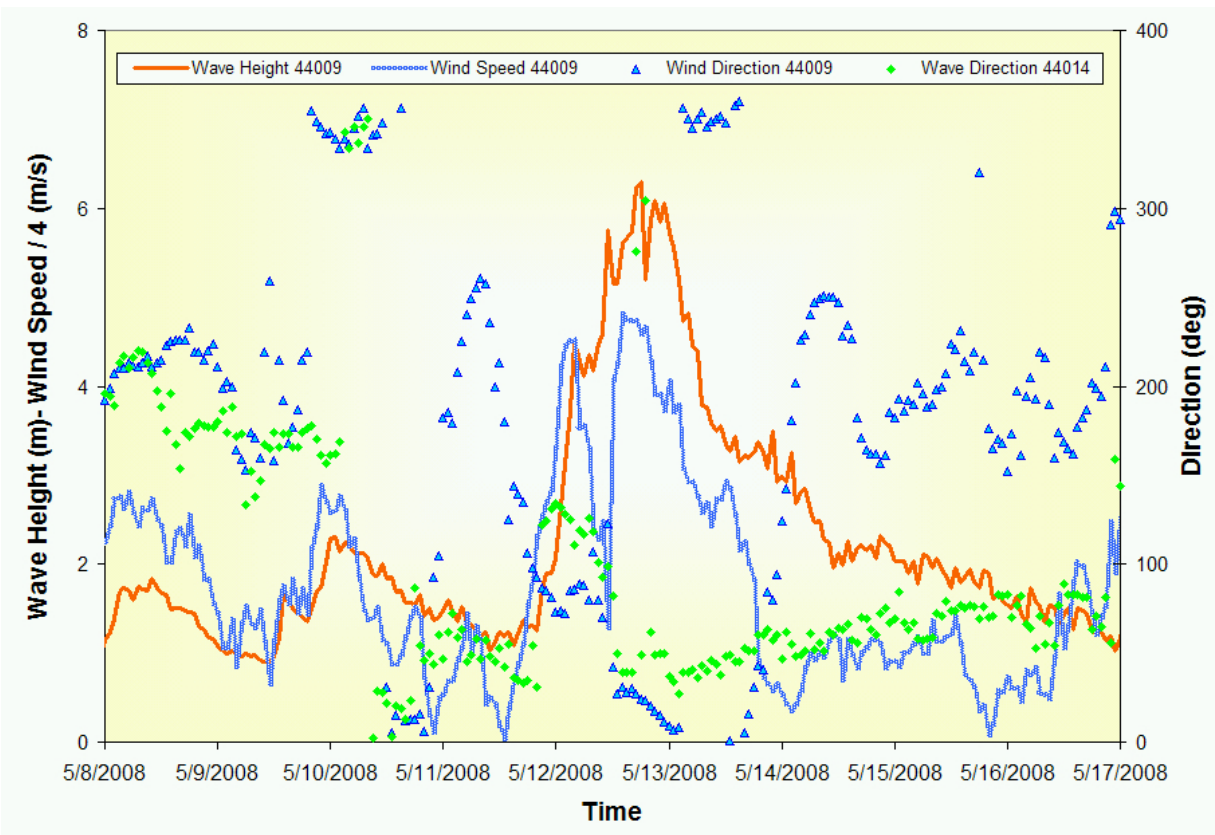
Figure 6.18 ADCP wave height vs. Buoy 44009

Figure 6.19 Wave height, wind speed and direction measured by Buoy 44009 during a nor'easter event.

As for the measured coastal currents in the calculation area, Figure 2.10 shows the location of MARCOOS data points relative to the Isle of Wight and other shoals in the study area. MARCOOS data Point 227 is a few kilometers east of Isle of Wight where the depth is approximately 20 m. Inter-comparison of MARCOOS velocity data showed little difference between recorded data at the four points. Figure 6.20 provides comparison between Point 227 and Point 275 data as an example. Recorded current velocity at the two locations is very similar. Therefore, the data from Point 227 which is the closest point to Isle of Wight was used for the present study.
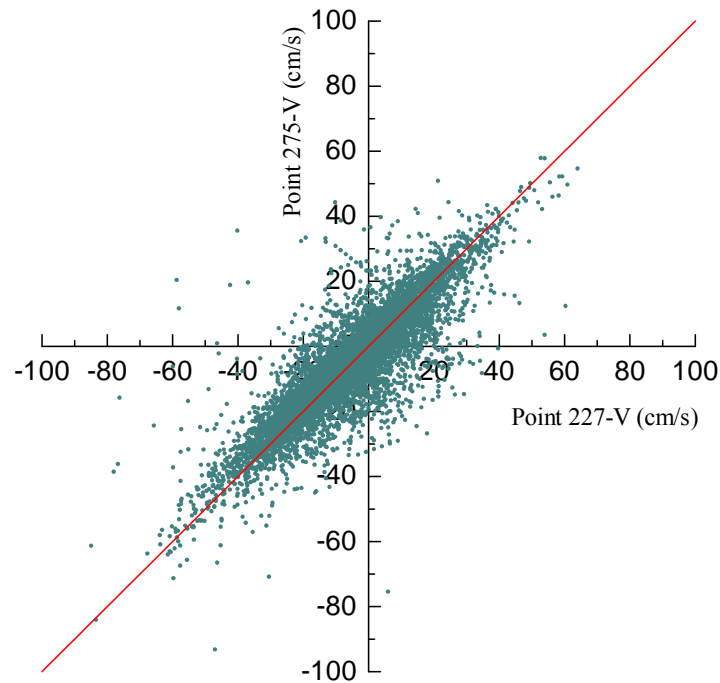
Figure 6.20 Comparison between northward components of MARCOOS surface current velocity data at points 227 and 275.

MARCOOS provides surface velocity data. On the other hand, most sediment transport relationships for tidal and subtidal environments use depth-averaged currents as the input velocity. This is because the bottom shear stress is normally formulated in terms of depth-averaged currents in these environments. Therefore, MARCOOS surface currents needed to be converted to depth-averaged currents before being used in sediment transport calculations. The relationship between surface and depth-averaged currents at the site was thus investigated using ADCP data. Figures 6.21 and 6.22 provide quantile-quantile (QQ) statistical (top figures) as well as the actual current velocity (bottom figures) comparison plots of surface vs. depth-averaged currents at SE and NW ADCP locations, respectively. The statistical parameters (Bias, RMSE, SI, SIB and r) are also given in the figures (see Appendix C for definitions). The quantile-quantile plots compare the exceedance levels for depth-averaged and surface current velocity. In other words, they are plots of the corresponding velocity in both data sets at

equivalent values of cumulative probability. The analysis shows that surface currents are statistically representative of the depth-averaged currents. Correlation factors (r=0.80 and 0.71) are reasonably high and it may be concluded from both figures that depth-averaged currents are almost the same as surface currents. This is again an indication of a well developed system of subtidal and wind-driven currents. MARCOOS surface currents measured at Point 227 were therefore used uniformly over the entire calculation domain.
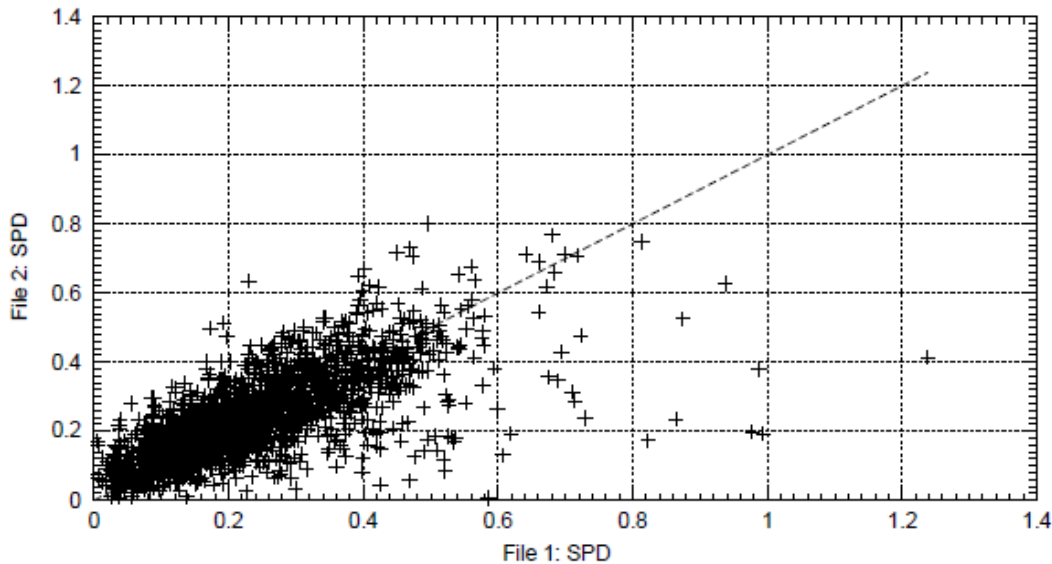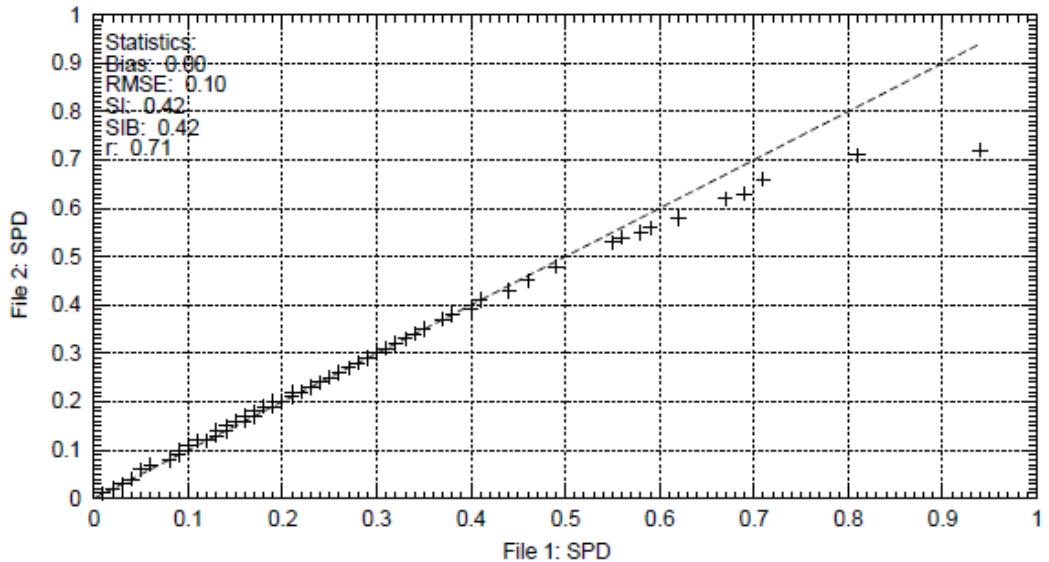
Number of Points: 2031
File 1: SE_DepthAveraged.bts
File 2: SE_Surface.bts
Directional Interval: 1. - 360.
Linear fit coeff: 0.9988

Start Date: 2007 3 1
End Date: 2007 5 24
Threshold: 0.00

QQ Version 2.0

Figure 6.21 QQ and velocity plots of surface vs. depth-averaged current at SE ADCP.

Figure 6.22 QQ and velocity plots of surface vs. depth-averaged current at NW ADCP.

Time series plots of the one-year wave-current data thus developed are presented in Appendix B. The developed one-year input wave and current file contains 8764 hourly conditions. Calculation of morphology change for a single wave condition required a minimum of 5 minutes on an Intel Quad Core (Q9550 @ 2.83 GHz) machine. Including all the above hourly conditions in the simulation would thus require a very long calculation time that is impractical. It was

necessary to set a threshold bed shear stress and consider only those wave conditions that exceed the set threshold value. Sensitivity of calculated transport rates to various threshold bed shear stresses (Shields stress) was examined. Wave-induced Shields stress for cutoff purposes was calculated in 7 m depth, which is the depth at the top of the Isle of Wight shoal. Transport rate calculations were conducted for a water depth of 10 m. Cumulative transport volumes are shown in Figure 6.23.

Note that using a threshold Shields stress of 0.5 reduces the number of hourly conditions from 8,764 to 987 conditions. Applying threshold values of 0.6, 0.8, and 1.0 would further reduce the number of hourly conditions to 698, 373, and 258 conditions, respectively. It was decided to use a threshold Shields stress of 1.0 to keep calculation time within practical limits. Figure 6.23 indicates that this would result in an underestimation of cumulative transport of about 40%.
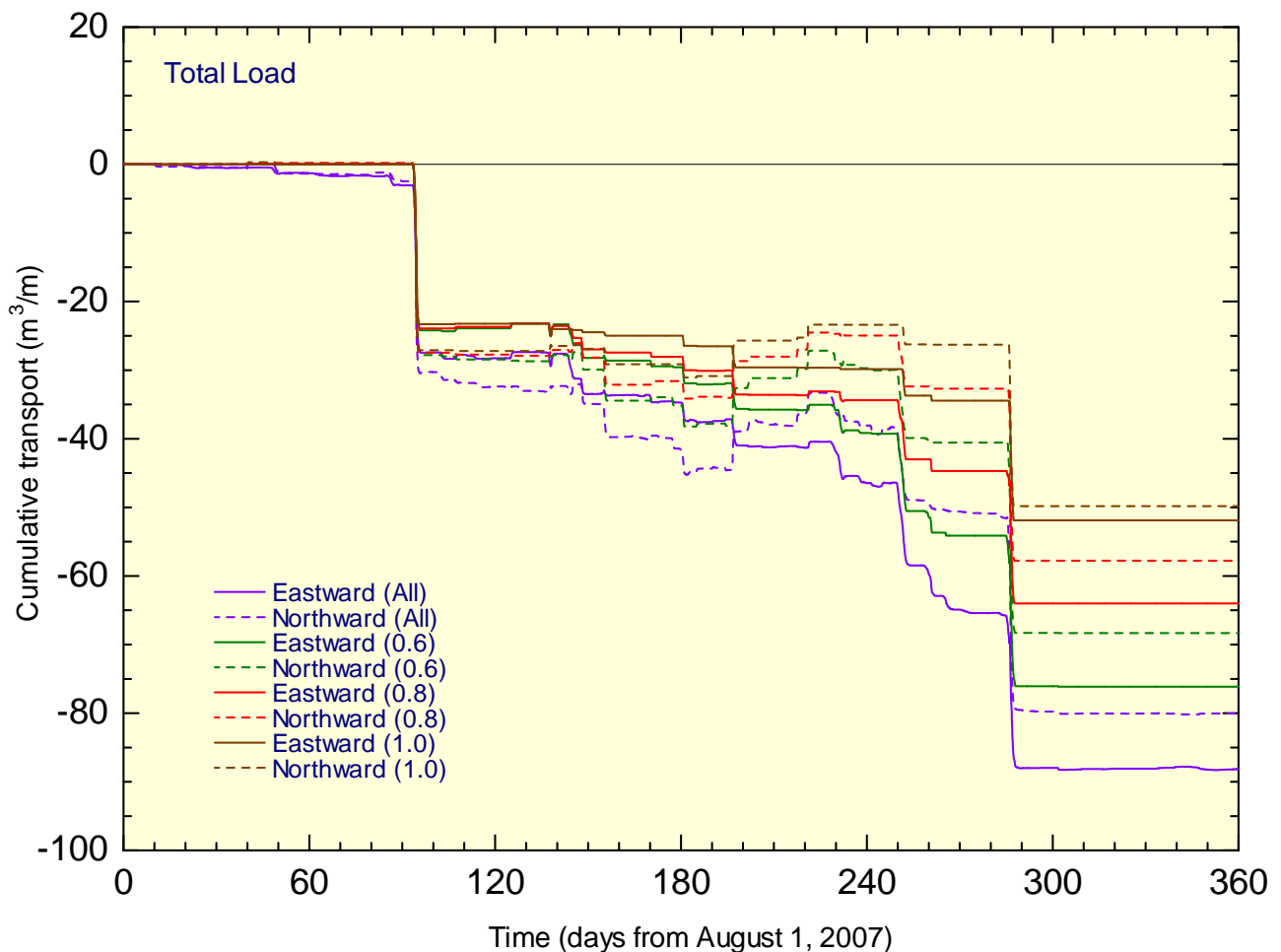

Figure 6.23 Cumulative sediment transport volumes calculated for the developed wave-current field using Van Rijn sediment transport model.

Referring to Figure 5.3, the percentage of nor'easters in the above representative wave-current field is 245 hours which is about 28% more than the average of 196 hours. This is because nor'easters occurred rather frequently in 2008.

6.7   Simulation of Existing Conditions

The existing bathymetry of the calculation domain was constructed using the overall survey of 1975 and the USACE 2002 surveys of Isle of Wight and Weaver. The model was run with the one-year wave and current data developed in Section 6.6 as the input driving force. As discussed in Section 4.3, surface sediment samples from IOW indicate a median grain size ranging from 0.3 mm to 1.5 mm. Modeling of morphology change with graded sediments is presently an area of ongoing research requiring representation of spatial (both horizontal and vertical) and temporal variations of the grain size in the calculation domain and is beyond the scope of this study. Generally, however, the movement of graded sands involves various processes (or modes of transport) and grain size distribution on a morphodynamically active shoal is subject to temporal variability and depends on the type and intensity of hydrodynamic forcing that prevailed prior to sediment sampling. Usually, the coarser sand fraction tends to expose itself and armor the surface under a moderate wave climate regardless of its low percentage in the mixture. During extreme events, however, both fine and coarse fractions move together and the overall transport is expected to be governed by the movement of the finer fraction (Dibajnia and Watanabe, 2000). Therefore, a median sediment grain size of 0.3 mm was selected for the present simulations. The D&W transport formula was used.

Calculated transport rates were multiplied by a factor of 10 to calculate the change in morphology over 10 years. The use of a morphological scaling factor is a common practice in morphology calculations for simulating evolution over long time periods to reduce the required calculation time, provided that the rate of morphology change is gradual (Roelvink, 2006). It is expected to provide similar results to when the 1 year forcing dataset over ten years is used. Note that the shoals migrate at a rate of a few m/year, which is very small compared to overall shoal dimensions. Furthermore, since the developed one-year wave-current dataset includes an above-average number of nor'easters, the predicted change in morphology is expected to correspond to a longer than 10 year period (closer to 13 years considering that the input time series contains 28% more nor'easters than average) . Furthermore, using a threshold Shields value of 1.0 excludes nearly all non-storm wave conditions resulting in emphasizing the effect of storm events, particularly those of nor'easters.
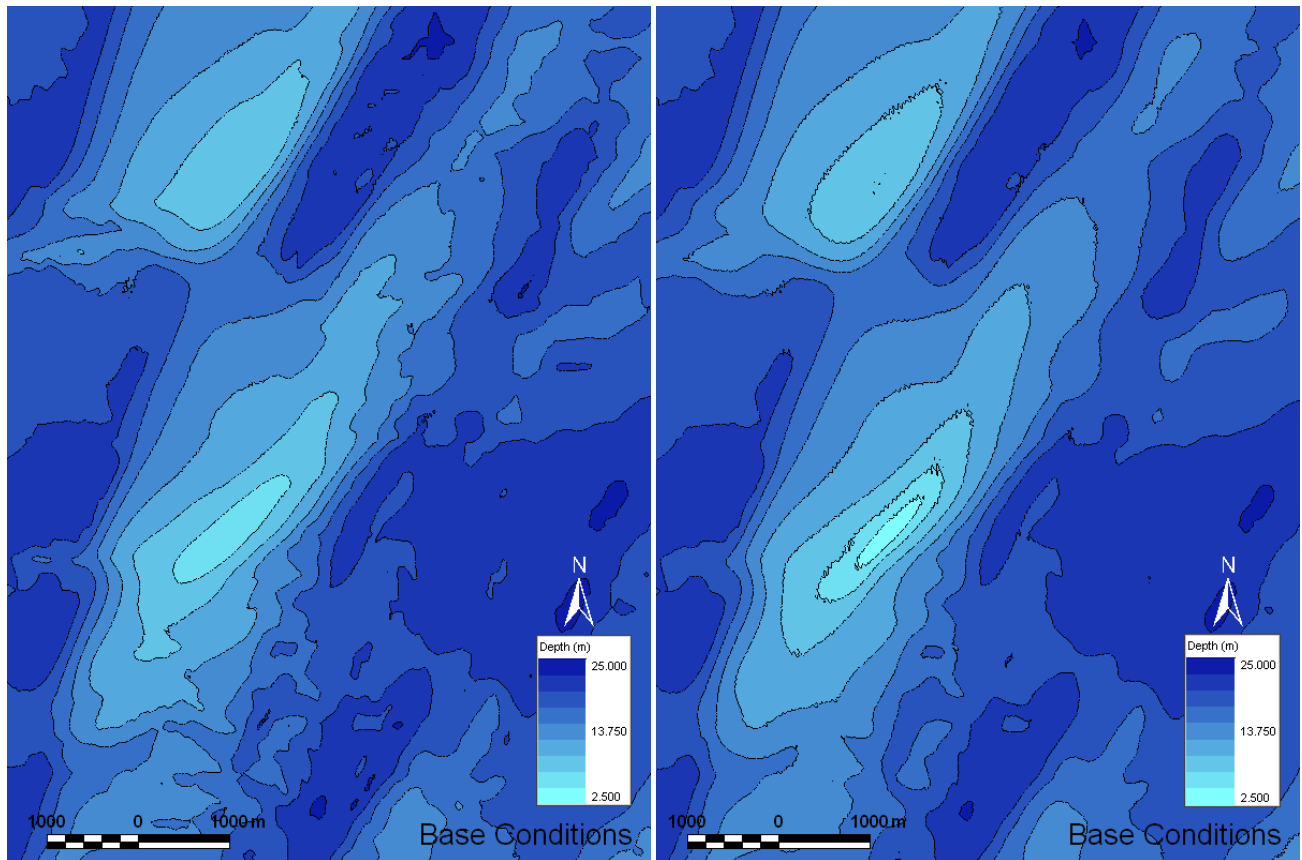
Figure 6.24 Initial (left) and final (right) morphology for the existing (Base) conditions.

Figure 6.24 shows the initial and predicted future bathymetry for the existing shoal configurations. Both IOW and Weaver shoals have moved towards the south. The predicted morphology represents a slightly higher shoal than the initial shoal. This is the result of wave focusing over the shoal under nor'easter events. Figure 6.25 shows the initial and final depth contours (5.0, 7.5, 10.0 and 15.0 m) as well as a map of change in bottom elevations. The overall contour movement and depth change are in agreement with observations of comparisons between historic bathymetries described in Section 5.4.
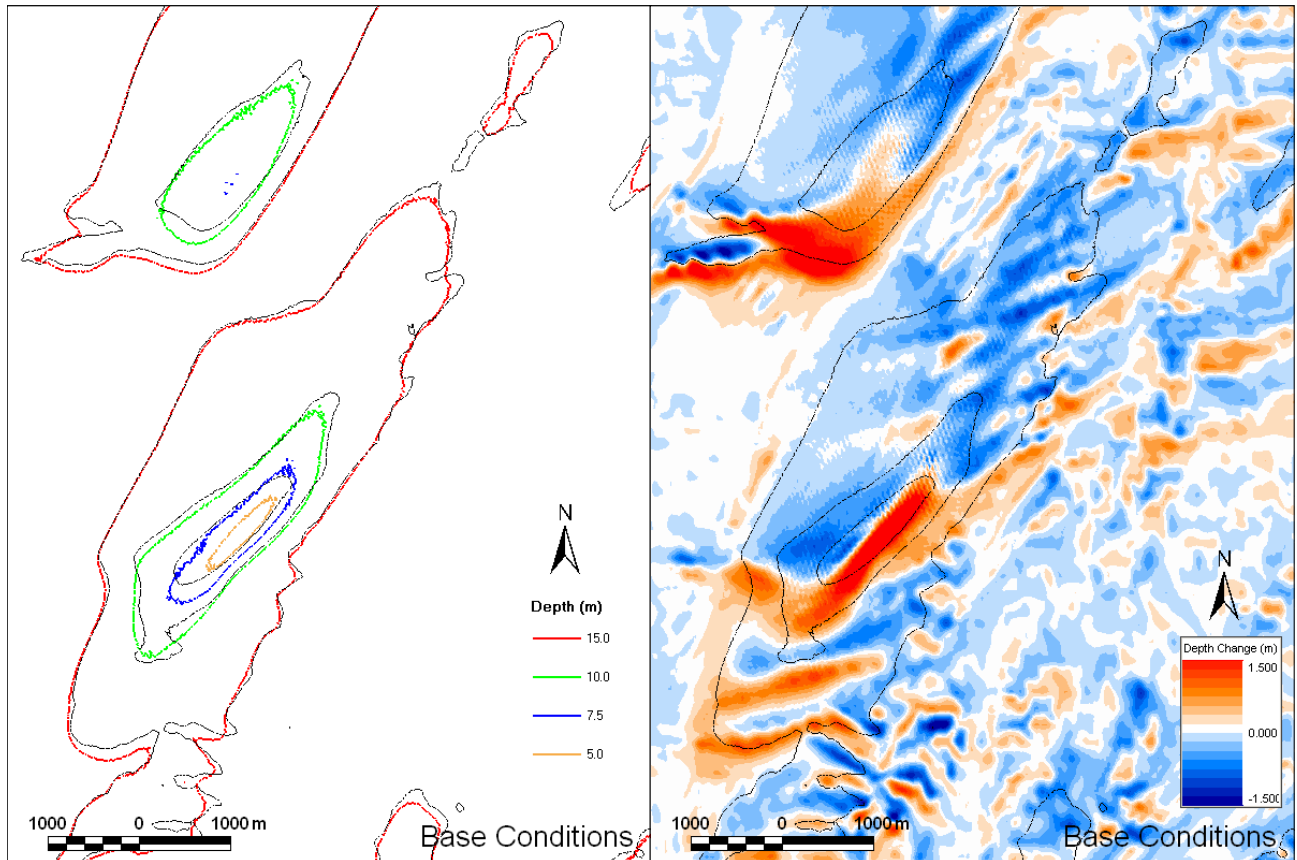
Figure 6.25 Initial and final depth contours (left) and depth change (right) for the existing (Base) conditions.

To obtain a better understanding of the results, several transects were extracted and compared across the shoal. Figure 6.26 shows locations of transects (3 along the shoal and 7 in transverse direction). Transects 1 and 7 cross at the shoal crest.

Figure 6.27 compares the evolution of Isle of Wight along the 3 longitudinal transects (1, 2 and 3) since 1929 with the predicted future profile. Note that the input to the morphology model was the 2002 bathymetry. Similarly Figure 6.28 shows the evolution of Isle of Wight along 4 transverse transects (5, 7, 9 and 10) since 1929 with the predicted future profile.
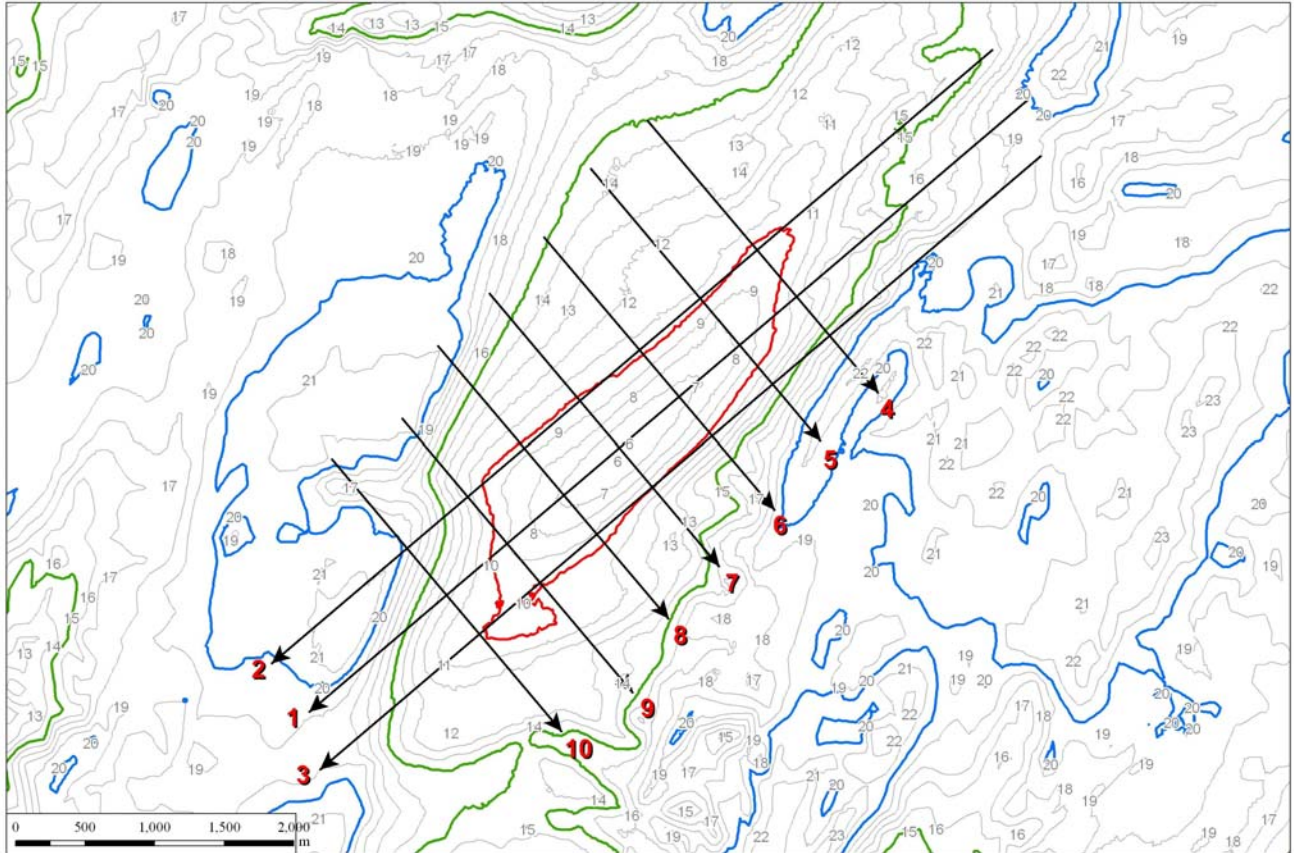
Figure 6.26 Extracted transects along and across Isle of Wight

In Figure 6.27, the overall movement of the shoal and its southwest flank towards southwest is fairly well simulated. The predicted shoal height at Transect 1 is slightly overestimated as a result of wave focusing effect of nor'easters. The predicted excess height (also observed in Transect 7, Figure 6.28) is expected to smooth out by the action of less severe daily waves and currents that are not included in the simulations. Comparisons at Transects 9 and 10 (Figure 6.28) show that sediment accumulation on the west side of the shoal is also properly simulated.

From the above comparisons it is concluded that the predicted future shoal morphology represents the overall historic evolution and movement of Isle of Wight. The model thus has the capability of evaluating and comparison of the impacts of various dredging scenarios.
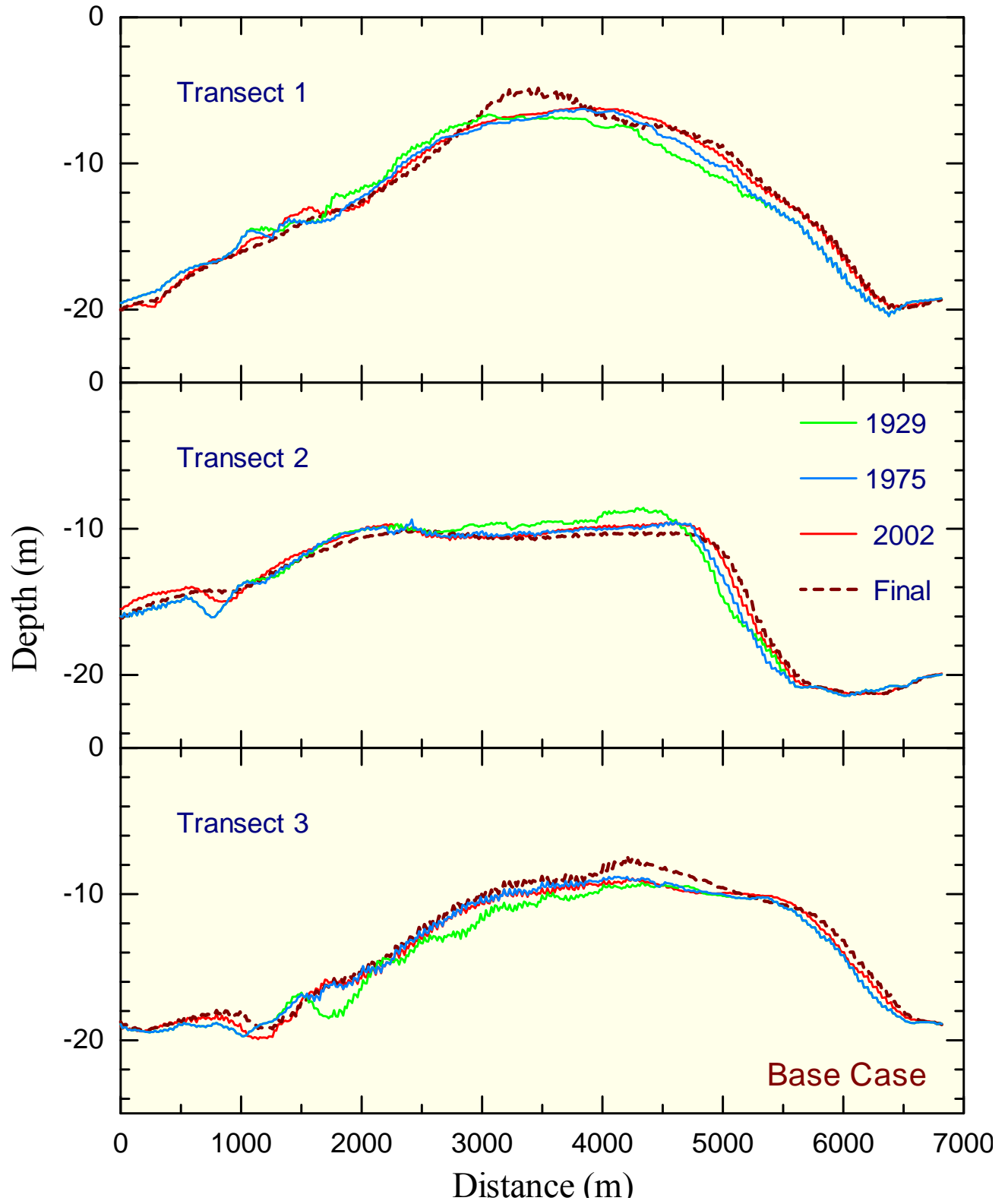
Figure 6.27 Evolution of IOW since 1929 along transects 1, 2 and 3 compared to predicted profiles.
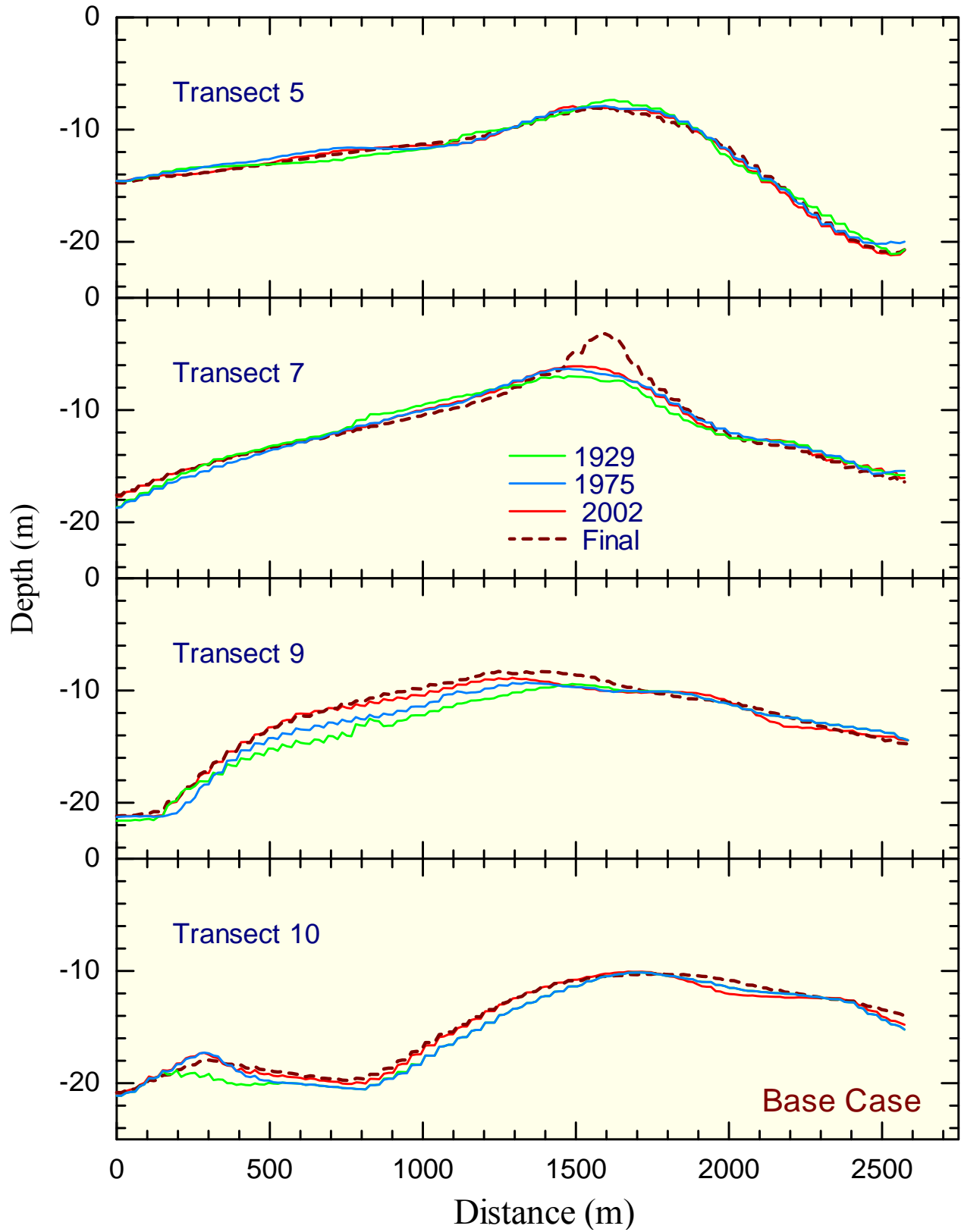
Figure 6.28 Evolution of IOW since 1929 along transects 5, 7, 9 and 10 compared to predicted profiles.
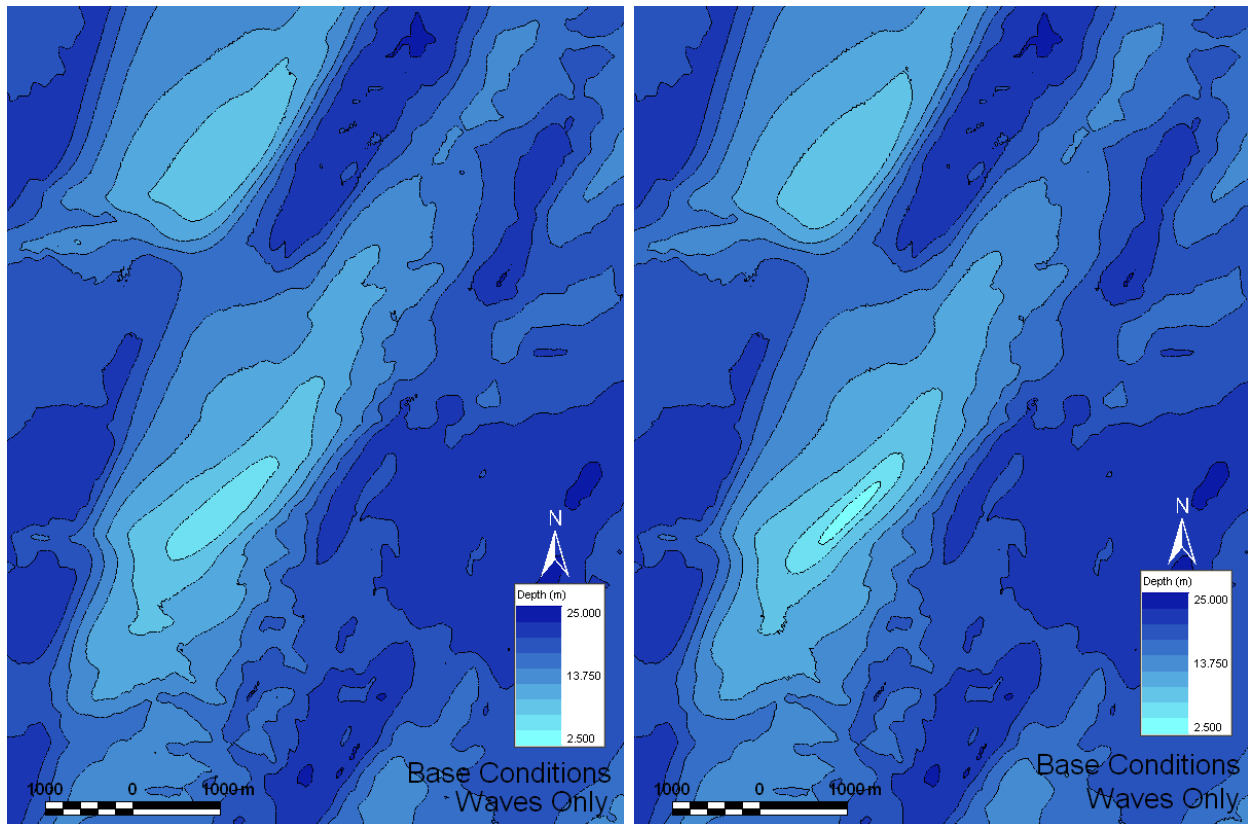
Figure 6.29 Initial (left) and final (right) morphology for the Base Conditions under waves' action only.

In order to provide a better understanding of the contribution from the waves to the resulting shoal morphology, simulations were completed using zero input current velocity. Figure 6.29 shows the initial and predicted future bathymetry for the existing shoal configurations when only waves are considered as the model driving force. There is accumulation of sediment along the crest of IOW and the predicted morphology represents a higher shoal than the initial shoal. As discussed before, this is the result of wave focusing over the shoal under nor'easter events. Figure 6.30 shows the initial and final depth contours (5.0, 7.5, 10.0 and 15.0 m) as well as a map of change in bottom elevations. Initial contours are shown by black lines while their corresponding final contours are shown in color. There is only a limited movement of contours and depth change is limited to the area around the shoal crest.

Figure 6.31 compares the evolution of Isle of Wight along the 3 longitudinal transects (1, 2 and 3) since 1929 with the predicted future profile. Again, note that the input to the morphology model was the 2002 bathymetry. Similarly Figure 6.32 shows the evolution of Isle of Wight along 4 transverse transects (5, 7, 9 and 10) since 1929 with the predicted future profile.
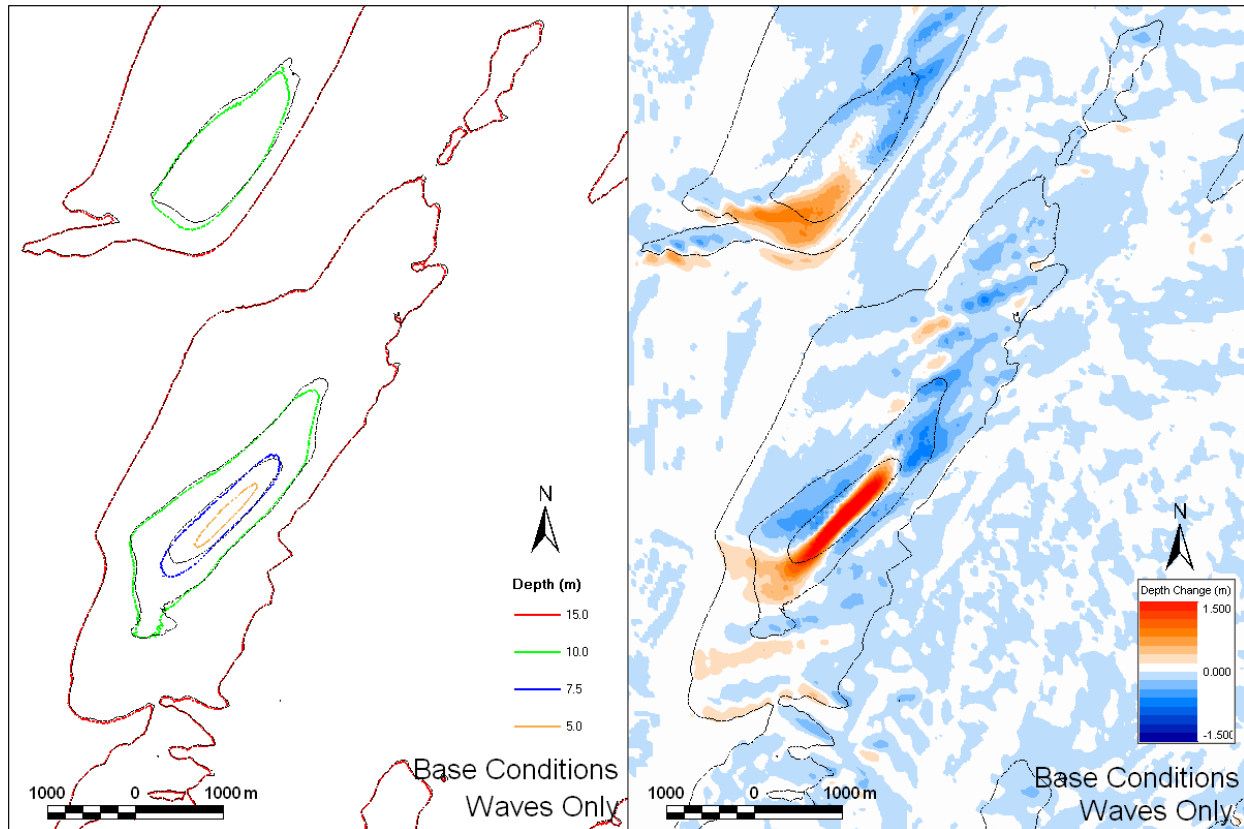
Figure 6.30 Initial and final depth contours (left) and depth change (right) for the Base Conditions umder waves' action only.

In Figure 6.31, there is no movement of the shoal and its southwest flank towards the southwest as in the case of simulation with waves and currents (Figure 6.27). However, the predicted shoal height at Transect 1 is similar to the results shown in Figure 6.27. Comparisons at Transects 9 and 10 (Figure 6.32) show no signs of sediment accumulation on the west side of the shoal as was the case in simulations with waves and currents (Figure 6.28).

From the above comparisons it may be concluded that waves are the primary factor in shoal growth and maintenance while currents are more responsible for shoal migration. This is in agreement with the findings of Section 5.5.

Figure 6.31 Evolution of IOW since 1929 along transects 1, 2 and 3 compared to predicted profiles when only waves are considered.

Figure 6.32 Evolution of IOW since 1929 along transects 5, 7, 9 and 10 compared to predicted profiles when only waves are considered.

7.0   SIMULATION OF DREDGING SCENARIOS

A total of 11 shoal dredging scenarios were considered and model runs completed for each scenario. In each scenario, the Isle of Wight was partially excavated to the -10 m contour to provide sand volumes in the range of 1 to 2 million cubic meters. Table 7.1 provides a s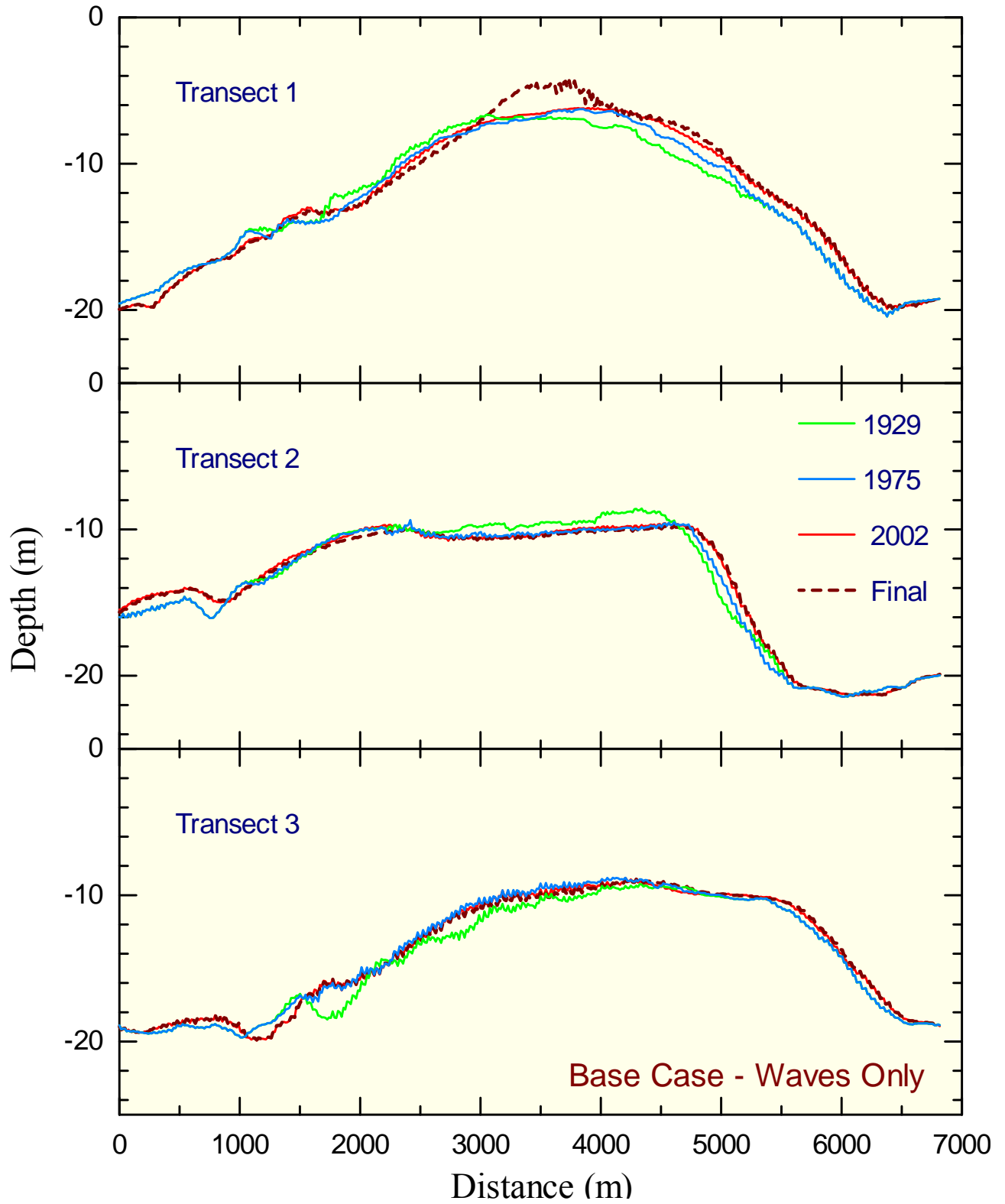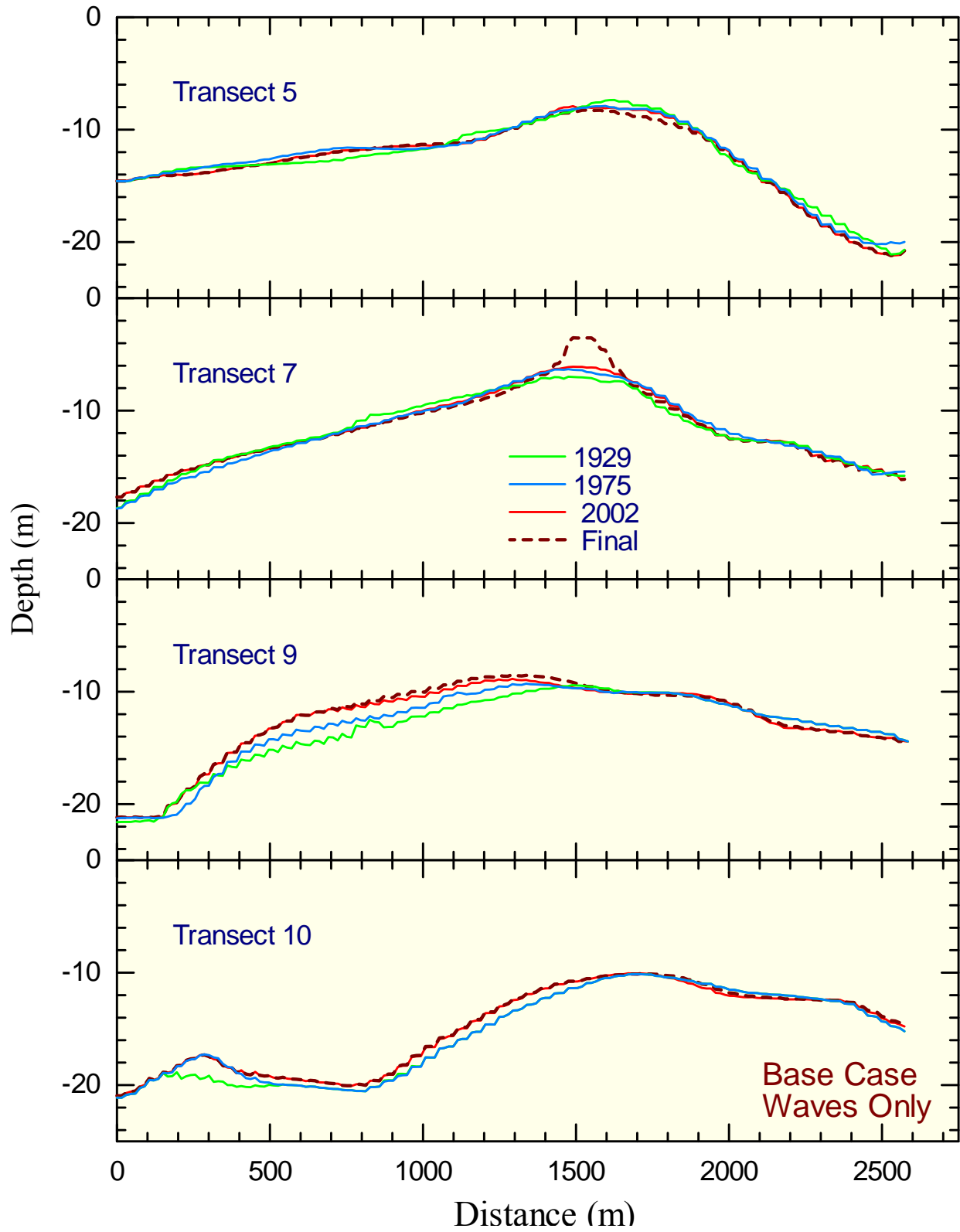ummary. Numerical excavation was conducted on the 2002 bathymetry representing the existing conditions. Similar to the simulation of existing conditions (Section 6.7), the model was run with the one-year wave and current data developed in Section 6.6 as the input driving force. The median sediment grain size was 0.3 mm and the D&W transport formula was used. Calculated transport rates were multiplied by a factor of 10 and the predicted change in morphology is expected to roughly correspond to a 13-year period. The results have provided valuable insights on response of different dredging plans that can be used for the development of dredging guidelines. The results obtained for individual dredging scenarios are presented and discussed in this section.

Table 7.1 – Dredging scenarios.

Dredging Scenario	Excavation Area	Volume Dredged (milliom m^3)
1	southeastern half of the crest	1.9
2	northwestern half of the crest	1.6
3	southwestern half of the crest	1.8
4	northeastern half of the crest	1.8
5	top 1/3 of the volume between shoal crest and -10 m contour	0.3
6	top 2/3 of the volume between shoal crest and -10 m contour	1.5
7	southwestern quarter of the crest	0.95
8	southwestern and northeastern quarters of the crest	1.75
9	southwestern 1/3 of the crest	1.0
10	middle 1/3 of the crest	1.9
11	northeastern 1/3 of the crest	0.75

7.1   Numerical Modeling of Dredging Alternatives

Scenario 1

In this scenario the southeastern half of the crest of Isle of Wight is dredged to -10 m contour, as shown in Figure 7.1, to provide about 1.9 million m^3 of sand.
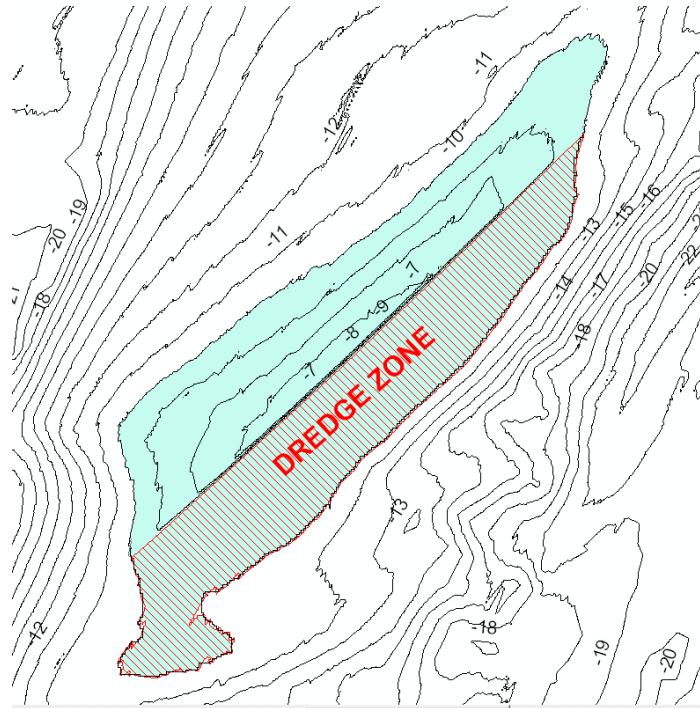

Figure 7.1 Dredging Scenario 1.

Figure 7.2 shows the initial and predicted future bathymetry for the Scenario 1 dredging configurations. IOW is reintegrated into a slightly narrower shoal. The shoal height of the predicted morphology is close to the initial shoal height before dredging. This is the result of wave focusing over the shoal under nor'easter events. Figure 7.3 shows the initial and final depth contours (5.0, 7.5, 10.0 and 15.0 m) as well as a map of change in bottom elevations. Initial contours are shown by black lines, while their corresponding final contours are shown in color. There is accumulation over the dredged part of the shoal and a new shoal crest is created. Comparisons at selected transects (Figures 7.4 and 7.5) show that the reformed shoal is about 1.5 m to 2 m lower (at its crest) than the pre-dredge shoal. Note that the pre-dredge shoal is also shown (green line marked as 2002) in these figures to provide a base for comparisons. When a certain transect is outside of the excavated area (e.g. Transect 2), then the green line does not appear in the corresponding transect figure because the green and red (initial) lines are identical.

Figure 7.2 Initial (left) and final (right) morphology for Scenario 1 conditions

Figure 7.3 Initial and final depth contours (left) and depth change (right) for Scenario 1 conditions.

Figure 7.4 Predicted evolution of IOW along transects 1, 2 and 3 after dredging Scenario 1.

Figure 7.5 Predicted evolution of IOW along transects 5, 7, 9 and 10 after dredging Scenario 1.

Scenario 2

In this scenario the northwestern half of the crest of Isle of Wight is dredged to -10 m contour, as shown in Figure 7.6, to provide about 1.6 million m^3 of sand.

Figure 7.6 Dredging Scenario 2.

Figure 7.7 shows the initial and predicted future bathymetry for the Scenario 2 dredging configurations. IOW is reintegrated into a slightly narrower shoal. Figure 7.8 shows the initial and final depth contours as well as a map of change in bottom elevations. There is not much accumulation over the dredged part of the shoal as the overall net transport is towards the non-dredged (southeast) side of the shoal. Comparisons at the transects presented in Figures 7.9 and 7.10 show that a new shoal crest is formed along Transect 3, i.e. shoal crest is shifted towards southeast. Looking at comparisons at Transect 1 and Transect 3, the new crest is at 7 m depth, while the pre-dredge crest was at 6 m depth. Therefore, this dredging scenario is expected to result in a more asymmetric shoal with a crest height at about 1 m lower than the pre-dredge conditions.
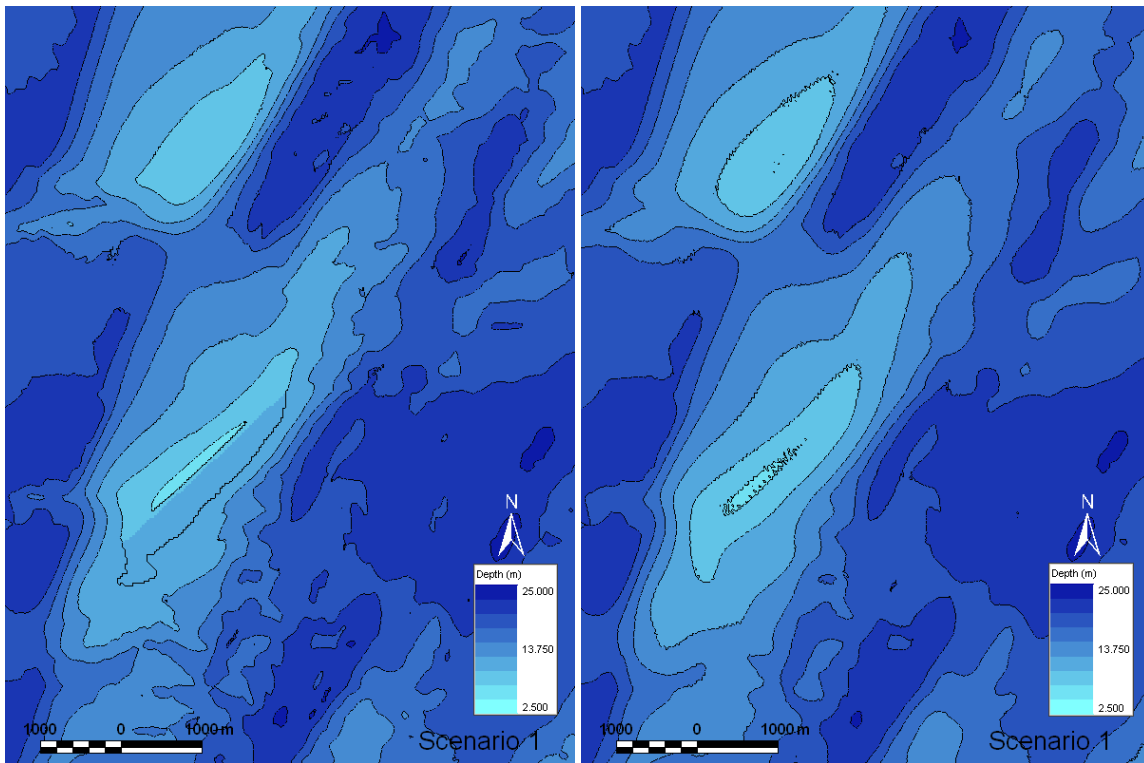
Figure 7.7 Initial (left) and final (right) morphology for Scenario 2 conditions
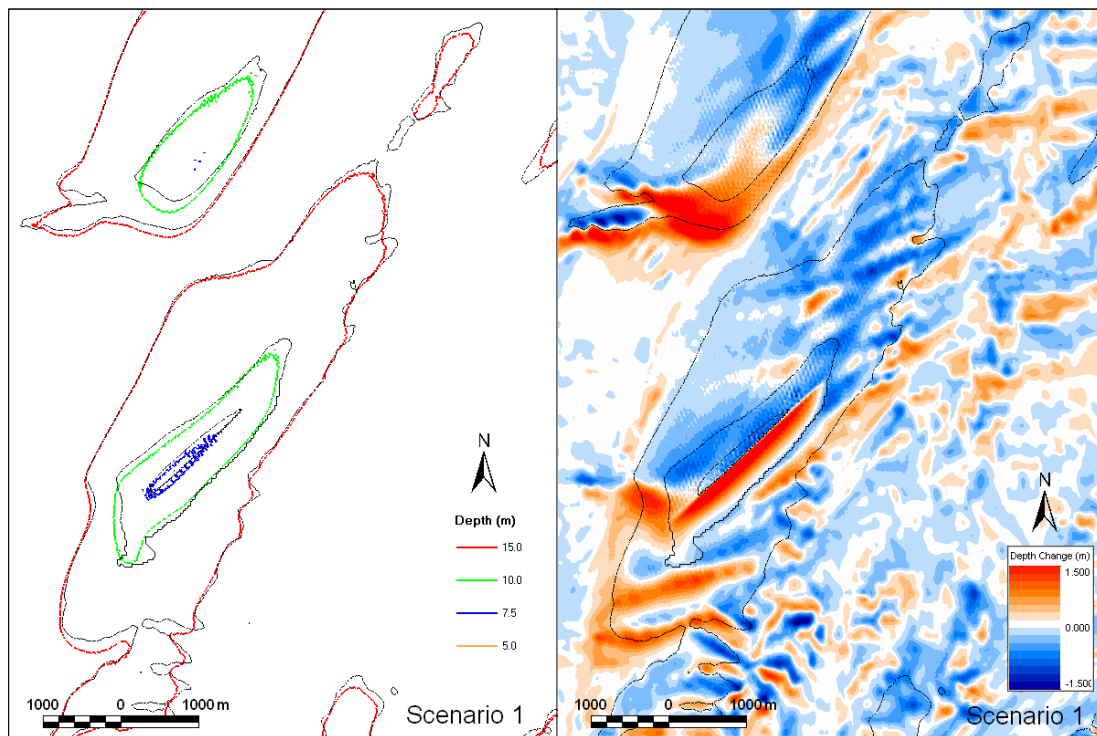

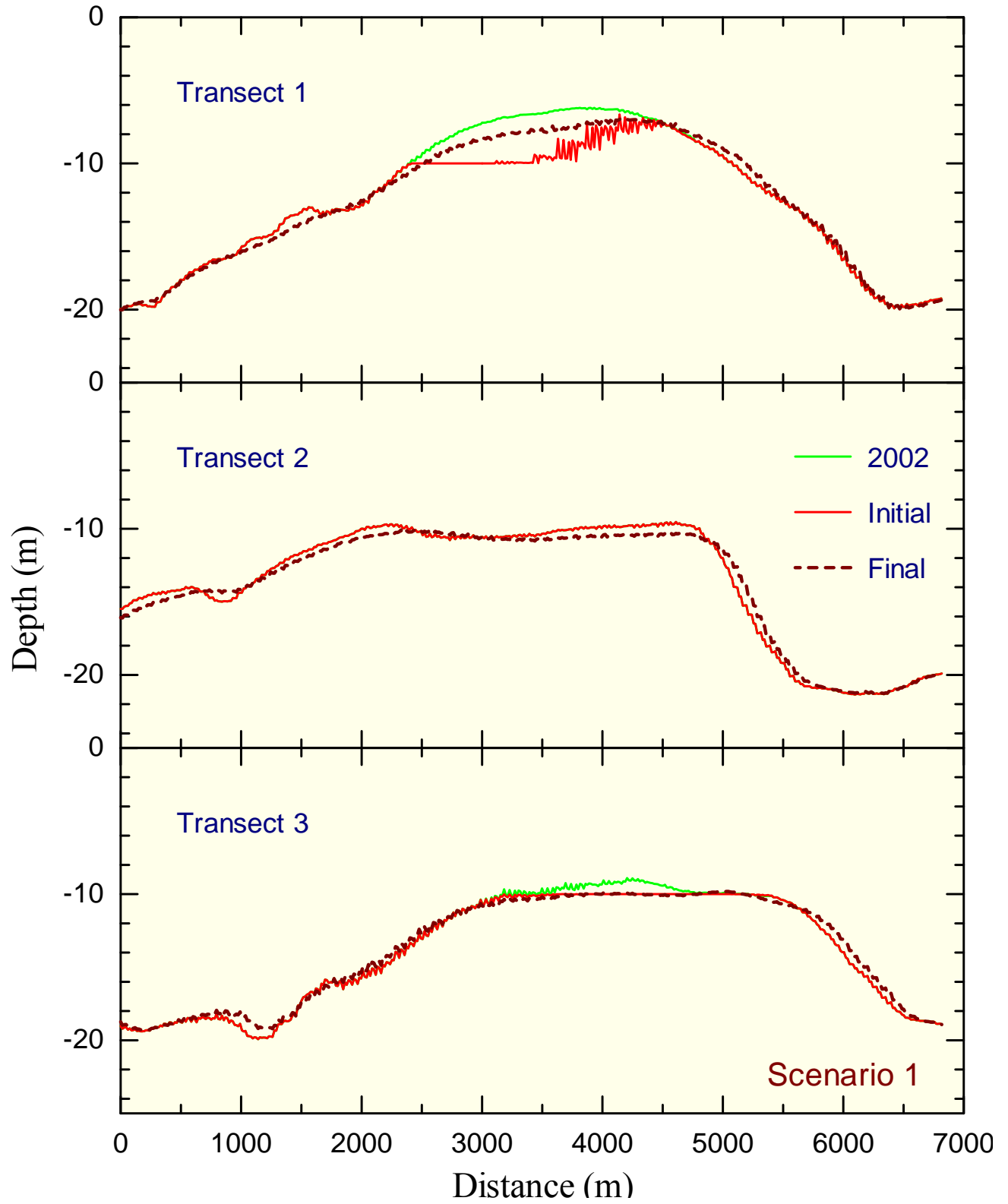**Figure 7.8 Initial and final depth contours (left) and depth change (right) for Scenario 2 conditions.**

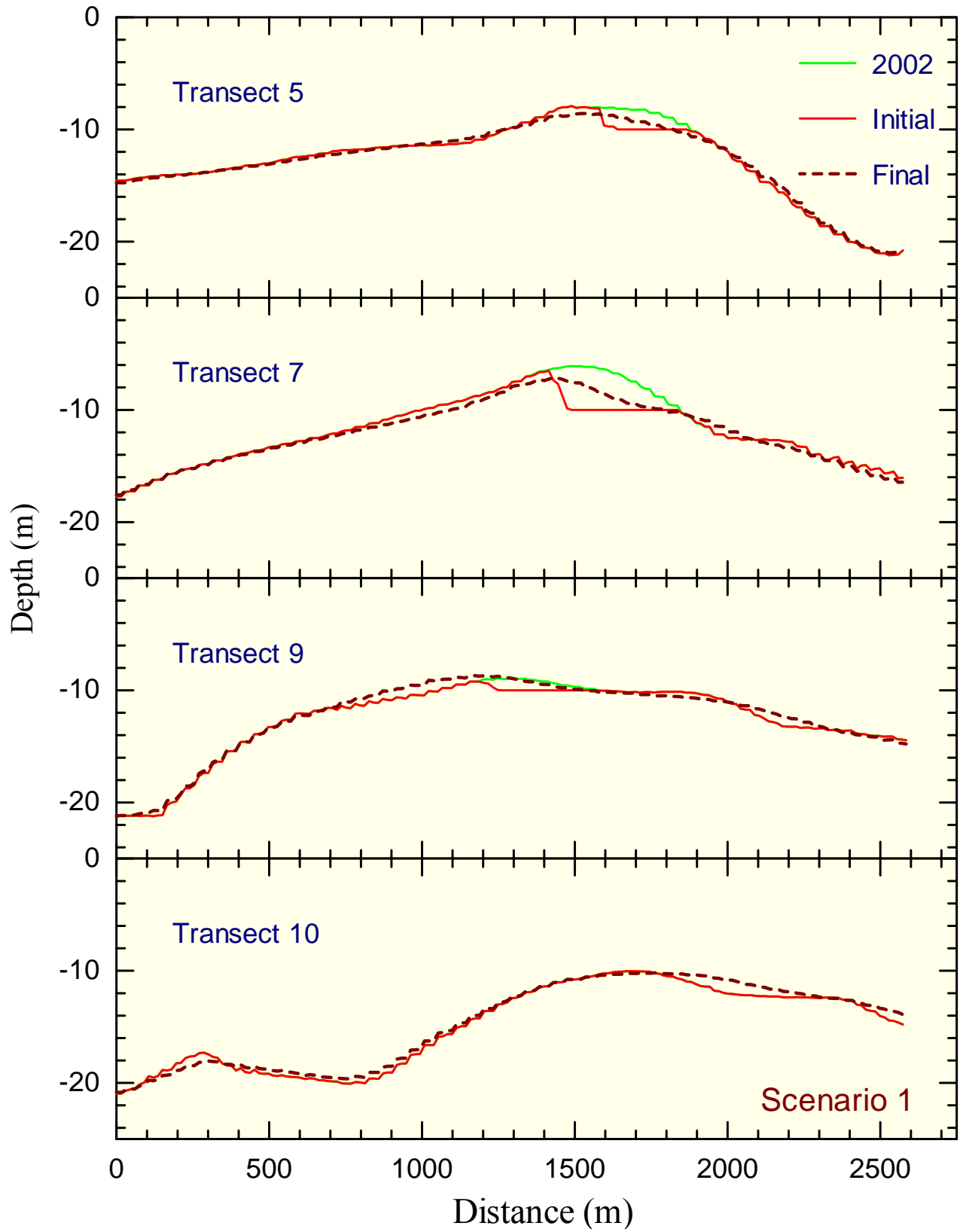**Figure 7.9 Predicted evolution of IOW along transects 1, 2 and 3 after dredging Scenario 2.**

Figure 7.10 Predicted evolution of IOW along transects 5, 7, 9 and 10 after dredging Scenario 2.

Scenario 3

In this scenario the southwestern half of the crest of Isle of Wight is dredged to -10 m contour, as shown in Figure 7.11, to provide about 1.8 million m^3 of sand.
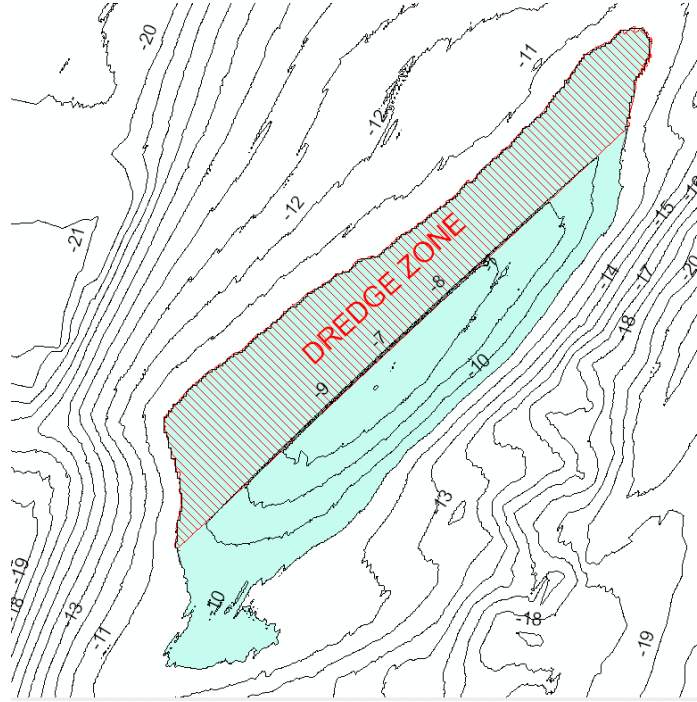

Figure 7.11 Dredging Scenario 3.

Figure 7.12 shows the initial and predicted future bathymetry for the Scenario 3 dredging configurations. IOW is reintegrated into a shoal with shorter crest length than the pre-dredge conditions. Figure 7.13 shows the initial and final depth contours as well as a map of change in bottom elevations. There is considerable accumulation over the northeast half of the dredged part. The rest of the dredged platform stays nearly unchanged. Comparisons at selected transects presented in Figures 7.14 and 7.15 show that the reformed shoal crest has the same height as the pre-dredge shoal. The new crest, however, is shorter and does not extend far beyond Transect 7 towards southwest. Therefore, this dredging scenario is expected to result in a shoal with the same height but with a shorter crest length than the pre-dredge conditions.
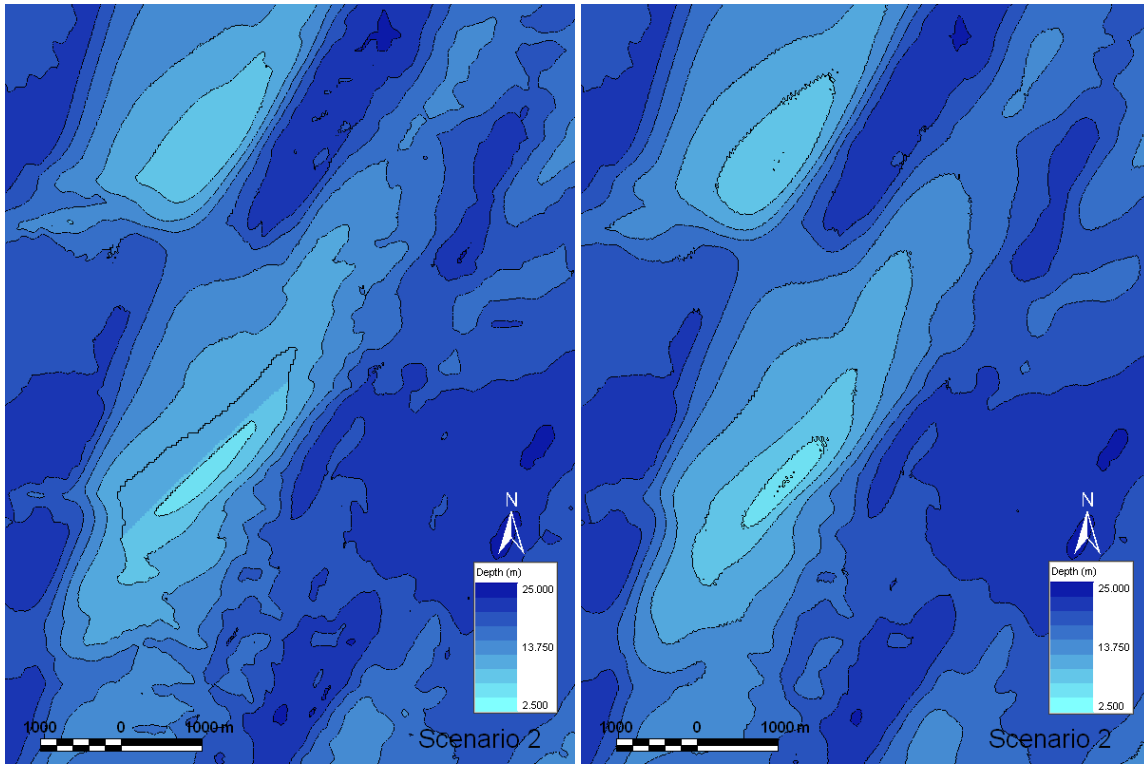
Figure 7.12 Initial (left) and final (right) morphology for Scenario 3 conditions
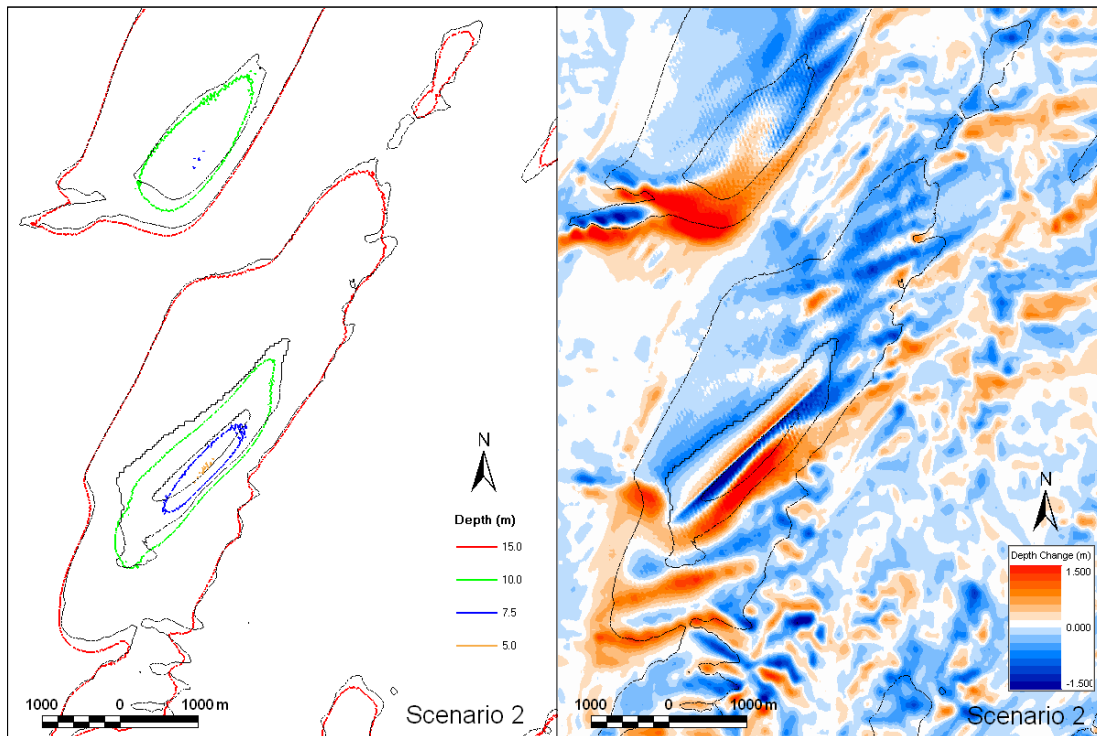

Figure 7.13 Initial and final depth contours (left) and depth change (right) for Scenario 3 conditions.
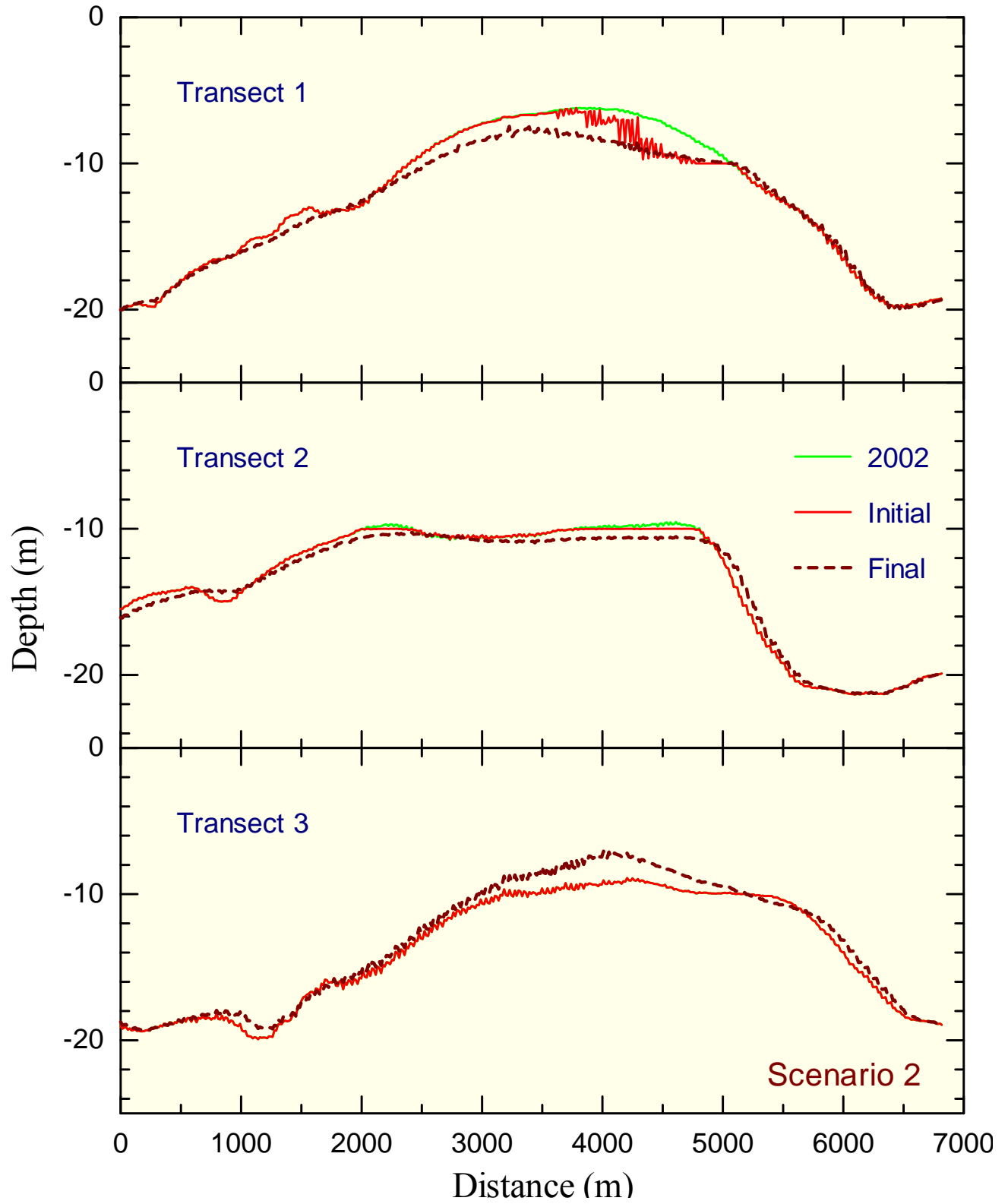
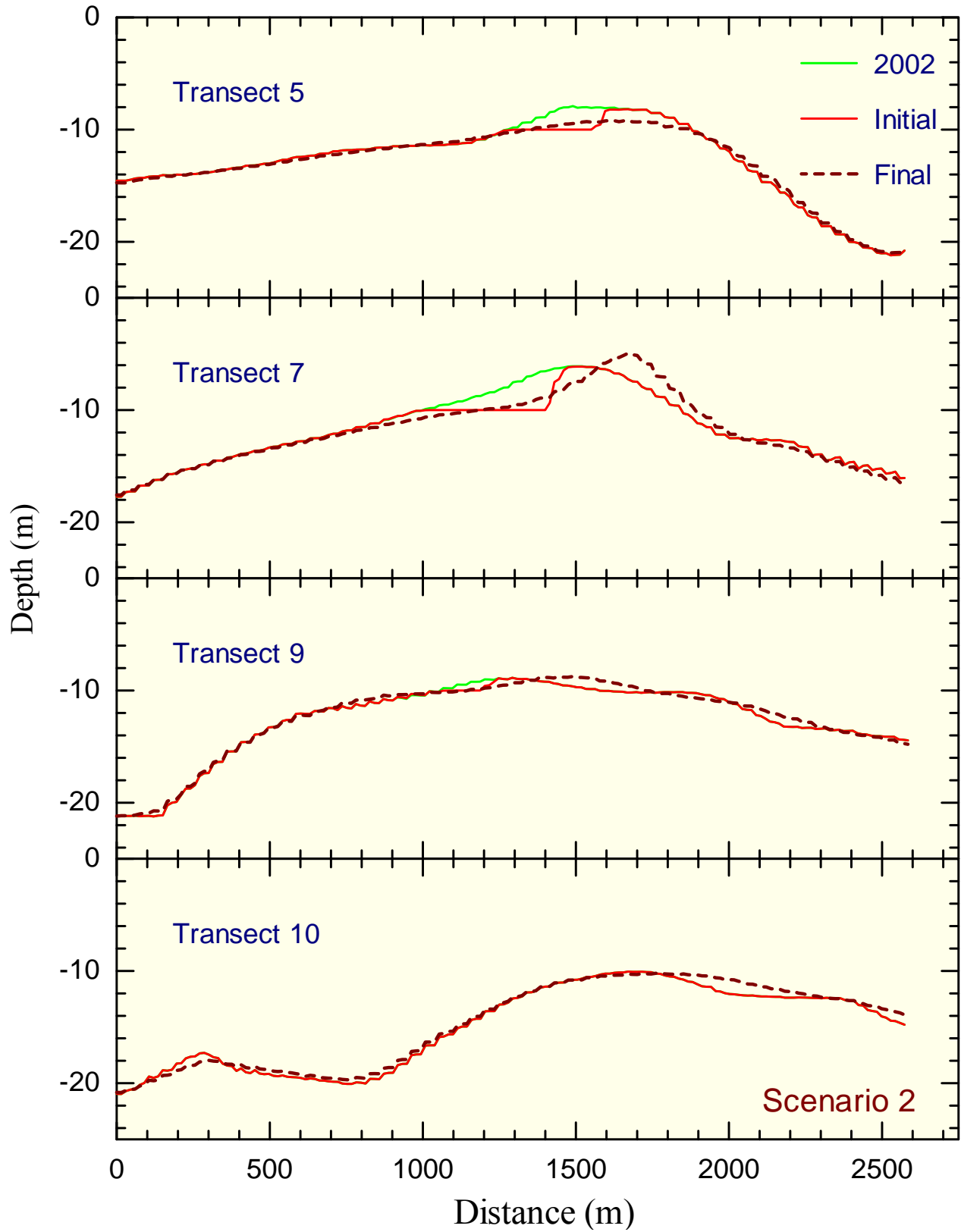**Figure 7.14 Predicted evolution of IOW along transects 1, 2 and 3 after dredging Scenario 3.**

Figure 7.15 Predicted evolution of IOW along transects 6, 7, 8 and 9 after dredging Scenario 3.

Scenario 4

In this scenario the northeastern half of the crest of Isle of Wight is dredged to -10 m contour, as shown in Figure 7.16, to provide about 1.8 million m^3 of sand.
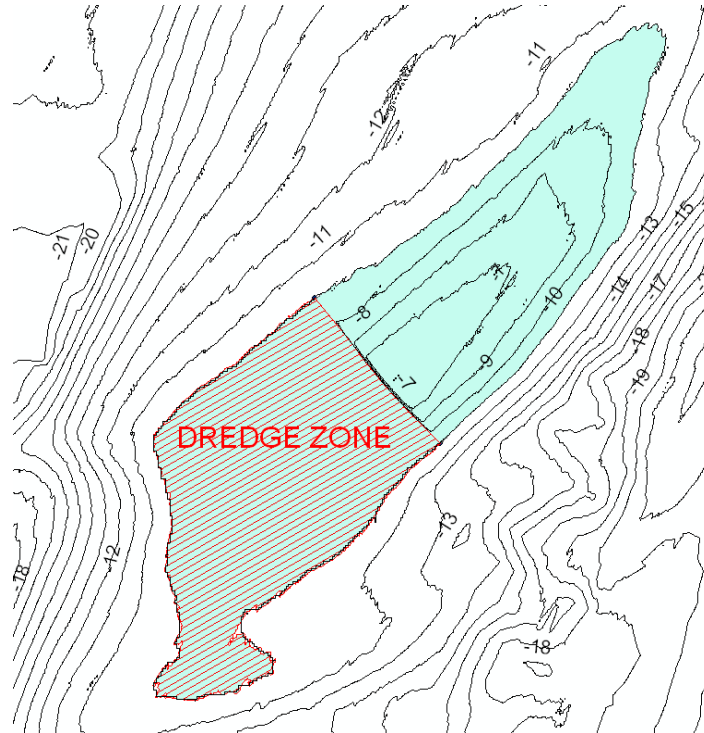

Figure 7.16 Dredging Scenario 4.

Figure 7.17 shows the initial and predicted future bathymetry for the Scenario 4 dredging configurations. IOW is reintegrated into a shoal with shorter crest length than the pre-dredge conditions. Figure 7.18 shows the initial and final depth contours as well as a map of change in bottom elevations. There is almost no accumulation over the dredged part of the shoal and the dredged platform stays unchanged. The new crest is formed on the southwest half of the shoal as the overall transport (shoal migration) is towards southwest. Comparisons at selected transects presented in Figures 7.19 and 7.20 show that the dredged area undergoes very little change. The reformed shoal crest has the same height as the pre-dredge shoal. The new crest, however, is shorter and limited to the southwest half of the shoal. Therefore, this dredging scenario is expected to result in a shoal with the same height but with a shorter crest length located on the southwest half of the shoal compared to the pre-dredge conditions.
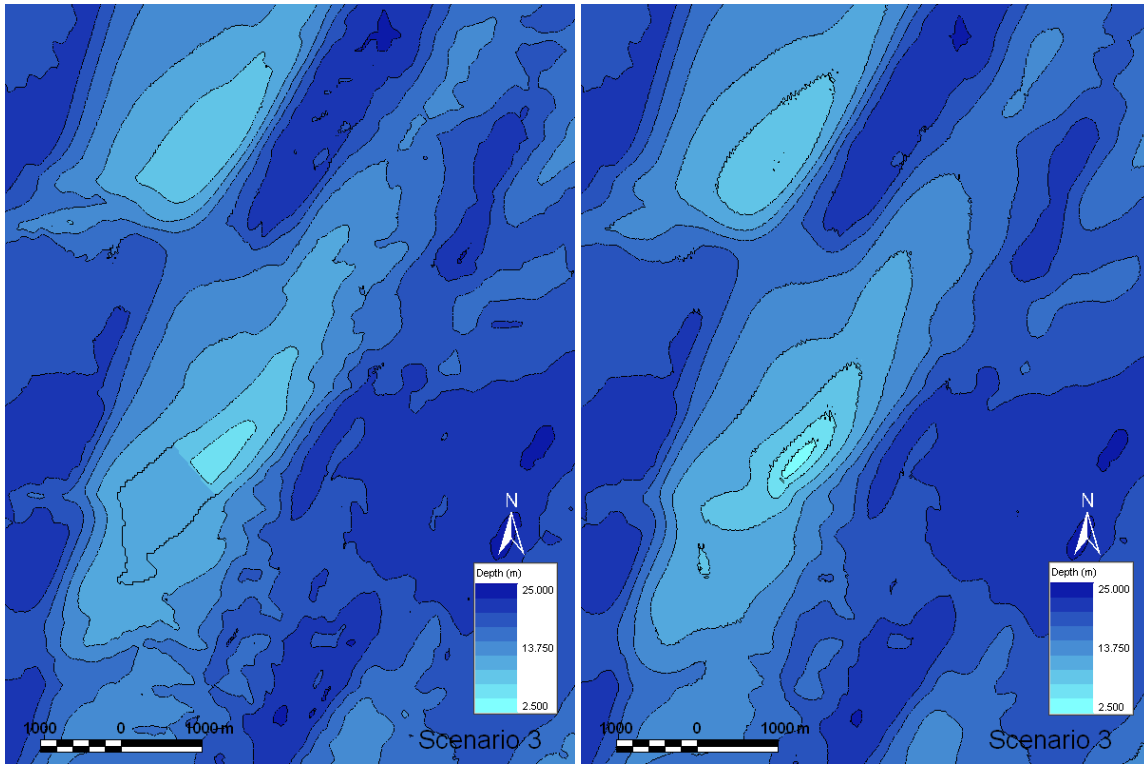
Figure 7.17 Initial (left) and final (right) morphology for Scenario 4 conditions
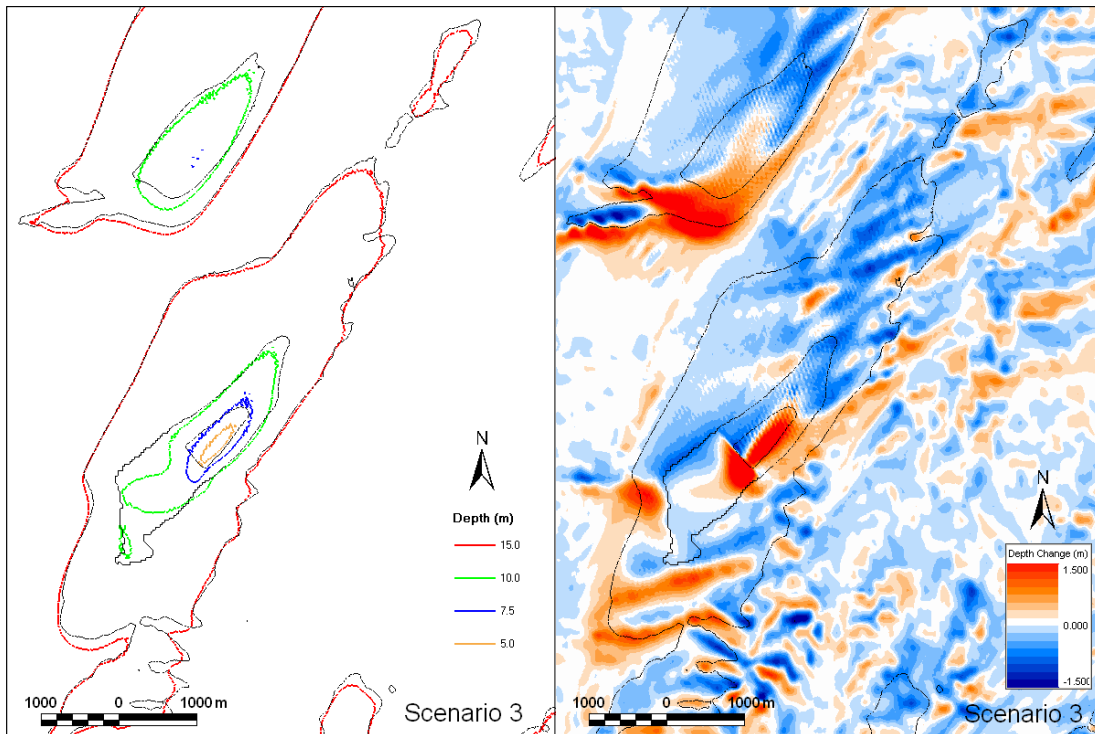

Figure 7.18 Initial and final depth contours (left) and depth change (right) for Scenario 4 conditions.
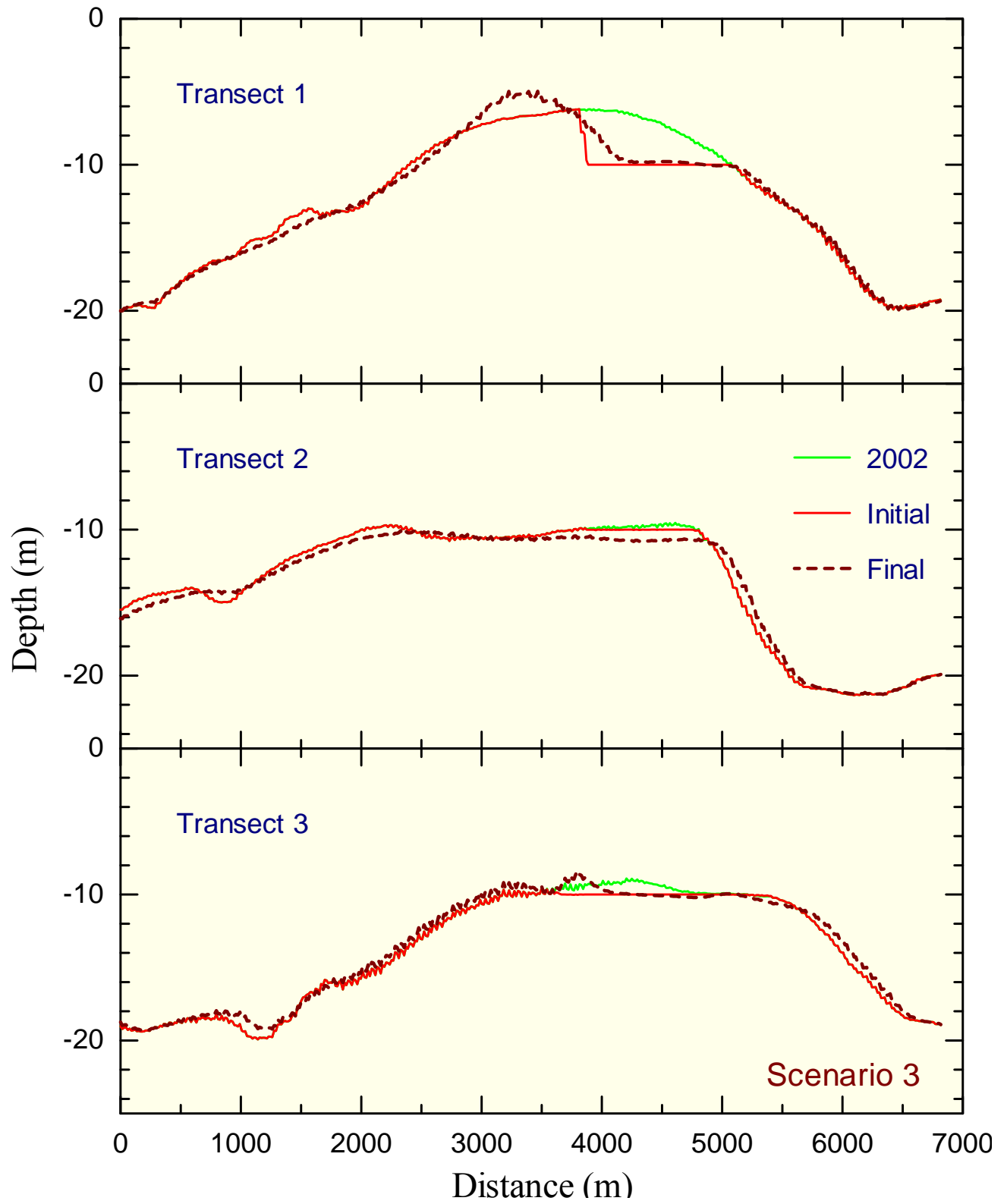
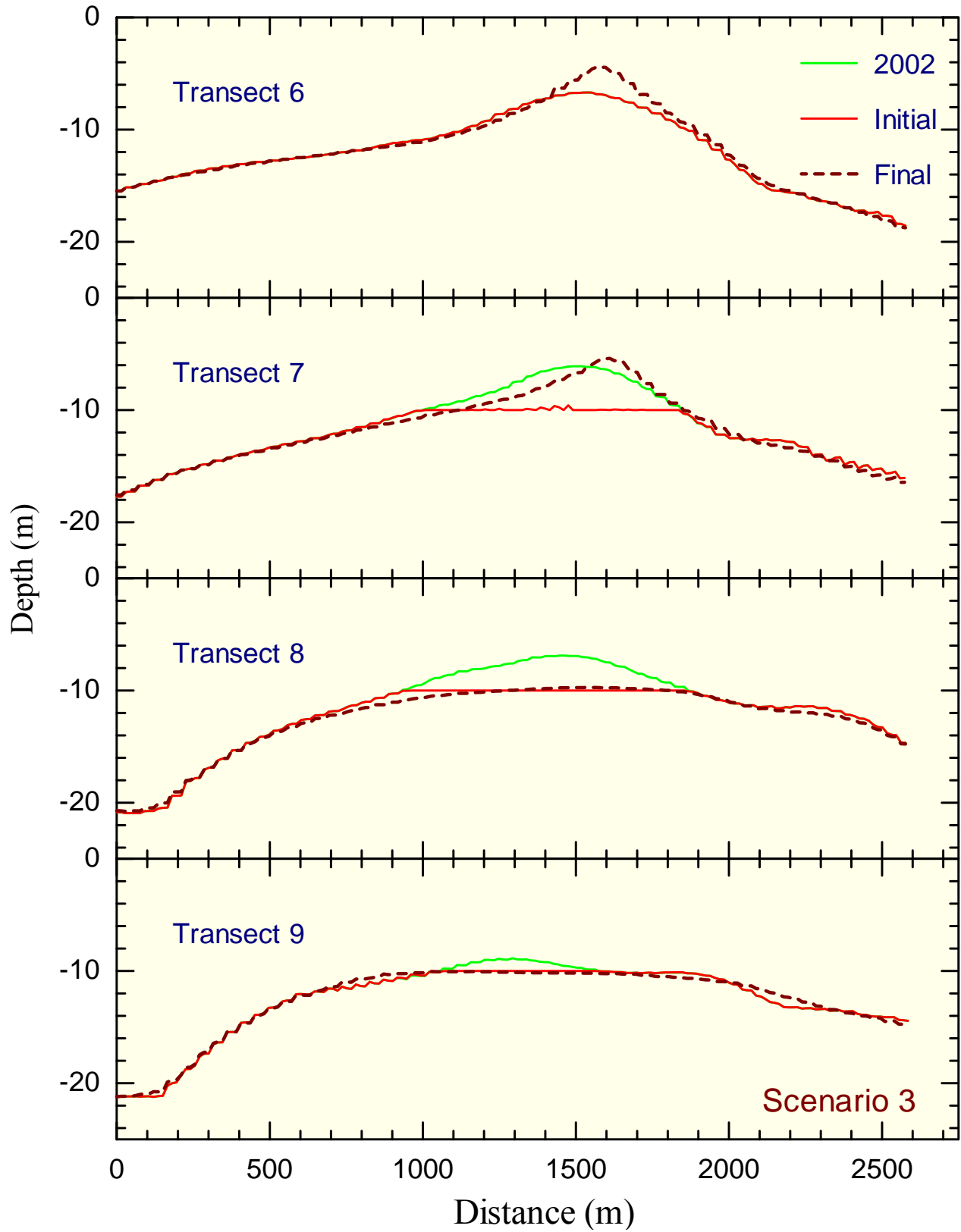**Figure 7.19 Predicted evolution of IOW along transects 1, 2 and 3 after dredging Scenario 4.**

Figure 7.20 Predicted evolution of IOW along transects 4, 5, 6 and 7 after dredging Scenario 4.

Scenario 5

In this scenario the top 1/3 of the volume between shoal crest and -10 m contour is dredged (i.e. from top to -7.3 m contour), as shown in Figure 7.21, to provide about 0.3 million m^3 of sand.
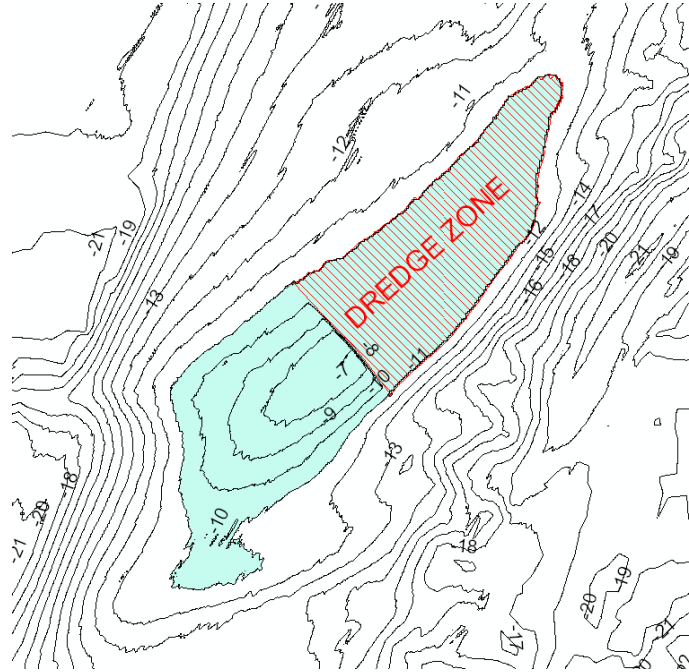

Figure 7.21 Dredging Scenario 5.

Figure 7.22 shows the initial and predicted future bathymetry for the Scenario 5 dredging configurations. IOW keeps its overall shape but with a slightly lower crest. Figure 7.23 shows the initial and final depth contours as well as a map of change in bottom elevations. The excavated part of the shoal is covered again by sand. Comparisons at the transects presented in Figures 7.24 and 7.25 show that the reformed shoal crest is at the same location and has almost the same height as the pre-dredge conditions. Therefore, this dredging scenario is expected to result in essentially the same shoal with a crest height nearly the same as the pre-dredge conditions.

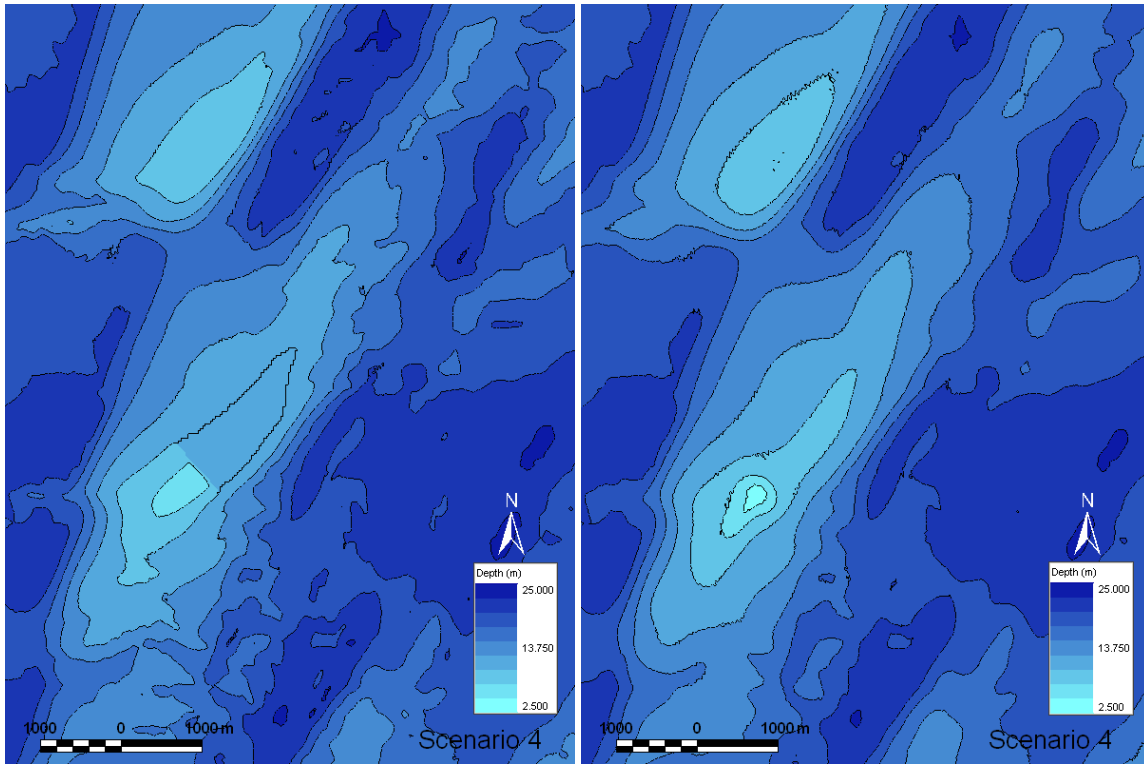**Figure 7.22 Initial (left) and final (right) morphology for Scenario 5 conditions**

Figure 7.23 Initial and final depth contours (left) and depth change (right) for Scenario 5 conditions.

Figure 7.24 Predicted evolution of IOW along transects 1, 2 and 3 after dredging Scenario 5.

Figure 7.25 Predicted evolution of IOW along transects 6, 7, 8 and 9 after dredging Scenario 5.

Scenario 6

In this scenario the top 2/3 of the volume between shoal crest and -10 m contour is dredged (i.e. from top to -8.7 m contour), as shown in Figure 7.26, to provide about 1.5 million m^3 of sand.

Figure 7.26 Dredging Scenario 6.

Figure 7.27 shows the initial and predicted future bathymetry for the Scenario 6 dredging configurations. IOW keeps its overall shape but with a lower crest. Figure 7.28 shows the initial and final depth contours as well as a map of change in bottom elevations. There is little accumulation over the dredged part of the shoal. Comparisons at the transects presented in Figures 7.29 and 7.30 show that the shoal crest stays almost flat (as dredged) and is about 2 m to 3 m lower then the pre-dredge conditions. Therefore, this dredging scenario is expected to result in essentially the same shoal but with a much (2 m to 3 m) lower crest height than the pre-dredge conditions.

Figure 7.27 Initial (left) and final (right) morphology for Scenario 6 conditions
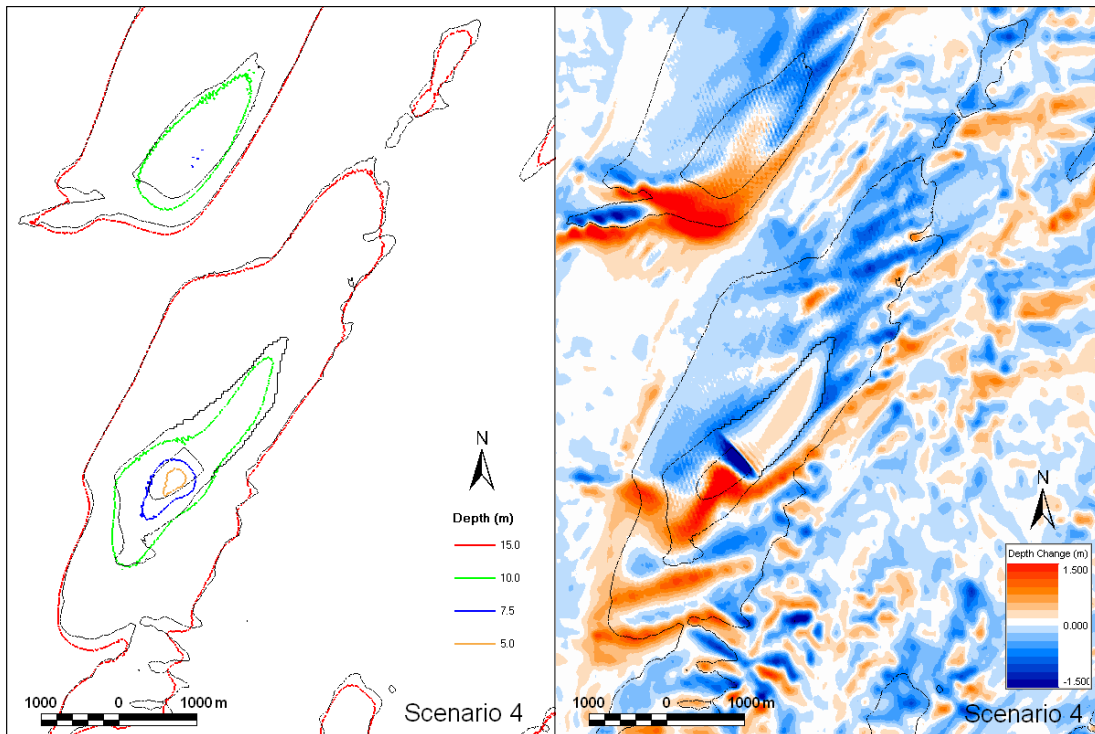

Figure 7.28 Initial and final depth contours (left) and depth change (right) for Scenario 6 conditions.
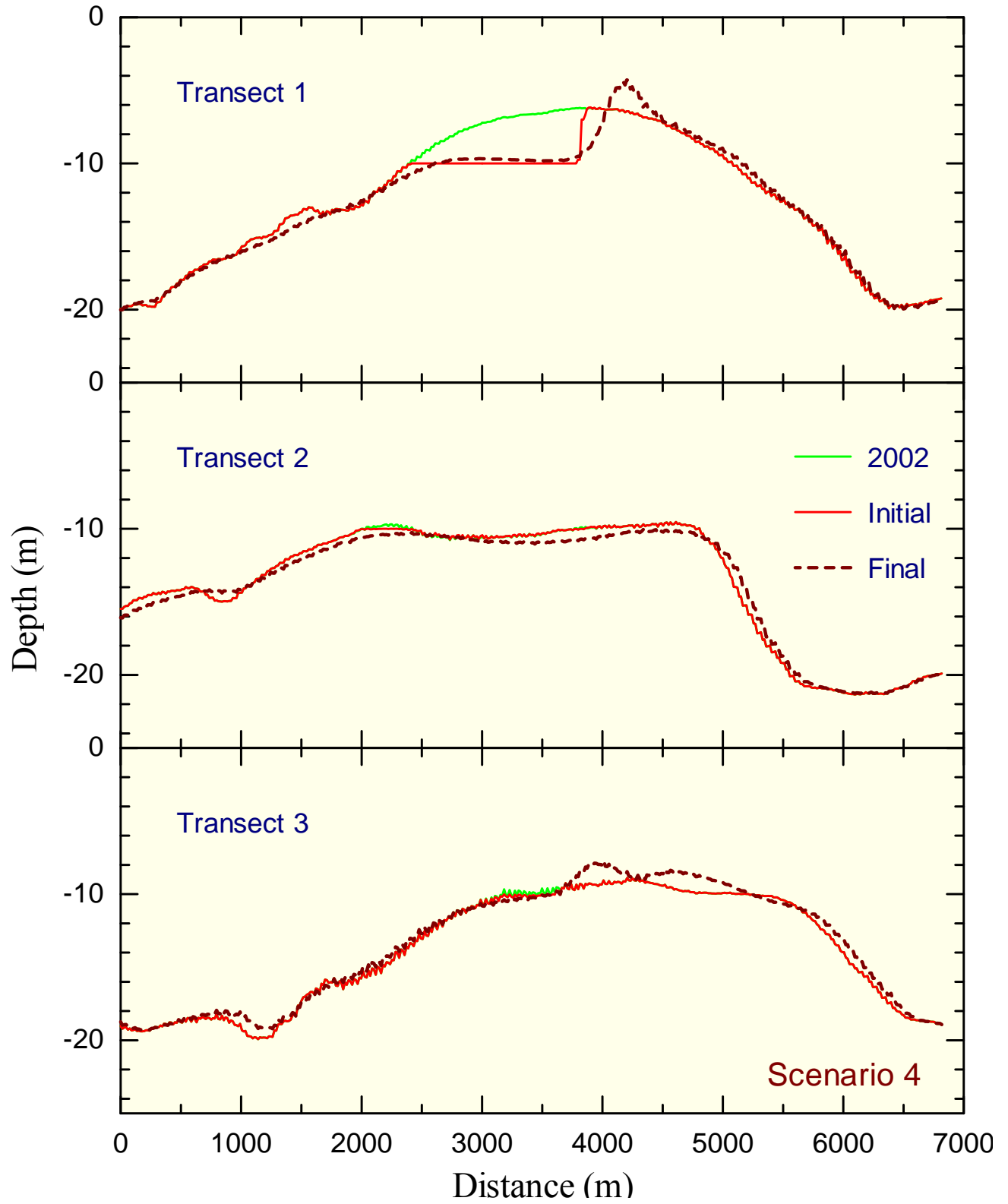
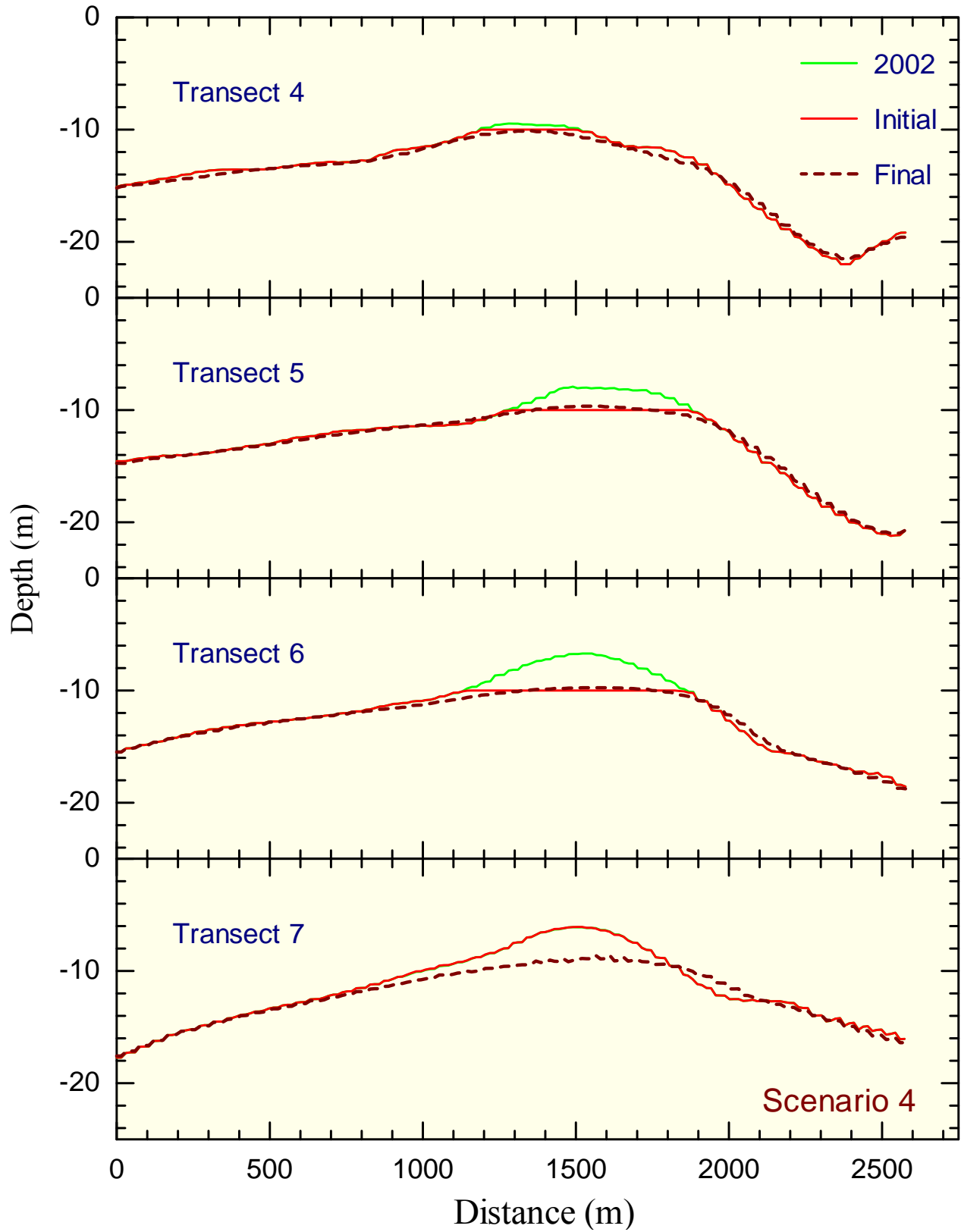**Figure 7.29 Predicted evolution of IOW along transects 1, 2 and 3 after dredging Scenario 6.**

Figure 7.30 Predicted evolution of IOW along transects 5, 7, 9 and 10 after dredging Scenario 6.

Scenario 7

In this scenario the southwestern quarter of the crest of Isle of Wight is dredged to -10 m contour, as shown in Figure 7.31, to provide about 0.95 million m^3 of sand.
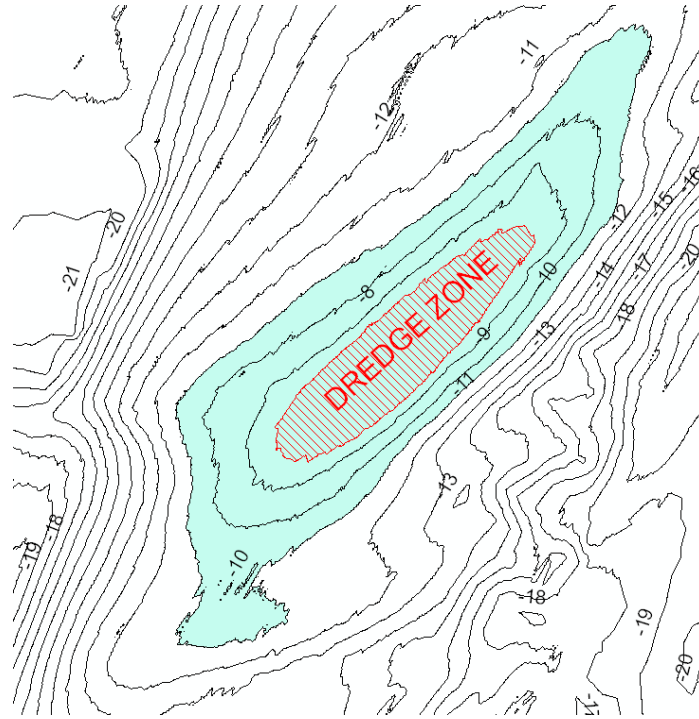

Figure 7.31 Dredging Scenario 7.

Figure 7.32 shows the initial and predicted future bathymetry for the Scenario 7 dredging configurations. IOW is reintegrated into a shoal with a smaller shoal crest than the pre-dredge conditions. The new shoal crest is centered towards the northeast side of the shoal where the most of wave-focusing effect occurs. Figure 7.33 shows the initial and final depth contours as well as a map of change in bottom elevations. There is considerable accumulation over the dredged part. Comparisons at selected transects presented in Figures 7.34 and 7.35 show that the reformed shoal crest has the same height as the pre-dredge shoal. The new crest is on the northeast side of the shoal likely due to the fact that the southwest side has been dredged and does not grow equally. Therefore, this dredging scenario is expected to result in a shoal with the same height but with a shorter crest length than the pre-dredge conditions.
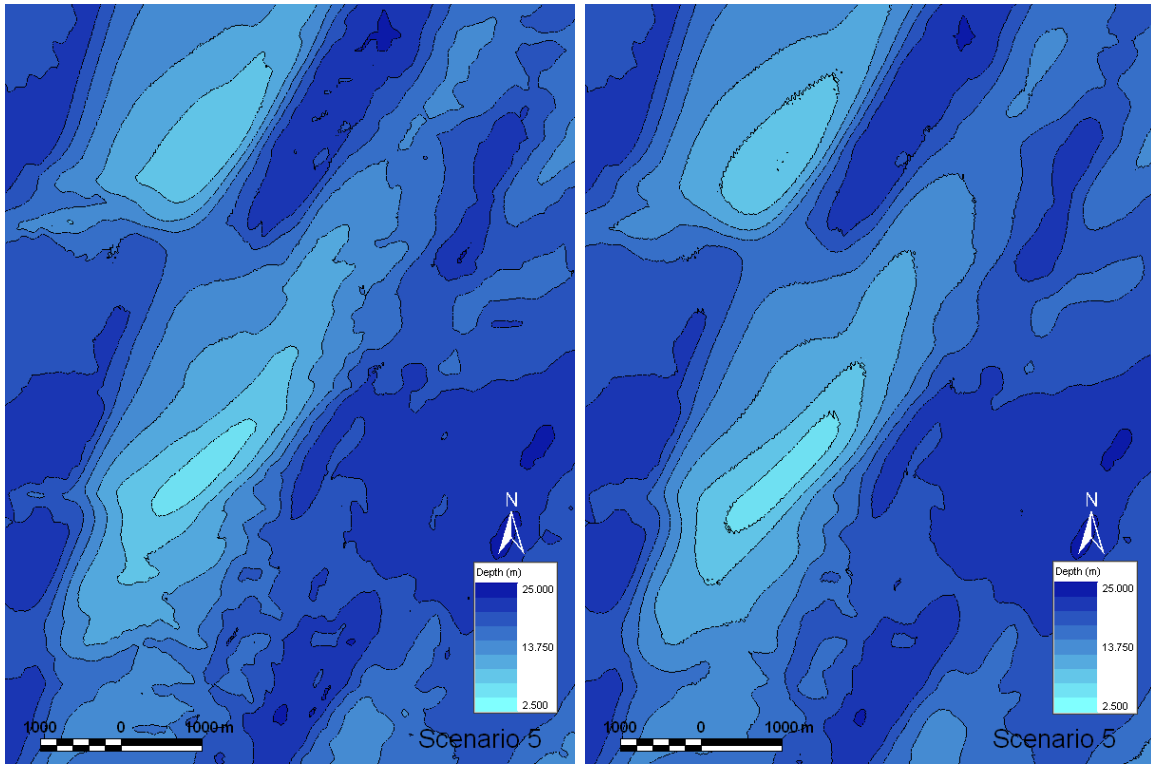
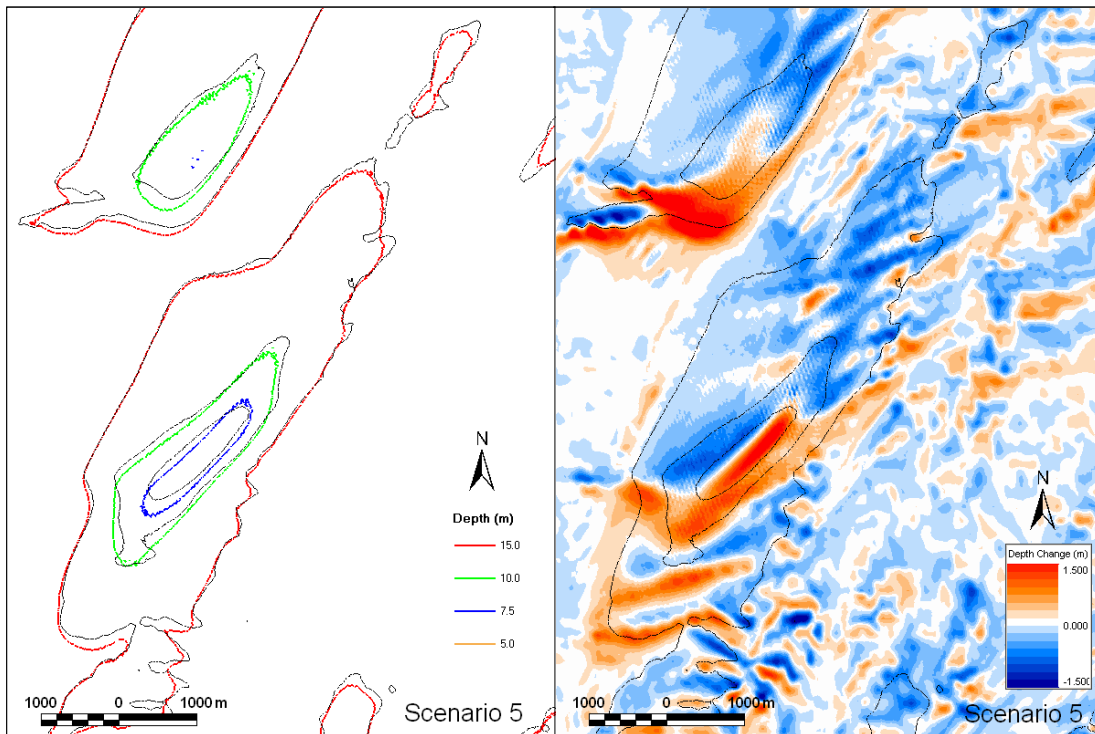**Figure 7.32 Initial (left) and final (right) morphology for Scenario 7 conditions**

Figure 7.33 Initial and final depth contours (left) and depth change (right) for Scenario 7 conditions.
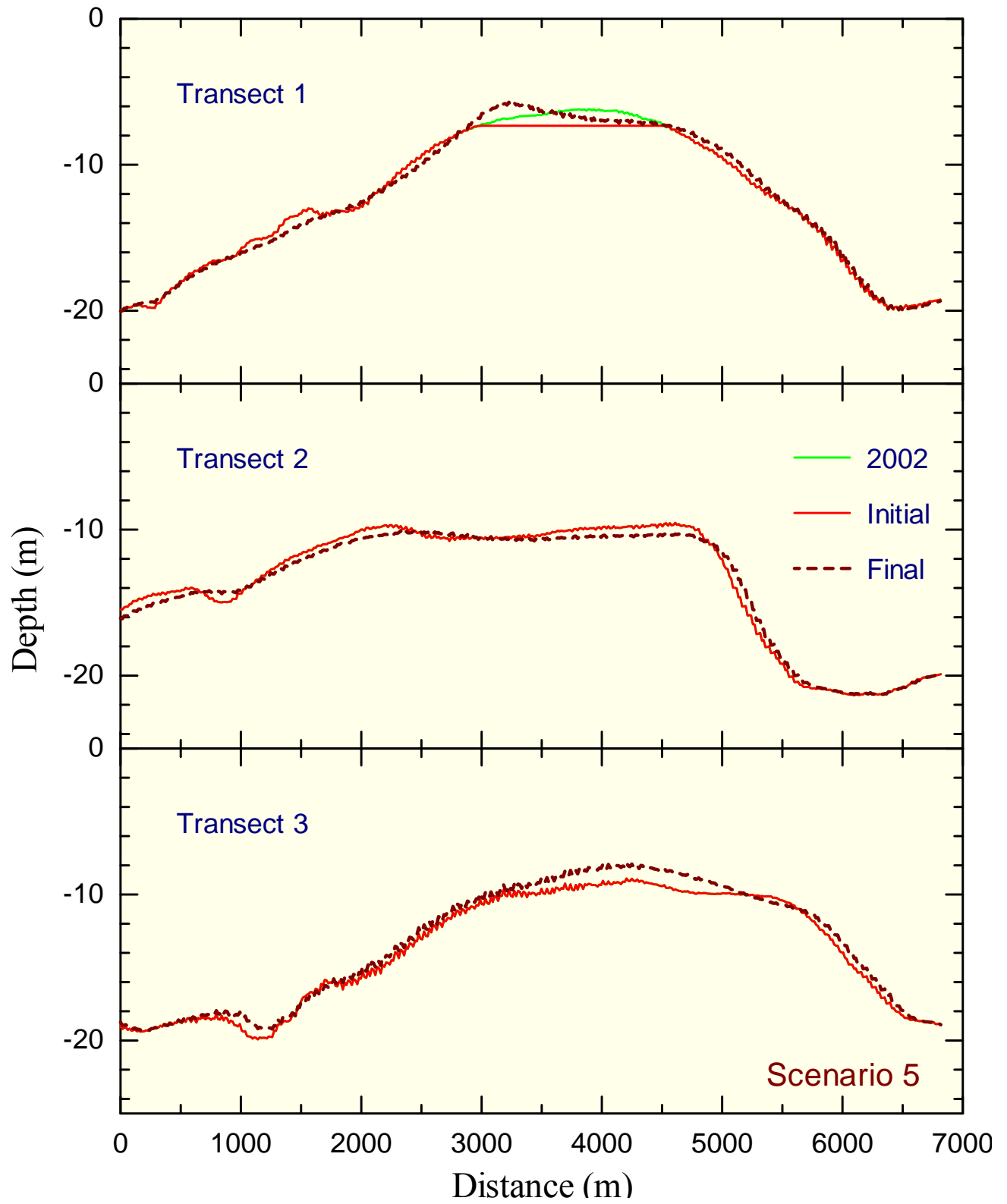
Figure 7.34 Predicted evolution of IOW along transects 1, 2 and 3 after dredging Scenario 7.
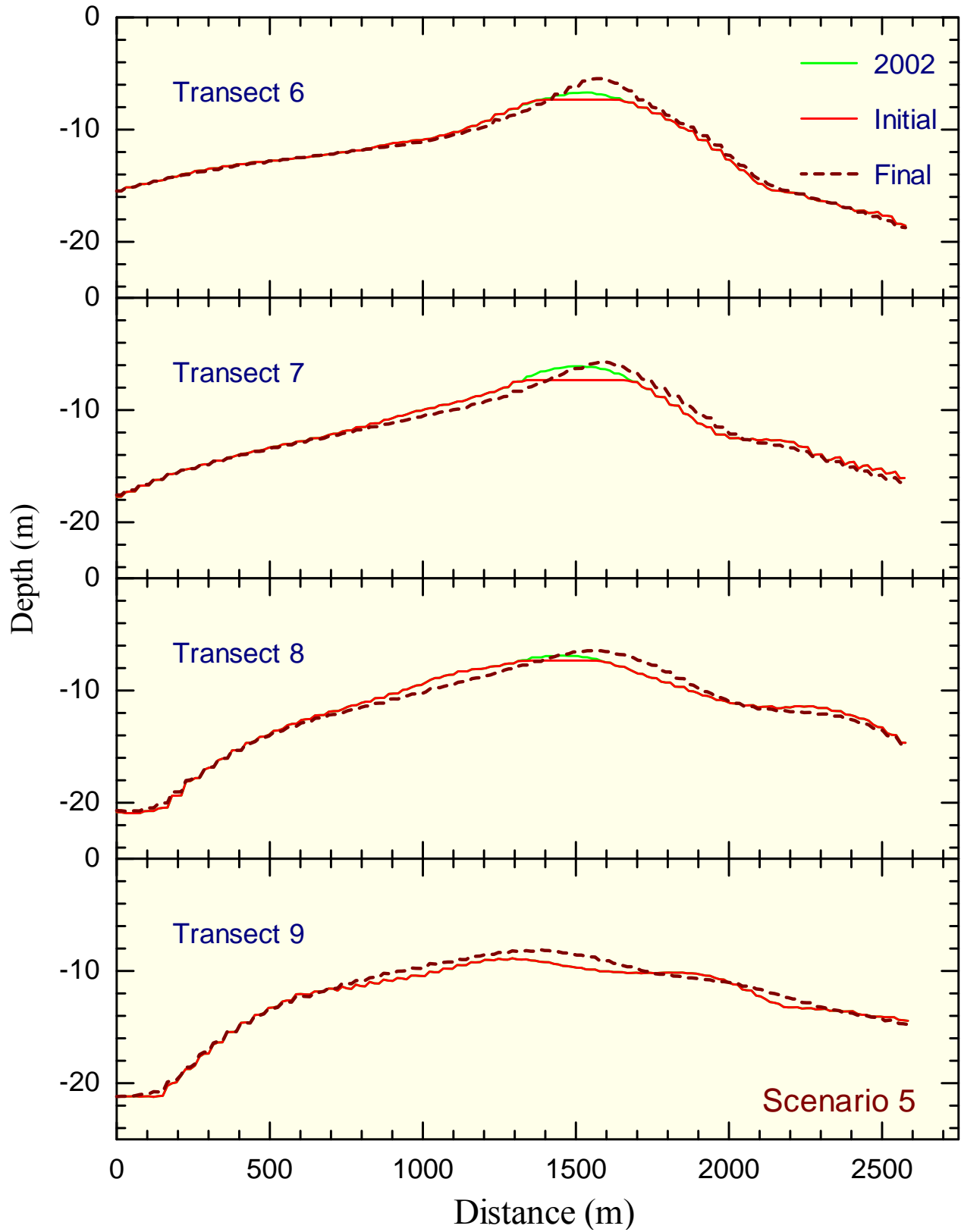
Figure 7.35 Predicted evolution of IOW along transects 6, 7, 8 and 9 after dredging Scenario 7.

Scenario 8

In this scenario both southwestern and northeastern quarters of the crest of Isle of Wight are dredged to -10 m contour, as shown in Figure 7.36, to provide about 1.75 million m^3 of sand.
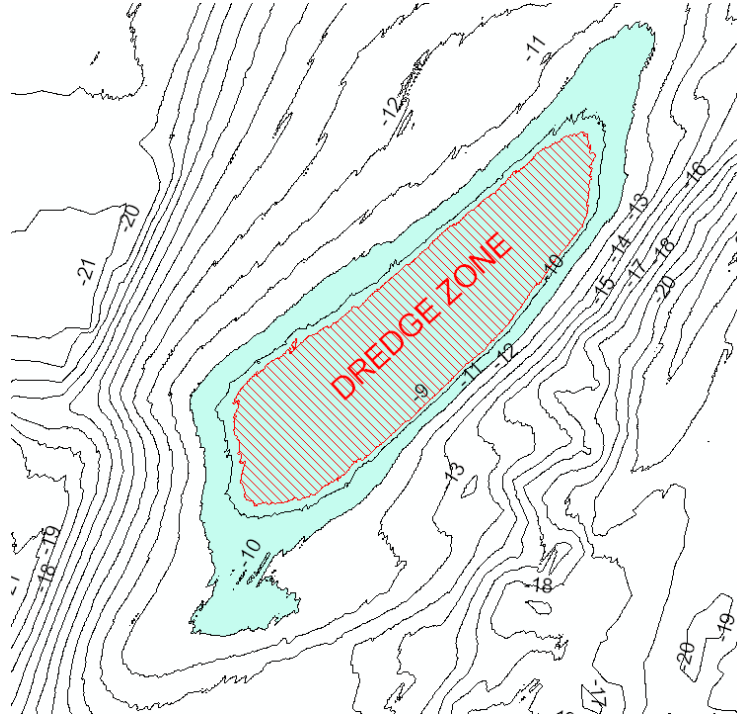

Figure 7.36 Dredging Scenario 8.

Figure 7.37 shows the initial and predicted future bathymetry for the Scenario 8 dredging configurations. IOW is reintegrated into a shoal with a smaller shoal crest than the pre-dredge conditions. The new shoal crest is centered on the southeast side of the shoal where most of the wave-focusing effect occurs. Figure 7.38 shows the initial and final depth contours as well as a map of change in bottom elevations. There is considerable accumulation over the southwest dredged quarter in line with the overall shoal migration direction. Comparisons at selected transects presented in Figures 7.39 and 7.40 show that the reformed shoal does not reach the same height as the pre-dredge shoal and is about 1 m to 2 m lower. The new crest is on the southeast quarter side of the shoal likely due to the fact that the southwest side has been dredged and does not grow equally. Therefore, this dredging scenario is expected to result in a shoal with lower height and shorter crest length than the pre-dredge conditions.
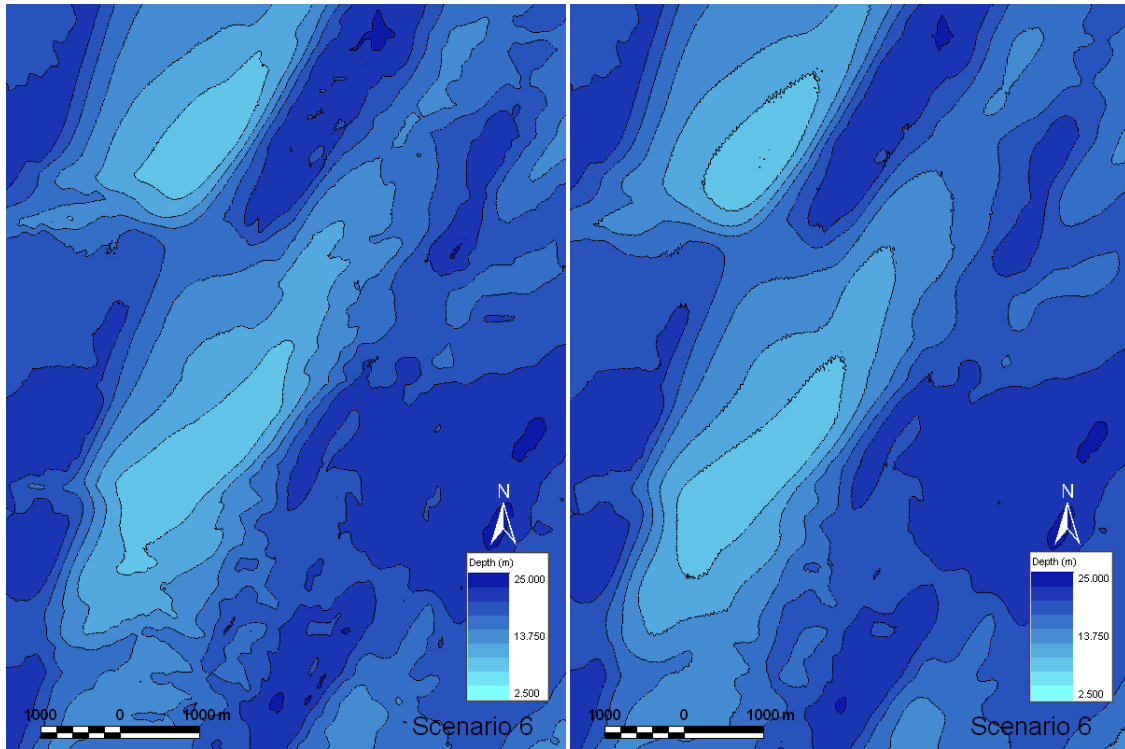
Figure 7.37 Initial (left) and final (right) morphology for Scenario 8 conditions
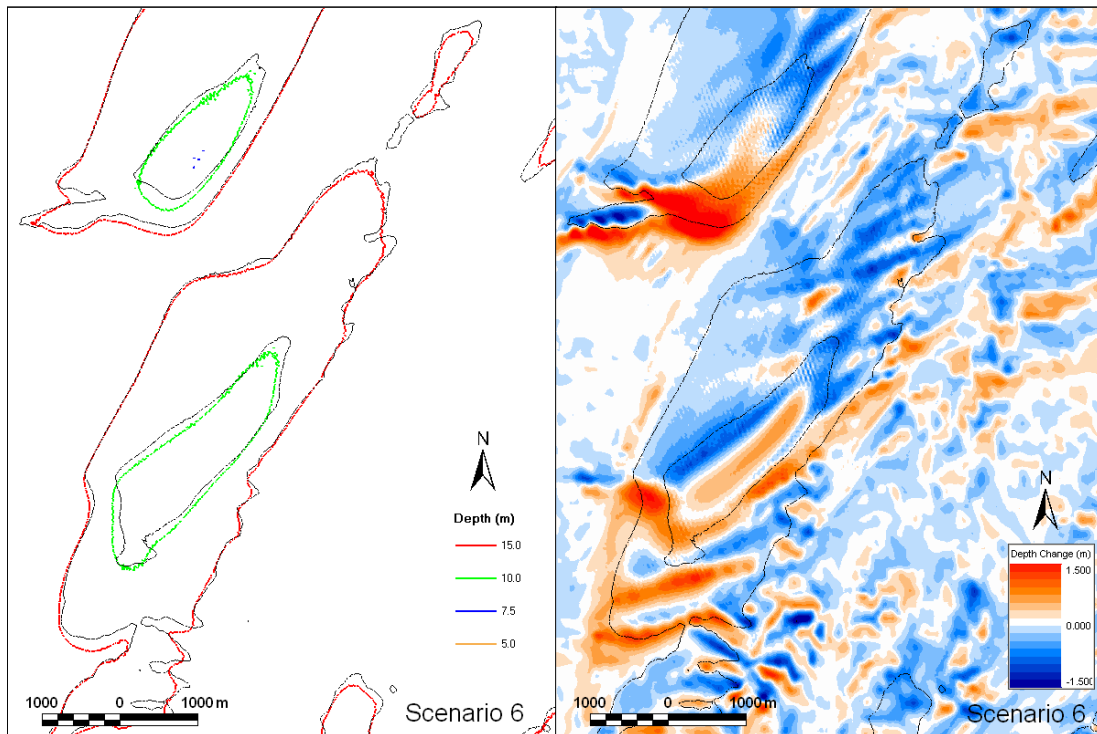

Figure 7.38 Initial and final depth contours (left) and depth change (right) for Scenario 8 conditions.
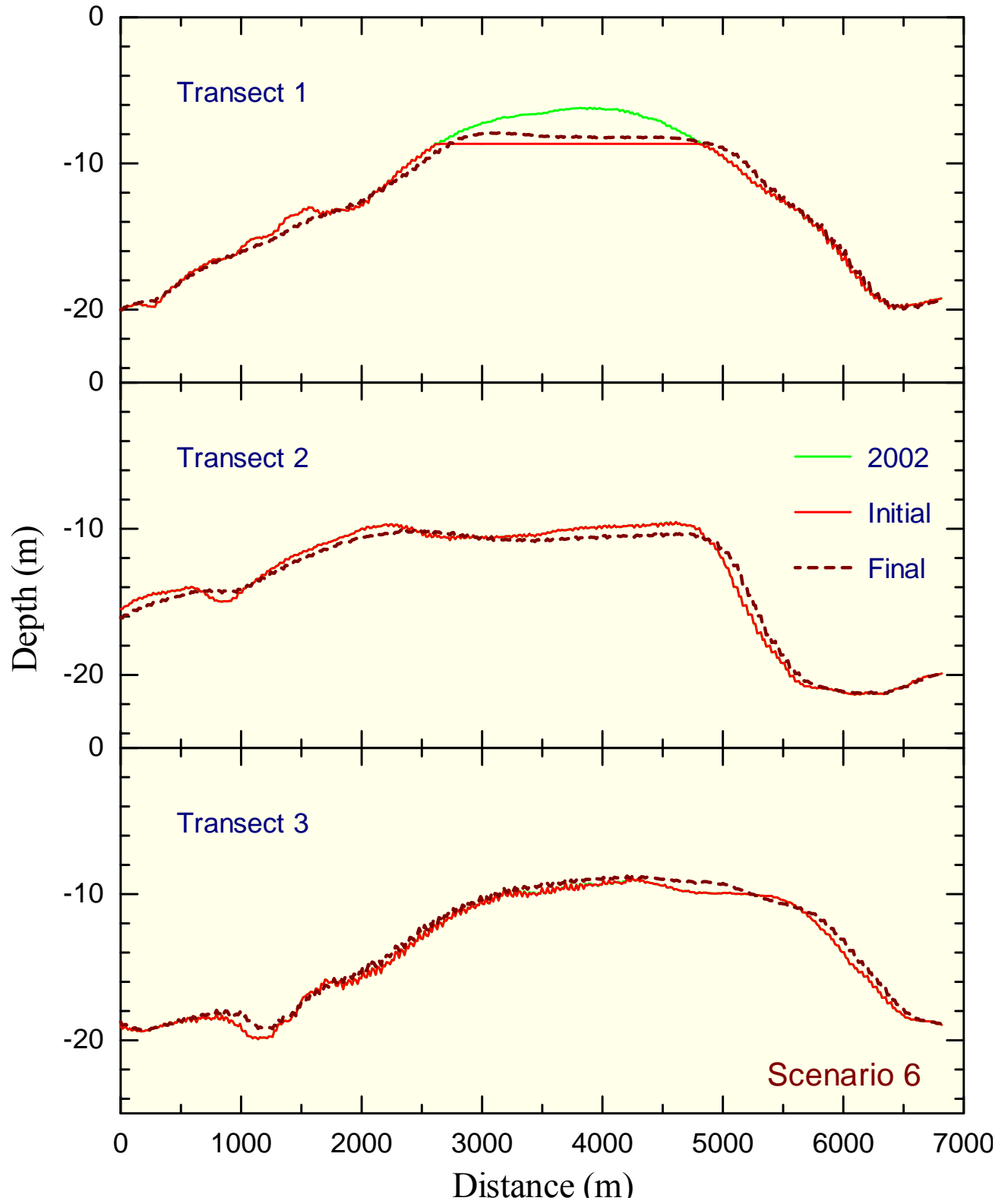
Figure 7.39 Predicted evolution of IOW along transects 1, 2 and 3 after dredging Scenario 8.
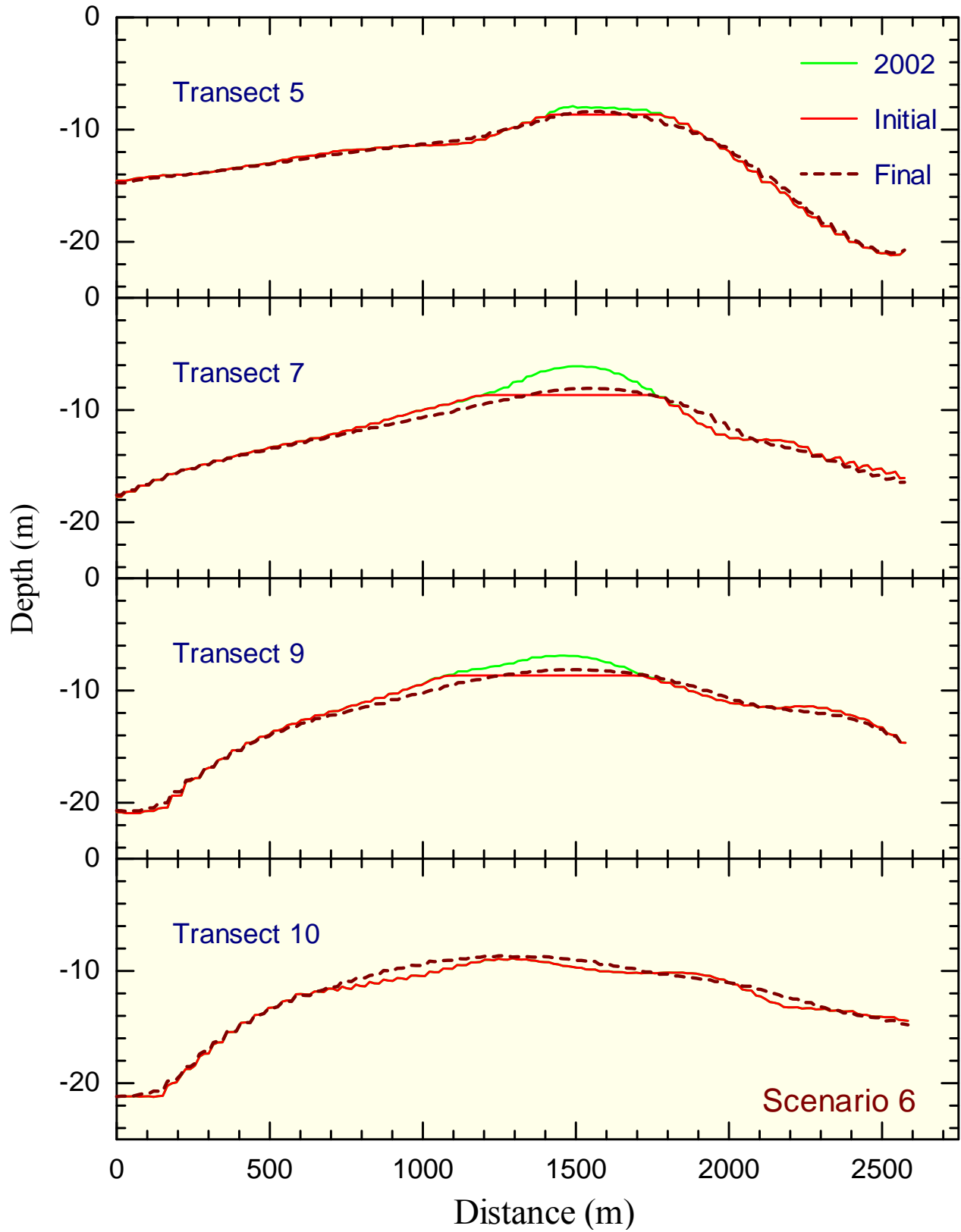
Figure 7.40 Predicted evolution of IOW along transects 5, 6, 7 and 8 after dredging Scenario 8.

Scenario 9

In this scenario the southwestern 1/3 of the crest of Isle of Wight is dredged to -10 m contour, as shown in Figure 7.41, to provide about 1.0 million m^3 of sand.
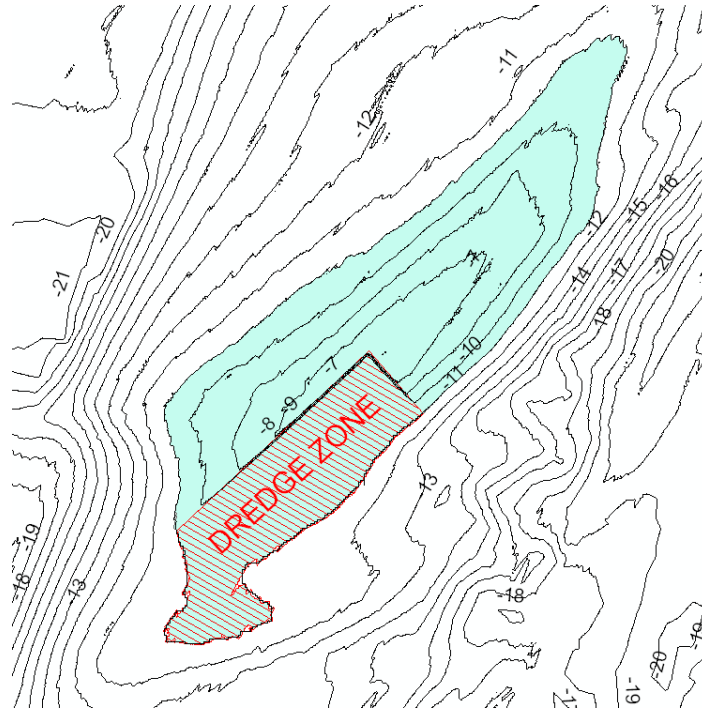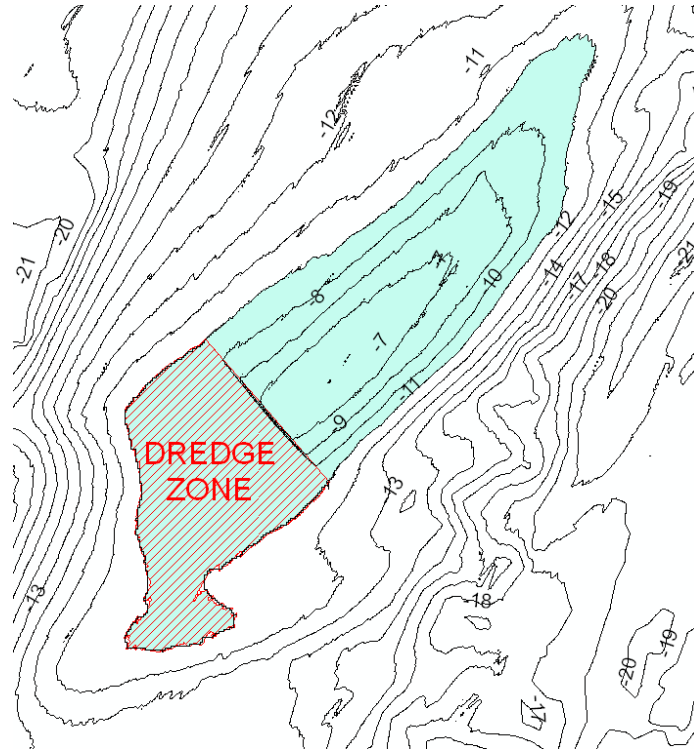

Figure 7.41 Dredging Scenario 9.

Figure 7.42 shows the initial and predicted future bathymetry for the Scenario 9 dredging configurations. Similar to Scenario 3, IOW is reintegrated into a shoal with shorter crest length than the pre-dredge conditions. Figure 7.43 shows the initial and final depth contours as well as a map of change in bottom elevations. There is considerable accumulation over the northeast half of the dredged part. Comparisons at selected transects presented in Figures 7.44 and 7.45 show that although the dredged platform stays partly unchanged, the reformed shoal crest has the same height as the pre-dredge shoal. The new crest, however, is shorter and does not extend far beyond Transect 8 towards the southwest. Therefore, this dredging scenario is expected to result in a shoal with the same height but with a shorter crest length than the pre-dredge conditions.
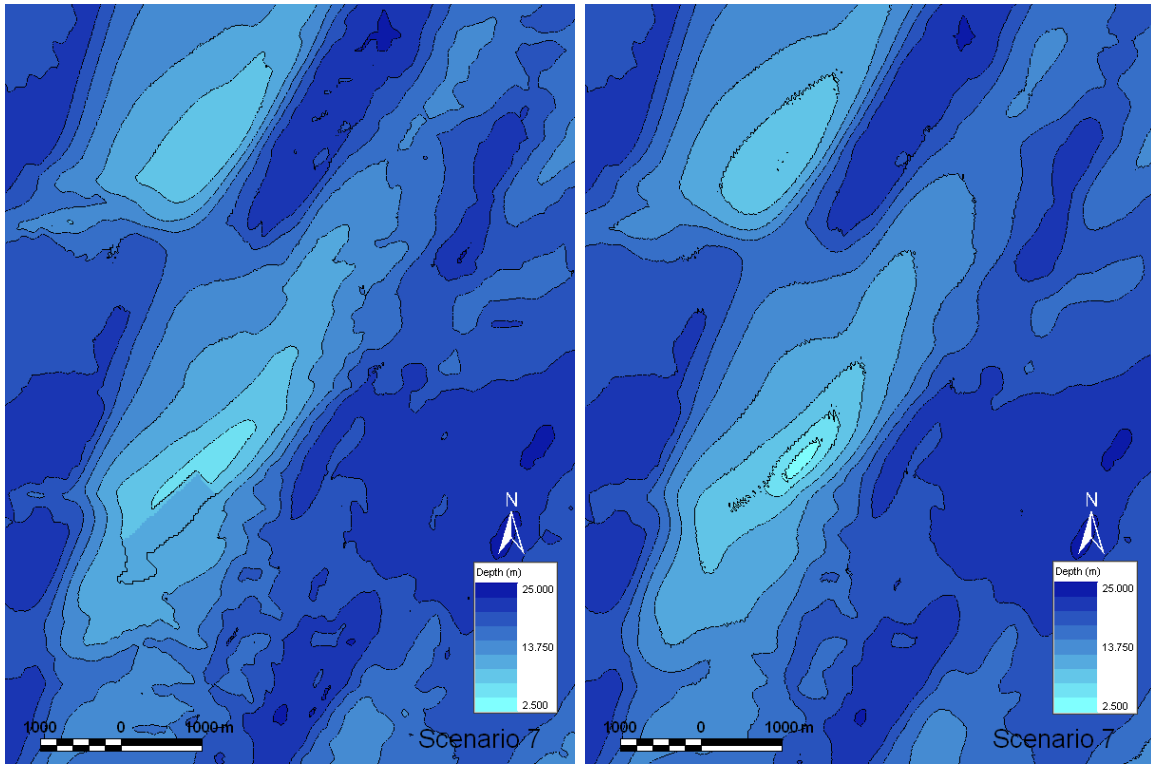
Figure 7.42 Initial (left) and final (right) morphology for Scenario 9 conditions
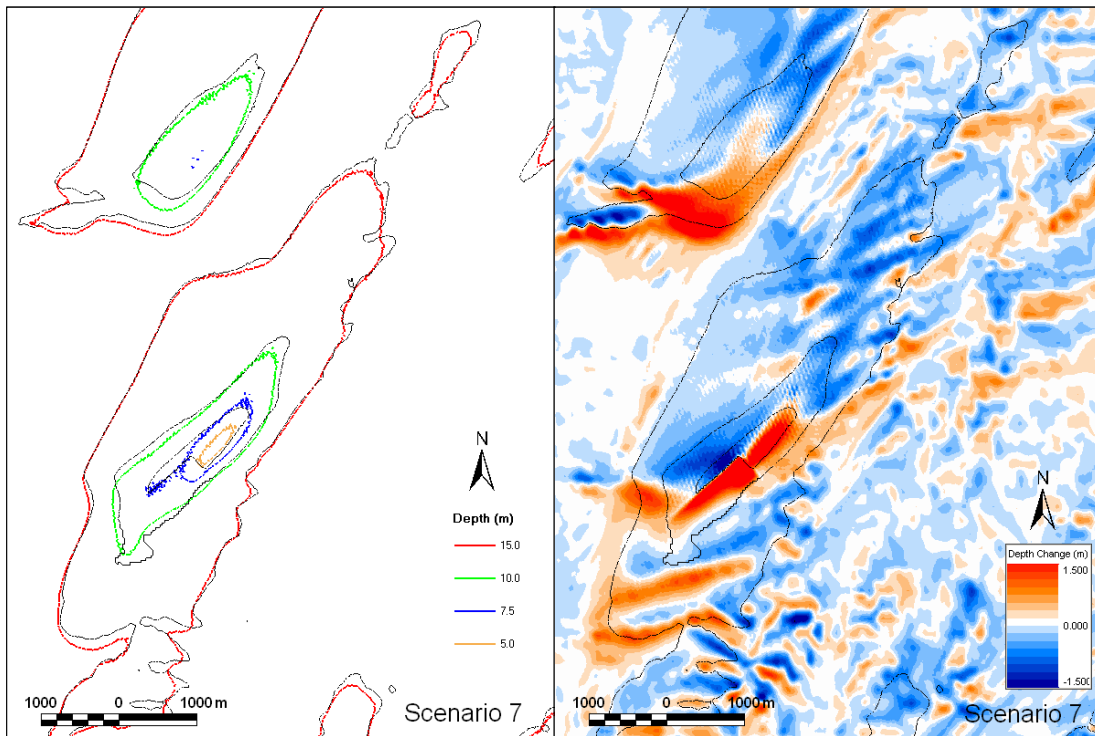

Figure 7.43 Initial and final depth contours (left) and depth change (right) for Scenario 9 conditions.
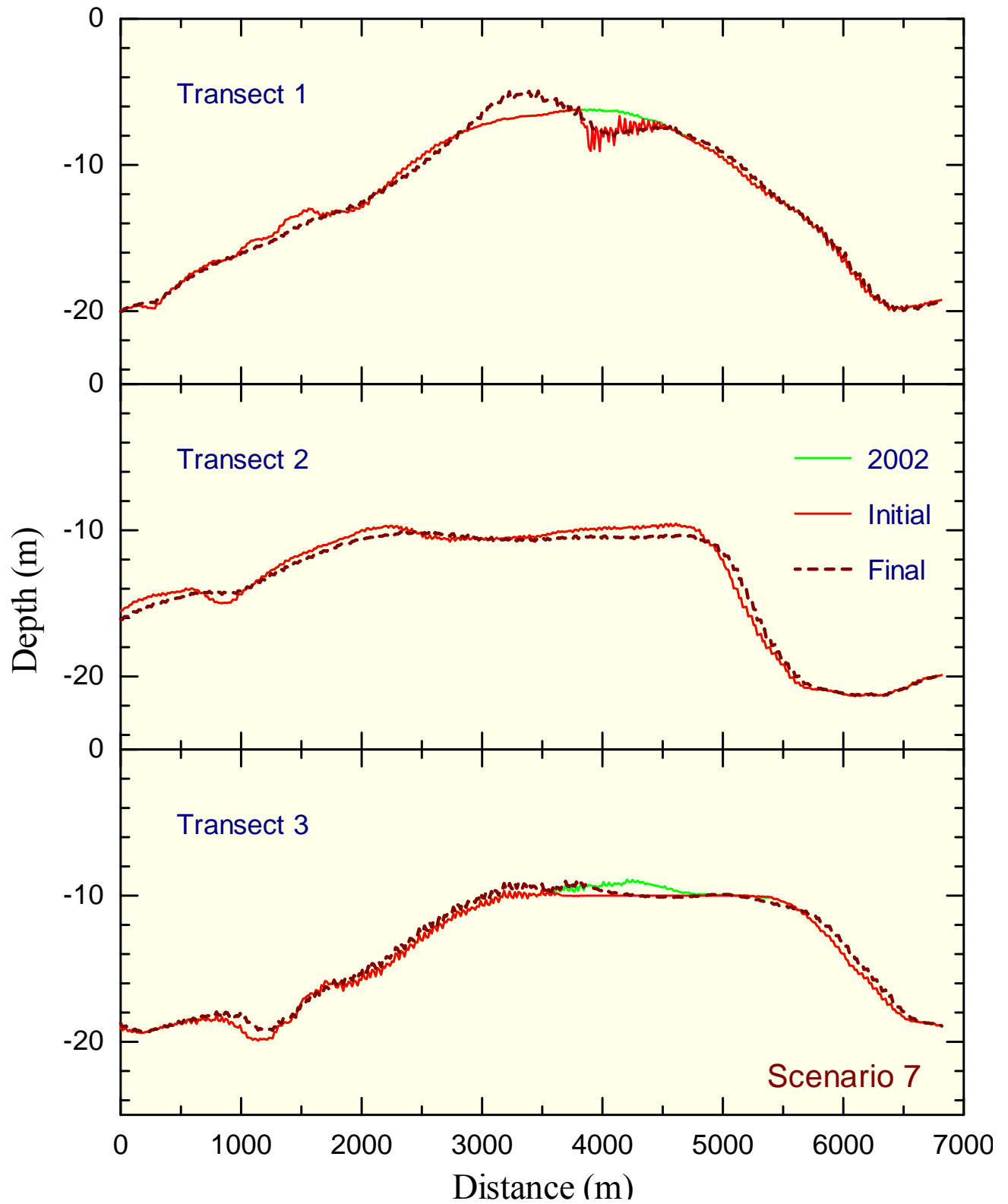
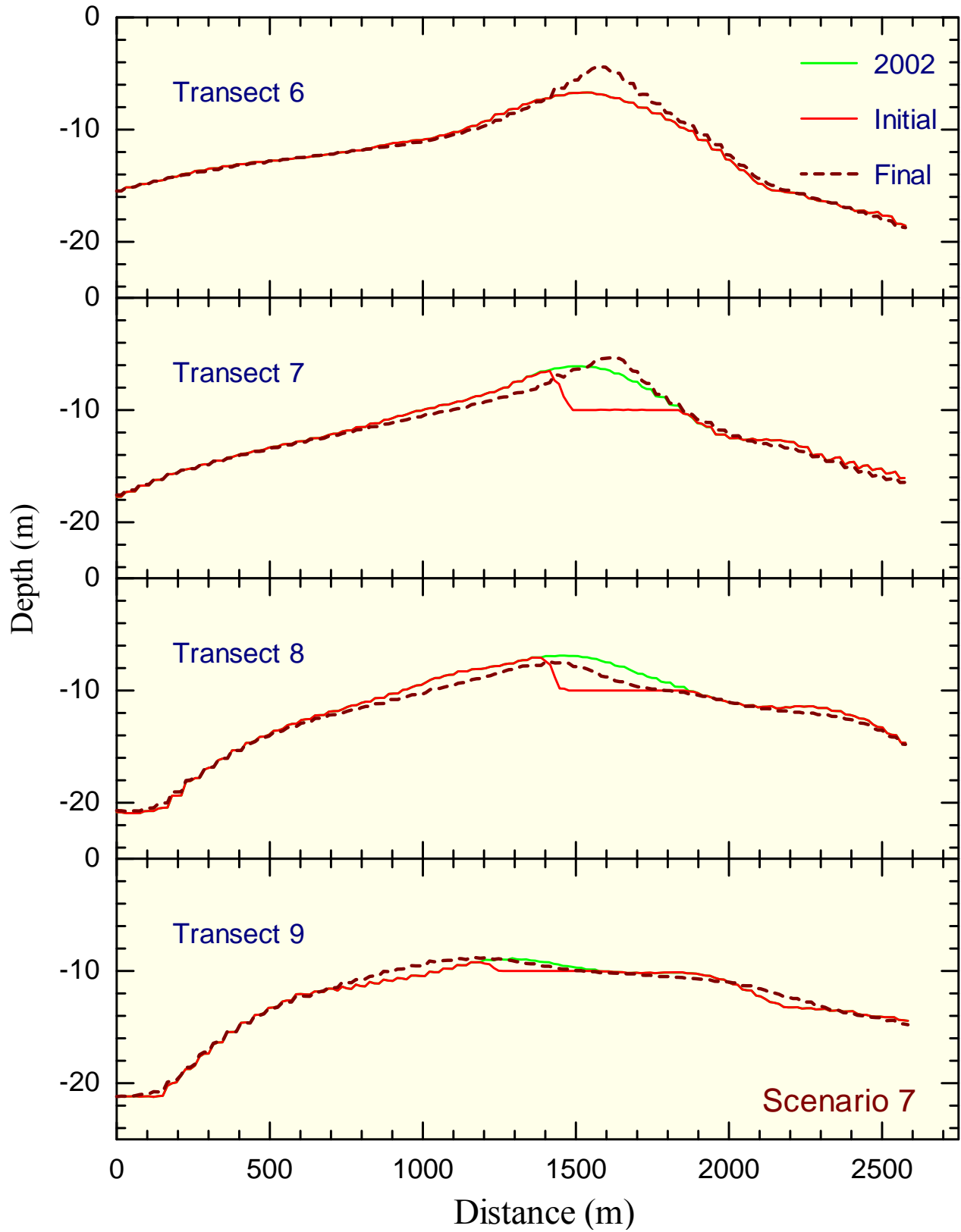Figure 7.44 Predicted evolution of IOW along transects 1, 2 and 3 after dredging Scenario 9.

Figure 7.45 Predicted evolution of IOW along transects 7, 8, 9 and 10 after dredging Scenario 9.

Scenario 10

In this scenario the middle 1/3 of the crest of Isle of Wight is dredged to -10 m contour, as shown in Figure 7.46, to provide about 1.9 million m^3 of sand.
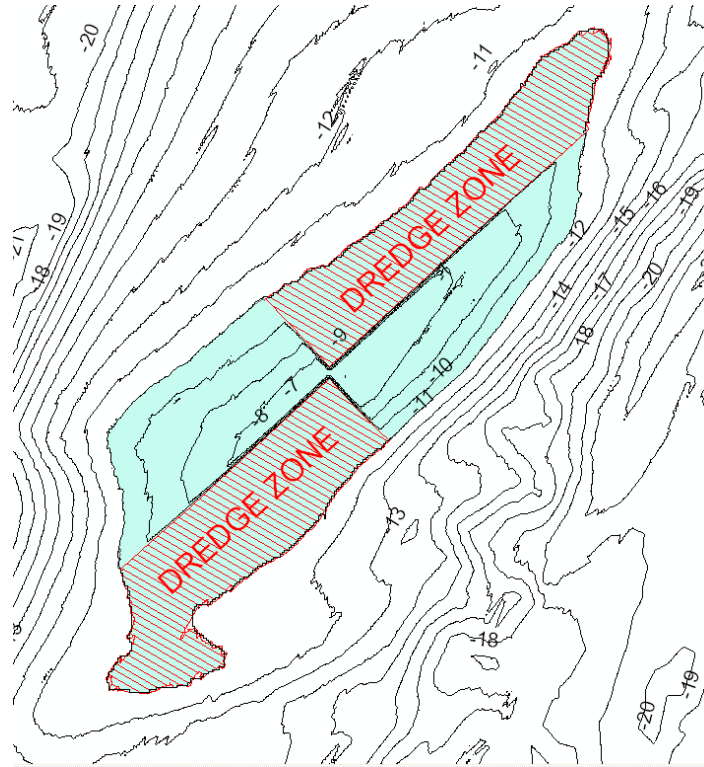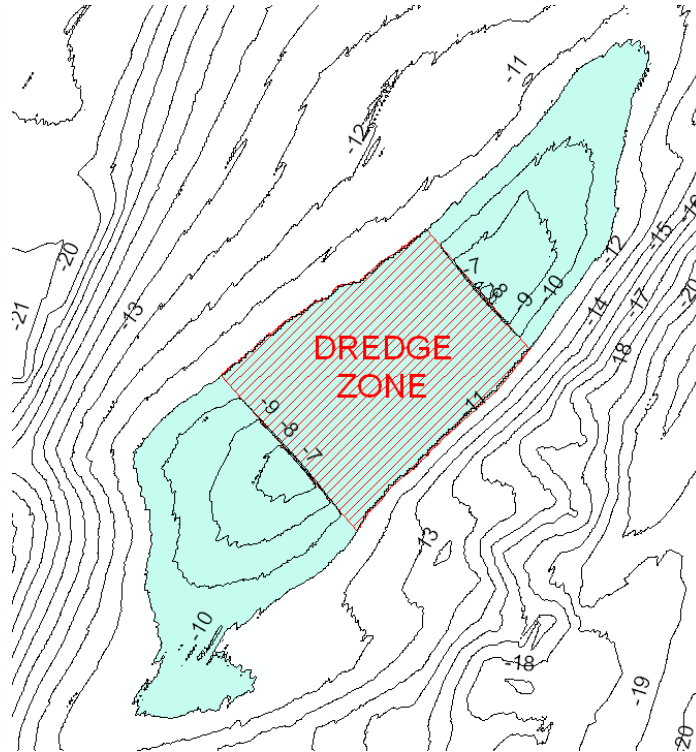

Figure 7.46 Dredging Scenario 10.

Figure 7.47 shows the initial and predicted future bathymetry for the Scenario 10 dredging configurations. IOW is reintegrated into a shoal with double crests. Figure 7.48 shows the initial and final depth contours as well as a map of change in bottom elevations. There is considerable accumulation over the northeast half of the dredged part, while the southwest half receives little accumulation. In fact the remaining southwest part of the shoal crest has moved towards southwest to form a new crest. Comparisons at the transects presented in Figures 7.49 and 7.50 show that the dredged platform stays almost unchanged and the two crests are formed by remains of the initial shoal crest on both sides of the dredged area. The overall shoal height is expected to be the same as that of the pre-dredge shoal. Therefore, this dredging scenario is expected to result in a shoal with two smaller crests, both expected to be at the same level of the shoal crest in the pre-dredge conditions.
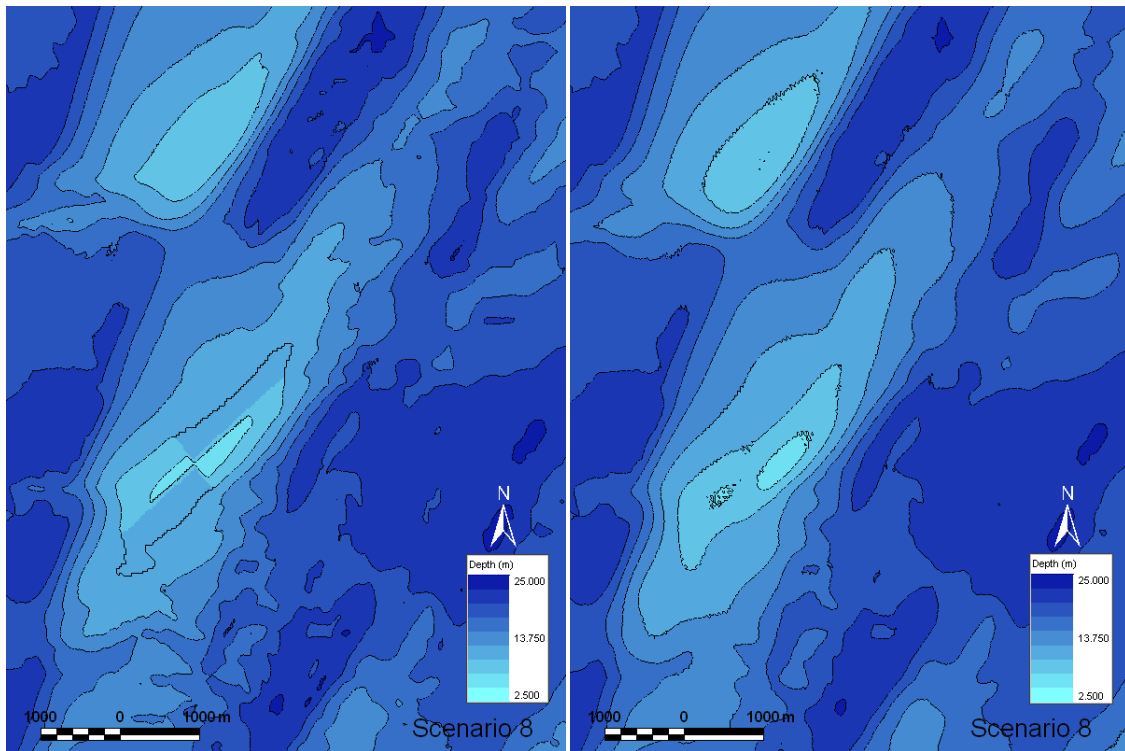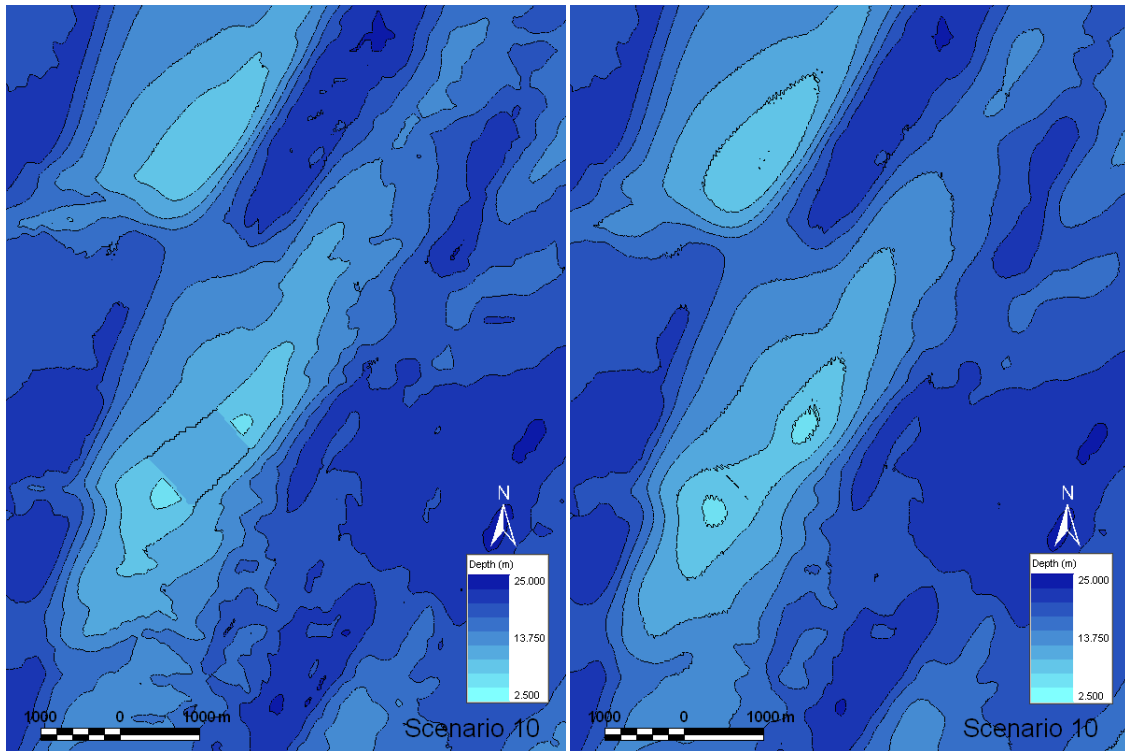
Figure 7.47 Initial (left) and final (right) morphology for Scenario 10 conditions
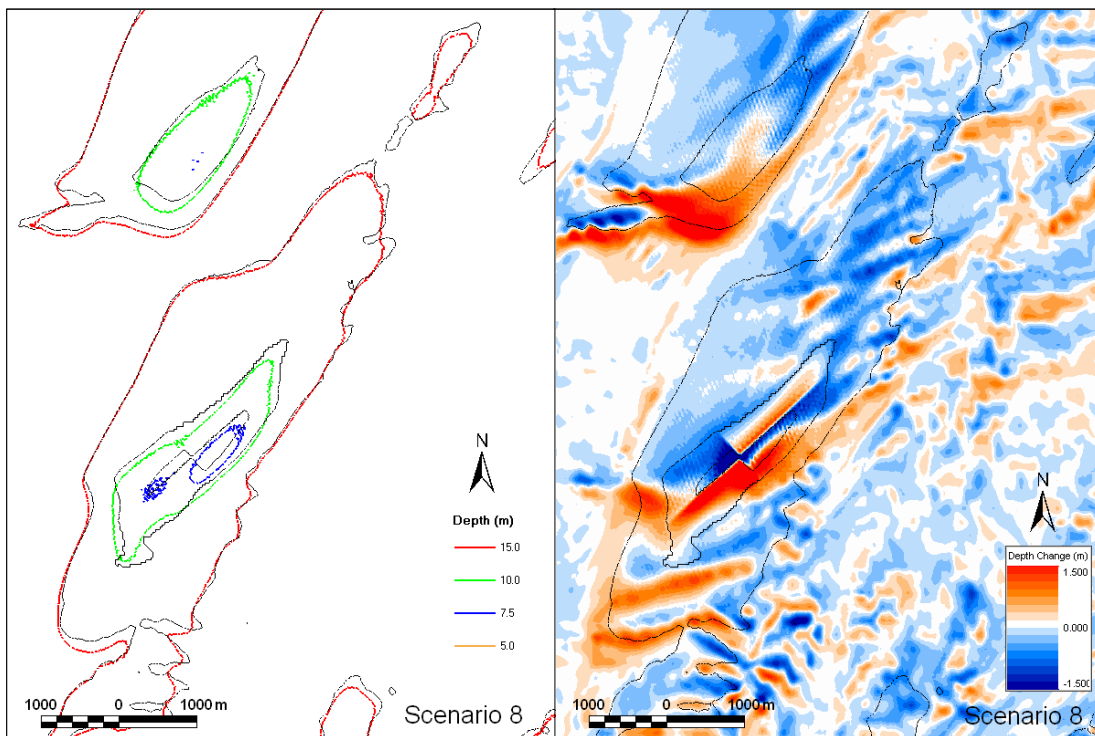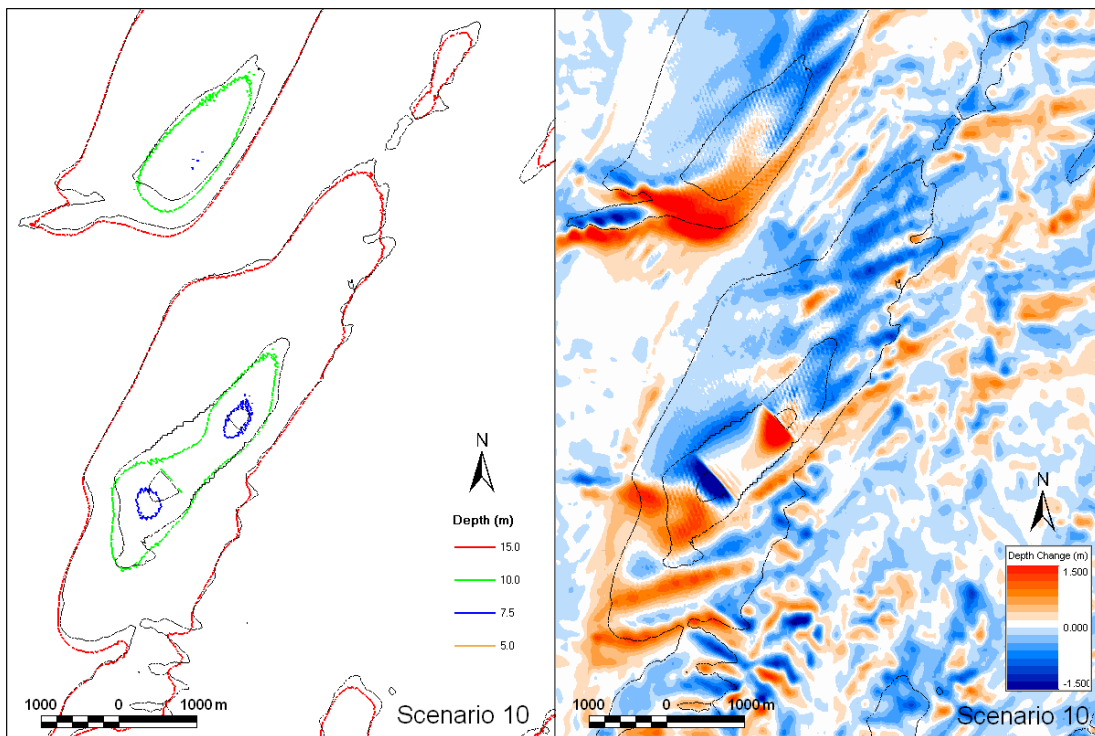

Figure 7.48 Initial and final depth contours (left) and depth change (right) for Scenario 10 conditions.
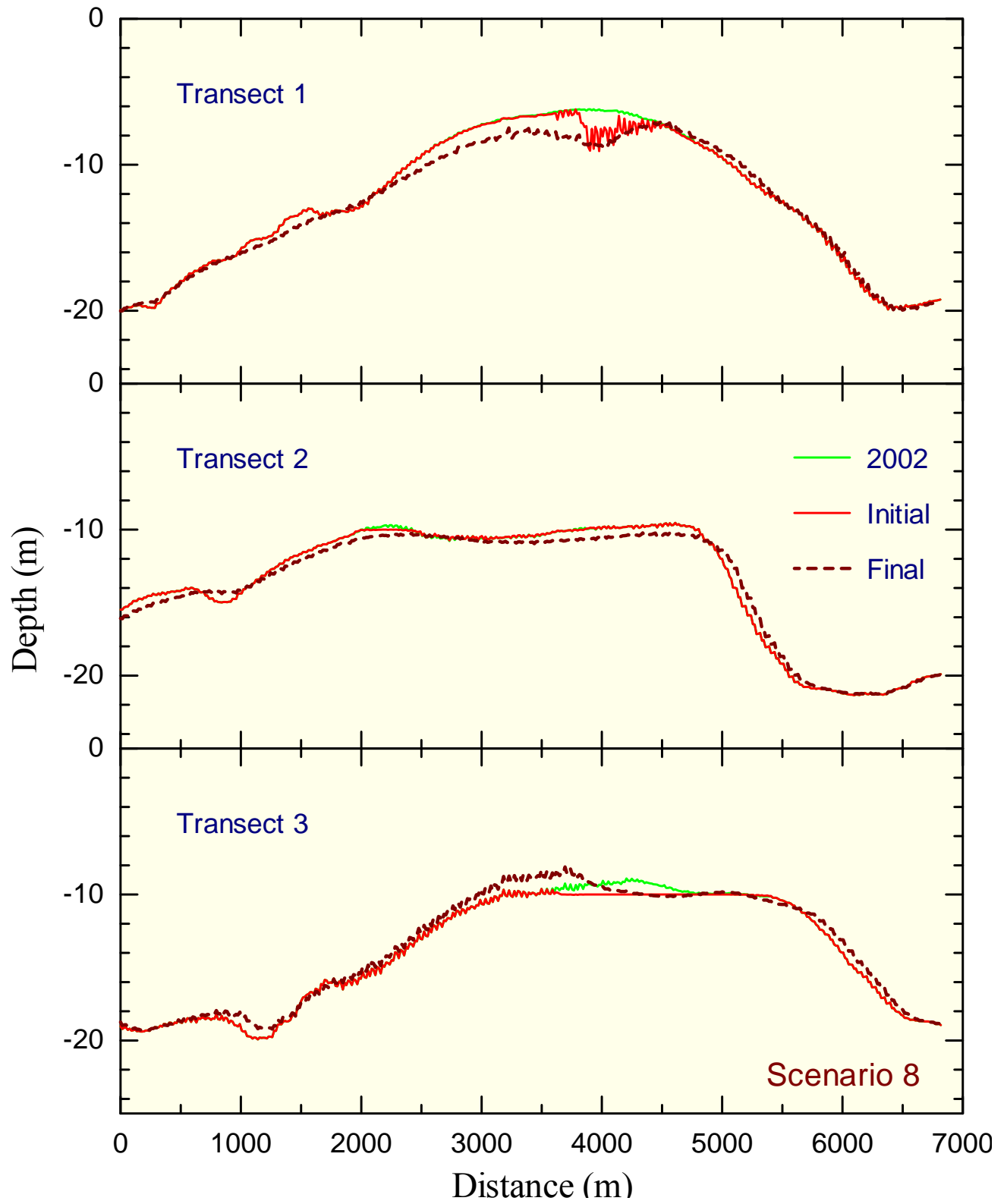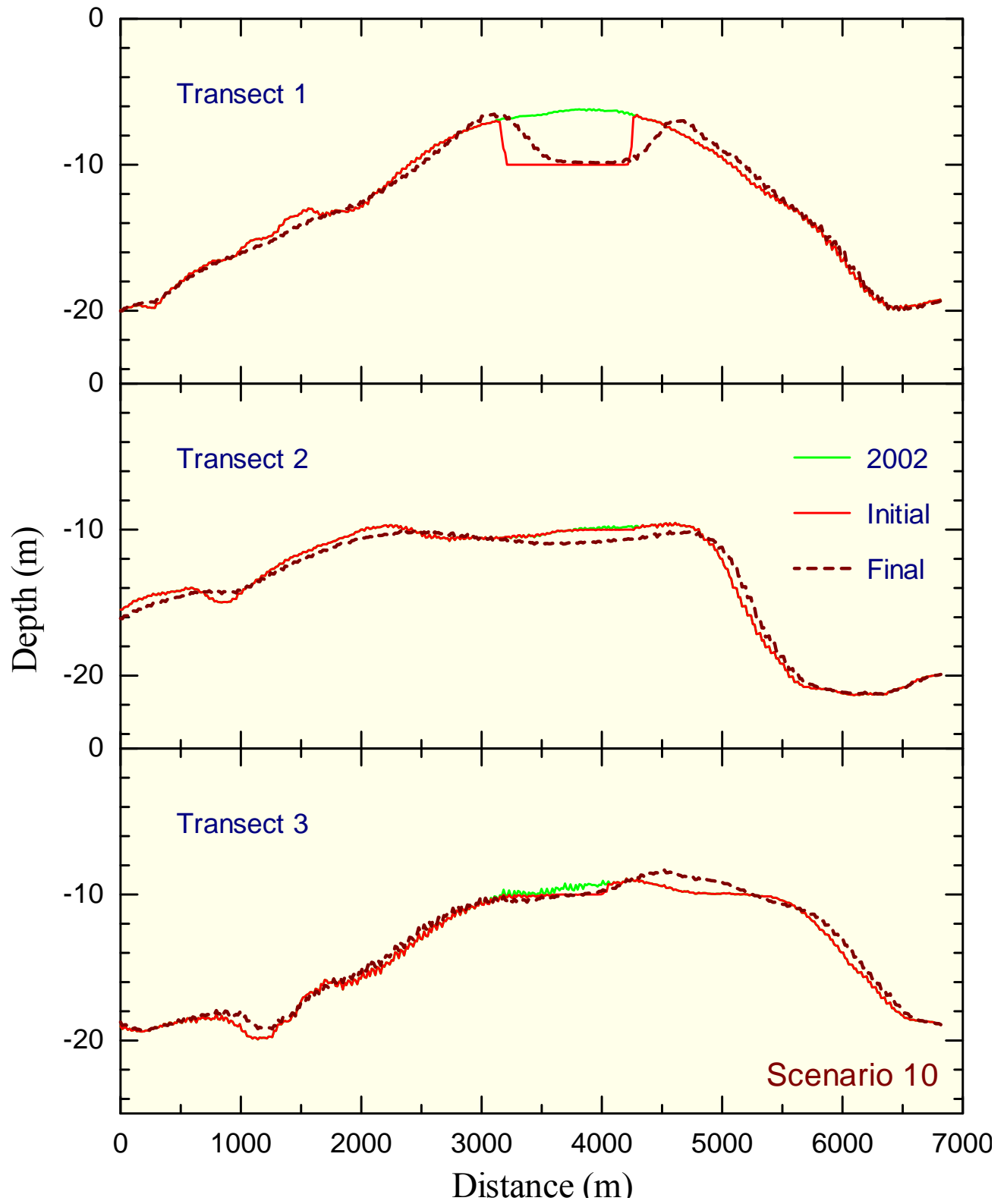
Figure 7.49 Predicted evolution of IOW along transects 1, 2 and 3 after dredging Scenario 10.
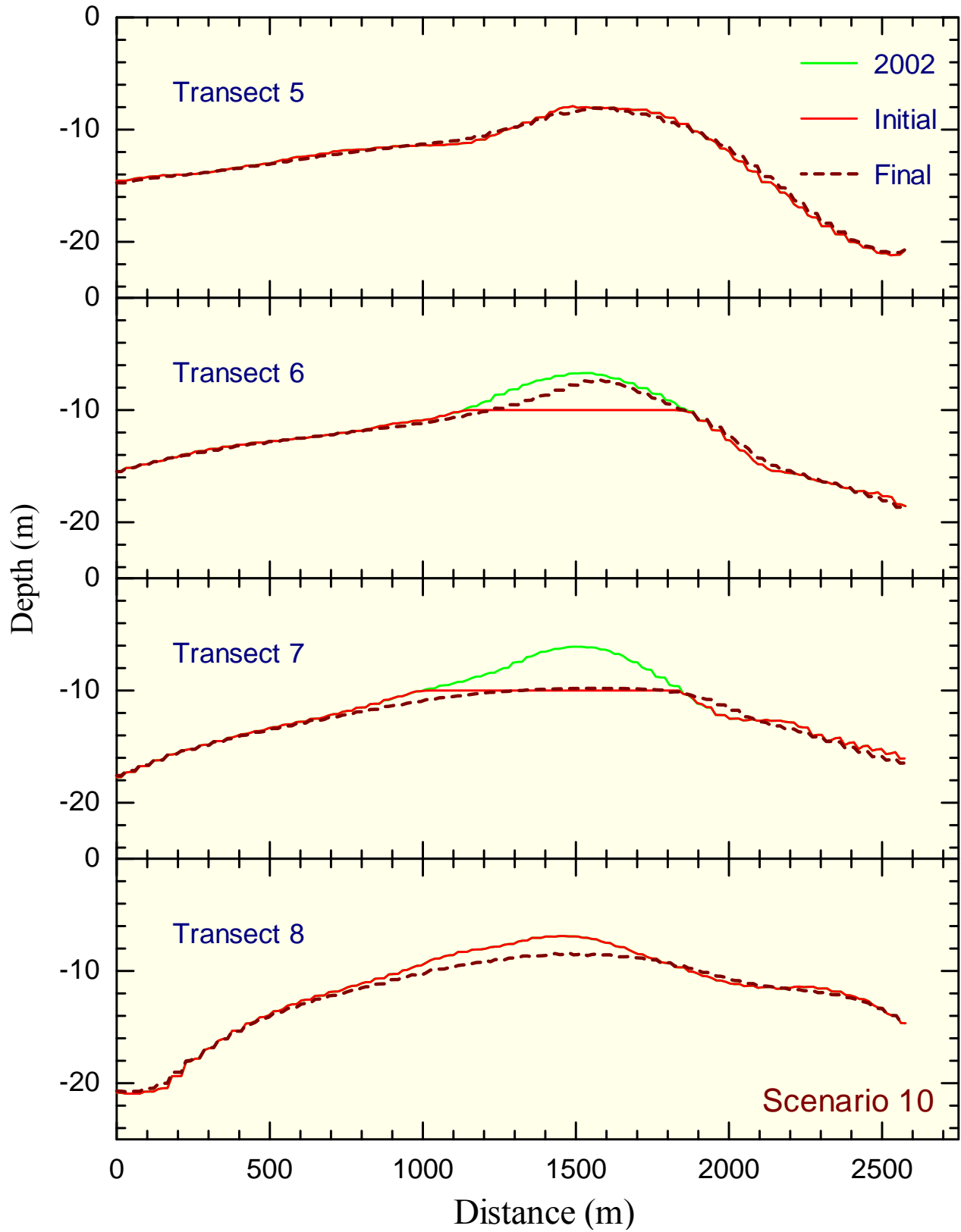
Figure 7.50 Predicted evolution of IOW along transects 5, 6, 7 and 8 after dredging Scenario 10.

Scenario 11

In this scenario the northeastern 1/3 of the crest of Isle of Wight is dredged to -10 m contour, as shown in Figure 7.51, to provide about 0.75 million m³ of sand.
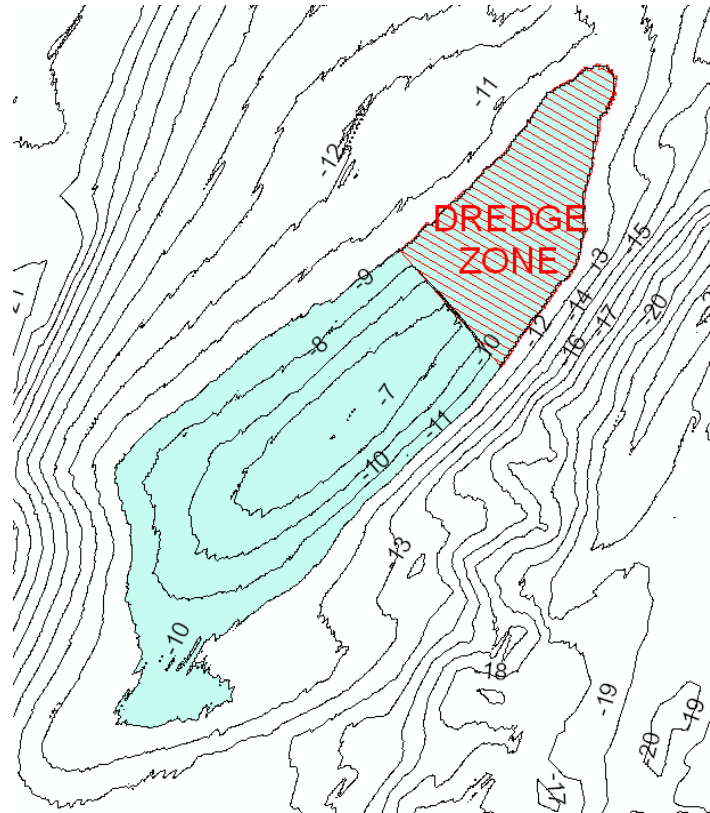
Figure 7.51 Dredging Scenario 11.

Figure 7.52 shows the initial and predicted future bathymetry for the Scenario 11 dredging configurations. IOW is reintegrated into a shoal with shorter crest length than the pre-dredge conditions. Figure 7.53 shows the initial and final depth contours as well as a map of change in bottom elevations. There is little accumulation over the dredged part of the shoal. The new crest covers the southwest 2/3 of the shoal as the overall transport (shoal migration) is towards southwest. Comparisons at selected transects presented in Figures 7.54 and 7.55 show that while the dredged platform undergoes very little change, the reformed shoal crest has the same height as the pre-dredge shoal. The new crest, however, is shorter and limited to the southwest 2/3 of the shoal. Therefore, this dredging scenario is expected to result in a shoal with the same height but with a shorter crest length centered on the southwest 2/3 of the shoal compared to the pre-dredge conditions.
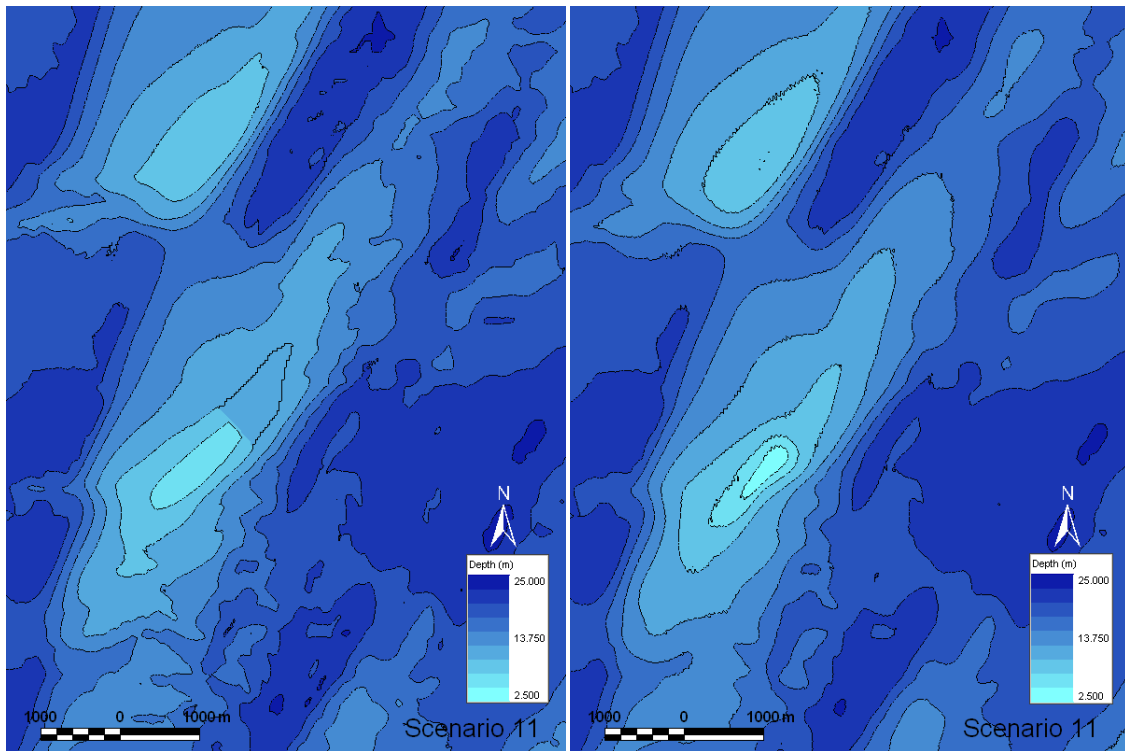
Figure 7.52 Initial (left) and final (right) morphology for Scenario 11 conditions
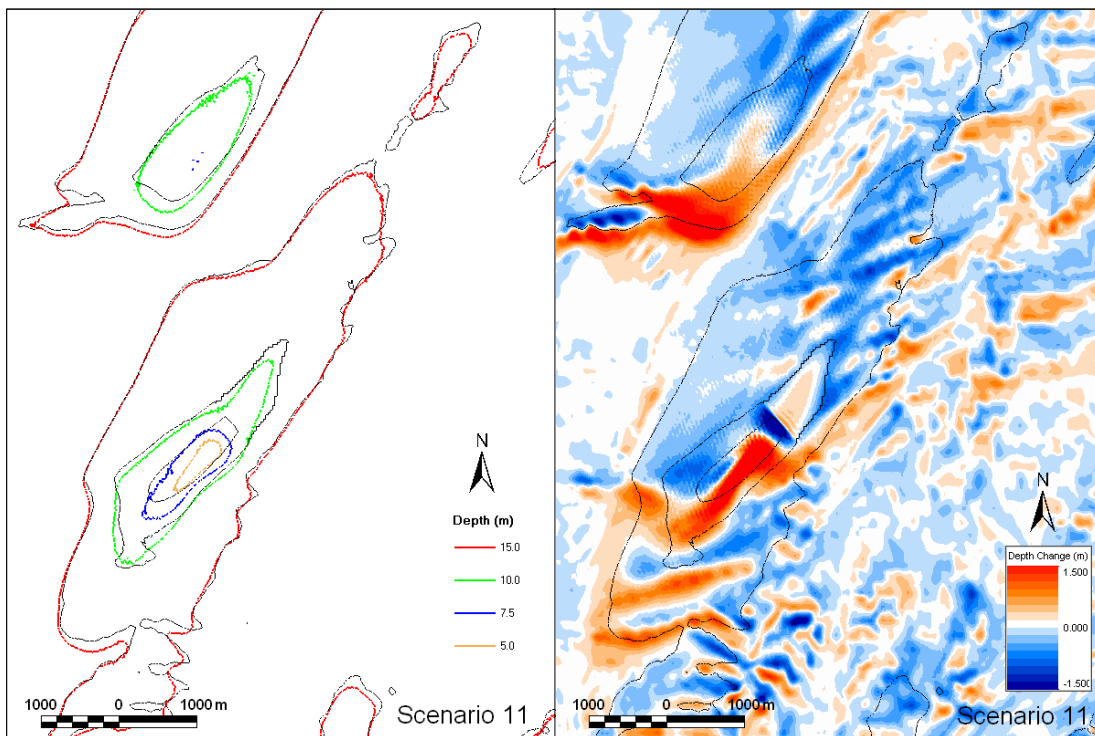
Figure 7.53 Initial and final depth contours (left) and depth change (right) for Scenario 11 conditions.
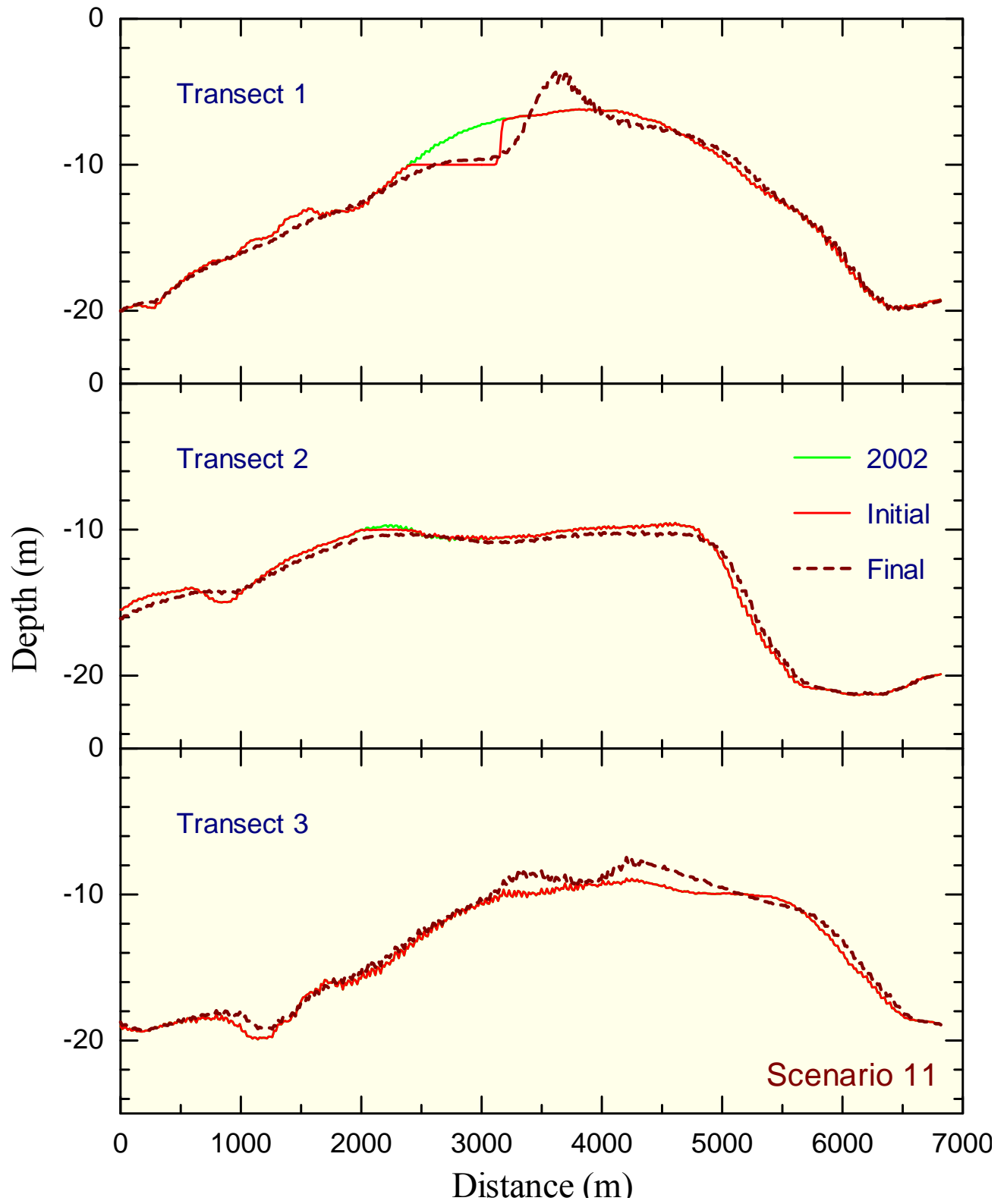
Figure 7.54 Predicted evolution of IOW along transects 1, 2 and 3 after dredging Scenario 11.
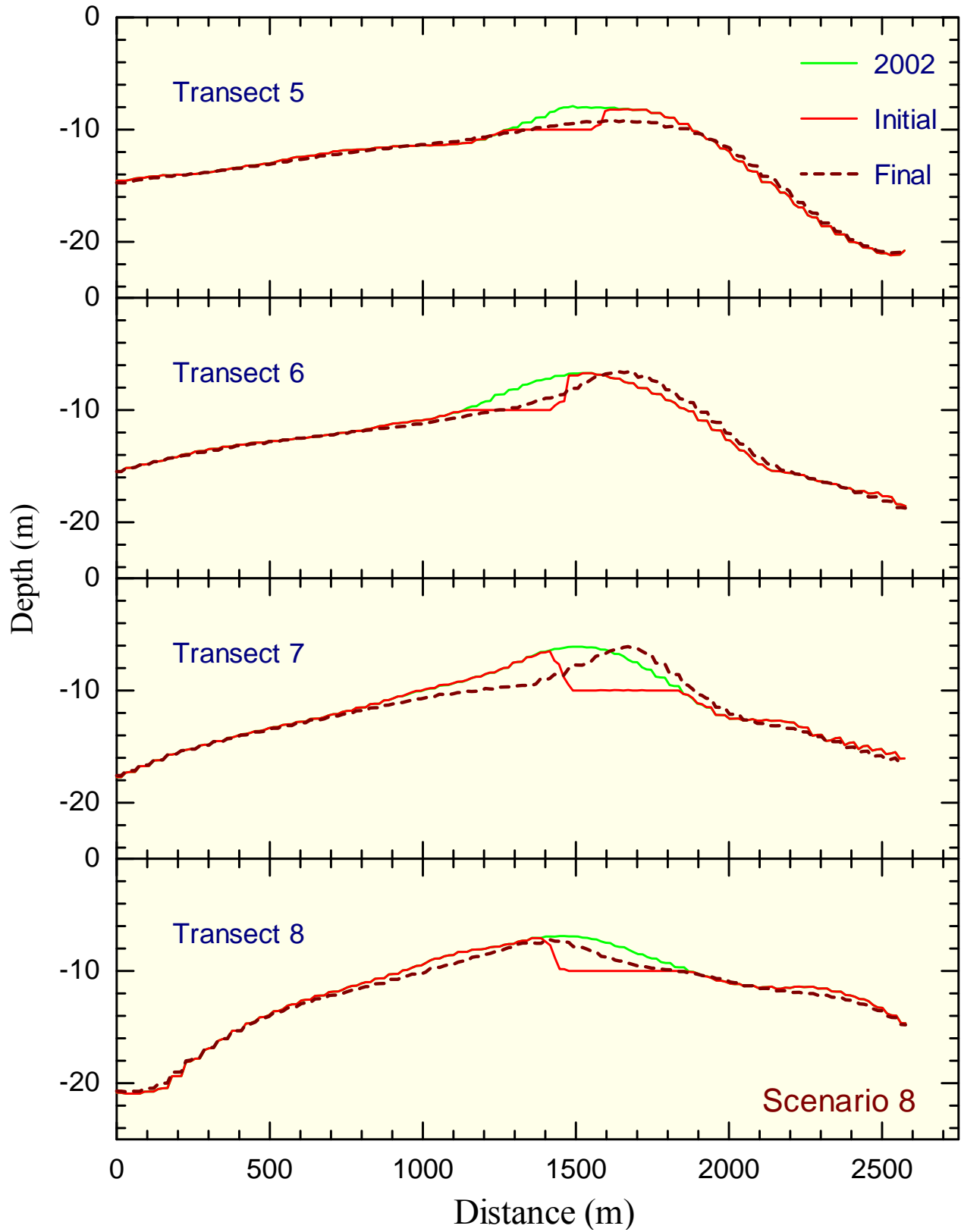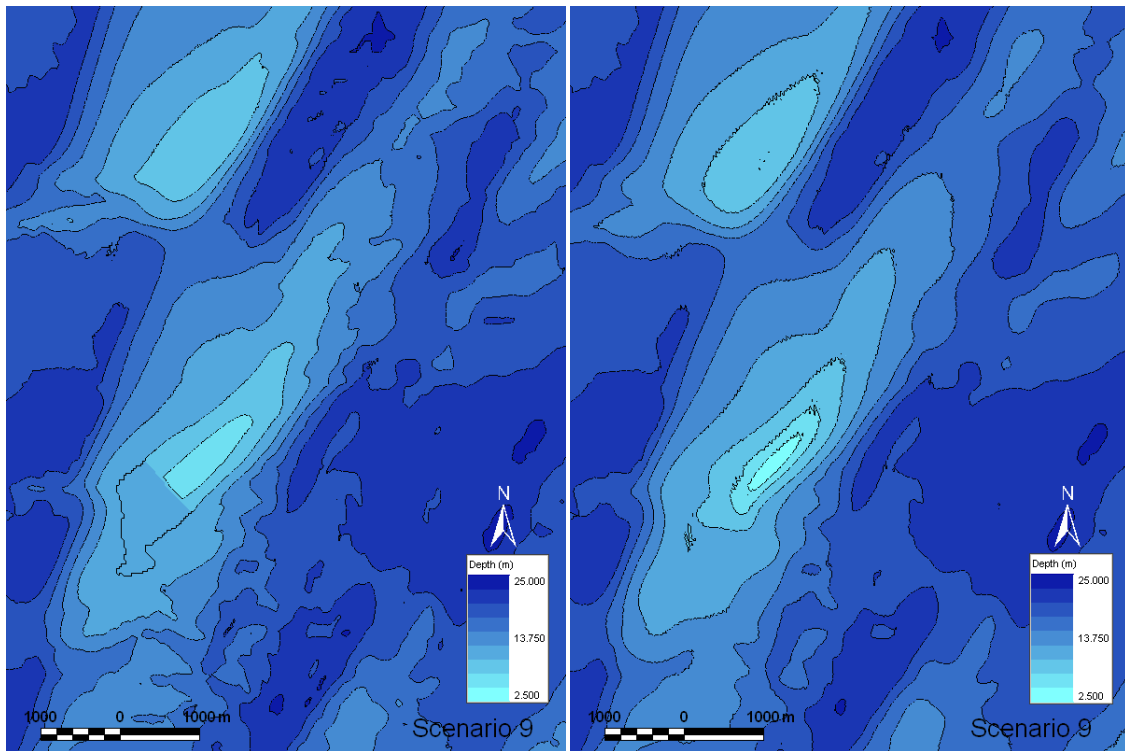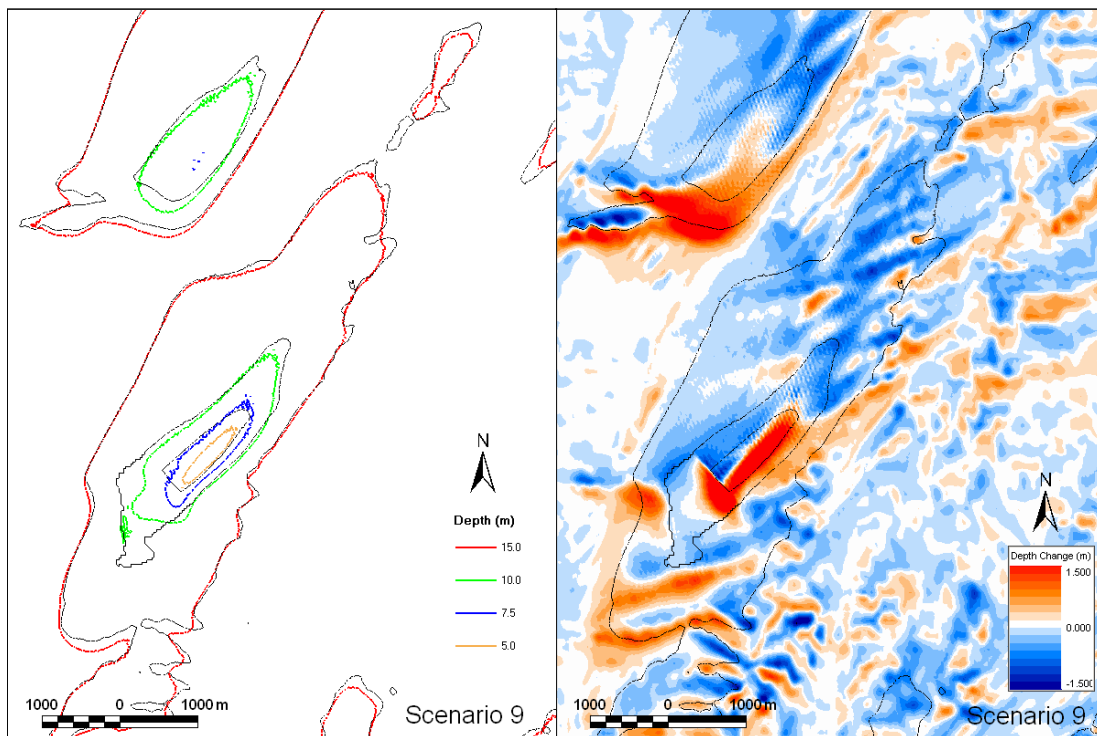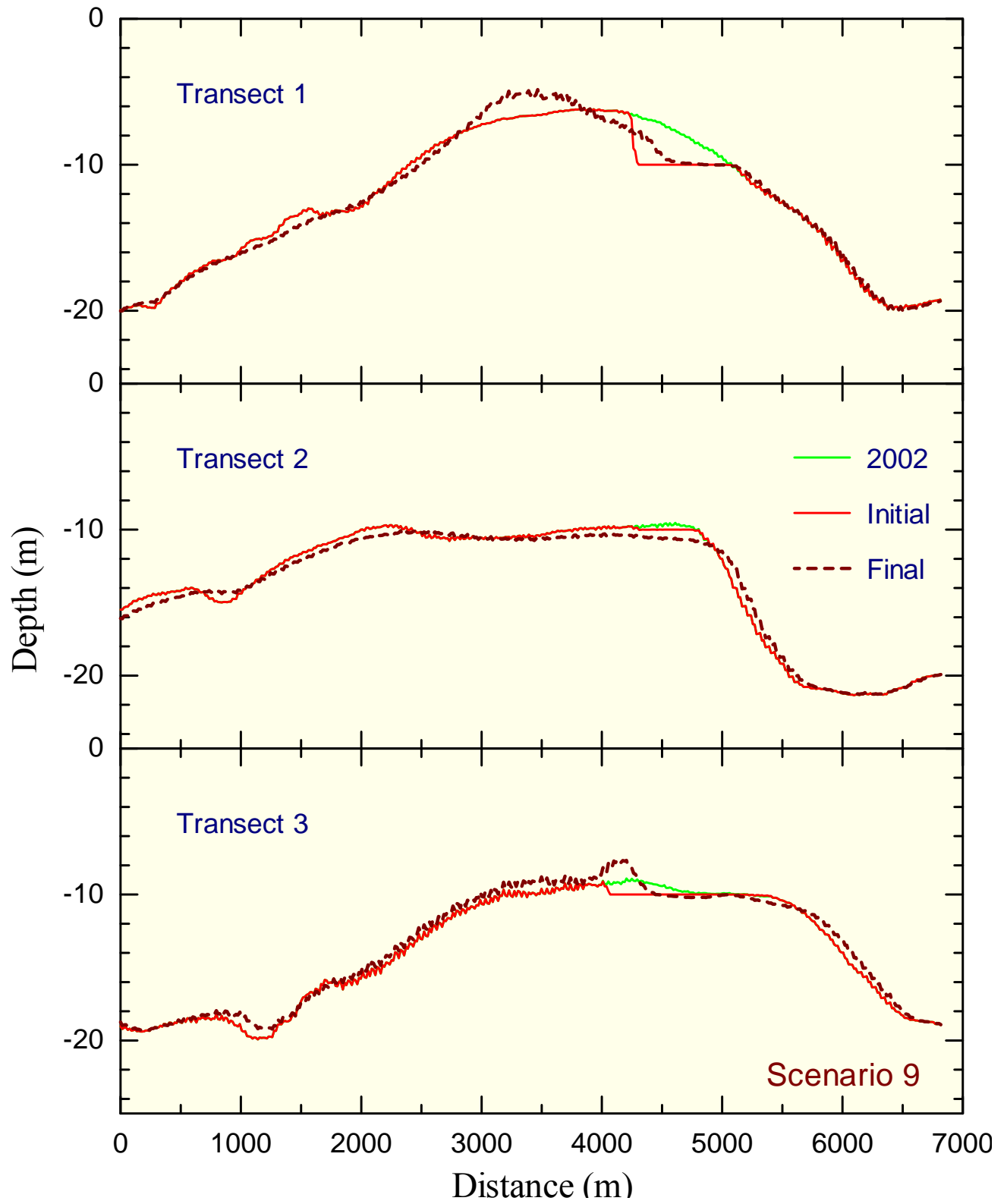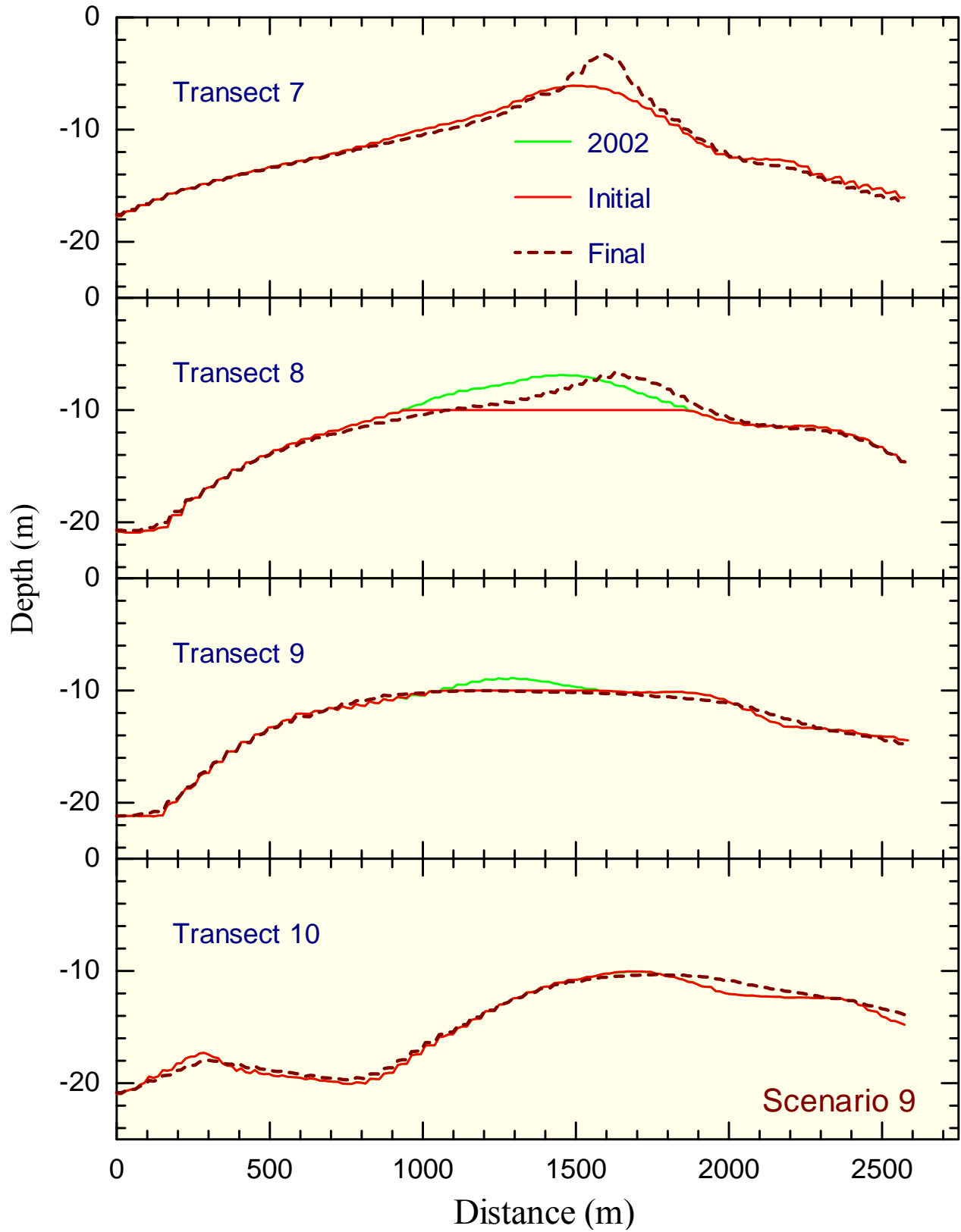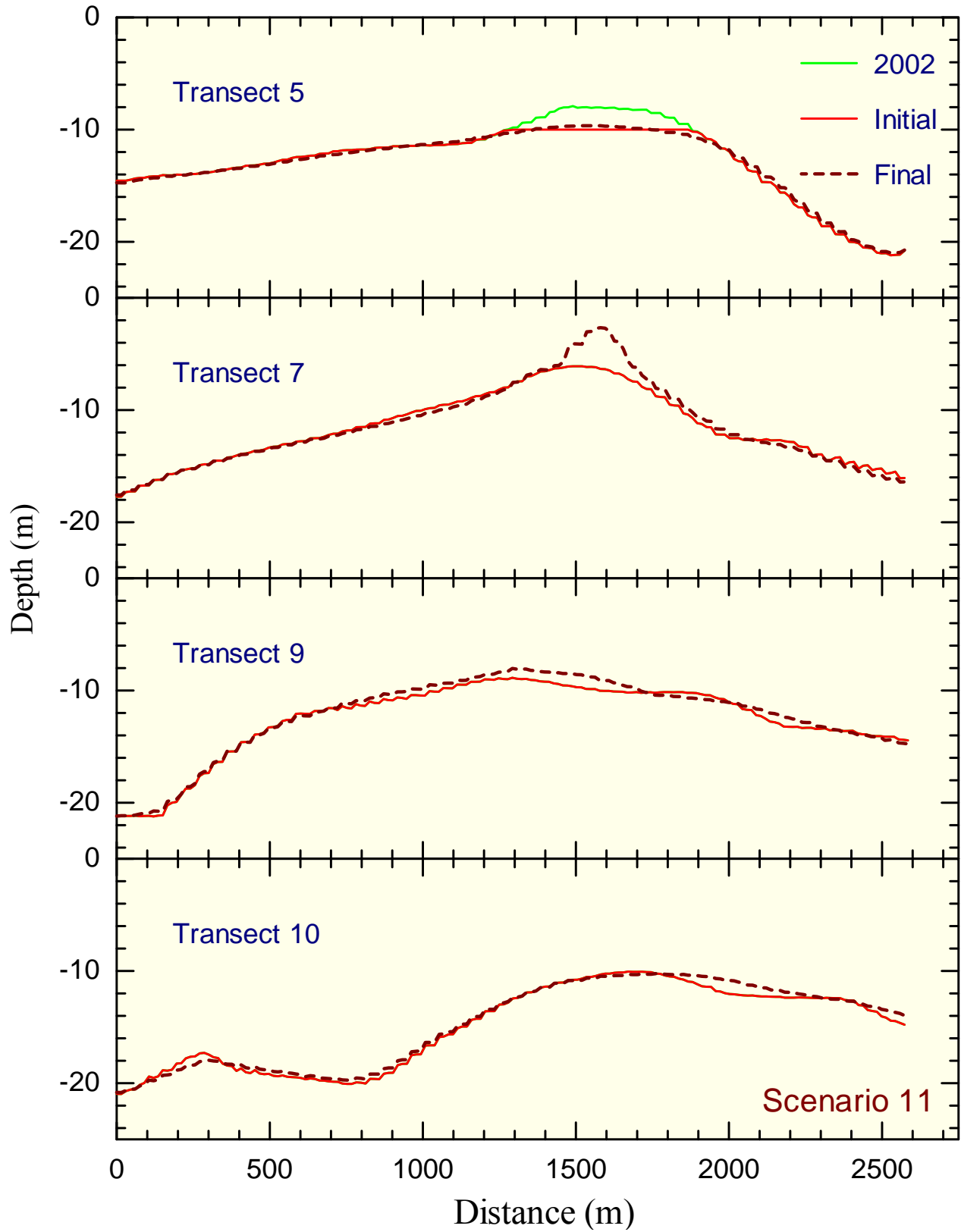
Figure 7.55 Predicted evolution of IOW along transects 5, 7, 9 and 10 after dredging Scenario 11.

7.2　Summary of the Numerical Modeling Results

A total of 11 different dredging scenarios were considered and the evolution of the resulting dredged shoals over a 10 to 15 year period was simulated using the numerical model developed for this study. Table 7.2 provides a summary of the results. A bullet point summary of the findings is also presented here:
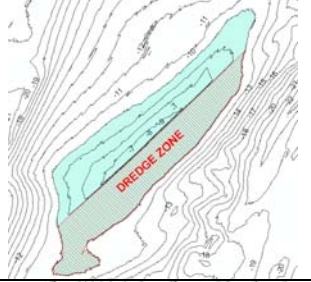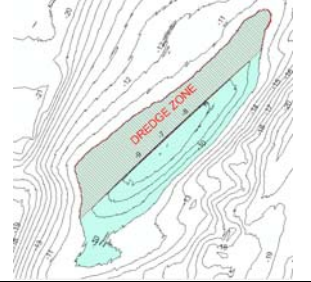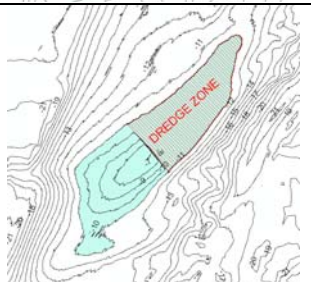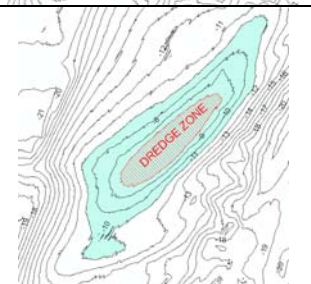
- For all the simulated scenarios, the shoal was reformed to a shoal with a smaller volume due to removal of the sediment. In other words, the volume taken by dredging was not compensated by transport of material from outside of the shoal.

- Despite the reduction in volume, the reformed shoal had the same height as that of the pre-dredge shoal conditions for some of dredging scenarios.
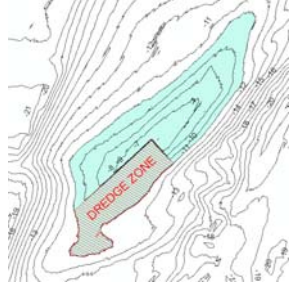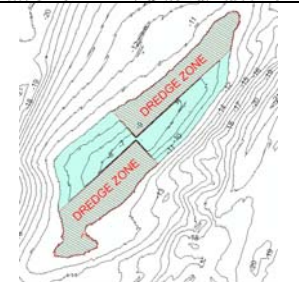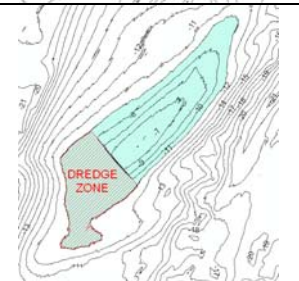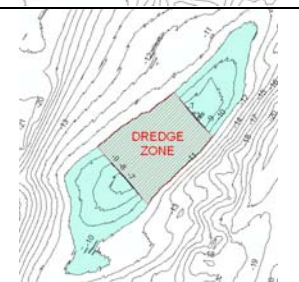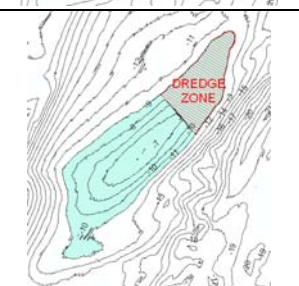
There is a limit for shoal height recovery when the sediment is taken directly from the top of the shoal. When 1.3 m of the shoal was removed (Scenario 5), the reformed shoal height was nearly the same as the height of the pre-dredge conditions. However, when 2.7 m was removed from the top of the shoal (Scenario 6), the shoal height did not recover back to its pre-dredge conditions. Considering that the crest of IOW shoal is at -6 m, this means that lowering the shoal crest to deeper than -7.5 m would result in a permanent reduction of shoal height to that level. Note that IOW has a Relative Shoal Height (H/BD) of 0.71. Therefore, it is not expected to re-grow once its Relative Shoal Height becomes less than 0.65 (i.e. removal of more than 1.3 m). As an example, we note that Weaver has a Relative Shoal Height of 0.62 and has not grown as high as IOW or Fenwick.

- Among other simulated cases, Scenarios 1, 2 and 8 resulted in a lower shoal height than the pre-dredge conditions. All these scenarios correspond to cases when material is taken from the entire length of the shoal crest (i.e. along the longer axis of the shoal).

- Under Scenarios 4 and 11 the reformed shoal height was nearly equivalent to the pre-dredge conditions but the dredged platform stayed unchanged. These correspond to the cases where material was taken from the northeast half or 1/3 of the shoal. The new shoal crest was formed on the southwest side.

- Under Scenarios 3, 7 and 9 the reformed shoal height was nearly equal to the pre-dredge conditions and the dredged platform was either partially (Scenario 3) or fully (Scenarios 7 and 9) integrated into the newly formed shoal. These correspond to the cases where material was taken from the southwest quarter, 1/3, or half the shoal. The new shoal crest was formed on the southwest side as the overall shoal migration is towards the southwest.

- Under Scenario 10 where sediment was taken from the middle 1/3 of the shoal, the reformed shoal had double crests. The shoal height was equal to the pre-dredge conditions, but the dredged platform stayed relatively unchanged.

- In the present simulations, only dredging from above the -10 m contour was considered as this is the most active part of a shoal. Regarding dredging from shoal flanks below the -10 m contour, it should be noted that the important process of wave focusing occurs over the shoal flanks of the northeast half of the shoal. Therefore, dredging from below the -10 m contour over the southwest half of the shoal is expected to have little effect on shoal integrity and little change is anticipated in the dredged area.

- The present investigation was focused on excavation of sand from between shoal crest and the -10 m contour providing from 1 to 2 million m^3 of material. Dredging scenarios involving excavation from shoal crest to below the -10 m contour, thus generating more than 2 million m^3 of sand, were not investigated. Additional modeling would be required to address such larger scale dredging scenarios.

- Although the above predictions represent shoal evolution over a nearly 13-year period, it is expected that the result can be considered to be representative of the trend in a period of 2 to 3 decades given the overall slow rate of shoal morphology change. The 13-year period is considered long enough for observation of shoal crest response to dredging and evolution of the excavated platform. Simulation of longer periods would suffer from accumulated numerical errors masking the actual morphology change results.

Table 7.2 – Summary of dredging scenarios.

Dredging Scenario	Excavation Area	Volume Dredged (milliom m³)	Morphologic Response
1		1.9	Reforms into a slightly narrower shoal with a shoal height that is about 1.5 m to 2 m lower (at its crest) than the pre-dredge shoal. There is accumulation over the dredged part of the shoal and a new shoal crest is created.
2		1.6	Reforms into a slightly narrower shoal with a shoal height that is about 1 m lower (at its crest) than the pre-dredge shoal. Little accumulation occurred over the dredged part of the shoal resulting in a more asymmetric shoal than the pre-dredge conditions.
3		1.8	Reforms into a shoal with shorter crest length but the same shoal height as the pre-dredge conditions. There is considerable accumulation over the northeast half of the dredged part. The rest of the excavated platform stays nearly unchanged.
4		1.8	Reforms into a shoal with shorter crest length but the same shoal height as the pre-dredge conditions. The new crest is formed on the southwest half of the shoal. The excavated platform stays nearly unchanged.
5		0.3	The shoal keeps its overall shape with almost the same shoal height as the pre-dredge conditions. The excavated part of the shoal is covered again by sand.

6		1.5	The shoal keeps its overall shape but with a much (i.e. 2 m to 3 m) shorter shoal height than the pre-dredge conditions. Little accumulation occurred over the excavated area and the shoal crest stayed almost flat (as dredged).
7		0.95	Reforms into a shoal with a shorter crest length but the same shoal height as the pre-dredge conditions. The new shoal crest is centered towards the northeast side of the shoal. Considerable accumulation occurred over the excavated area.
8		1.75	Reforms into a shoal with a shorter crest and (1 m to 2 m) shorter shoal height than the pre-dredge conditions. The new shoal crest is centered on the southeast side of the shoal. There is also considerable accumulation over the southwest excavated part.
9		1.0	Reforms into a shoal with shorter crest length but the same shoal height as the pre-dredge conditions. There is considerable accumulation over the northeast half of the dredged part. The rest of the excavated platform stays nearly unchanged.
10		1.9	Reforms into a shoal with double crests both have the same shoal height as the pre-dredge conditions. There is considerable accumulation over the northeast half of the excavated area, while the southwest half receives little accumulation.
11		0.75	Reforms into a shoal with shorter crest length but the same shoal height as the pre-dredge conditions. Little accumulation occurred over the excavated area. The new crest was centered on the southwest 2/3 of the shoal.

7.3   Comparison with CSA/ACR Findings

In a recent study (OCS Study MMS 2010-010), CSA International, Inc. in cooperation with Applied Coastal Research and Engineering and others investigated geomorphologic changes associated with potential sand mining scenarios on shoals offshore Fenwick Island, Maryland, using numerical models. Tidal hydrodynamic, wave process, and sediment transport pattern models were coupled to assess the morphologic response of offshore sand shoals to various "dredging" scenarios in support of future beach nourishment requirements. The excavation scenarios simulated were

- Dredging a hole over a designated area on the shoal;

- Dredging the leading edge of a shoal;

- Dredging the trailing edge of a shoal; and

- Dredging in a striped pattern to facilitate recruitment of benthic invertebrates into dredged areas.

Tidal hydrodynamics for the continental shelf and nearshore areas offshore the Delmarva Peninsula were modeled using the Advanced Circulation Model for Oceanic Coastal and Estuarine Waters (ADCIRC). Tidal velocities were found to be very small (on the order of 0.05 m/s) and therefore, incident wave energy was considered to play a primary role in sediment movement and morphology change at the offshore shoals. Nearshore wave heights and directions across Weaver Shoal, Isle of Wight Shoal, and Shoal A were estimated using the USACE STeady state spectral WAVE (STWAVE) half-plane model.

Bathymetric change at and adjacent to the shoals in response to various "dredging" geometries was investigated under a 3-day storm from the northeast (peak storm wave height of 6 m) and a 3-day storm from the east (peak storm wave height of 5 m). In addition to a baseline scenario for each of the shoals, three dredging geometries for Weaver and Isle of Wight shoals were simulated, along with two dredging scenarios at Shoal A. Results from the Baseline scenario indicated dominant sand transport from northeast to southwest and south, where sand is eroded from shoal crests and deposited on the leading edge of the shoal. Although these results are in overall agreement with our findings in Section 6.7, details on shoal crest erosion are not be supported by the fact that wave influence is mainly to build up the shoal crest through wave focusing processes. Sand is mainly eroded from trailing edge and deposited on the leading edge of the shoal.

CSA/ACR modeling results illustrated that if dredging is performed on a portion of a shoal that is not active under present conditions, there will be a lack of sand availability to replenish the removed sand. On the other hand, material removed from active areas of a shoal will be replenished by normal wave conditions at the site. Shallow shoal crests, like Isle of Wight Shoal, and the leading edge of all above-mentioned three shoals are noted as the active areas of

erosion/deposition. These active transport and deposition areas will recover to original conditions more rapidly than inactive portions of shoals. These findings are in agreement with the results of the present study although the CSA/ACR report does not discuss quantitative details on long-term recovery of the shoal height.

For the dredging scenarios examined, the CSA/ACR report recommends that the most desirable location or subarea (crest, leading edge, or trailing edge) of a shoal for dredging is the leading edge from a physical standpoint, followed by the crest as the second choice, and the trailing edge. In the present study, it was found that only dredging of the leading edge of a shoal has the potential for complete shoal height recovery.

Considering physical processes, the CSA/ACR report also provides the following general recommendations:

1. Extracting sand from a depocenter, leading edge, or downdrift margin of a shoal, to avoid interrupting natural shoal migration and potentially reduce the time required for site refilling;

2. Avoid dredging in erosional areas that source downdrift depocenters, which also may be slow to refill after dredging;

3. Dredging in a striped pattern to leave sediment sources adjacent to and interspersed throughout target areas, leading to a more uniformly distributed infilling process; and

4. Excavation should occur on shoal crests and higher areas of the leading edge rather than lower areas of the shoals because of greater sediment mobility, which potentially results in more rapid sediment reworking and site infilling.

The above recommendations are in general agreement with the findings of this study. However, we note that recommendations #3 and #4 could result in a reformed shoal that has a shorter shoal Height than the pre-dredged conditions.

The CSA/ACR report also generally states that based on geological models of shoal formation, there does not appear to be a mechanism supporting the idea that the structural integrity of a feature will "deflate" or "unravel" when subject to repeated dredging. The report continues that as long as a seafloor irregularity remains upon which to reform the ridge, dominant shelf processes will construct these features as described by shelf ridge process models. The CSA/ACR report does not provide quantitative discussions on the geometry of the required irregularity and dimensions of the expected reconstructed feature. Therefore, the above conclusion may generally be interpreted that upon being dredged, a shoal will unconditionally re-grow (to its pre-dredged conditions) as long as its remaining is left as an irregularity on the seafloor. In the present investigation, we also did not identify any "shoal deflating" processes. In other words, there was no indication that there exists a critical threshold for dredging that once crossed, ridge and shoal features may deflate, losing their morphologic integrity. However, the

present study suggests that shoals are initially generated at the shoreline and continue to grow due to wave action under rising sea levels. Once a shoal is in 10 m of water or deeper, it will only reform into a smaller shoal upon dredging. That is, the more material removed from the shoal, the smaller the volume of the resulting shoal. It is only under certain dredging conditions that the reformed shoal may become as high as the pre-dredged shoal.

8.0   RECOMMENDATIONS FOR DREDGING GUIDELINES

8.1   Summary of Findings

An analysis of shoal parameters was conducted in Section 5.5 and numerical modeling of several dredging scenarios was completed in Section 7.1 to assess long-term and short-term shoal morphology evolution aspects, respectively. A summary of key findings is provided here to be used for development of dredging guidelines in the next section.

i.   Analysis of more than 180 offshore shoals in the study area suggested that there is a Shoal Height Growth Zone between 10 m and 30 m depth. This zone was further divided into two areas. In the 10 m to 20 m depth range, shoals can potentially grow in height up to the minimum Crest Depth of 5 m. In the 20 m to 30 m depth range, shoals may still grow but to a lesser extent. The 20 m to 30 m Base Depth range is a transition zone over which the predominant forcing changes from wave-dominated at 20 m depth to current-dominated at 30 m depth.

ii.   The Relative Shoal Height defined as the ratio of shoal Height to Base Depth (H/BD) was found to be an appropriate indicator of the shoal Height growth. The maximum Relative Shoal Height, $(H/BD)_{max}$, varies from 0.5 at 10 m depth to 0.75 at 20 m depth. A shoal that has reached the maximum relative shoal height of its Base Depth may be considered as a fully grown shoal (in height) at that depth, but may still grow under rising sea levels. A fully grown shoal is more likely to re-grow and rebuild itself to the same height upon being dredged.

iii.   Shoals located in waters deeper than 30 m show a decrease in height with increasing depth representing a possible Shoal Height Decrease Zone beyond 30 m depth. These shoals are not expected to grow and will not recover in height once they are dredged.

iv.   Numerical modeling results indicated that after removal of material from a shoal, the shoal was reformed to a shoal with a smaller volume due to removal of the sediment. In other words, the volume taken by dredging was not compensated by transport of material from outside of the shoal. However, despite the reduction in volume, the reformed shoal had the same height as that of the pre-dredge shoal conditions for certain dredging scenarios.

v.   Numerical modeling results indicated that there is a limit for shoal height recovery when the sediment is taken directly from top of the shoal. When 1.3 m of the shoal was removed from top of IOW, the reformed shoal height was nearly the same as the height of the pre-dredge conditions. However, when 2.7 m was removed from top of this shoal, the shoal height did not recover back to its pre-dredge conditions. IOW has a Relative Shoal Height (H/BD) of 0.71. Therefore, it is not expected to re-grow once its Relative Shoal Height becomes less than 0.65 (i.e. removal of more than 1.3 m). As an

example, it is noted that Weaver has a Relative Shoal Height of 0.62 and has not grown as high as IOW or Fenwick.

vi. Numerical modeling results indicated that when material was taken from the southwest quarter, 1/3, or half the shoal, the reformed shoal height was nearly equal to the pre-dredge conditions and the dredged platform was either partially or fully integrated into the newly formed shoal. The new shoal crest was formed on the southwest side as the overall shoal migration is towards the southwest.

vii. Numerical modeling results indicated that when material was taken from the entire length of the shoal crest the reformed shoal height was less than the pre-dredge conditions. When material was taken from the northeast 1/3 or half the shoal, the reformed shoal height was nearly equal to the pre-dredge conditions but the dredged platform stayed unchanged.

viii. Only dredging from above the -10 m contour was considered in numerical simulations. Regarding dredging from shoal flanks below the -10 m contour, it should be noted that wave focusing occurs over the shoal flanks of northeast half of the shoal and dredging from this area should be avoided. Dredging from below the -10 m contour over the southwest half of the shoal is expected to have little effect on shoal integrity and little change is anticipated in the dredged area.

8.2   Proposed Guidelines

Based on the findings of the present study summarized in Section 8.1, the following dredging guidelines are proposed to maintain and protect the integrity of offshore ridge and shoal regimes. The proposed guidelines deal with dredging of offshore shoals as well as evaluation of offshore shoal dredging projects.

The shoal Height (H) was found to be the most important parameter representing the integrity of a shoal. The present study showed that after removal of material from a shoal, the shoal is reformed to a shoal with a smaller volume due to removal of the sediment. In other words, the volume taken by dredging is not compensated by transport of material from outside of the shoal. However, despite the reduction in volume, the reformed shoal may attain the same height as that of the pre-dredge shoal conditions for certain dredging scenarios. The following guidelines, therefore, are intended to provide dredging practices that result in a reformed shoal that has the same height as the pre-dredge shoal.

- The final dredging approach should be determined based on suitability of the dredged sand for nourishment as well as ecosystem services associated with the reformed shoal shape. A determination is required regarding the importance of maintaining the pre-dredge shoal Height from an ecological perspective.

- The proposed guidelines are not universal and are dictated by the local storm wave height, storm wave direction, storm related subtidal currents. They are recommended for the shoals in the area offshore Delaware, Maryland and Virginia between Delaware Bay and Chesapeake Bay.

- Only those shoals located in less than 30 m depth have the potential to re-grow after dredging, and therefore, shoals with a Base Depth of greater than 30 m should not be dredged if it is determined to be important to maintain the pre-dredge shoal Height from an ecological perspective.

- Shoals with Relative Shoal Height (defined as H/BD) of less than 0.5 are not likely to recover after dredging. Therefore, shoals with Relative Shoal Height of less than 0.5 should not be dredged if shoal recovery to its pre-dredge height is desired from an ecological perspective.

- The maximum Relative Shoal Height, $(H/BD)_{max}$, varies from 0.5 at 10 m depth to 0.75 at 20 m depth. A shoal that has reached the maximum relative shoal height corresponding to its Base Depth may be considered as a fully grown shoal at that depth. A fully grown shoal (in height) can potentially re-grow and rebuild itself to the same height upon being dredged. Therefore, if shoal recovery to its pre-dredge height is desired, shoals that have reached their maximum relative shoal height are recommended for dredging. For the present study area, maximum Relative Shoal Height at a certain Base Depth (BD) may be estimated as: $(H/BD)_{max} = (BD-5)/BD$.

- In case of Isle of Wight or other shoals with the same Base Depth (i.e. 21 m), when dredging from the top of the shoal, the relative shoal height should not be reduced to less than 0.65 (i.e. removal of more than 1.3 m) after dredging or it will not re-grow to the same pre-dredge height. Dredging directly from the shoal crest is thus not recommended in this case.

- Sand should not be removed from the entire length of the shoal. Longitudinal dredging (i.e. dredging all along the longer axis) is not preferred because it affects wave focusing processes and the shoal does recover to the same pre-dredge height.

- In the present study area, it is recommended to dredge sand from the SW side of a shoal. This is because 1) wave focusing is concentrated on the NE side of a shoal, and 2) overall shoal migration is towards the southwest. Therefore, after removal of material from the SW side of a shoal, a new shoal crest is formed over the excavated area by transport of material from the NE side.

- In case of Isle of Wight, dredging from SW side of the shoal above -10 m contour is recommended as it would result in creation of a smaller shoal with the same shoal height as the pre-dredge conditions.

- Dredging from shoal flanks below the -10 m contour over the SW half of the shoal is expected to have little effect on shoal integrity and little change is anticipated to happen to the dredged area. This dredging option is thus recommended if it can provide sand suitable for nourishment.

- Similar guidelines are expected to apply to shoals in areas other than present study area. Details, however, would be dictated by local wave and current conditions. It is recommended that a similar study be completed for other regions when the ecological role of the shoal height/shape is very important to justify the associated study cost. Note that USACE (2008) determined that cost differences between dredging scenarios with vs. without comparable guidelines in place are below level of cost concern for future Ocean City borrow work. Below are a few guidelines for such a study:

  o The study should involve analysis of historic and recent bathymetry data to determine shoal migration trends, field measurements of waves and currents to identify the driving forces involved, sediment sampling, dimensional analysis of shoal parameters to define those parameters critical to shoal integrity, and long-term morphological numerical modeling to evaluate dredged shoal response.

  o When planning hydrographic surveys of offshore shoals, as recognized by most hydrographic survey standards, it is important to deploy a tide gage in the survey area at the time of the hydrographic survey to apply proper tidal corrections and reference the survey to a correct datum. If comparison of successive hydrographic surveys is intended, the two surveys need to be several years apart as errors commonly involved in a hydrographic survey are comparable in magnitude to the annual slow rate of change of bottom morphology and affect short-term bathymetry comparisons.

  o Numerical modeling of long-term morphologic evolution of the shoals is a challenging task. One of the difficulties is regarding definition of proper input driving forces. Measurement of waves and currents are recommended to identify key driving forces and mechanisms affecting local shoal morphology. Appropriate representative wind, wave, tide and current conditions should then be prepared to drive the model for long-term morphology simulations. Measured data, if available, may be used to develop the model input file. Otherwise, significant modeling efforts may be required to develop appropriate model input conditions.

  o Full plane spectral (or equivalent) wave models must be used for wave transformation calculations. Standard (half-plane) spectral wave models cannot accurately simulate wave transformation processes over offshore shoals even if the models are applied within their recommended ±45° limitation. Generally, these shoals feature a number of slopes in various directions and provide severe conditions for refraction and wave focusing calculations by conventional half-plane spectral wave transformation models.

9.0   CONCLUSIONS

W.F. Baird & Associates Ltd. (Baird) was retained by the Minerals Management Service (MMS) for execution of the project "Investigation of Dredging Guidelines to Maintain and Protect the Integrity of Offshore Ridge and Shoal Regimes/Detailed Morphologic Evaluation of Offshore Shoals".   The purpose of this study was to formulate and recommend offshore dredging guidelines to protect and maintain the integrity of the ridge and shoal features found on the Outer Continental Shelf (OCS) which are being targeted as sand borrow sites for beach nourishment and coastal restoration efforts.

A series of investigations were completed in the present study to support the guidelines through an improved understanding of the morphologic evolution of ridge and shoal features.   These investigations included a field measurement program, analysis of historic data and numerical modeling.

The field measurements involved deployment of three Acoustic Doppler Current Profilers (ADCP) for 3 months (March to May 2007) to measure waves and currents in the study area. Sediment sampling and analysis and limited hydrographic survey of Isle of Wight were also completed. A number of severe storm events were recorded by the ADCPs during the three-month deployment and provided invaluable insight on various driving forces contributing to costal processes in the study area. Measured current velocities indicated the presence of both tidal and subtidal (storm-driven) current components. Further analysis of ADCP data indicated that synoptic scale pressure gradients associated with nor'easters result in large scale circulations that play an important role in movement of sediment in the study area. Initial sediment transport calculations indicated that the contribution of subtidal currents is as important as that from nor'easter waves themselves.

Analysis of water surface elevations measured by the ADCPs indicated that tides in the study area are very similar in range to those measured at Atlantic City. This is despite the fact that Ocean City is much closer to the present site and all hydrographic surveys are referenced to Ocean City datum. It is, therefore, important to deploy a tide gage in the survey area at the time of any hydrographic survey. Two hydrographic surveys of the leading (SW) edge of Isle of Wight were completed in March 2007 and January 2008 and compared with each other. It was found that errors commonly involved in a hydrographic survey are comparable in magnitude to the annual slow rate of change of bottom morphology in the study area, affecting short-term bathymetry comparisons.

Long-term morphological evolution of Isle of Wight was investigated in GIS using surveys from 1929, 1975 and 2002. All surveys were referenced to MLLW at Ocean City, and the effect of sea level rise was taken into account (~ 4 mm/year). The 1929-2002 comparison showed an overall southward movement of the shoal, while the comparison between 1975 and 2002 surveys indicated a movement in SW direction. The reasons behind the differences observed between 1929-2002 and 1975-2002 comparisons are not clear. One possibility could be long-term (decadal or longer) shifts/variations in the wave and current climate of the area.

A dimensional analysis of shoal parameters was completed. More than 180 offshore shoals were identified and analyzed in the study area offshore Delmarva Atlantic Coast. The dataset contains a wide range of shoals resulting in large scatter when shoal parameters are plotted against each other. A universal relationship was not observed between those parameters. Nevertheless, several important trends provided insight into shoal behavior and morphologic evolution. The data suggests that wave influence on the shoals is limited to shoals with Base Depth of less than 30 m. Waves were found to be the primary factor in shoal height growth and maintenance (as opposed to currents that have a greater influence on shoal migration).

The analysis suggested that there is a Shoal Height Growth Zone between 10 m and 30 m depth. This zone was further divided into two areas. In the 10 m to 20 m depth range, shoals can potentially grow in height up to the minimum Crest Depth of 5 m. In the 20 m to 30 m depth range, shoals may still grow but to a lesser extent. The 20 m to 30 m Base Depth range is a transition zone over which the predominant forcing changes from wave-dominated at 20 m depth to current-dominated at 30 m depth.

The Relative Shoal Height defined as the ratio of shoal Height to Base Depth (H/BD) was found to be an appropriate indicator of the shoal Height growth. The maximum Relative Shoal Height, $(H/BD)_{max}$, varies from 0.5 at 10 m depth to 0.75 at 20 m depth. A shoal that has reached the maximum relative shoal height of its Base Depth may be considered as a fully grown shoal (in height) at that depth, but may still grow under rising sea levels. A fully grown shoal is more likely to re-grow and rebuild itself to the same height upon being dredged. Shoals located in waters deeper than 30 m show a decrease in height with increasing depth representing a possible Shoal Height Decrease Zone beyond 30 m depth. These shoals are not expected to grow and will not recover in height once they are dredged.

Numerical modeling of long-term morphologic evolution of the shoals proved to be a challenge. One of the difficulties was regarding representation of subtidal currents in the model. Calculation of large scale circulations and corresponding subtidal currents across Northwestern Atlantic Ocean requires complicated coupled meteorological and hydrodynamic modeling which is not currently available. Given the importance of subtidal currents, it was decided to use measured wave and flow conditions as the input driving force to the shoal morphology evolution model. Therefore, model input driving forces (waves and currents) had to be assembled from a variety of sources including MARCOOS (Mid-Atlantic Regional Coastal Ocean Observing System) high frequency radar surface current data for currents and various NDBC Buoy data for waves.

An analysis of calculated wave field over the shoals by standard (half-plane) spectral wave models and its sensitivity to wave direction and grid orientation indicated that even if the models are applied within their recommended ±45° limitation, they cannot accurately simulate wave transformation processes over offshore shoals. Generally, these shoals feature a number of slopes in various directions and provide severe conditions for refraction and wave focusing calculations by conventional half-plane spectral wave transformation models. This results in inaccuracies in calculated wave directions even if the models are applied within their

recommended ±45° limitation. A full-plane model (SWAN) was used for the current morphology simulation effort to improve the accuracy of wave direction calculations.

The numerical model was used to simulate long-term evolution of the existing Isle of Wight shoal conditions. Comparisons with 1929, 1975 and 2002 surveys indicated that the predicted future shoal morphology represents the overall historic evolution and movement of Isle of Wight. The model thus has the capability to evaluate and compare the impacts of various dredging scenarios. Modeling results also indicated that waves are the primary factor in shoal growth and maintenance while currents are more responsible for shoal migration.

A total of 11 shoal dredging scenarios were considered and model runs completed for each scenario. In each scenario, the Isle of Wight was partially excavated to the -10 m contour to provide sand volumes in the range of 1 to 2 million cubic meters. The model was run to predict change in morphology over a 10 to 15 year period. The results provided valuable insights on response of different dredging plans that were used for the development of dredging guidelines.

It was found that after removal of material from a shoal, the shoal reforms itself with a smaller volume due to removal of the sediment. In other words, the volume taken by dredging is not compensated by transport of material from outside of the shoal. However, despite the reduction in volume, the reformed shoal may attain the same height as that of the pre-dredge shoal conditions for certain dredging scenarios. Although shoals get smaller as a result of dredging, there was no evidence of possible shoal diminishing/deflation after dredging. In other words, there was no indication that there exists a critical threshold for dredging that once crossed, ridge and shoal features may deflate, losing their morphologic integrity.

A series of dredging guidelines were provided with the objective to provide dredging practices that result in a reformed shoal that has the same height as the pre-dredge shoal. The provided guidelines are not universal and are recommended for the shoals in the area offshore Delaware, Maryland and Virginia between Delaware Bay and Chesapeake Bay.

Similar guidelines are expected to apply to shoals in areas other than present study area. Details, however, would be dictated by local wave and current conditions. It is recommended that a similar study be completed for other regions. The study should involve analysis of historic bathymetry data to determine shoal migration trends, field measurements of waves and currents to identify the driving forces involved, dimensional analysis of shoal parameters to define those parameters critical to shoal integrity, and long-term morphological numerical modeling to evaluate dredged shoal response.

10.0 REFERENCES

Amato, Roger, 2002, Great Gull Bank: Balancing multiple use of a shoal with the renourishment of Assateague Island, Maryland. American Shore & Beach Preservation Association, Northeast Chapter Annual Meeting Abstracts.

Byrnes, M.R., Baker, J.L., and Li, F., 2002. Quantifying potential measurement errors and uncertainties associated with bathymetric change analysis. ERDC/CHL CHETN-IV-50, Coastal and Hydraulics Laboratory, U.S. Army Engineer Research and Development Center, Vicksburg, MS, 17 p.

Calvete, D., Falques, A., De Swart, H.E. and Walgreen, M., 2001. Modelling the formation of shoreface-connected sand ridges on storm-dominated inner shelves. Journal of Fluid Mechanics, 441: 169-193.

Diaz, R.J., Cutter Jr., G.R., Able, K.W., "The Importance of Physical and Biogenic Structures to Juvenile Fishes on the Shallow Inner Continental Shelf", Estuaries, vol. 26, n. 1, pp 12-20, Feb, 2003.

Dibajnia, M., Moriya, T., and Watanabe, A., 2001. A representative wave model for estimation of nearshore local transport rate, Coastal Engineering Journal, Vol. 43, No.1, pp. 1-38.

Dibajnia, M., and Watanabe, A., 1992. Sheet flow under nonlinear waves and currents, Proc. 23rd Int. Conf. on Coastal Eng., ASCE. pp. 2015-2028.

Dibajnia, M., and Watanabe, A., 2000. Moving layer thickness and transport of graded sand, Proc. 27th Int. Conf. on Coastal Eng., ASCE. pp. 2752-2765.

Duane, D.B., Field, M.E., Meisburger, E.P., Swift, D.J.P. and Williams, S.J., 1972. Linear shoals on the Atlantic inner continental shelf, Florida to Long Island. In: D.J.P. Swift, D.P. Duane and O.H. Pilkey (Editors), Shelf Sediment Transport: Process and Pattern. Dowden, Hutchinson & Ross, Stroudsburg, Pennsylvania, pp. 447-498.

Dyer, K.R. and Huntley, D.A., 1999. The origin, classification and modeling of sand banks and ridges. Continental Shelf Research, 19: 1285-1330.

Field, M.E., 1980. Sand bodies on coastal plain shelves: Holocene record of the U.S. Atlantic inner shelf off Maryland. Journal of Sedimentary Petrology, 50(2): 505-528.

Figueiredo, A.G., Swift, D.P., Stubblefield, W.L., and Clarke, T.L., 1981. Sand ridges on the inner Atlantic shelf of North America: morphometric comparisons with Huthnance stability model. Geomarine Letters, 1, 187-191.

Glenn S.M., C. Jones, M. Twardowski, L. Bowers, J. Kerfoot, J. Kohut, D. Webb, O. Schofield, 2008. Glider Observations of Sediment Resuspension in a Middle Atlantic Bight Fall Transition Storm, Limnology and Oceanography. 53 (6): 2180-2196.

Hayes, M.O., and Nairn, R.B. (2004). "Natural Maintenance of Sand Ridges and Linear Shoals on the US Gulf and Atlantic Coast Shelves and the Potential Impacts of Dredging". Journal of Coastal Research, Vol. 20, 138-148.

Lentz, S.J., 2008. Observations and a model of the mean circulation of the Middle Atlantic Bight Continental Shelf, Journal of Physical Oceanography, 38(6), 1203-1221.

Maa, J.P.Y., C.H. Hobbs, III, S.C. Kim, and E. Wei. 2004. Potential impacts of sand mining offshore of Maryland and Delaware: Part 1 - impacts on physical oceanographic processes. Journal of Coastal Research, 20(1): 44-60.

McBride, R.A. and Moslow, T.F. (1991). Origin, evolution, and distribution of shoreface sand ridges, Atlantic inner shelf, U.S.A., Marine Geology, 97, 57-85.

McHone, J.F., JR. 1973. Morphologic time series from a submarine sand ridge on the southern Virginia coast. Norfolk, Virginia: Old Dominion University, M.S. thesis, 55 pp.

Moore, K., Wilcox, D., Anderson, B. and Orth, R. 2003. Analysis of historical distribution of SAV in the eastern shore Coastal Basins and Mid-Bay Islands complexes as evidence of historical water quality conditions and a restored bay ecosystem. Special Report No. 383 in Applied Marine Science and Ocean Engineering. The Virginia Institute of Marine Science, School of Marine Science, College of William and Mary Gloucester Point, Virginia, 23062.

Nishimura, H., 1988. Computation of nearshore current. In: Horikawa, K. (Editor), Nearshore Dynamics and Coastal Processes, University of Tokyo Press, Tokyo, pp. 271-291.

OCS Study MMS 2000-055: Environmental Survey of Potential Sand Resource Sites Offshore Delaware and Maryland, Hobbs C.H, III, Virginia Institute of Marine Science, 2000.

OCS Study MMS 2010-010: Analysis of Potential Biological and Physical Impacts of Dredging on Offshore Ridge and Shoal Features. Prepared by CSA International, Inc. in cooperation with Applied Coastal Research and Engineering, Inc., Barry A. Vittor & Associates, Inc., C.F. Bean, L.L.C., and the Florida Institute of Technology for the U.S. Department of the Interior, Minerals Management Service, Herndon, VA. 160 pp. + apps.

Pattiaratchi, C.B. and Collins, M.B., 1987. Mechanisms for linear sandbank formation and maintenance in relation to dynamical oceanographic observations. Progress in Oceanography, 19, 117-176.

Restrepo, J.M., 2001. Sediment dynamics and wave-current interactions. Continental Shelf Research, 21: 1331-1360.

Roelvink, J.A., 2006. Coastal morphodynamic evolution techniques. Coastal Engineering 53, 277–287.

Sanay R., G. Voulgaris, and J.C. Warner, 2007. Influence of Tidal Asymmetry and Residual Circulation on Sediment Transport in Linear Sandbanks: A Processes-Oriented Numerical Study. Journal of Geophysical Research, Oceans, Vol 112, C12015, doi:10.1029/2007JC004101.

Slacum, H.W. Jr., W.H. Burton, E. T. Methratta1, E. Weber, R. Llansó, J. Dew-Baxter, 2010.Assemblage Structure in Shoal and Flat-bottom Habitats on the Inner Continental Shelf of the Middle Atlantic Bight, U.S.A., Marine and Coastal Fisheries Journal, in press.

Snedden, J.W. and Dalrymple, R.W., 1999. Modern shelf sand ridges: from historical perspective to a unified hydrodynamic and evolutionary model. In: K.M. Bergman and J.W. Snedden (Editors), Isolated Shallow Marine Sand Bodies: Sequence Stratigraphic Analysis and Sedimentologic Interpretation. Society for Sedimentary Geology, Tulsa, OK, pp. 13-28.

Swift, D.J.P. and Field, M.E., 1981. Evolution of a classic sand ridge field: Maryland sector, North American inner shelf. Sedimentology, 28: 461-482.

Swift, D.J.P., Kofoed, J.W., Saulsbury, F.P. and Sears, P., 1972. Holocene evolution of the shelf surface, central and southern Atlantic Shelf of North America. In: D.J.P. Swift, D.B. Duane and O.H. Pilkey (Editors), Shelf Sediment Transport: Process and Pattern. Dowden, Hutchinson & Ross, Stroudsberg, Pennsylvania, pp. 499-574.

Trowbridge, J.H., 1995. A mechanism for the formation and maintenance of shore-oblique sand ridges on storm–dominated shelves. Journal of Geophysical Research, 100(C8): 16,071-16,086.

Van Rijn, L.C., 1993. Principles of sediment transport in rivers, estuaries and coastal seas. Aqua Publications, Amsterdam, The Netherlands.

Van Rijn, L.C. 1998. "Principles of coastal morphology", Aqua Publications, Amsterdam, The Netherlands, 4.376-4.389.

Van Rijn, L.C., 2000. General view on sand transport by currents and waves. Report Z2899.20/Z2099.30/Z2824.30, Delft Hydraulics, Delft, The Netherlands.

Vasslides, J.M. and K.W. Able., 2008. Importance of shoreface sand ridges as habitat for fishes off the northeast coast of the United States. Fishery Bulletin 106: 93-107.

U.S. Army Corps of Engineers. 1998. Ocean City, Maryland, and vicinity water resources study- final integrated feasibility report and Environmental Impact Statement. U.S. Army Corps of Engineers, Baltimore District. June 1998. Pagination by chapter.

U.S. Army Corps of Engineers. 2008. Atlantic Coast of Maryland Project Borrow Sources for 2010—2044; Final Supplemental Environmental Impact Statement. Baltimore District. August 2008. Pagination by chapter, plus annexes.

Wozencraft, J.M., Hardegree, L., Bocamazo, L.M., Rosati,J.D., and Davis, J. E. 2001. Tools for Regional Sediment Management. US Army Corps of Engineers ERDC/CHL CHETN-XIV-2.

Zuzek, P. J., R. B. Nairn, Thieme, S.J. 2003. Spatial and temporal considerations for calculating shoreline change rates in the Great Lakes Basin. Journal of Coastal Research, 38: 125 – 146.

APPENDIX A
Time Series of ADCP Measurements

Deepwater ADCP
X:0516771
Y: 4254870
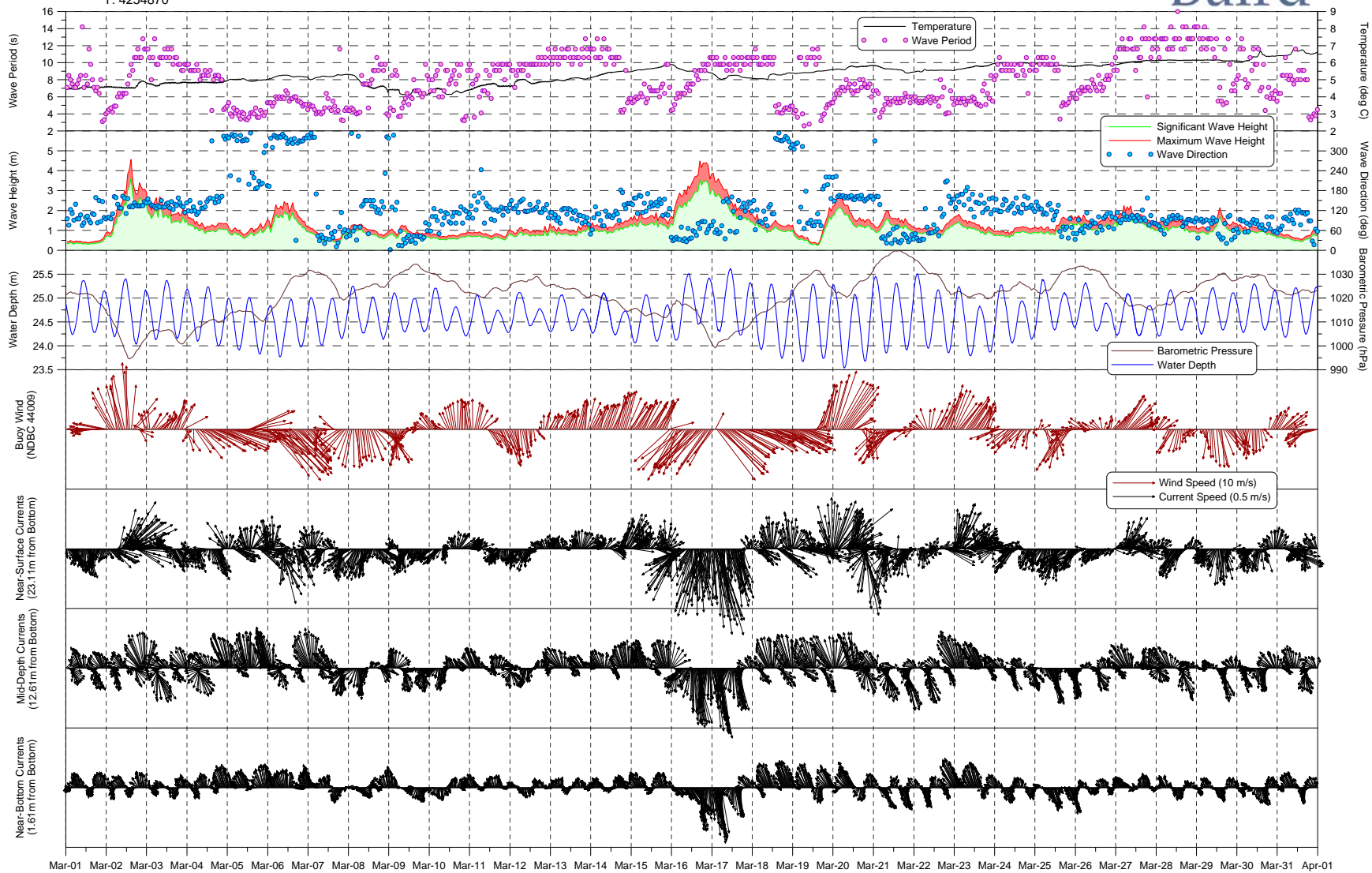
Baird

Deepwater ADCP
X:0516771
Y: 4254870
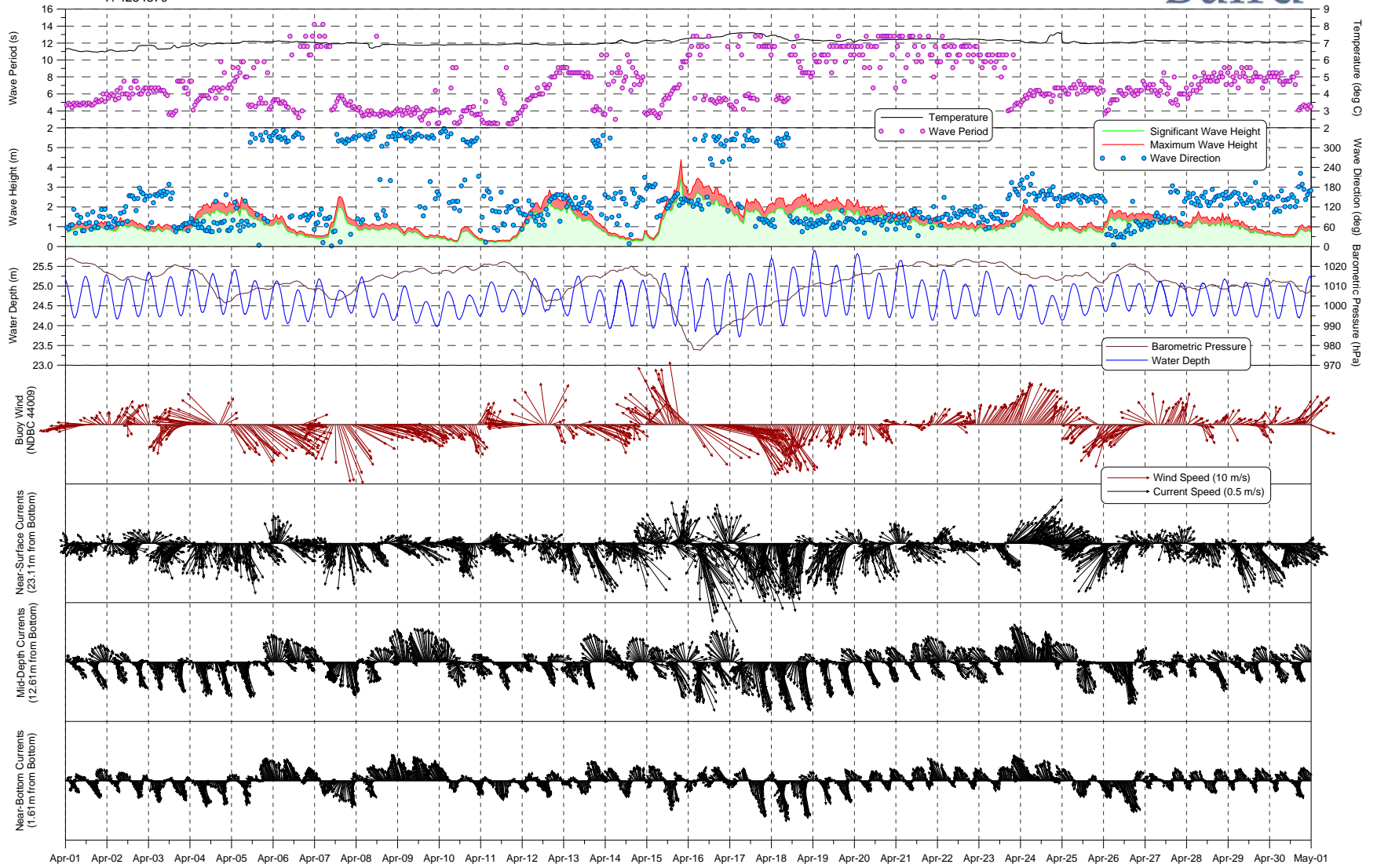
Baird

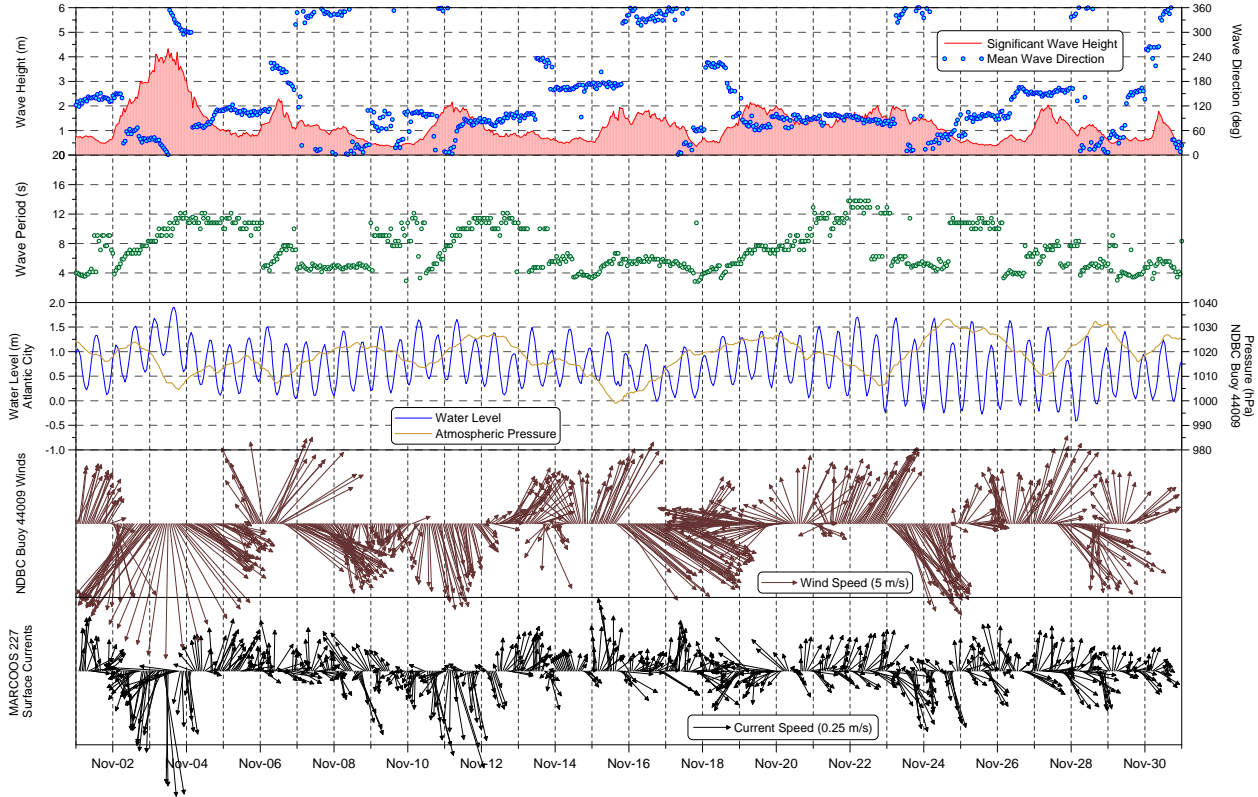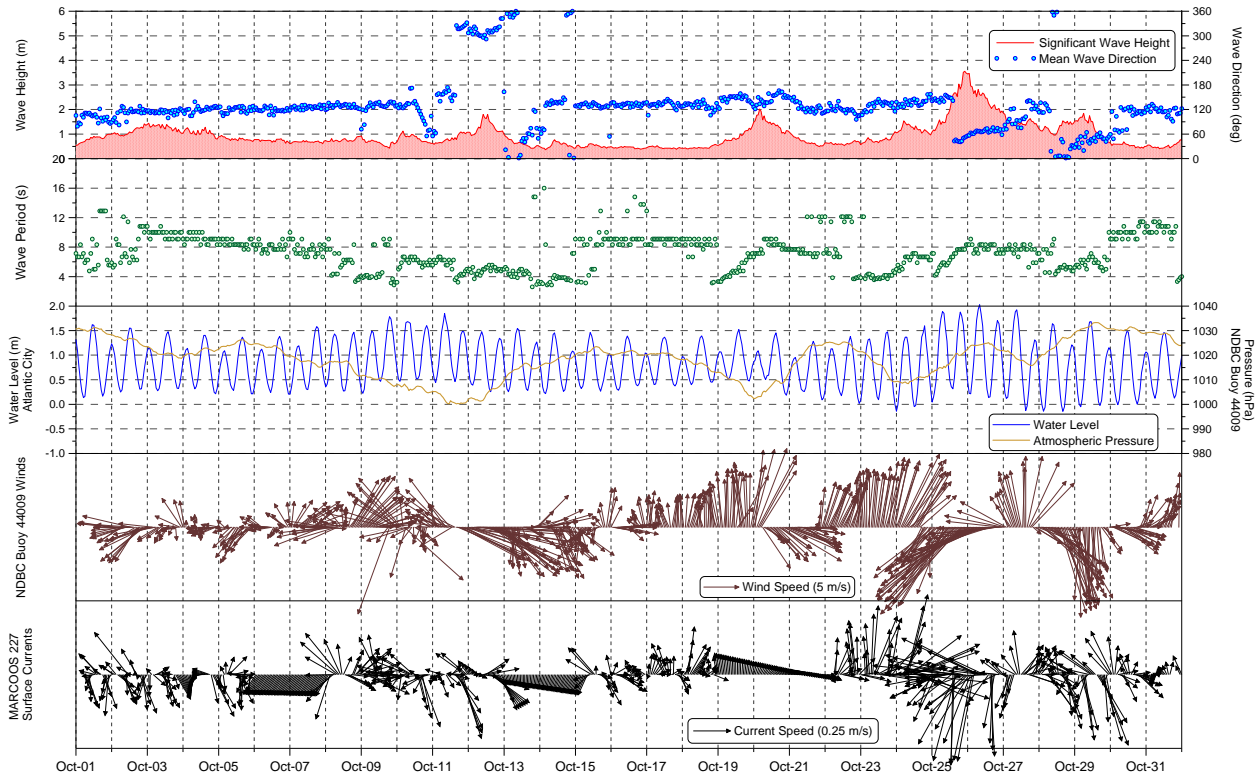Deepwater ADCP
X:0516771
Y: 4254870
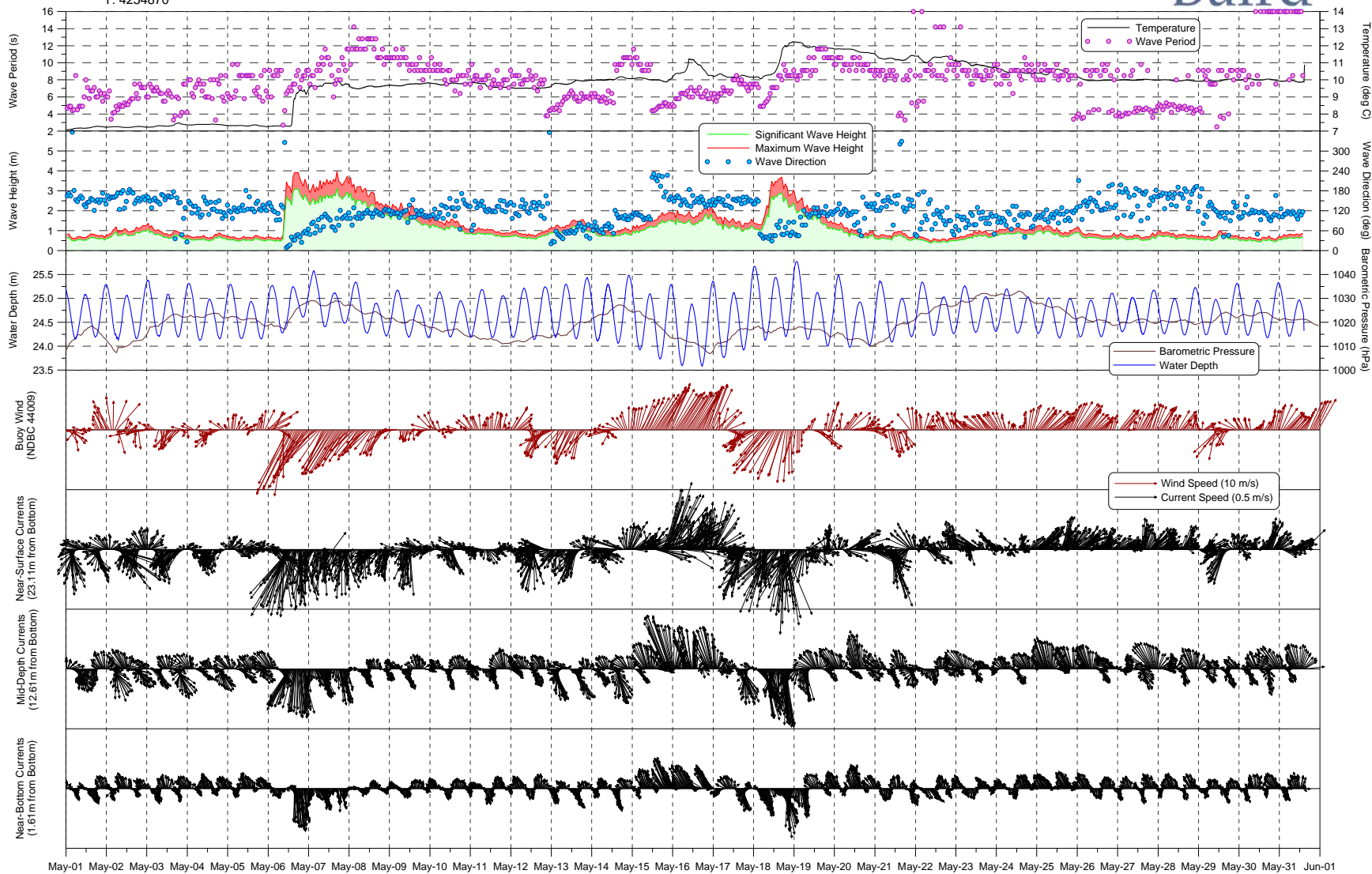
Baird

NW ADCP
X: 0505772
Y: 4248948
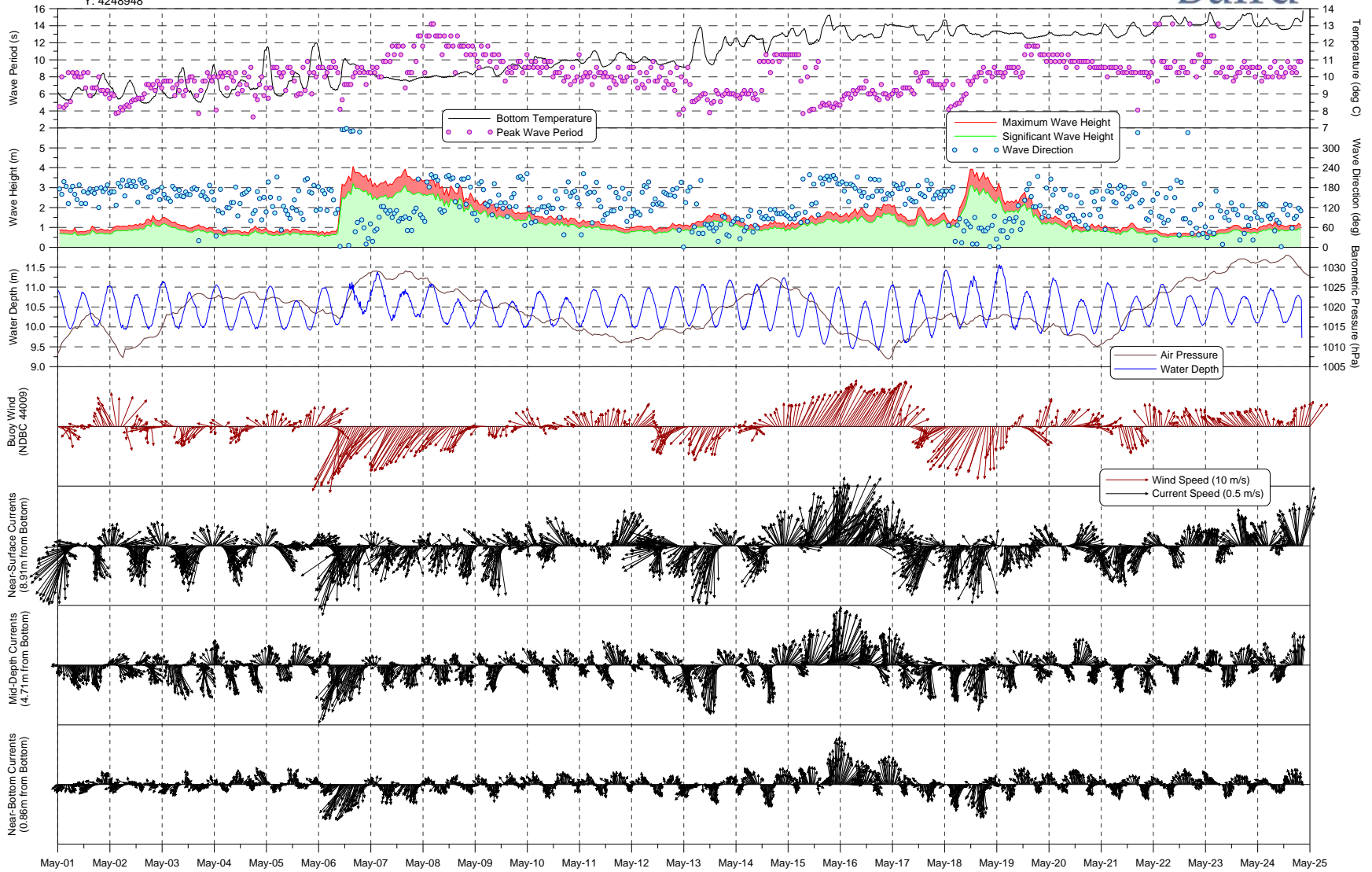
Baird

SE ADCP
X: 0506456
Y: 4248317

Baird
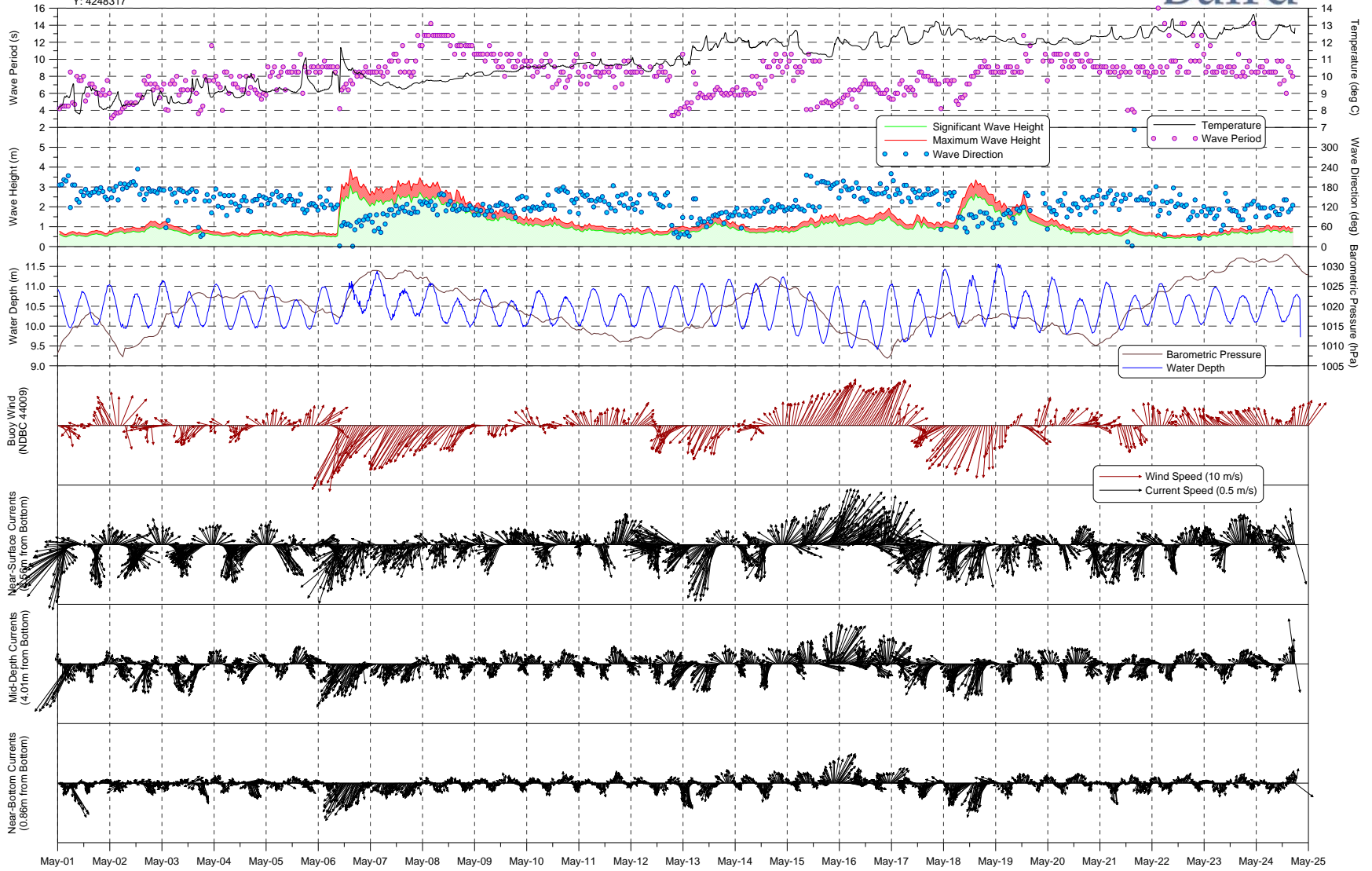
APPENDIX B
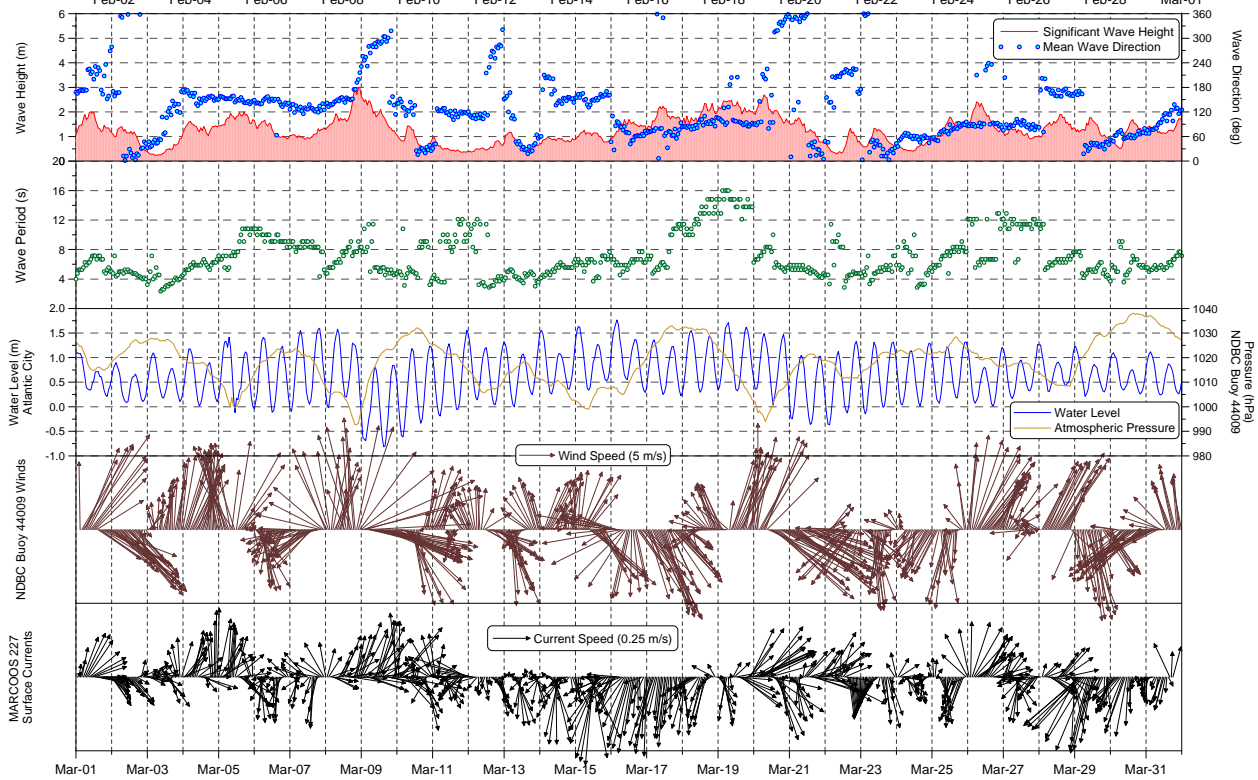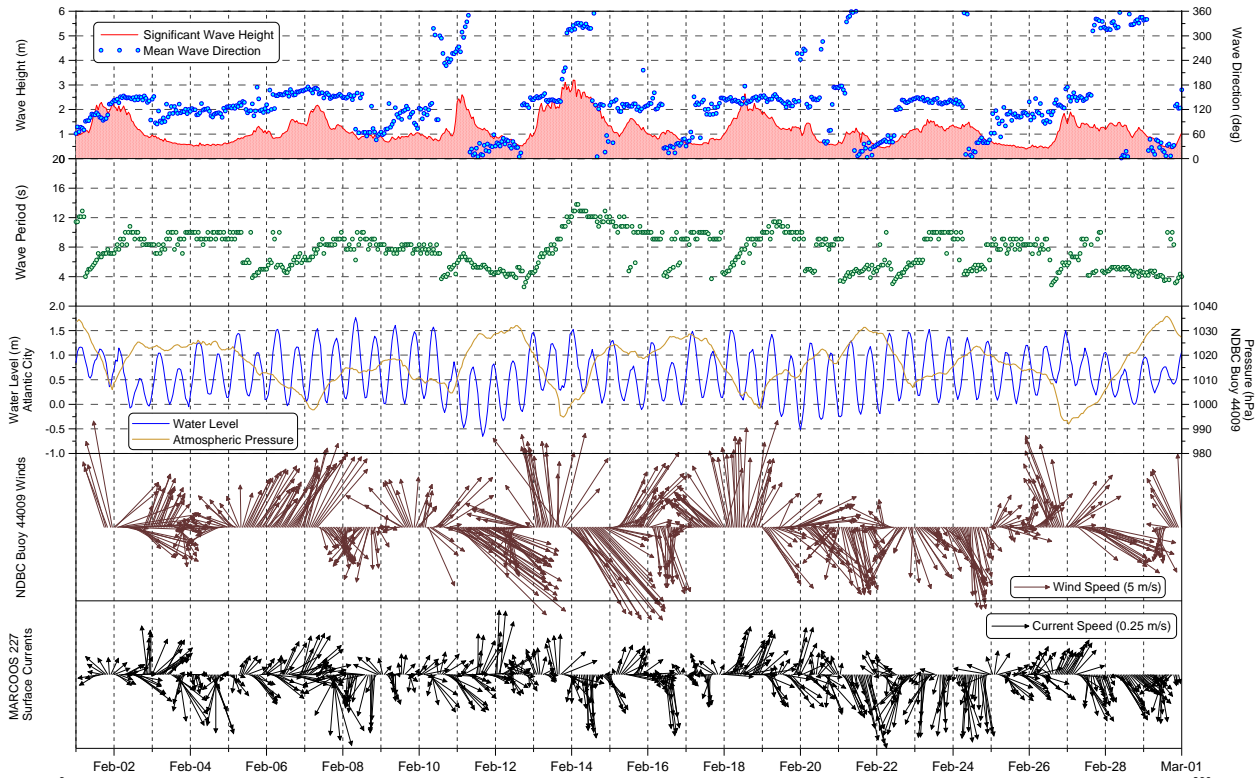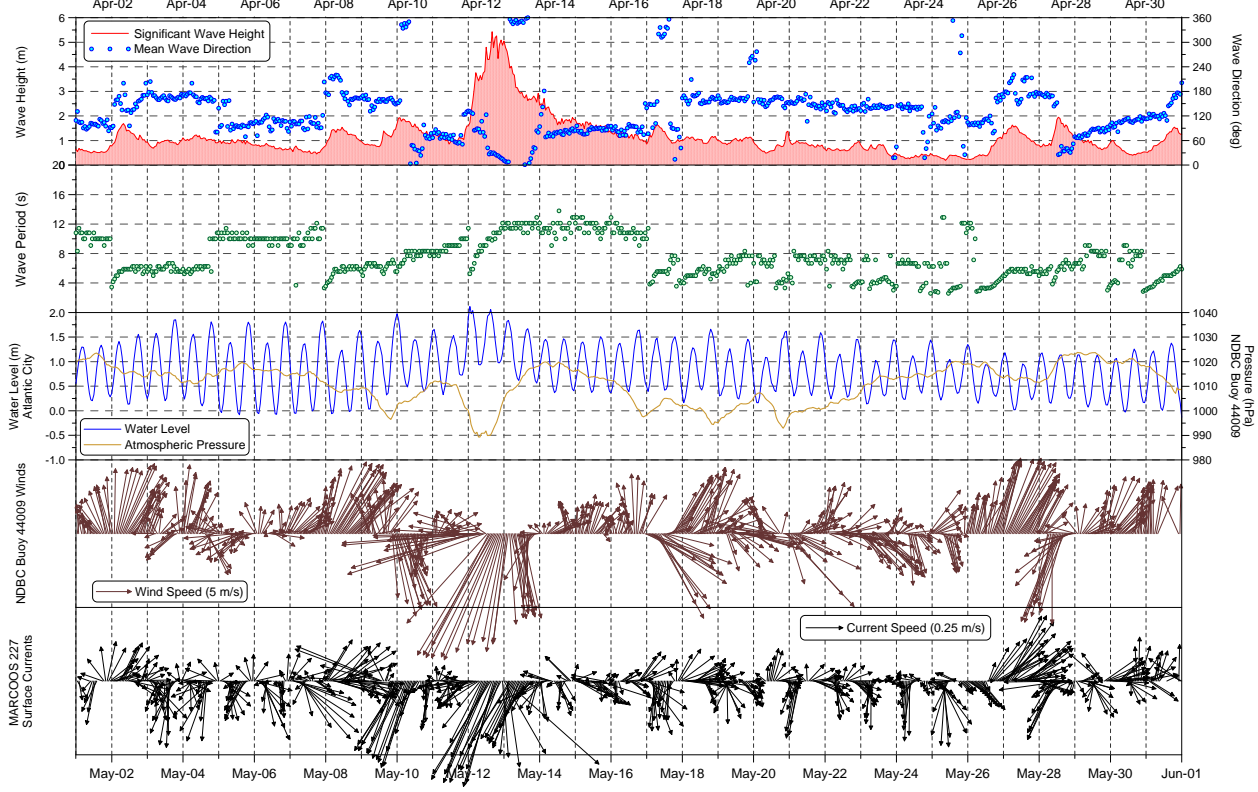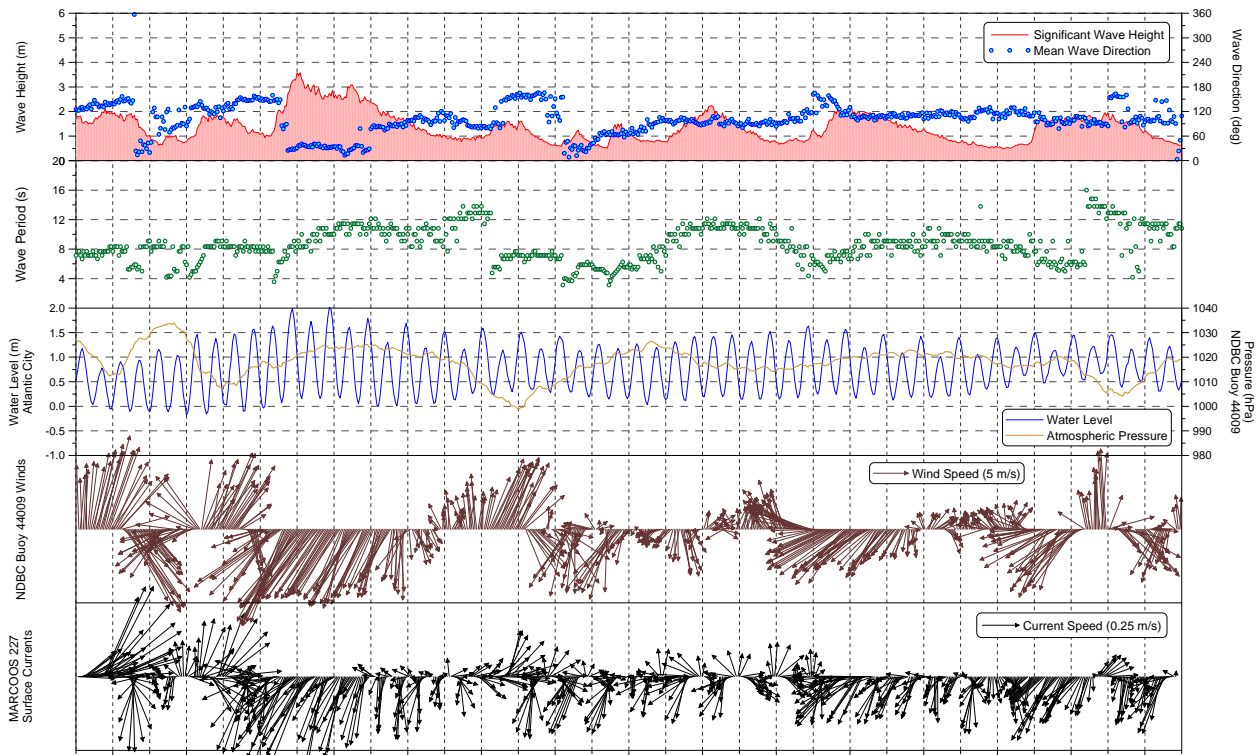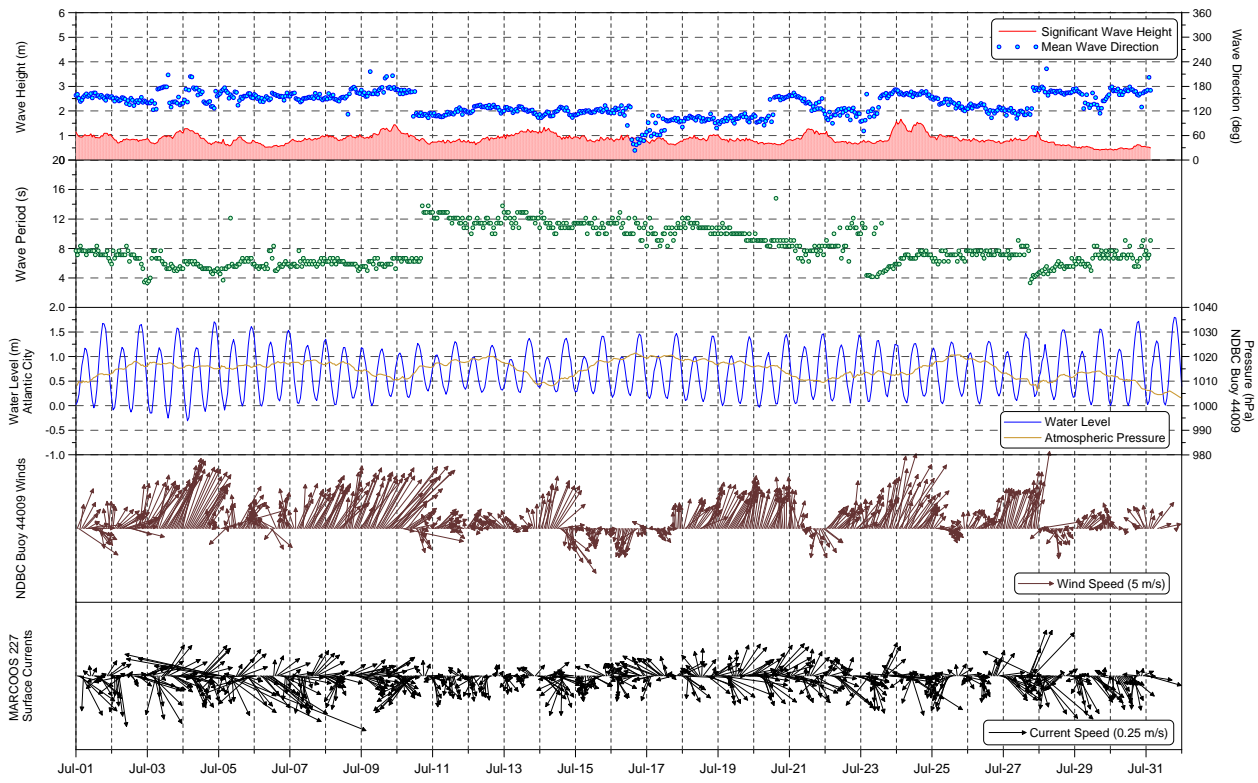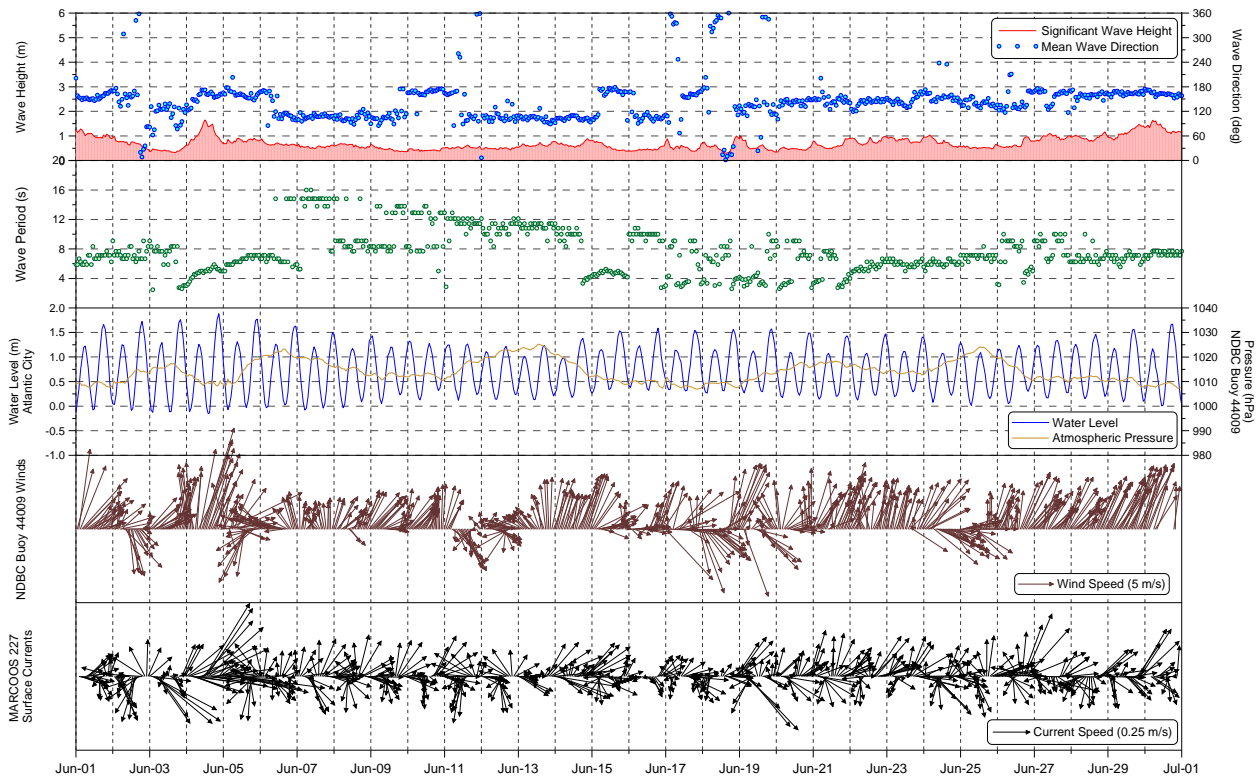**Time Series of the Developed One-year Wave and Current Input Data**
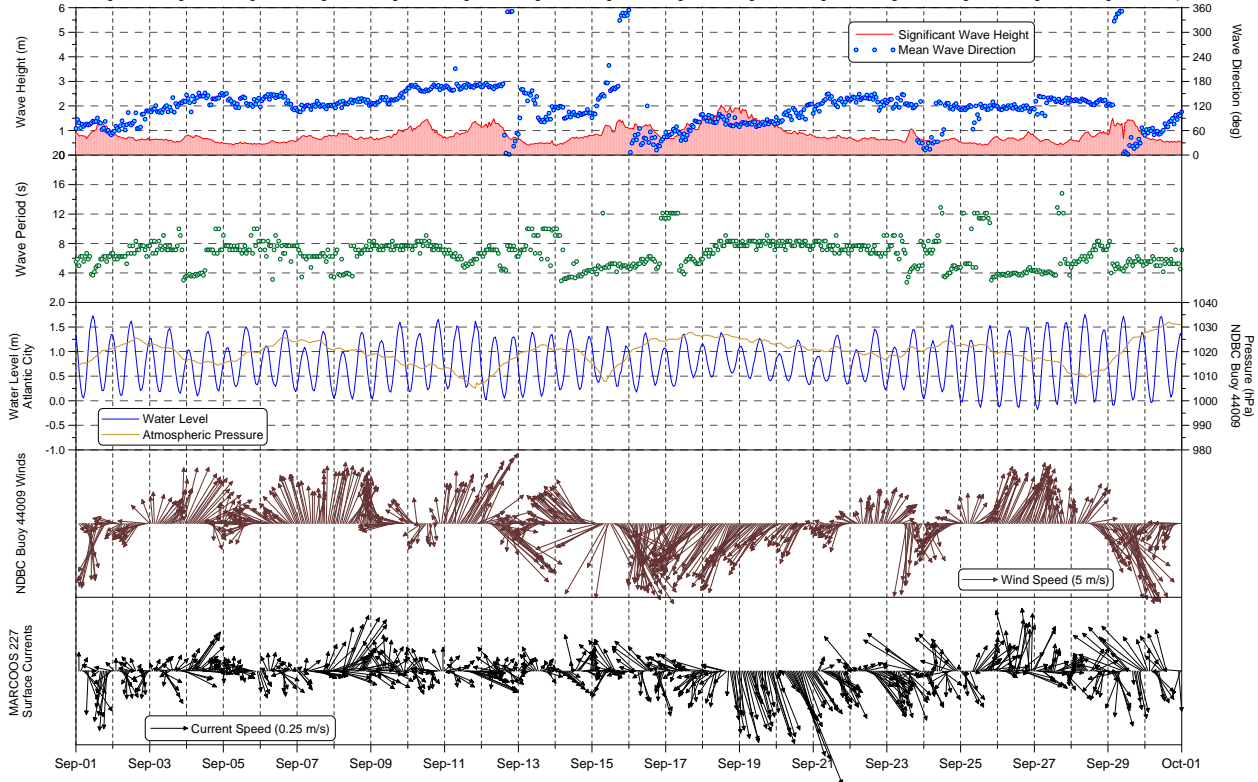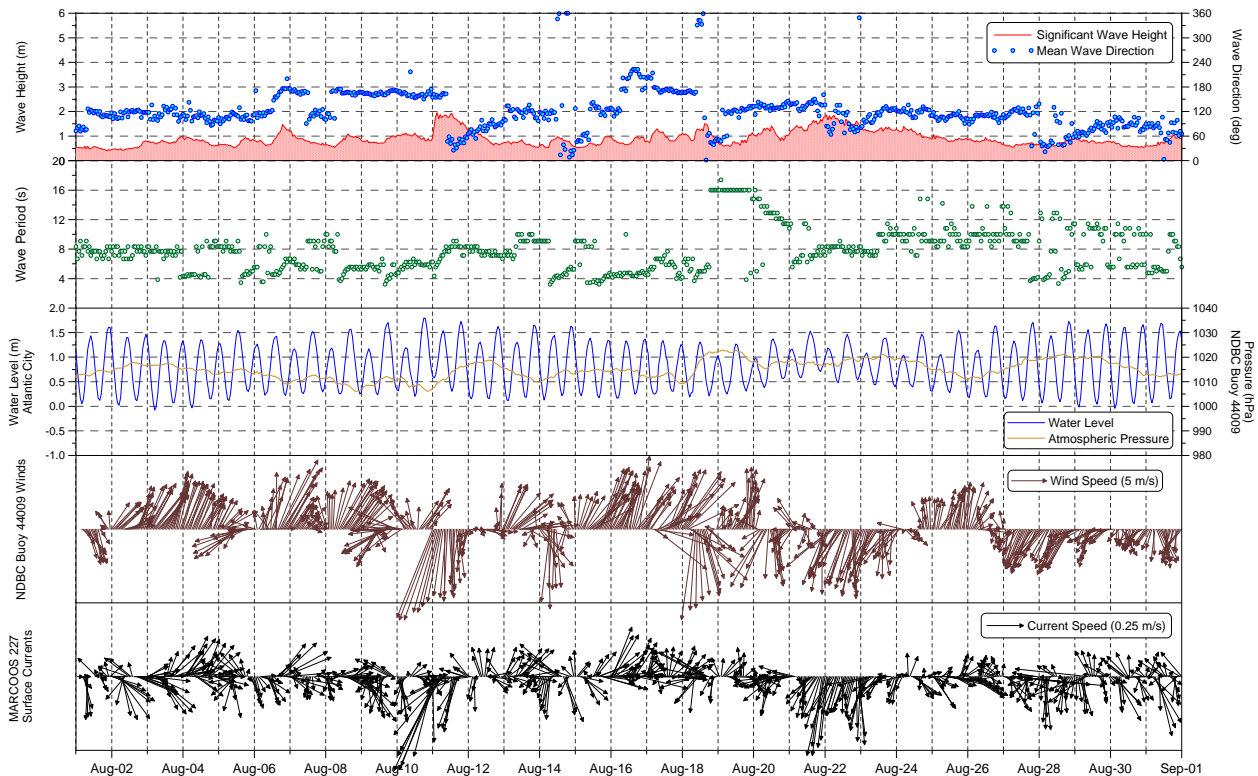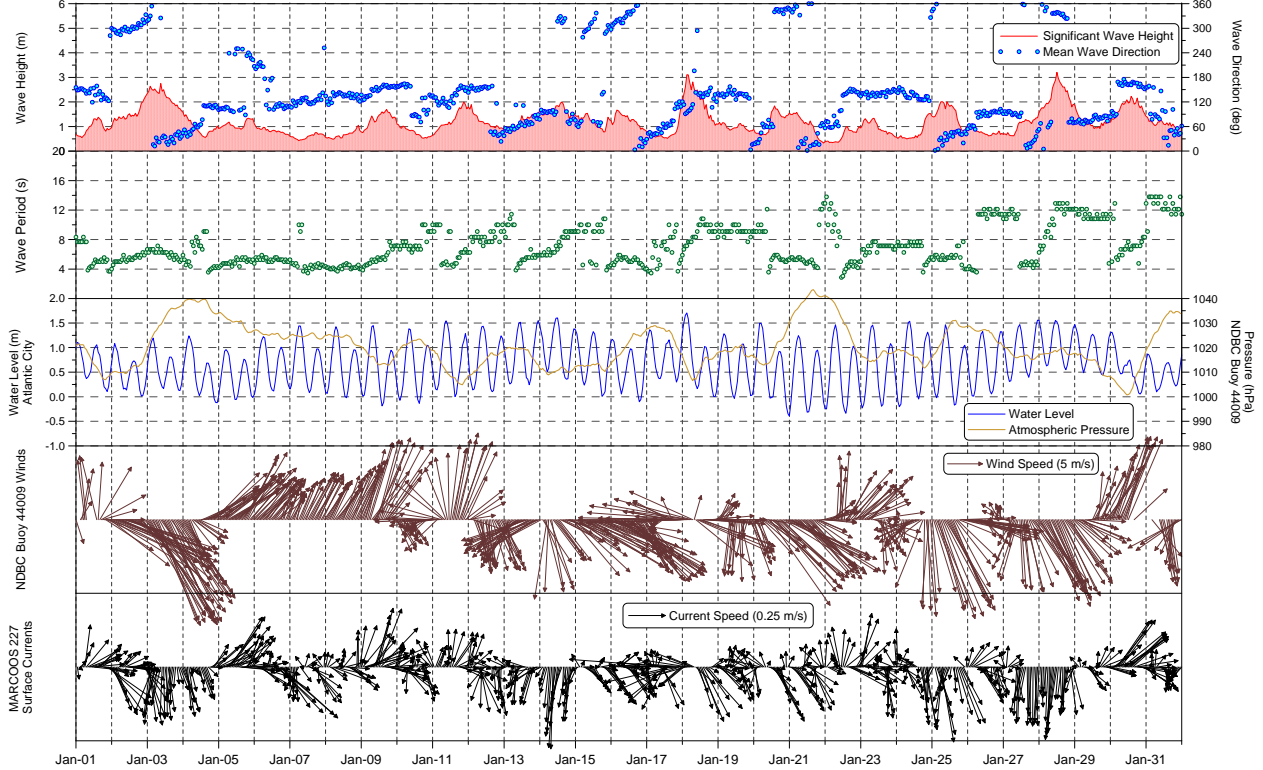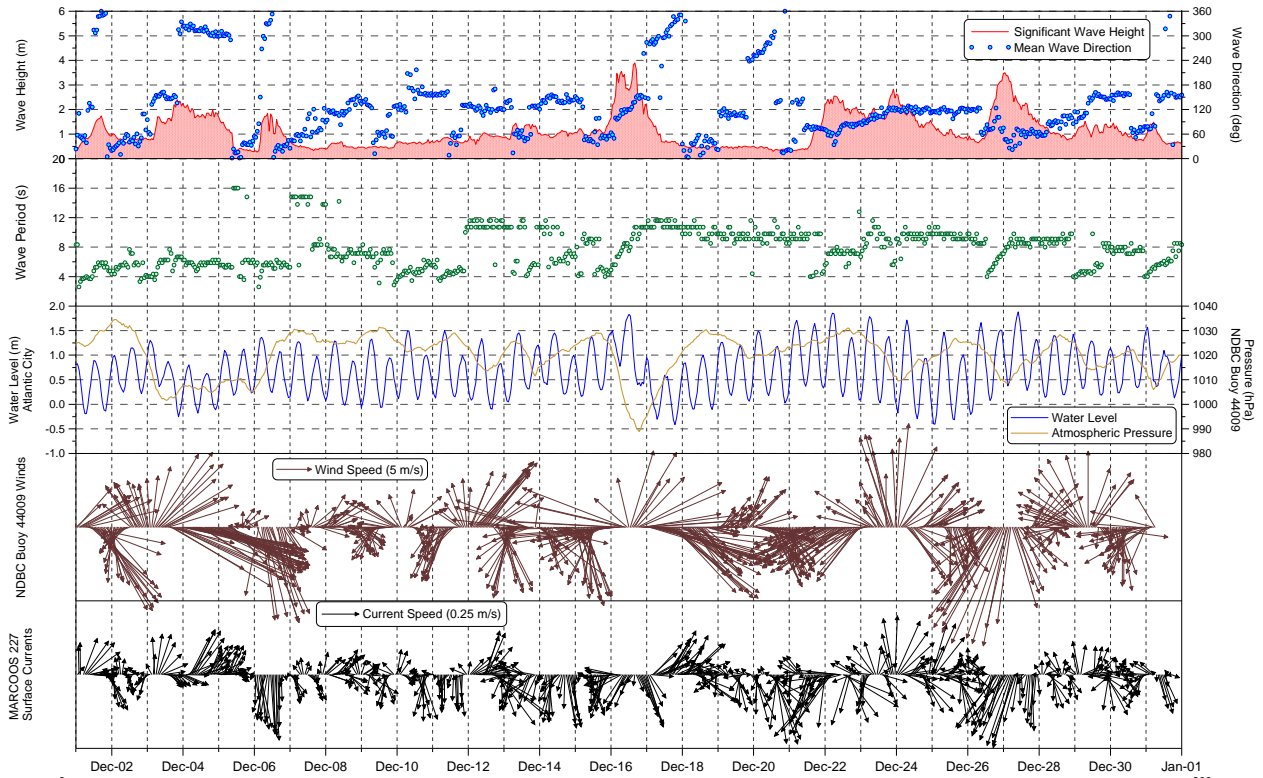
APPENDIX C
STATISTICAL MEASURES OF ERROR

Bias:

Bias is the difference between the variable and the expected value of the estimator of the variable.

$$Bias = (\bar{y} - \bar{x})$$

Root Mean Square Error (RMSE):

RMSE is the measure of total error defined as the square root of the sum of the variance and the square of the bias.

$$RMSE = \sqrt{1/n \sum (y_i - x_i)^2}$$

Scatter Index (SI):

Root Mean Square Error divided by Bias

$$SI = \frac{\sqrt{1/n \sum ((y_i - \bar{y}) - (x_i - \bar{x}))^2}}{\bar{X}}$$

Scatter Index (Bias Removed):

$$SI = \sqrt{1/n \sum ((y_i - \bar{y}) - (x_i - \bar{x}))^2}$$

Correlation Coefficient (r):

Correlation (CC) or "r" is a measure of the closeness of the relationship between two or more variables. Correlation coefficients can range from -1.00 to +1.00. Perfect negative correlation is represented by –1 and perfect positive correlation is given by +1.0, while a value of 0.0 represents a lack of correlation

$$CC = \frac{\sum (x_i - \bar{x})(y_i - \bar{y})}{\sqrt{\sum (x_i - \bar{x})^2 \sum (y_i - \bar{y})^2}}$$